Université du Québec

Institut national de la recherche scientifique

Énergie, Matériaux et Télécommunications

Approaches for Adaptive Resource Allocation in Cognitive Radio Networks

By

Vahid Reza Asghari

A dissertation submitted in partial fulfillment of the requirements for the degree of
Doctor of Philosophy (Ph.D.) in Telecommunications

Evaluation Jury

External examiner	Prof. Tho Le-Ngoc McGill University
External examiner	Prof. Octavia A. Dobre Memorial University
Internal examiner	Prof. Douglas O'Shaughnessy INRS–Énergie, Matériaux et Télécommunications
Internal examiner	Prof. Charles Despins INRS–Énergie, Matériaux et Télécommunications
Research director	Prof. Sonia Aïssa INRS–Énergie, Matériaux et Télécommunications

To my dear Mom and Dad.

Abstract

Proposing efficient spectrum utilization techniques to alleviate spectrum congestion is one of the most important challenges in wireless communication technologies operating at specific spectrum bands. In fact, the growth of wireless application demands has caused the frequency allocation table for wireless services to become over congested. On the other hand, recent measurement studies have shown that the radio frequency spectrum in its current shape is inefficiently utilized. Hence, for the purpose of alleviating the long-standing problem of spectrum congestion, the federal communication commission (FCC) is actively revising the traditional spectrum allocation policies and moving towards the adoption of *opportunistic spectrum-sharing* techniques using cognitive radio. Cognitive radio (CR) is a technology that has the ability of sensing the environment in which it operates and adapting to its changes. For instance, through sensing, CR detects the portions of the spectrum that are un-occupied (also referred to as spectrum holes) at a specific location or time. One of the most efficient ways to identify spectrum holes is to sense the activity of the primary users operating within the secondary users' (cognitive user) range of communication. In this dissertation, we study different approaches for adaptive resource allocation in spectrum-sharing CR networks. In this context, we propose utilizing spectrum sensing information about the primary users' activity and secondary channel knowledge to adaptively adjust the secondary transmission parameters such as time, power and rate while adhering to the generated interference at the primary receivers. In this case, a proper resource management is needed so as to maximize the throughput performance of the secondary users and avoid performance degradation for the primary users. The existence and specification of such resource allocation are necessary issues and will be investigated in this dissertation for different operating scenarios. We also propose adopting cooperative relaying techniques in spectrum-sharing CR systems to more effectively and efficiently utilize the available transmission resources while adhering to the quality of service requirements of the primary (licensed) users of the shared spectrum band. In particular, while the moment generating function approach is commonly used to evaluate the performance analysis of

cooperative relaying systems, we propose a unified framework which relies on the first-order statistics and convolutional methods to investigate the end-to-end performance of cooperative relaying spectrum-sharing systems. Furthermore, we quantify the advantages of utilizing relaying transmissions in spectrum-sharing CR networks for different operating scenarios and conditions.

Student   Research Director

Acknowledgments

"**And that there is not for man except that [good] for which he strives**", Surat An-Najm.

I am deeply grateful to my advisor, professor Sonia Aïssa, for her guidance and continuous support and encouragement. Working with Dr. Aïssa and learning from her has been a true privilege, and her depth of knowledge and availability to answer my questions and discuss research ideas kept me focused and motivated throughout my research. I also want to express my gratitude to my thesis committee members for their comments and suggestions on my dissertation.

My most heartfelt gratitude goes to my family and most of all my mother Heshmat and my father Javad, and my wife Marzieh, for their endless love, caring, and pride. I thank them for always being there and believing in me; this work is dedicated to them. I also thank my brother Hossein and my sisters Mahtab, Fariba, Farahnaz and Sara and my brother-in-law Masoud for helping me reach this goal in my life.

Many friends at INRS-EMT contributed to making the years of graduate school enjoyable. I will mention a few of special importance. I would like to thank my brother Hossein to make these years memorable. I am also thankful to my friends Leila, Daniel, Jian, Kais, Marcelo, Florian and Reza, for their friendship and sense of humor. I am also grateful to the support staff at INRS-EMT specially Helene, for their friendly and skilled assistance.

Finally and most, I praise Allah for giving me his greatest inspiration throughout my life.

Table of Contents

List of Figures

List of Acronyms

AF	Amplify-and-Forward
AWGN	Additive White Gaussian Noise
BC	Broadcast Channels
BER	Bit Error Rate
BPSK	Binary Phase Shift Keying
BS	Base Station
CDF	Cumulative Distribution Function
CR	Cognitive Radio
CRTC	Canadian Radio-television Telecommunications Commission
CSI	Channel State Information
DF	Decode-and-Forward
DTV	Digital Television
ENP	Effective Noise Power
FCC	Federal Communications Commission
I.I.D.	Independent and Identically Distributed
KKT	Karush-Kuhn-Tucker
MAC	Multiple Access Channels
MHR	Multi-Hop Relaying
MIMO	Multiple-Input Multiple-Output
MGF	Moment Generating Function
M-QAM	M-ary Quadrature Amplitude Modulation
MRC	Maximal Ratio Combining
OP	Outage Probability
PAM	Pulse Amplitude Modulation
PDF	Probability Distribution Function

PR	Primary Receiver
PRS	Partial Relay Selection
PT	Primary Transmitter
PU	Primary User
QAM	Quadrature Amplitude Modulation
QoS	Quality of Service
SASN	Spectrum-Aware Sensor Network
SEP	Symbol Error Probability
SER	Symbol Error Rate
SIR	signal-to-interference ratio
SNR	signal-to-noise ratio
SR	Secondary Receiver
SSI	Soft-Sensing Information
ST	Secondary Transmitter
SU	Secondary User
TD	Time Division
TDMA	Time Division Multiple Access
tifr	truncated channel inversion with fixed-rate
USA	United States of America
WRAN	Wireless Regional Area Network

Chapter 1

Introduction

1.1 Background and Motivation

1.1.1 Cognitive Radio Tasks: An Overview

As of late June 2009, the United States of America (USA) has completed the shutting down process of analog terrestrial broadcasting. The Canadian Radio-television Telecommunications Commission (CRTC) has also set the deadline for the transition to digital television (DTV), namely to August 31, 2011 [1]. By that date, Canadian over-the-air television stations will stop broadcasting in the analog domain and use digital signals instead. Around the world, most developed countries have begun the analog shutdown, a process that will accelerate during the next five years. The transition to digital will free up some valuable spectrum resources for other important services like advanced wireless and public safety, such as for police and emergency applications[1]. Indeed, DTV uses up less spectrum resources than analog TV. In addition, DTV transmission is less affected by interference and also operates at lower power levels than analog TV signals.

On the other hand, driven by the consumers' increasing interest in wireless services, demands for the radio spectrum have increased dramatically. Moreover, the conventional approach to spectrum management is very inflexible in the sense that each operator is granted an exclusive license to operate in a certain frequency band. However, with most of the useful radio spectrum being already allocated, it is becoming excessively hard to find vacant bands to either deploy new services or to enhance the existing ones. In this context,

---

[1]This conversion will also offer more channels, and better picture/sound quality to TV users.

for the purpose of improving the spectral efficiency in TV bands, the Federal Communications Commission (FCC) in the USA has allowed unlicensed (secondary) systems to operate within the spectrum band allocated to DTV services while ensuring that no harmful interference is caused to DTV broadcasting [2]. Taking this into account, the IEEE 802.22 working group is developing the so-called WRAN standard, which will operate as a secondary system in the DTV bands based on cognitive radio technology [3].

Cognitive radio (CR) technology has the ability of sensing the environment in which it operates, and to exploit this information to opportunistically provide wireless links that can best meet the demand of the user and of its radio environment. CR technology has a huge potential to increase the radio spectrum utilization by efficiently reusing and sharing licensed spectrum bands while adhering to the interference limitations of their primary users. Accordingly, two main functions in CR systems are *spectrum sensing* and *spectrum access*.

Spectrum sensing consists of observing the radio spectrum band and processing observations in order to acquire information about the licensed-transmission in the shared spectrum band. Spectrum sensing is an important task in CR systems, and considered compulsory in the IEEE 802.22 standard [4]. Various spectrum sensing problems have been observed in the literature [5–8]. The necessary requirement in spectrum sensing is to adopt sophisticated sensing techniques and practical algorithms for exchanging the sensing information between secondary nodes.

Spectrum access, on the other hand, consists of providing efficient allocation and management of the available resources among the secondary users. Chief among the challenges in opportunistic CR networks is spectrum access [9]. Indeed, how to efficiently and fairly allocate the radio resources between secondary users in a CR network is a fundamental problem (see e.g. [10–13]).

In this dissertation, we focus on several issues related to CR spectrum-sharing systems namely, adaptive resource allocation, capacity limits, multi-user communications and the benefits of utilizing cooperative communications in CR networks.

1.1.2   Adaptive Resource Allocation

Adaptive resource allocation is a promising technique to improve the performance of CR communication systems [14]. Using this technique, a CR node has the ability to change

its transmission parameters based on active monitoring of several factors in the radio environment, such as radio spectrum, licensed users' activity and traffic, and fading channel variations [9]. In this context, usually in spectrum-sharing systems, the secondary channel state information (CSI) is used at the secondary transmitter to adaptively adjust the transmission resources [15, 16]. In this regard, knowledge of the secondary link CSI and information about the channel between the secondary transmitter (ST) and the primary receiver (PR), both at the ST, have been used in [16] to obtain the optimal power transmission policy of the secondary user (SU) under constraints on the peak and average received-power at the PR. The same approach has also been used in [17] and [18] to optimize the SU's transmission policy under different types of resource and quality of service (QoS) constraints. In [19], in addition to the aforementioned channel information, CSI pertaining to the primary user (PU) link was also assumed available at the ST to optimally adjust the transmit power so as to maximize capacity subject to a constraint on the average capacity loss of the primary link.

1.1.3   Capacity Limits

For performance evaluation and design of CR systems, using the appropriate capacity metric is of paramount importance. Usually, ergodic capacity is used as a long-term throughput measure in these systems [20]. The ergodic capacity is the maximum average achievable rate over all fading states without any constraint on delay. However, in CR systems, by imposing constraints on the interference generated by the cognitive users while adhering to the PUs' activity levels, it is obvious that some percentage of outage is unavoidable [16]. Hence, for delay-sensitive applications, delay-limited capacity is a more appropriate metric [21]. In this regard, the delay-limited capacity of spectrum-sharing systems under different types of power constraints, was investigated in [22] and [23], considering availability of the CSI pertaining to the SU link and the one corresponding to the interference channel between the secondary transmitter (ST) and primary receiver (PR), both at the ST. On the other hand, in many real-time applications, the required rate is not necessarily constant. For example, in wireless systems where a specific rate is needed for voice communication, any excess rate can be used for other applications. Motivated by this fact, the service-rate based capacity notion was proposed in [24, 25]. In particular, in CR systems where the transmission is limited by the PUs' activity, it is desirable for

the SUs to fully utilize the radio resources while they have access to the shared spectrum band. In this regard, considering availability of the secondary CSI and information about the interference channel at the ST, the service-rate capacity of spectrum-sharing systems is investigated in [22].

1.1.4 Multi-User Communications

As mentioned before in Section 1.1.1, spectrum access means how to efficiently and fairly allocate the radio resources between secondary users in a CR network [12]. This issue is similar to the broadcast channel (BC) problem in current wireless communication systems. In BC systems, typically and traditionally, CSI has been utilized to adaptively allocate the transmission resources, such as time, power, bandwidth and rate, among users [26]. In particular, considering perfect CSI at the base station and receivers, the optimal time and power allocation policies that maximize the ergodic capacity of fading BCs was investigated in [26]. In spectrum-sharing CR networks, the problem of fair resource allocation among secondary users was investigated in [12] subject to QoS constraints at the SUs and interference constraints at the PRs. In the latter works, CSI is the only information based on which the base station decides how to distribute the resources between users.

1.1.5 Performance Analysis of Cooperative Relaying Communications

Resource management is indeed of fundamental importance in spectrum-sharing systems as explained in Section 1.1.1. However, when the available spectrum resources are not sufficient enough to guarantee reliable transmission at the secondary party, the resource allocation policy may not be able to fulfill the secondary users' requirements. In such cases, the secondary system has to implement sophisticated techniques to meet its performance requirements. One notable technique is cooperative communication, which exploits the natural spatial diversity of multi-user systems. The concept of cooperative diversity has been recently gaining increasing interest [27–31]. The key idea is that terminals located in different geographical positions may share their antennas in order to mimic a virtual antenna array and exploit the advantages of spatial diversity even when the source and destination nodes are single-antenna devices. In fact, cooperative transmissions enable two nodes, one source and one destination, to reach one another through a set of cooperating

relays, the aim of which is to propagate the signal from the source to the destination in order to enhance coverage and increase the achievable throughput between the end nodes. In this context, the performance evaluation of multi-branch multihop cooperative wireless systems has been investigated in [32] by proposing a unified framework which relies on the MGF-based approach. Furthermore, outage probability and end-to-end performance of cooperative relaying systems were analyzed in [33, 34].

1.1.6 Cooperative Relaying CR Communications

Communication using relay nodes is a promising way to combat signal fading due to multipath radio propagation, and improve the system performance and coverage area [35]. Roughly speaking, there are two main types of signal processing at the relaying nodes: Amplify-and-forward (AF) whereby the relay simply amplifies the received signal without any sort of decoding and forwards the amplified version to the destination node, which is the most straightforward and practical option, and decode-and-forward (DF) whereby the relay decodes the received signal and then re-encodes it before forwarding it to the destination node. In this context, the concept of relaying has been applied in the CR context to assist the transmission of SUs and improve spectrum efficiency, e.g., see [36–39].

1.2 Research Objectives

In this dissertation, as highlighted in the above, we investigate different approaches in adaptive resource allocation in spectrum-sharing CR networks. In this regard, we consider CR networks making use of sensing information about the PU's activity in the CR neighboring area and operating under interference constraints. In this case, a proper resource management is needed so as to guarantee the QoS requirements at the PUs. The existence and specification of such resource allocation under various service requirements at the secondary system are necessary issues and will be investigated in this dissertation. We will also develop dynamic resource allocation techniques and propose proper adaptation policies for CR networks. In particular, we will consider a spectrum-sharing BC scenario and develop advanced techniques for spectrum sensing and resource management in conjunction with the adaptation policies and protocols so as to utilize the radio spectrum in an efficient manner. Thereafter, we will adopt the cooperative relaying transmission technique

for the secondary communication in a spectrum-sharing CR system, to more effectively use the available spectrum resources and decrease the interference at the primary receivers. In this context, initially, we consider a source/destination transmission link and investigate the performance evaluation of single- and multi-hop relaying communication systems by using the moment generating function (MGF)-based approach. Then, we consider a typical cooperative relaying spectrum-sharing system and investigate its end-to-end performance by proposing a unified framework which relies on the first-order statistics and convolutional approaches.

1.3   Contribution of the Dissertation

1.3.1   Accomplishment

The contribution of this dissertation can be summarized in several respects as follows:

In Chapter 2, we consider a spectrum-sharing system where the power of the ST is controlled based on soft-sensing information about the PU's activity and CSI pertaining to the secondary link. Spectrum sensing information is obtained by a spectrum sensing detector mounted on the secondary side to assess the PU's activity state in the shared spectrum band and the system is characterized by resource constraints on the average interference at the PR and peak transmit power at the ST. Considering these limitations, the ergodic capacity of the SU's channel in a fading environment is investigated, and the optimal power allocation scheme for achieving capacity, namely *variable power* policy, is derived. However, while most modulation schemes do not adapt their performance to the fading conditions, a reconfigurable CR is able to select a modulation strategy that adapts the transmission rate and power to provide reliable communication across the channel all the time. In this context, we also investigate a *variable rate and power* multilevel quadrature amplitude modulation (M-QAM) transmission strategy in a CR communication system where the rate and power of the ST are adaptively controlled based on availability of the secondary link CSI and soft-sensing information about the PU's activity. Furthermore, considering imperfect soft-sensing information is used at the secondary system, we investigate the optimal power transmission policy in terms of false-alarm and detection probabilities and explore the impact of detection uncertainties on the performance of spectrum sharing cognitive radio systems.

In Chapter 3, different capacity notions, namely, ergodic, delay-limited and service-rate capacities, in CR systems are investigated while the transmission parameters of the cognitive users are adaptively changed based on availability of the CSI pertaining to the SU link, and soft-sensing information about the activity of the PU. We first study the ergodic capacity of the SU's link in fading environments and derive the associated optimal power allocation policy. Then, the power allocation policy under outage probability constraint is obtained, and the achievable capacity with such transmission policy is investigated in different fading environments. Finally, we propose the service-rate capacity as a service-based capacity notion for CR networks that not only provides a minimum constant rate for cognitive users, but also increases the average long-term achievable rate of the secondary communication link through utilization of the available excess power.

In Chapter 4, we consider a primary/secondary spectrum-sharing system, and study adaptive resource management in CR fading BC channels. In this context, while focusing on the capability of CR systems to sense the environment in which they operate, we obtain an optimal time-sharing and transmit power allocation policy for CR-BC systems, based on local observations about the primary system activity around each SR. Our approach is novel relative to utilizing local soft-sensing information in order to determine which SU should have access to the shared spectrum band at each sensing state. We also implement a discrete sensing mechanism in order to limit the overall system complexity, without compromising the system performance significantly.

In Chapter 5, we consider a source/destination transmission link and investigate the performance evaluation of single- and multi-hop relaying communication systems by using the MGF-based approach. First, considering a generalized fading scenario in a single-hop communication system, we investigate the performance of the proposed system in terms of the average symbol error probability (SEP) of arbitrary M-ary QAM constellations in maximal-ratio combining (MRC) schemes over non-identical correlated channels. Then, we consider a multi-hop relaying system with amplify-and-forward (AF) transmission and no line-of-sight between the source and destination nodes, operating over Nakagami fading channels with arbitrary fading parameters. In this context, making use of the MGF approach, we investigate the performance of cooperative relaying networks in terms of average SEP, ergodic capacity and outage probability subject to independent and non-identically distributed Nakagami-m fading.

In Chapter 6, we adopt a cooperative relaying technique for the secondary transmission in a spectrum-sharing system, to more effectively use the available spectrum resources, and decrease the interference at the PRs. We consider a dual-hop cooperative relaying spectrum-sharing system and investigate the end-to-end performance of this cooperative system by proposing a unified framework which relies on the first-order statistics and convolutional approaches. Specifically, assuming an intermediate decode-and-forward (DF) relay node is employed in the communication between the secondary source and destination nodes, the end-to-end performance of the dual-hop cooperative system is studied by obtaining the first-order statistics pertaining to the first and second transmission channels. Furthermore, we consider the scenario when a cluster of relays is available between the secondary source and destination nodes. In this case, using partial relay selection scheme, the results presented for the single-relay scenario are generalized. Finally, we consider that the communication between the secondary source and destination nodes is assisted by an intermediate relay that uses AF relaying. We propose a framework based on the standard convolutional approach to investigate the overall performance of the cooperative spectrum-sharing system for different propagation conditions.

1.3.2   List of Original Publications

- [1] V. Asghari and S. Aissa, "Adaptive Rate and Power Transmission in Spectrum Sharing Systems", *IEEE Transactions on Wireless Communications*, vol. 9, no. 10, pp. 3272 – 3280, Oct. 2010.

- [2] V. Asghari and S. Aissa, "Resource Management in Spectrum-Sharing Cognitive Radio Broadcast Channels: Adaptive Time and Power Allocation", *IEEE Transactions on Communications*, vol. 59, no. 5, pp. 1446 – 1457, May 2011.

- [3] V. Asghari and S. Aissa, "End-to-End Performance of Cooperative Relaying in Spectrum-Sharing Systems with Quality of Service Requirements", *IEEE Transactions on Vehicular Technology*, vol. 60, no. 5, pp. 2656 – 2668, July 2011.

- [4] V. Asghari and S. Aissa, "Spectrum Sharing in Cognitive Radio Systems: Service-Oriented Capacity and Power Allocation", Accepted for publication at *IET Communications, Special Issue on: Cognitive Communications*, pp. 1 – 13, May 2011.

- [5] V. Asghari and S. Aissa, "Performance of Cooperative Spectrum-Sharing Systems with Amplify-and-Forward Relaying", Accepted for publication at *IEEE Transactions on Wireless Communications*, Nov. 2011.

- [6] V. Asghari, D. da Costa and S. Aissa, "Symbol Error Probability of Rectangular QAM in MRC Systems with Correlated η-μ Fading Channels", *IEEE Transactions on Vehicular Technology*, vol. 59, no. 3, pp. 1497 – 1503, Mar. 2010.

- [7] V. Asghari, D. da Costa and S. Aissa, "Closed-Form Upper Bounds for the Ergodic Capacity of Multihop Relaying Networks with Nakagami-m Fading", Submitted to *IEEE Transactions on Communications*, Jan. 2011.

- [8] V. Asghari and S. Aissa, "Impact of Detection Uncertainties on the Performance of Spectrum Sharing Cognitive Radio with Soft Sensing", Submitted to *IEEE Transactions on Vehicular Technology*, July 2011.

- [9] V. Asghari and S. Aissa, "Resource sharing in cognitive radio systems: Outage capacity and power allocation under soft sensing," in Proc. *IEEE Global Telecommunications Conference* (GLOBECOM'08), New Orleans, LA, USA, Nov.-Dec. 2008, pp. 1 – 5.

- [10] V. Asghari and S. Aissa, "Rate and power adaptation for increasing spectrum efficiency in cognitive radio networks," in Proc. *IEEE International Conference on Communications* (ICC'09), Dresden, Germany, June 2009, pp. 1 – 5.

- [11] V. Asghari and S. Aissa, "Adaptive Time-Sharing and Power Allocation for Cognitive Radio Fading Broadcast Channels", in Proc. *IEEE International Conference on Communications* (ICC'10), Cape Town, South Africa, May. 2010, pp. 1 – 5.

- [12] V. Asghari, A. Maaref and S. Aissa, "Symbol Error Probability Analysis for Multihop Relaying over Nakagami Fading Channels", in Proc. *IEEE Wireless Communications and Networking Conference* (WCNC'10), Sydney, Australia, April, 2010, pp. 1 – 6.

- [13] V. Asghari and S. Aissa, "Cooperative Relay Communication Performance Under Spectrum-Sharing Resource Requirements", in Proc. *IEEE International Conference on Communications* (ICC'10), Cape Town, South Africa, May. 2010, pp. 1 – 6.

- [14] V. Asghari and S. Aissa, "Parallel-Serial Concatenated Coding: Design and Bit Error Probability Performance", in Proc. *IEEE 21st Canadian Conference on Electrical and Computer Engineering* (CCECE'08), pp. 489 – 492, Niagara Falls, ON, Canada, May 2008.

- [15] V. Asghari and S. Aissa, "Capacity Analysis of Spectrum-Sharing Cognitive Radio Systems With/Without Delay Constraint," Submitted to *IEEE International Conference on Communications* (ICC'12), Ottawa, Canada, Jun. 2012, pp. 1 – 6.

1.4   Organization of the Dissertation

The remainder of the dissertation is organized as follows.

Chapter 2 investigates the optimal power and rate allocation schemes that maximize the ergodic capacity of the secondary user's channel in fading environment for CR spectrum-sharing systems. In Chapter 3, we study three capacity notions, namely, ergodic, delay-limited and service-rate (with and without outage), for CR spectrum-sharing systems operating under constraints on the average received-interference and peak transmit-power. In Chapter 4, we investigate adaptive time sharing and power allocation policy in CR fading broadcast channels when spectrum-sensing information is utilized at the base station of the secondary network. Then, we propose adopting cooperative relaying transmission technique in spectrum-sharing systems to more efficiently use the available spectrum resources. In this context and as an initial step, in Chapter 5, a performance analysis of cooperative relaying communication systems is investigated in different fading environments. In Chapter 6, we consider a cooperative relaying spectrum-sharing CR system and develop a performance analysis of the proposed cooperative system while adhering to the QoS requirements of the primary users of the shared spectrum band. Finally, the dissertation conclusions are provided in Chapter 7.

Chapter 2

Adaptive Rate and Power Transmission in Spectrum-Sharing Systems[1]

2.1 Variable Rate and Variable Power Transmission Policies

As mentioned earlier in Chapter 1.1.2, adopting adaptive resource allocation technique, a secondary transmitter finds the ability to change its transmission parameters based on active monitoring of several factors in the radio environment, such as the primary users' activity and fading channel variations [9]. In particular, the transmission parameters of the secondary users, such as modulation level and transmit power, may be adjusted according to the channel variations while ensuring no harmful interference is caused to the licensed (primary) users of the spectrum band.

In this context, availability of CSI at the cognitive transmitter was initially considered in [40], where the optimum adaptive power transmission scheme that achieves the Shannon capacity [41], under fading and average transmit power constraint, was presented. The latter power optimization problem but subject to peak and average transmit power constraints was investigated in [42]. Usually, in spectrum-sharing systems, the secondary CSI is used at the secondary transmitter to adaptively adjust the transmission resources as presented

---

in [15–17, 19]. Common to the latter works is the fact that they all considered knowledge about the interference channel at the ST. However, a CR network can be deployed in different ways, e.g., centralized (with infrastructure) or Ad-hoc (distributed) [9]. In particular, in CR networks such as WRAN [43], knowledge of the channel between the ST and the PR, i.e., TV receivers in $IEEE$802.22 WRAN standard [44], may not be accessible by the SU network. Hence, in such networks, the capability of sensing the environment [14] can be utilized by the cognitive users to optimize their transmission policy. Concerning the sensing techniques, one of the most efficient ways to determine spectrum occupancy is to sense the activity of PUs operating in the SU's range of communication [44]. From a practical point of view, it is difficult for a SU to have direct access to the CSI pertaining to the PU link. Thus, recent works on spectrum-sharing systems concentrated on sensing the primary transmitter's activity, based on local processing at the SU side [8]. In this context, the sensing ability is provided by a sensing detector, mounted on the SU's equipment, which scans the spectrum band for a specific time. Then, the activity statistics of the PU's signal in the shared spectrum band is calculated.

Based on this sensing information, the cognitive user has this capability to determine if a signal from a primary transmitter is locally present in a specific spectrum band [9]. For instance, the received signals at an energy-based detector were used in [45] and [46] to detect the presence of unknown transmitters. Using this soft-sensing information obtained from the spectrum sensor and considering that the ST does not have information about the state of its corresponding channel, the power adaptation strategy that maximizes the capacity of the SU's link was investigated in [47]. On the other hand, in a spectrum-sharing system, to avoid deteriorating the QoS of the PUs of the band, a received-interference constraint at the PR can be considered more relevant than the transmit power constraint [48]. Indeed, in such systems, it is necessary to control the transmit power at the STs so as to limit the amount of interference caused to the PUs. In this regard, using CSI pertaining to the SU's link and adopting a soft-sensing technique at the ST in an independent manner, the outage capacity lower-bound of Rayleigh fading channel in a primary/secondary spectrum-sharing system was investigated in [8].

In this chapter, we consider a spectrum-sharing system where the power of the ST is controlled based on soft-sensing information about the PU's activity and CSI pertaining to the secondary link. The system is characterized by resource constraints on the average

interference at the PR (hereafter referred to as interference constraint) and peak transmit
power at the ST. Considering these limitations, we investigate the ergodic capacity of the
SU's fading channel, and derive the optimal power allocation scheme for achieving capac-
ity, namely *variable power* policy. However, while most modulation schemes do not adapt
their performance to the fading conditions, a reconfigurable CR is able to select a modula-
tion strategy that adapts the transmission rate and power to provide reliable communication
across the channel all the time [14]. This strategy, referred to as *variable rate and power*,
was proposed in [49, 50]. In the latter works, assuming CSI availability at the transmitter
side, the rate and power strategy that maximizes channel capacity was investigated under
average transmit power and bit error rate (BER) constraints. In this context, we also in-
vestigate *variable rate and power* multilevel quadrature amplitude modulation (*M*-QAM)
transmission strategy in a CR communication system where the rate and power of the ST
are adaptively controlled based on availability of the secondary link CSI and soft-sensing
information about the PU's activity.

In detailing these contributions, the remainder of this chapter is organized as follows.
Based on the system and channel models which are described in section 2.1.1, at first,
the variable power strategy that maximizes the ergodic capacity of the SU link under pre-
defined resource constraints is investigated in section 2.1.2. Thereby, a discussion about
the benefits of using soft-sensing information under the considered adaptive transmission
policy over fading channels, is provided. Then, in section 2.1.3, considering *M*-QAM mod-
ulation[2], we determine the adaptation policy for varying the transmission rate and power
so as to maximize the achievable capacity of the secondary link, while satisfying the afore-
mentioned power constraints and BER requirements. Finally, numerical results followed
by concluding remarks and summary are presented in sections 2.1.4 and 2.1.5, respectively.

2.1.1 Spectrum Sharing System

2.1.1.1 System Model

We consider a typical spectrum-sharing system with a pair of primary transmitter and
receiver (PT and PR) and a pair of secondary transmitter and receiver (ST and SR). In
this scenario, the SU is allowed to use the spectrum band originally assigned to the PU as

---

[2]Although our focus is on *M*-QAM modulation, the proposed rate and power adaptation policy can be
applied to other *M*-ary modulation schemes as well.
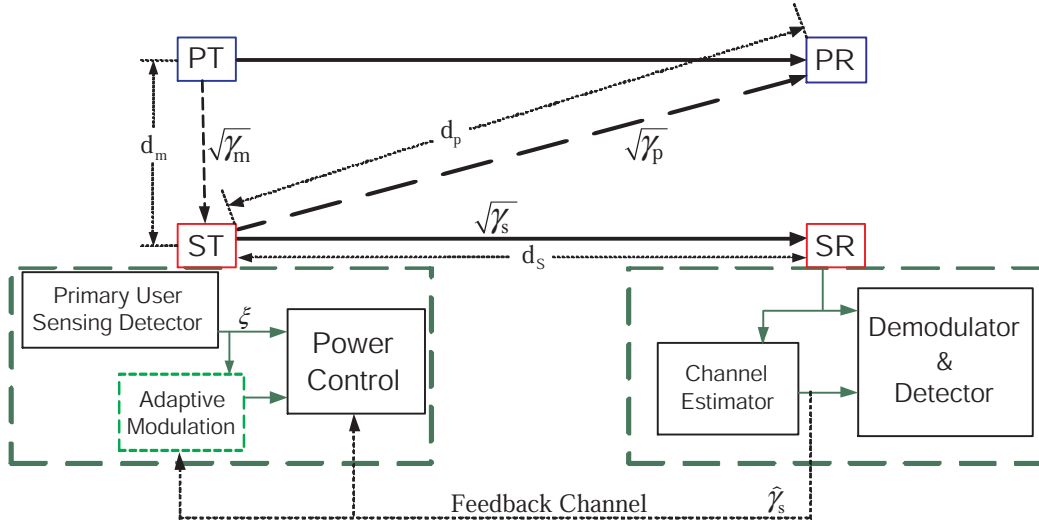
Figure 2.1: Spectrum-sharing system model.

long as the interference power imposed on the PR is limited by a predefined value. The
system model is illustrated in Fig. 2.1. We assume that the PU link is a stationary block-
fading channel with coherence time, T_c. According to the definition of block-fading, the
channel gain remains constant over T_c time epochs after which the gain changes to a new
independent value. The PT is assumed to use a Gaussian codebook with average transmit
power P_t. In this work, it is assumed that the PU's activity follows a block static model
where the duration of a block is equal to the coherence time of the fading channel, T_c. This
implies that for at least T_c time period, the activity state of the PU remains unchanged.
Accordingly, we may consider that the PT remains active (ON state) with probability α or
inactive (OFF state) with probability $\bar{\alpha} = 1 - \alpha$, in T_c time periods.

We further consider a discrete-time flat-fading channel with perfect CSI at the receiver
and transmitter of the SU. As illustrated in Fig. 2.1, the SR generates an estimate of the
channel power gain between ST and SR: $\widehat{\gamma}_s$. We assume that the latter information is fed
back to the ST error-free and without delay. We denote the channel gain between the
transmitter and receiver of the SU by $\sqrt{\gamma_s}$, the one between the ST and PR by $\sqrt{\gamma_p}$, and the
one between PT and ST by $\sqrt{\gamma_m}$. The channel power gains, γ_s, γ_p and γ_m, are independent,
and we assume unit-mean distribution for γ_s,[3] and exponential distribution for γ_p and γ_m
with variances that depend on the distances between the associated nodes ($\frac{1}{d_p^2}$ for γ_p and

---

[3]The expressions derived hereafter can be applied for any fading distribution. In the numerical results
section, however, we will assume $\sqrt{\gamma_s}$ to be distributed according to Rayleigh and Lognormal functions.

$\frac{1}{d_{\mathrm{m}}^2}$ for γ_{m}). Moreover, it is assumed that the channel gains are stationary, ergodic and
mutually independent from the noise. We also consider that the additive noise (including
interference from the PT) at the SR can be modeled as a zero-mean Gaussian random
variable with variance $N_0 B$, where N_0 and B denote the noise power spectral density and
the signal bandwidth, respectively.

2.1.1.2   Spectrum-Sensing Module

As shown in Fig. 2.1, the ST is equipped with a spectrum-sensing detector whose
function is to assess the frequency band for primary transmissions. Based on the received
signals, the detector calculates a single sensing metric, ξ, [45]. We consider that the statis-
tics of ξ conditioned on the PU's activity being in an ON or OFF state, are known a priori to
the ST. Using energy-based sensing, it has been shown in [45] that conditioned on the PU
being ON or OFF, the sensing parameter ξ can be modeled according to Chi-square prob-
ability distribution functions (PDFs) with ν degrees of freedom, where ν is related to the
number of samples used in the sensing period, N. We define the PDFs of ξ given that the
PT is ON or OFF by $f_1\left(\xi\right)$ and $f_0\left(\xi\right)$, respectively. According to [51, pp. 941], for a large
number of ν (e.g., $\nu \geq 30$), one can approximate a Chi-square distribution with a Gaussian
PDF. Since the number of observation samples can be large enough for the approximation
to be valid, we choose $f_1(\xi) \sim \mathcal{N}(\mu_1, \delta_1^2)$ and $f_0(\xi) \sim \mathcal{N}(\mu_0, \delta_0^2)$ where $(\mu_1,\, \delta_1^2)$ and $(\mu_0,\, \delta_0^2)$ are respectively given by [8][4]:

$$
\begin{aligned}
\mu_1 &= N\left(\frac{P_{\mathrm{t}}}{d_{\mathrm{m}}^2}+1\right), \quad \delta_1^2 = 2N\left(\frac{P_{\mathrm{t}}}{d_{\mathrm{m}}^2}+1\right)^2, \\
\mu_0 &= N, \qquad\qquad\quad \delta_0^2 = 2N,
\end{aligned}
\tag{2.1}
$$

where P_{t} is the PU transmit power and d_{m} denotes the distance between PT and ST.

The ST uses these statistics ($f_1(\xi)$ and $f_0(\xi)$) to optimally adjust its transmission power
and rate while satisfying predefined power constraints. Given that transmission pertaining
to the SU should not deteriorate the QoS of the PU, we impose a constraint on the average

---

[4]Note that we use Gaussian approximation according to energy detection technique, but, in the expressions
provided hereafter, there is no restriction as to the distribution of the sensing information. Such distribution
can be changed according to the sensing technique adopted by the cognitive users.

interference-power inflicted at the PR when the PU is ON. This constraint is defined as

$$\mathrm{E}_{\gamma_{\mathrm{s}},\xi,\gamma_{\mathrm{p}}}\left[S(\gamma_{\mathrm{s}},\xi)\gamma_{\mathrm{p}}\middle|\mathrm{PU\ is\ ON}\right] \leq Q_{\mathrm{inter}}; \ \ \forall \ \gamma_{\mathrm{s}},\gamma_{\mathrm{p}},\xi, \tag{2.2}$$

where $S(\gamma_{\mathrm{s}},\xi)$ denotes the transmit power of the SU, and $\mathrm{E}_{\gamma_{\mathrm{s}},\xi,\gamma_{\mathrm{p}}}[\cdot]$ defines the expectation over the joint PDF of random variables γ_{s}, ξ and γ_{p}.

In practice, the SU's transmit power needs to be limited according to the operation range of power amplifiers. Thus, in addition to the interference constraint in (2.2), we impose a peak transmit power limit at the ST, namely,

$$S(\gamma_{\mathrm{s}},\xi) \ \leq \ Q_{\mathrm{peak}}; \ \ \forall \ \gamma_{\mathrm{s}},\xi. \tag{2.3}$$

Hereafter, considering knowledge of the secondary link CSI at the ST and availability of said soft-sensing information at the latter, we obtain the adaptation policies, pertaining to *variable power* and *M*-QAM based *variable rate and power*, that maximize the achievable capacity of the secondary link under the above presented resource constraints. Then, we illustrate the benefits of using soft-sensing information in CR systems under the aforementioned power and rate adaptation techniques.

2.1.2   Power Adaptation Policy

We start by investigating the power adaptation policy under the aforementioned constraints. Then, we analyze the benefits of using soft-sensing information in our primary/secondary spectrum-sharing system.

The ergodic capacity is defined as the maximum long-term achievable rate, over all possible channel states, with arbitrary small probability of error [41]. By considering the average transmit power constraint, the ergodic capacity of a fading channel with CSI at both the transmitter and receiver is obtained in [40]. Using the same approach, the capacity of fading channels subject to peak and average transmit power constraints is derived in [42], which shows that a multiplexed Gaussian codebook with optimally allocated power in time, such that both constraints are satisfied, can achieve the ergodic capacity.

In our case, the ST uses the CSI pertaining to the SU's link and soft-sensing information about the PU's activity, in order to achieve optimum channel capacity under interference

(2.2) and peak transmit-power (2.3) constraints. Adopting an approach similar to that used
in [42], the channel capacity can be shown to be achieved through optimal utilization of
the transmit power over time, such that both constraints are met. Therefore, the ergodic
capacity, in bits/sec/Hz, represents the solution to the following maximization problem:

$$\frac{C_{\text{er}}}{B} = \max_{\gamma_{\text{s}}, \xi} \left\{ \text{E}_{\gamma_{\text{s}}, \xi} \left[\log_2 \left(1 + \frac{S\left(\gamma_{\text{s}}, \xi\right)\gamma_{\text{s}}}{N_0 B} \right) \right] \right\}, \tag{2.4}$$

$$\text{s.t. } \text{E}_{\gamma_{\text{s}}, \xi} \left[S(\gamma_{\text{s}}, \xi) \middle| \text{PU is ON} \right] \leq Q'_{\text{inter}}, \tag{2.5}$$

$$S\left(\gamma_{\text{s}}, \xi\right) \leq Q_{\text{peak}}, \tag{2.6}$$

where $\max_{\gamma_{\text{s}}, \xi}\{\cdot\}$ denotes the maximization over the distributions of γ_{s} and ξ. In (2.5), the
interference constraint is simplified by taking the expectation over the distribution of γ_{p},
where $Q'_{\text{inter}} = Q_{\text{inter}} d_{\text{p}}^2$ with d_{p} denoting the distance between ST and PR. We now state
the following result, giving the power adaptation policy that maximizes the ergodic capacity
presented in (2.4).

Theorem: In a primary/secondary spectrum-sharing system, considering availability of
sensing information about the primary user activity and secondary CSI knowledge at the
secondary transmitter, the optimal power adaptation policy under constraints on average
interference and peak transmit power is given by:

$$S\left(\gamma_{\text{s}}, \xi\right) = \begin{cases} Q_{\text{peak}} & \frac{1}{\gamma_{\text{s}}} < \frac{\gamma_{\text{v}}(\xi)}{N_0 B}, \\ \frac{\gamma_{\text{u}}(\xi)}{\lambda_1} - \frac{N_0 B}{\gamma_{\text{s}}} & \frac{\gamma_{\text{v}}(\xi)}{N_0 B} \leq \frac{1}{\gamma_{\text{s}}} \leq \frac{\gamma_{\text{u}}(\xi)}{\lambda_1 N_0 B}, \\ 0 & \frac{1}{\gamma_{\text{s}}} > \frac{\gamma_{\text{u}}(\xi)}{\lambda_1 N_0 B}, \end{cases} \tag{2.7}$$

where λ_1 is the Lagrangian multiplier, which is calculated such that the average interference
constraint in (2.5) is satisfied, and the terms $\gamma_{\text{u}}(\xi)$ and $\gamma_{\text{v}}(\xi)$ are given by

$$\gamma_{\text{u}}(\xi) = \alpha + \bar{\alpha}\frac{f_0\left(\xi\right)}{f_1\left(\xi\right)}, \quad \gamma_{\text{v}}(\xi) = \frac{\gamma_{\text{u}}(\xi)}{\lambda_1} - Q_{\text{peak}}. \tag{2.8}$$

Proof 1 *In order to obtain the optimal power allocation policy, we adopt Lagrangian op-
timization [52, 5.5.3]. The objective function, J_{C}, of the capacity formula in (2.4), can be*

expressed as given in (2.9), where λ_1, $\lambda_2(\gamma_{\mathrm{s}}, \xi)$ and $\lambda_3(\gamma_{\mathrm{s}}, \xi)$ are the Lagrangian multipliers.

$$
\begin{aligned}
J_{\mathrm{C}}\left[S\left(\gamma_{\mathrm{s}}, \xi\right), \lambda_1, \lambda_2\left(\gamma_{\mathrm{s}}, \xi\right), \lambda_3\left(\gamma_{\mathrm{s}}, \xi\right)\right] = {} & \mathrm{E}_{\gamma_{\mathrm{s}}, \xi}\left[\log_2\left(1+\frac{S\left(\gamma_{\mathrm{s}}, \xi\right)\gamma_{\mathrm{s}}}{N_0 B}\right)\right] \\
& -\lambda_1\left(\mathrm{E}_{\gamma_{\mathrm{s}}, \xi|\mathrm{PU\,ON}}\left[S\left(\gamma_{\mathrm{s}}, \xi\right)-Q'_{\mathrm{inter}}\right]\right) \\
& +\int_0^\infty\!\!\int_0^\infty \lambda_2\left(\gamma_{\mathrm{s}}, \xi\right)S\left(\gamma_{\mathrm{s}}, \xi\right)d\gamma_{\mathrm{s}}d\xi \\
& -\int_0^\infty\!\!\int_0^\infty \lambda_3\left(\gamma_{\mathrm{s}}, \xi\right)\left(S\left(\gamma_{\mathrm{s}}, \xi\right)-Q_{\mathrm{peak}}\right)d\gamma_{\mathrm{s}}d\xi. \quad (2.9)
\end{aligned}
$$

It is easy to show that J_{C} is a concave function of $S(\gamma_{\mathrm{s}}, \xi)$ and that the interference constraint in (2.4) is convex. Then, taking the derivative of J_{C} with respect to $S(\gamma_{\mathrm{s}}, \xi)$ and setting it to zero yields (2.10) under the necessary and sufficient Karush-Kuhn-Tucker (KKT) conditions given by (2.11)-(2.13).

$$
\begin{aligned}
\left(\left(\alpha f_1\left(\xi\right)+\bar{\alpha}f_0\left(\xi\right)\right)\left(\frac{\gamma_{\mathrm{s}}}{S\left(\gamma_{\mathrm{s}}, \xi\right)\gamma_{\mathrm{s}}+N_0 B}\right)-\lambda_1 f_1\left(\xi\right)\right)f_{\gamma_{\mathrm{s}}}\left(\gamma_{\mathrm{s}}\right) & \\
+\lambda_2\left(\gamma_{\mathrm{s}}, \xi\right)-\lambda_3\left(\gamma_{\mathrm{s}}, \xi\right) & = 0. \quad (2.10) \\
\lambda_1\left(\mathrm{E}_{\gamma_{\mathrm{s}}, \xi|\mathrm{PU\,ON}}\left[S\left(\gamma_{\mathrm{s}}, \xi\right)-Q'_{\mathrm{inter}}\right]\right) & = 0, \quad (2.11) \\
\lambda_2\left(\gamma_{\mathrm{s}}, \xi\right)S\left(\gamma_{\mathrm{s}}, \xi\right) & = 0, \quad (2.12) \\
\lambda_3\left(\gamma_{\mathrm{s}}, \xi\right)\left(S\left(\gamma_{\mathrm{s}}, \xi\right)-Q_{\mathrm{peak}}\right) & = 0. \quad (2.13)
\end{aligned}
$$

For each value of γ_{s} and ξ, the optimal transmit power can take values satisfying $Q_{\mathrm{peak}} \geq S(\gamma_{\mathrm{s}}, \xi) \geq 0$. Assume that $S(\gamma_{\mathrm{s}}, \xi) = 0$ for some γ_{s} and ξ. In this case, (2.13) requires $\lambda_3(\gamma_{\mathrm{s}}, \xi) = 0$ and (2.12) implies that $\lambda_2(\gamma_{\mathrm{s}}, \xi) \geq 0$ which, when substituted into (2.10), yield

$$
\left(\alpha f_1\left(\xi\right)+\bar{\alpha}f_0\left(\xi\right)\right)\left(\frac{\gamma_{\mathrm{s}}}{N_0 B}\right)-\lambda_1 f_1\left(\xi\right) < 0,
$$

which, after further manipulation, simplifies to

$$
\frac{1}{\gamma_{\mathrm{s}}} > \frac{\gamma_{\mathrm{u}}(\xi)}{\lambda_1 N_0 B}, \quad\quad\quad (2.14)
$$

*where λ_1 is the Lagrangian multiplier that satisfies the condition in (2.11) (or equivalently
the interference constraint (2.5) at equality).*

*Assume that $S(\gamma_s, \xi) = Q_{\text{peak}}$ for some γ_s and ξ. In this case, (2.12) requires $\lambda_2(\gamma_s, \xi) =
0$ and (2.13) implies that $\lambda_3(\gamma_s, \xi) \geq 0$ which, when substituted in (2.10), yield*

$$(\alpha f_1(\xi) + \bar{\alpha} f_0(\xi)) \left(\frac{\gamma_s}{N_0 B} \right) - \lambda_1 f_1(\xi) > 0,$$

which, after further manipulation, simplifies to

$$\frac{1}{\gamma_s} < \frac{\gamma_v(\xi)}{\lambda_1 N_0 B}. \tag{2.15}$$

*Now suppose that $0 < S(\gamma_s, \xi) < Q_{\text{peak}}$, then the conditions in (2.12) and (2.13) imply
that $\lambda_2(\gamma_s, \xi) = \lambda_3(\gamma_s, \xi) = 0$. According to (2.10), it follows that*

$$\left(\alpha f_1(\xi) + \bar{\alpha} f_0(\xi) \right) \left(\frac{\gamma_s}{S(\gamma_s, \xi) \gamma_s + N_0 B} \right) - \lambda_1 f_1(\xi) = 0.$$

*Then, after simple manipulation, the power adaptation policy for $0 < S(\gamma_s, \xi) < Q_{\text{peak}}$
can be expressed as,*

$$S(\gamma_s, \xi) = \frac{\gamma_u(\xi)}{\lambda_1} - \frac{N_0 B}{\gamma_s}. \tag{2.16}$$

*Finally, according to the results in (2.14), (2.15) and (2.16), the power adaptation
policy that maximizes the capacity expression in (2.4), can be expressed according to (2.7),
thus concluding the proof.*

The power adaptation policy, shown in (2.7), is partitioned into three regions depending
on the variation of $\frac{1}{\gamma_s}$ with respect to two thresholds, namely, $T_1 = \frac{\gamma_u(\xi)}{\lambda_1 N_0 B}$ and $T_2 = \frac{\gamma_v(\xi)}{N_0 B}$.
The schematic illustration of these thresholds is shown in Fig. 2.2. As observed, in the first
region, we do not use the channel for values of $\frac{1}{\gamma_s}$ exceeding T_1. In other words, transmis-
sion is suspended when the channel inversion is strong compared to threshold $\frac{\gamma_u(\xi)}{\lambda_1 N_0 B}$. The
second region is defined by the range $T_2 \leq \frac{1}{\gamma_s} \leq T_1$, where the power allocation is in the
form of water-filing. Finally, a constant power equal to Q_{peak} is considered for the third
region which corresponds to $\frac{1}{\gamma_s} < T_2$. The threshold values of the power allocation policy,
$\frac{\gamma_u(\xi)}{\lambda_1 N_0 B}$ and $\frac{\gamma_v(\xi)}{N_0 B}$, are determined such that the interference constraint (2.5) is satisfied at
equality. Accordingly, the interference constraint can be simplified by inserting $S(\gamma_s, \xi)$,
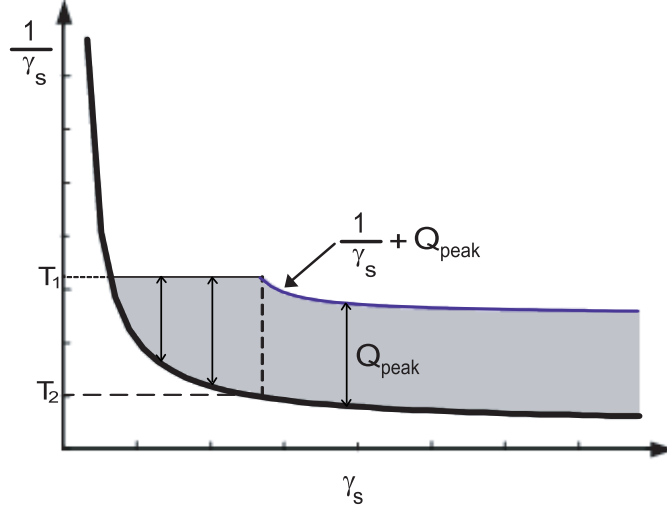
Figure 2.2: Schematic illustration of the variation of the transmit power using water-filling under peak power-constraint (Q_{peak}).

as given in (2.7), into (2.5), thus yielding

$$Q'_{\text{inter}} = \iint\limits_{\frac{\gamma_{\text{v}}(\xi)}{N_0 B} \leq \frac{1}{\gamma_{\text{s}}} \leq \frac{\gamma_{\text{u}}(\xi)}{\lambda_1 N_0 B}} \left(\frac{\gamma_{\text{u}}(\xi)}{\lambda_1} - \frac{N_0 B}{\gamma_{\text{s}}} \right) f_{\gamma_{\text{s}}}(\gamma_{\text{s}}) f_1(\xi) \, d\gamma_{\text{s}} d\xi$$

$$+ \iint\limits_{\frac{1}{\gamma_{\text{s}}} < \frac{\gamma_{\text{v}}(\xi)}{N_0 B}} Q_{\text{peak}} f_{\gamma_{\text{s}}}(\gamma_{\text{s}}) f_1(\xi) \, d\gamma_{\text{s}} d\xi, \qquad (2.17)$$

where $f(x)$ represents the PDF of random variable x. Note that the integration in (2.17) depends on the random variables γ_{s} and ξ which are the secondary CSI and sensing information metric, respectively.

For comparison purposes, we address the case with no additional soft-sensing information at the ST and using the optimal power adaptation policy presented in [42]. Indeed, we can assume that in [42, eq. (8)], the PU is always active irrespective of its real activity. Now, by comparing (2.7) which considers soft-sensing information at the ST with the power adaptation in [42], we observe that the effect of soft-sensing information is reflected through a new parameter in (2.7). This parameter, $\gamma_{\text{u}}(\xi)$, is related to the soft-sensing PDFs according to (2.8). As defined in Section 2.1.1.2, $f_0(\xi)$ denotes the PDF of the sensing metric ξ given that the PU is OFF, and $f_1(\xi)$ denotes the one corresponding to ON states. As observed in (2.8), when the probability that the PU is OFF gets higher than that of be-

ing ON, then the value of $\gamma_{\mathrm{u}}(\xi)$ has an ascensional behavior and $\gamma_{\mathrm{u}}(\xi) \geq 1$. Otherwise, $\gamma_{\mathrm{u}}(\xi) < 1$. Hence, as the probability of the PU being OFF gets higher, $\gamma_{\mathrm{u}}(\xi)$ increases and, consequently, the SU's transmission power shown in (2.7) also increases. Note that when $\gamma_{\mathrm{u}}(\xi) = 1$, the power adaptation policies in (2.7) and [42, eq. (8)] become identical. In this case, the ST has no information about the PU activity. Accordingly, it considers that the PU is always active ($f_0(\xi)/f_1(\xi) = 1$) and continuously transmits with the same power level.

Finally, substituting the power allocation policy (2.7) into (2.4) yields the ergodic capacity formula pertaining to the SU's link as follows:

$$\frac{C_{\mathrm{er}}}{B} = \operatorname*{E}_{\substack{\gamma_{\mathrm{s}},\xi \\ \frac{\gamma_{\mathrm{v}}(\xi)}{N_0 B} \leq \frac{1}{\gamma_{\mathrm{s}}} \leq \frac{\gamma_{\mathrm{u}}(\xi)}{\lambda_1 N_0 B}}} \left[\log_2 \left(\frac{\gamma_{\mathrm{u}}(\xi)\,\gamma_{\mathrm{s}}}{\lambda_1 N_0 B} \right) \right] + \operatorname*{E}_{\substack{\gamma_{\mathrm{s}},\xi \\ \frac{1}{\gamma_{\mathrm{s}}} < \frac{\gamma_{\mathrm{v}}(\xi)}{N_0 B}}} \left[\log_2 \left(1 + \frac{Q_{\mathrm{peak}}\,\gamma_{\mathrm{s}}}{N_0 B} \right) \right]. \quad (2.18)$$

2.1.3   Rate and Power M-QAM Adaptation Policy

As previously stated, the *variable rate and power* is a transmission strategy that can adjust the transmit power and rate of CR systems to improve the efficiency in utilizing the shared spectrum [14]. In this section, considering knowledge of CSI and spectrum-sensing information at the ST side, we investigate the benefits of using soft-sensing information on the capacity and adaptation policy of the *variable rate and power* transmission strategy in an M-QAM signal constellation, while adhering to the constraints on the average interference at the PU and peak transmit power at the secondary user, and satisfying predefined BER requirements. In this context, the BER bound of M-QAM when $M \geq 4$ for different values of secondary CSI, γ_{s}, and PU's activity states, ξ, can be expressed as follows [49]:

$$P_{\mathrm{b}}\left(\gamma_{\mathrm{s}},\,\xi\right) \leq 0.2 \exp\left(\frac{-1.5}{M-1} \frac{S\left(\gamma_{\mathrm{s}},\,\xi\right)\gamma_{\mathrm{s}}}{N_0 B} \right), \quad (2.19)$$

where M is the constellation size, and $P_{\mathrm{b}}\left(\gamma_{\mathrm{s}},\,\xi\right)$ denotes the instantaneous BER. Accordingly, the maximum achievable capacity in bits/sec/Hz, for the spectrum-sharing system operating under interference and peak transmit power constraints and for a given BER requirement P_{b}, represents the solution to the following optimization problem over the

spectral efficiency of the modulation scheme:

$$\frac{C_{P_{\mathrm{b}}}}{B} = \max_{\gamma_{\mathrm{s}},\xi} \left\{ \mathrm{E}_{\gamma_{\mathrm{s}},\xi} \left[\log_2 \left(M \left(\gamma_{\mathrm{s}}, \, \xi \right) \right) \right] \right\} \tag{2.20}$$

subject to constraints in (2.5) and (2.6),

$$0.2 \exp \left(\frac{-1.5}{M \left(\gamma_{\mathrm{s}}, \, \xi \right) - 1} \frac{S \left(\gamma_{\mathrm{s}}, \, \xi \right) \gamma_{\mathrm{s}}}{N_0 B} \right) \geq P_{\mathrm{b}}. \tag{2.21}$$

For achieving a target BER value, the inequality (2.21) can be used to adjust the transmission power, $S \left(\gamma_{\mathrm{s}}, \, \xi \right)$, and modulation level, $M \left(\gamma_{\mathrm{s}}, \, \xi \right)$. Thus, after simple manipulations of (2.21), for a given BER target P_{b}, the maximum M-QAM constellation size can be obtained as follows:

$$M \left(\gamma_{\mathrm{s}}, \, \xi \right) = 1 + K \frac{S \left(\gamma_{\mathrm{s}}, \, \xi \right) \gamma_{\mathrm{s}}}{N_0 B}, \tag{2.22}$$

where

$$K = \frac{-1.5}{\ln \left(5 P_{\mathrm{b}} \right)} < 1, \tag{2.23}$$

is a constant parameter related to the BER target, usually set according to the QoS requirements. From (2.22), the maximization problem in (2.20) can be rewritten as

$$\frac{C_{P_{\mathrm{b}}}}{B} = \max_{\gamma_{\mathrm{s}},\xi} \left\{ \mathrm{E}_{\gamma_{\mathrm{s}},\xi} \left[\log_2 \left(1 + K \frac{S \left(\gamma_{\mathrm{s}}, \, \xi \right) \gamma_{\mathrm{s}}}{N_0 B} \right) \right] \right\}, \tag{2.24}$$

under the interference and peak power constraints, (2.5) and (2.6), and given P_{b}. We now state the following result, giving the power and rate adaptation policies that maximize the SU's channel capacity under adaptive rate and power M-QAM transmission.

To obtain the optimal power allocation policy, the Lagrangian objective function to maximize the capacity expression in (2.24), can be formulated according to (2.25), where

λ_1, $\lambda_2(\gamma_{\rm s}, \xi)$ and $\lambda_3(\gamma_{\rm s}, \xi)$ are the Lagrangian multipliers.

$$
\begin{aligned}
J_{C_{P_{\rm b}}} \left[S\left(\gamma_{\rm s}, \xi\right), \lambda_1, \lambda_2\left(\gamma_{\rm s}, \xi\right), \lambda_3\left(\gamma_{\rm s}, \xi\right) \right] = {}& {\rm E}_{\gamma_{\rm s}, \xi} \left[\log_2 \left(1 + K \frac{S\left(\gamma_{\rm s}, \xi\right) \gamma_{\rm s}}{N_0 B} \right) \right] \\
& - \lambda_1 \left({\rm E}_{\gamma_{\rm s}, \xi | {\rm PU\,ON}} \left[S\left(\gamma_{\rm s}, \xi\right) - Q'_{\rm inter} \right] \right) \\
& + \int_0^\infty \int_0^\infty \lambda_2\left(\gamma_{\rm s}, \xi\right) S\left(\gamma_{\rm s}, \xi\right) d\gamma_{\rm s} d\xi \\
& - \int_0^\infty \int_0^\infty \lambda_3\left(\gamma_{\rm s}, \xi\right) \left(S\left(\gamma_{\rm s}, \xi\right) - Q_{\rm peak} \right) d\gamma_{\rm s} d\xi.
\end{aligned}
$$

$$(2.25)$$

Then, the derivative $\frac{\partial J_{C_{P_{\rm b}}}}{\partial S(\gamma_{\rm s}, \xi)} = 0$ can be obtained as given by (2.26), and the associated KKT conditions are as expressed in (2.11)-(2.13).

$$
\left(\left(\alpha f_1\left(\xi\right) + \bar{\alpha} f_0\left(\xi\right) \right) \left(\frac{K \gamma_{\rm s}}{K S\left(\gamma_{\rm s}, \xi\right) \gamma_{\rm s} + N_0 B} \right) - \lambda_1 f_1\left(\xi\right) \right) f_{\gamma_{\rm s}}\left(\gamma_{\rm s}\right)
$$
$$
+ \lambda_2\left(\gamma_{\rm s}, \xi\right) - \lambda_3\left(\gamma_{\rm s}, \xi\right) = 0.
$$

$$(2.26)$$

Now, following the same approach presented in the proof of the theorem in section 2.1.2, it is easy to show that the power adaptation strategy that maximizes the capacity expression in (2.20) given a target BER value, can be formulated according to:

$$
S\left(\gamma_{\rm s}, \xi\right) = \begin{cases}
Q_{\rm peak} & \dfrac{1}{\gamma_{\rm s}} < \dfrac{K \gamma_{\rm v}(\xi)}{N_0 B}, \\[2ex]
\dfrac{\gamma_{\rm u}(\xi)}{\lambda_1} - \dfrac{N_0 B}{K \gamma_{\rm s}} & \dfrac{K \gamma_{\rm v}(\xi)}{N_0 B} \le \dfrac{1}{\gamma_{\rm s}} \le \dfrac{K \gamma_{\rm u}(\xi)}{\lambda_1 N_0 B}, \\[2ex]
0 & \dfrac{1}{\gamma_{\rm s}} > \dfrac{K \gamma_{\rm u}(\xi)}{\lambda_1 N_0 B},
\end{cases}
$$

$$(2.27)$$

where λ_1 is the Lagrangian multiplier, calculated such that the average interference constraint in (2.5) is satisfied.

Comparing the power adaptation policy pertaining to adaptive rate and power transmission strategy (2.27), with that presented in (2.7) which considers power adaptation at the ST, we observe that in both policies, the number of decision thresholds is the same, and

that for values of $\frac{1}{\gamma_\mathrm{s}}$ between these thresholds the power allocation is in the form of water-filling. However, we observe that parameter K in (2.27) imposes an effective amount of power loss in the M-QAM adaptation technique in comparison with the policy in (2.7). Note that this power degradation is independent of the SU's channel conditions, γ_s, and the soft-sensing metric, ξ, and accordingly, K is the maximum coding gain for this adaptive rate and power M-QAM transmission strategy.

Now, substituting the power transmission policy (2.27) into (2.22), the maximum adaptive M-QAM modulation level can be obtained according to the following allocation:

$$
M\left(\gamma_\mathrm{s},\,\xi\right) = \begin{cases} 1 + \dfrac{KQ_\mathrm{peak}\gamma_\mathrm{s}}{N_0 B} & \dfrac{1}{\gamma_\mathrm{s}} < \dfrac{K\gamma_\mathrm{v}(\xi)}{N_0 B}, \\[2ex] \dfrac{K\gamma_\mathrm{u}(\xi)}{\lambda_1 N_0 B}\gamma_\mathrm{s} & \dfrac{K\gamma_\mathrm{v}(\xi)}{N_0 B} \le \dfrac{1}{\gamma_\mathrm{s}} \le \dfrac{K\gamma_\mathrm{u}(\xi)}{\lambda_1 N_0 B}, \\[2ex] 1 & \dfrac{1}{\gamma_\mathrm{s}} > \dfrac{K\gamma_\mathrm{u}(\xi)}{\lambda_1 N_0 B}, \end{cases}
\tag{2.28}
$$

where $M(\gamma_\mathrm{s},\,\xi)$ is related to the transmission rate through the following expression:

$$
R(\gamma_\mathrm{s},\,\xi) = \log_2\left(M(\gamma_\mathrm{s},\,\xi)\right).
\tag{2.29}
$$

From (2.28), we can conclude that the modulation level used by the cognitive user may be adjusted adaptively depending on the ratio $f_0\left(\xi\right)/f_1\left(\xi\right)$ (cf., (2.8)) and the variations of γ_s. Furthermore, the factor K still yields a degradation effect on the adaptive modulation level policy in (2.28).

Finally, for the spectrum-sharing system operating under predefined power limitations (2.20) and a target BER value, P_b, the capacity expression of the SU's link achieved based on the adaptive rate and power M-QAM transmission policy, is obtained by substituting (2.28) into (2.20), thus yielding:

$$
\frac{C_{P_\mathrm{b}}}{B} = \underset{\frac{K\gamma_\mathrm{v}(\xi)}{N_0 B} \le \frac{1}{\gamma_\mathrm{s}} \le \frac{K\gamma_\mathrm{u}(\xi)}{\lambda_1 N_0 B}}{\mathrm{E}_{\gamma_\mathrm{s},\xi}}\left[\log_2\left(\frac{K\gamma_\mathrm{u}(\xi)\,\gamma_\mathrm{s}}{\lambda_1 N_0 B}\right)\right] + \underset{\frac{1}{\gamma_\mathrm{s}} < \frac{K\gamma_\mathrm{v}(\xi)}{N_0 B}}{\mathrm{E}_{\gamma_\mathrm{s},\xi}}\left[\log_2\left(1 + \frac{KQ_\mathrm{peak}\,\gamma_\mathrm{s}}{N_0 B}\right)\right].
\tag{2.30}
$$

2.1.4 Illustrative Numerical Results and Discussion

In this section, we numerically illustrate the adaptation strategies, *variable power* and
variable rate and power, presented respectively in sections 2.1.2 and 2.1.3, when the
spectrum-sharing system operates under constraints on the average received-interference
and peak transmit-power. The SU channel variations are modeled through Rayleigh PDF
with unit mean, or Lognormal PDF with standard deviation $\sigma = 6$ dB. The Rayleigh fading
distribution arises from the multipath effect, and the lognormal distribution arises from the
attenuation of the transmitted signal due to shadowing. We assume perfect CSI of the SU
link is available at the ST, through an error-free feedback channel. The position of nodes
(Fig. 2.1) is such that $d_{\mathrm{s}} = d_{\mathrm{p}} = 1$ and $d_{\mathrm{m}} = 3$. The interference channel gain $\sqrt{\gamma_{\mathrm{p}}}$ is also
distributed according to Rayleigh PDF. Furthermore, we assume $N_0 B = 1$.

On the other hand, the sensing detector is assumed to calculate the sensing-information
metric in $N = 30$ observation samples. We suppose that the PU remains active 50% of the
time ($\alpha = 0.5$) and we set the PU's transmit power to $P_{\mathrm{t}} = 1$. Based on these settings[5],
the variation of parameter $\gamma_{\mathrm{u}}(\xi) := \alpha + \bar{\alpha} f_0(\xi)/f_1(\xi)$ is plotted in Fig. 2.3 for the sensing
PDFs, $f_1(\xi)$ and $f_0(\xi)$, shown in the same figure. As shown in the figure, three regions can
be recognized for parameter $\gamma_{\mathrm{u}}(\xi)$, namely, $\gamma_{\mathrm{u}}(\xi) > 1$, $\gamma_{\mathrm{u}}(\xi) = 1$ and $\gamma_{\mathrm{u}}(\xi) < 1$.

2.1.4.1 Ergodic Capacity in Adaptive Power Policy

In Fig. 2.4, we plot the instantaneous SU's transmit power presented in (2.7), for a
system operating under limited average interference and peak transmit power values given
by $Q_{\mathrm{inter}} = -6$ dB and $Q_{\mathrm{peak}} = 0$ dB, respectively. We illustrate the variation of the
optimum power adaptation policy in three regions: $\gamma_{\mathrm{u}}(\xi) > 1$, $\gamma_{\mathrm{u}}(\xi) = 1$ and $\gamma_{\mathrm{u}}(\xi) < 1$.
The scenario without soft-sensing is identified by $\gamma_{\mathrm{u}}(\xi) = 1$ whereas the case where the
probability that the PU is OFF is higher than being ON will be represented by $\gamma_{\mathrm{u}}(\xi) > 1$
and, otherwise, by $\gamma_{\mathrm{u}}(\xi) < 1$. As shown in Figs. 2.4(a) and 2.4(b), the power transmission
policy adapts to the SU's channel variation and soft-sensing information about the PU
activity, by transmitting at higher levels when the SU's CSI is strong and the PU being
OFF is more probable (higher values of $\gamma_{\mathrm{u}}(\xi)$). It is noted that the average interference and

---

[5]Herein, the values of the means and variances pertaining to the sensing distributions are considered such
that we can show two regions for the PU activity states, i.e., for some values of the sensing metric, $f_1(\xi)$ can
be higher than $f_0(\xi)$ or vice-versa.
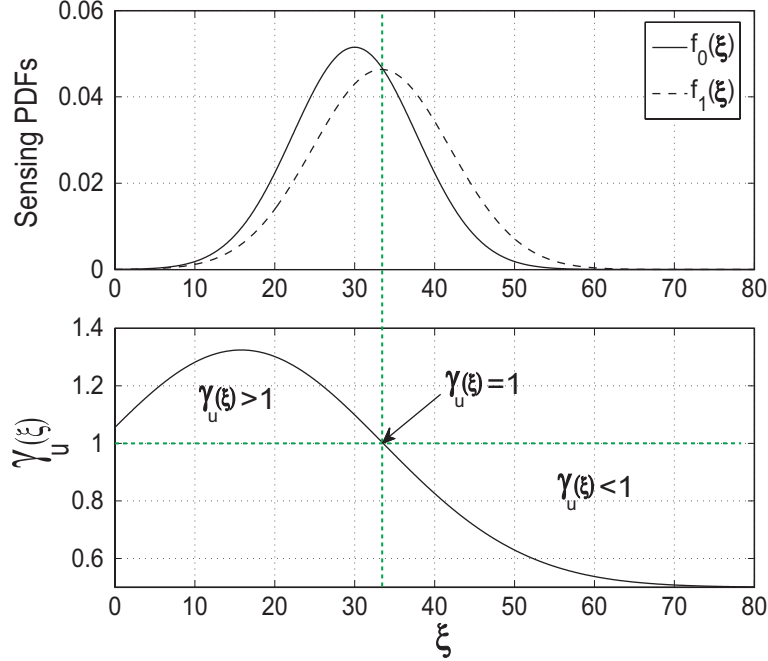
Figure 2.3: Sensing PDFs and $\gamma_{\mathrm{u}}(\xi)$ variations for $N = 30$, $P_{\mathrm{t}} = 1$, $\alpha = 0.5$ and $d_{\mathrm{m}} = 3$.

peak transmit power constraints are still maintained at the considered values for Q_{inter} and Q_{peak}.

Illustration of the ergodic capacity of the SU fading channel and the corresponding optimal Lagrangian multiplier, λ_1, are carried out in Figs. 2.5-2.8.

Figs. 2.5 and 2.6 plot the ergodic capacity of Rayleigh and Log-normal ($\sigma = 6$ dB) fading channels in bits/s/Hz, respectively, versus Q_{inter} and for different values of $\rho = \frac{Q_{\mathrm{peak}}}{Q_{\mathrm{inter}}}$. For comparison purpose, we also illustrate the result pertaining to the case when only the interference limit at the PU (Q_{inter}) is considered. The figures show that for a fixed value of Q_{inter}, as ρ increases (or Q_{peak} increases), the channel capacity increases and converges towards that of the system with no peak transmit-power constraint. In fact, this means that a higher Q_{peak} can be considered as an advantage for the system performance and increases the channel capacity, but after a certain value of ρ, for instance when Q_{peak} is much higher than Q_{inter} ($\rho > 2$), the capacity is only limited by the average interference constraint and does not increase as Q_{peak} increases.

The variation of the Lagrangian multiplier, λ_1, at which the interference constraint in (2.17) is satisfied, is plotted in Figs. 2.7 and 2.8 for the Rayleigh and Log-normal fading cases respectively, as a function of Q_{inter} and for various values of ρ. As observed, for
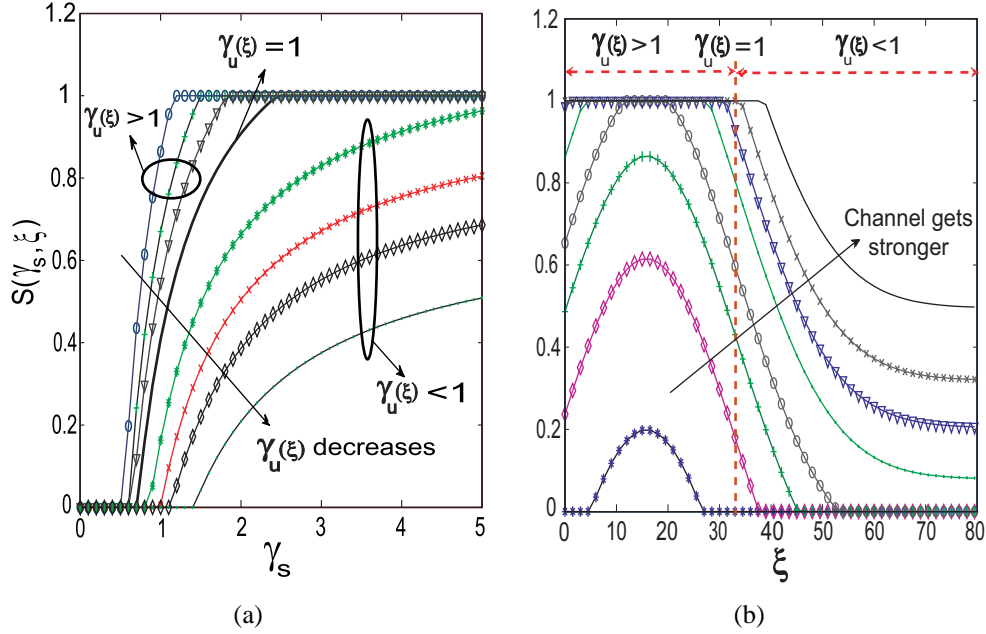
Figure 2.4: Instantaneous transmit power with $Q_{\text{inter}} = -6$ dB and $Q_{\text{peak}} = 0$ dB versus (a) secondary channel variation, γ_{s}, and (b) sensing metric, ξ.

a given value of Q_{inter}, λ_1 increases as the transmit power constraint gets less stringent, and converges towards the case with no peak transmit-power constraint. It is worth noting that considering the thresholds involved in (2.7), the water-filling area, $\frac{\gamma_{\text{v}}(\xi)}{N_0 B} \leq \frac{1}{\gamma_{\text{s}}} \leq \frac{\gamma_{\text{u}}(\xi)}{\lambda_1 N_0 B}$, becomes tighter for higher values of Q_{peak}.

2.1.4.2 Capacity with Adaptive Rate and Power M-*QAM* Policy

Considering adaptive rate and power M-QAM policy, the SU's transmission rate, $R(\gamma_{\text{s}}, \xi)$, is plotted in Fig. 2.9 as a function of the SU's channel variation, γ_{s}, and soft-sensing metric, ξ, for predefined constraint values given by: $Q_{\text{inter}} = -6$ dB, $Q_{\text{peak}} = 0$ dB and $P_{\text{b}} = 10^{-3}$. For clarity, the PDFs $f_1(\xi)$ and $f_0(\xi)$ obtained under the above system assumptions are shown in Fig. 2.9. As observed, the ST adapts to the PU's activity by transmitting at higher rates when the ratio $f_0(\xi)/f_1(\xi)$ increases and vice versa. At the other dimension of Fig. 2.9, the effect of channel gain variation is shown. It is clear that in strong CSI, the ST is able to transmit at higher rate, whereas in weak CSI conditions its transmission rate decreases.

The SU's capacity expression presented in (2.30) for the system using adaptive rate and power policy, is illustrated in Figs. 2.10 and 2.11, as a function of Q_{inter}, for Rayleigh and
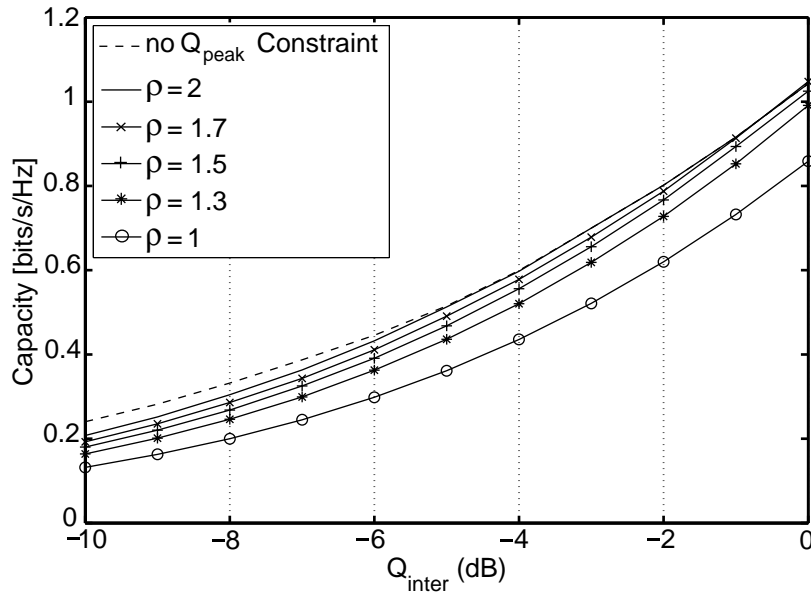
Figure 2.5: Ergodic capacity under adaptive power transmission in Rayleigh fading.
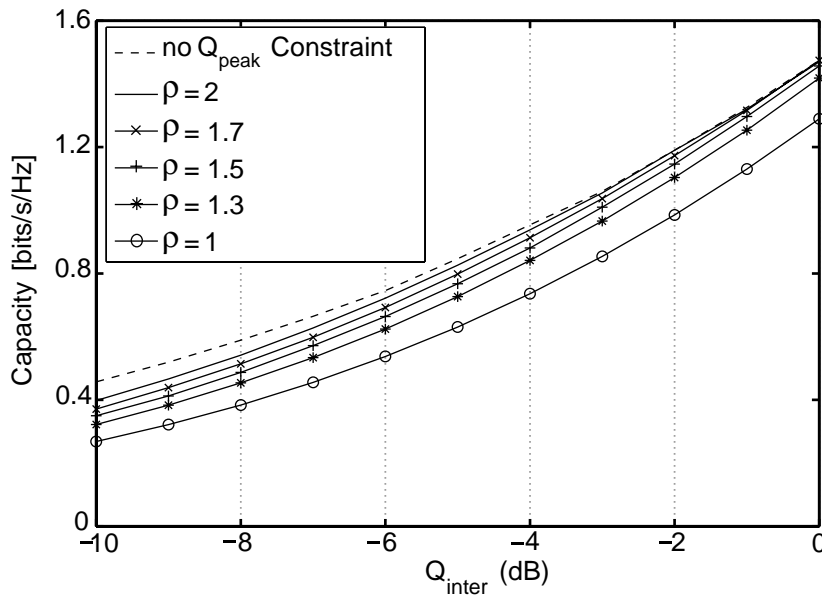
Figure 2.6: Ergodic capacity under adaptive power transmission in Log-normal fading with $\sigma = 6$ dB.
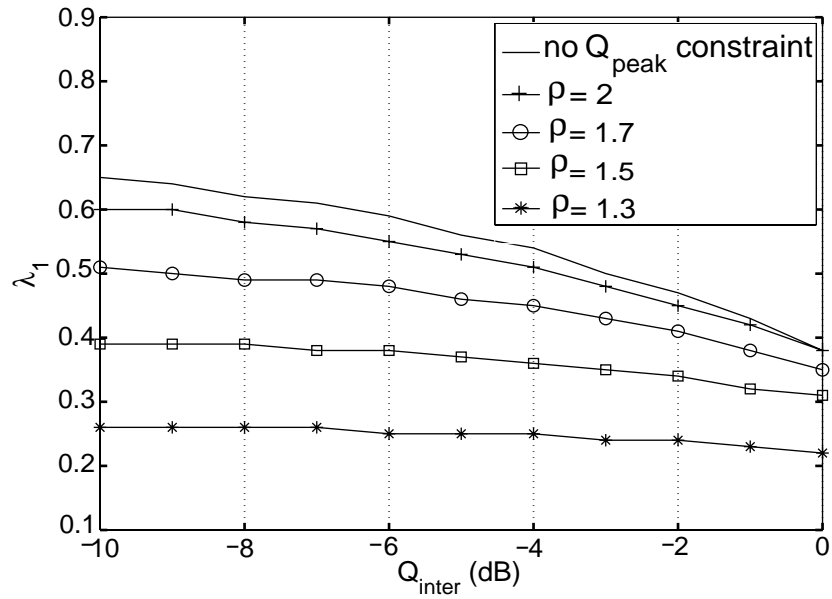
Figure 2.7: Variation of the Lagrangian parameter λ_1 for a Rayleigh fading channel.
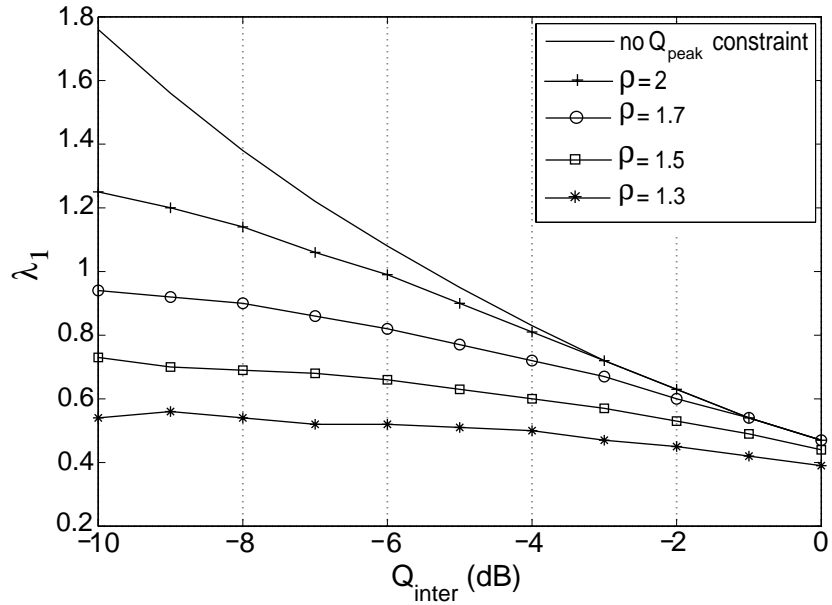
Figure 2.8: Variation of the Lagrangian parameter λ_1 for a Log-normal fading channel with $\sigma = 6$ dB.
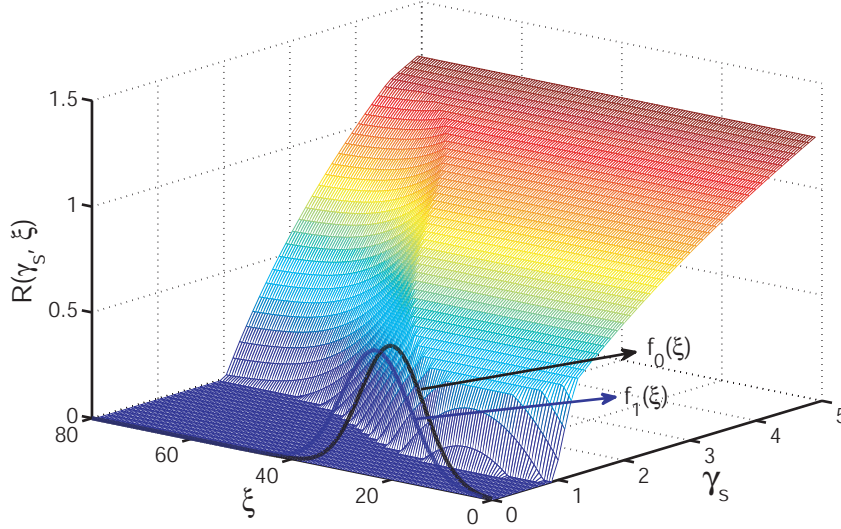
Figure 2.9: Instantaneous transmission rate using M-QAM, versus γ_s and ξ, with $Q_{\mathrm{inter}} = -6$ dB, $Q_{\mathrm{peak}} = 0$ dB and $P_{\mathrm{b}} = 10^{-3}$.

Lognormal ($\sigma = 6$ dB) fading distributions, respectively. We assume BER requirements given by: $P_{\mathrm{b}} = 10^{-2}$ and 10^{-3}. Moreover, we set $\rho = \frac{Q_{\mathrm{peak}}}{Q_{\mathrm{inter}}}$ to 1.7 and, for comparison purpose, we plot the ergodic capacity for the adaptive power strategy (2.18) as well. In these figures, we observe that there is a gap between the capacity results corresponding to (2.30) and (2.18), as discussed in section 2.1.3. The plots also show that this gap increases as the value of Q_{inter} increases and converges to a constant value.

2.1.5 Summary

We considered a CR-based spectrum-sharing system where the secondary user's transmit power and rate can be adjusted based on the secondary channel variations and soft-sensing information about the activity of the PU. The spectrum-sharing system was assumed to operate under constraints on average interference and peak transmit power. In this context, we first obtained the capacity gain offered by the SU's opportunistic access to the spectrum under variable power transmission strategy. Then, we investigated adaptive rate and power transmission approach such that the achievable capacity is maximized under said constraints and predefined BER requirements. Finally, numerical results and comparisons were provided and illustrated the throughput benefits of using soft-sensing information and CSI at the SU in CR systems. In particular, we showed that by using
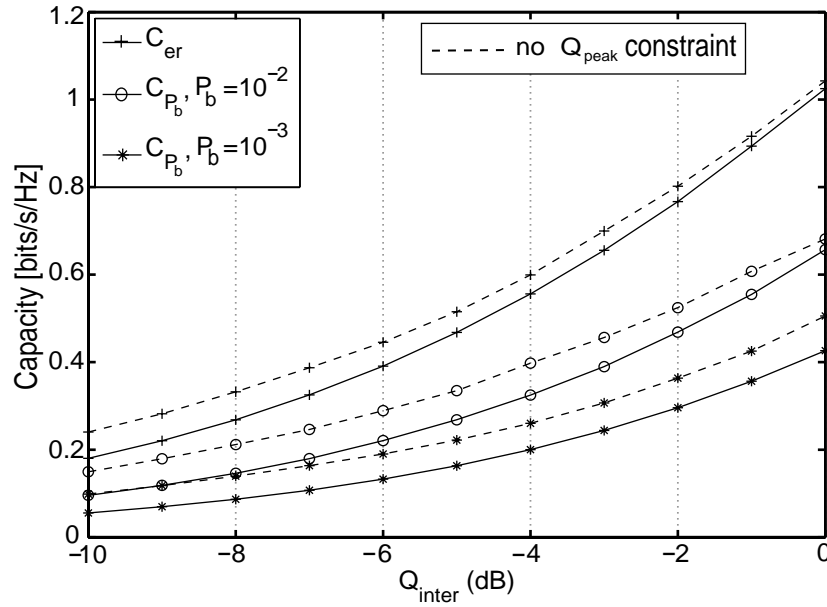
Figure 2.10: Achievable capacity under adaptive rate and power strategy using M-QAM in
Rayleigh fading channel for $\rho = 1.7$.
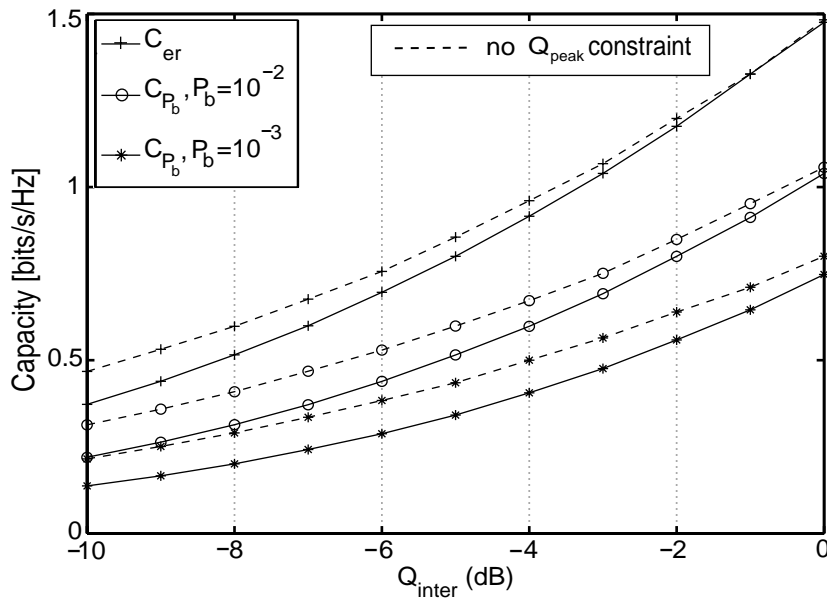
Figure 2.11: Achievable capacity under adaptive rate and power strategy using M-QAM in
Lognormal fading channel ($\sigma = 6$ dB) for $\rho = 1.7$.

soft-sensing technique, the SU may opportunistically control its transmission parameters such as rate and power, according to different PU's activity levels observed by the sensing detector. Moreover, it has been shown that there is a gap between the capacities achieved based on the above adaptive transmission policies.

In the next section, we consider imperfect soft-sensing mechanism at the secondary system and obtain the optimal power transmission policy in terms of false-alarm and detection probabilities and under constraint on the average interference power at the PR. Furthermore, we present a quantized sensing mechanism that considers only some restricted levels of sensing observations.

2.2 Impact of Detection Uncertainties on the Performance of Spectrum Sharing CR Systems

The reason for using sensing information in CR spectrum-sharing systems is to better adapt the transmission resources of the secondary user communications and of course, control the amount of interference caused to the primary system of the spectrum band. Through sensing, CR detects the portions of the spectrum that are available for the cognitive user (SU) at a specific location or time. Using a sensing detector at the secondary transmitter, the SU gets the ability to optimize its transmission power so as to maximize the channel capacity, while adhering to the interference limitations set by the PU.

It is important to note that if the SU fails to detect the PU's activity in the spectrum, harmful interference might occur. To prevent this, two issues must be considered: (i) the SU must control its transmit power such that a relatively low amount of interference affects the primary's communication [22, 53]. This can be addressed by implementing a power transmission policy which changes the transmission parameters adaptively based on the soft-sensing information about the PU's activity in the shared spectrum band as studied in Section 2.1. (ii) the detection mechanism must be able to determine the activity of the PU with sufficient certitude. In this regard, appropriate parameters need to be set, such as the number of sensing samples. In general, the performance of detection techniques is investigated in terms of the probability of detection and probability of false alarm [46]. Please note that the details about the performance of different detection techniques are available in the open literature (see, e.g., [7, 54] and references therein). Hence, in this section, we

consider that said estimation about the PU's activity, which is calculated at the sensing detector, is available to the SU with a predetermined false-alarm and detection probabilities. Specifically, we herein investigate the impact of imperfect spectrum sensing on the performance of CR spectrum-sharing systems in terms of false-alarm and detection probabilities, which can further affect the transmission parameters at the secondary transmitter and also the amount of interference caused to the primary receiver.

In this context, in [55], assuming a state transition model about the PU's channel activity, the effective capacity of CR spectrum-sharing system has been studied in order to assess the effect of false-alarm and detection probabilities on the throughput performance of the CR system under the statistical quality-of-service (QoS) constraints. In [56], the problem of designing the sensing-slot duration to maximize the throughput performance of the SU in a CR network was investigated under constraints on the false-alarm and detection probabilities. On the other hand, considering availability of soft-sensing information about the PU's activity state, the optimal power and rate transmission policies that maximize ergodic capacity of SUs' channels in fading environments, are investigated in Section 2.1. It is worth to note that in the latter section, we considered that the sensing information about the PU's activity is known a priori to the SU (perfect sensing).

In the following, in Section 2.2.1, we consider a CR spectrum-sharing system where the power of the SU is controlled based on soft-sensing information about the PU's activity and CSI pertaining to the secondary link, under a constraint on the average received-interference power at the primary receiver. We further assume an imperfect sensing mechanism at the SU, thus the uncertainty about the PU's activity is expressed by the false-alarm and detection probabilities in the system model. Our contribution, in this section, first consists of investigating the effect of imperfect spectrum sensing on the performance of CR spectrum-sharing in terms of false-alarm and detection probabilities while adhering to the interference limitation of the PU. In particular, in Section 2.2.2, we obtain the optimal power allocation policy that maximizes the ergodic capacity of the CR system under consideration. Then, a quantized sensing mechanism is implemented in Section 2.2.3 and the associated power allocation policy is derived. Numerical results and comparisons illustrating the impact of imperfect sensing information on the achievable capacity of the SU's link subject to the constraint on the average received-interference at the primary receiver, are provided in Section 2.2.4. Finally, concluding remarks and summary are presented in

Section 2.2.5.

2.2.1 Spectrum-Sharing System

Consider a CR spectrum-sharing system with a pair of primary transmitter and receiver (PT and PR), and a pair of secondary transmitter and receiver (ST and SR) operating in the same spectrum band. The SU transmits under a constraint on average interference inflicted at the PR. We consider a discrete-time flat-fading channel with perfect CSI at the receiver and transmitter of the SU. We define the channel gain pertaining to the SU's link by $\sqrt{h}$, and the one between the ST and the PR by $\sqrt{g}$. Channel gains are assumed to be independent and distributed according to a Rayleigh PDF with variances that depend on the distances between the associated nodes ($\frac{1}{d_h^2}$ for $\sqrt{h}$ and $\frac{1}{d_g^2}$ for $\sqrt{g}$). The channel gains are assumed to be stationary, ergodic and mutually independent of the noise.

Regarding the PU transmission strategy, it is assumed that PT transmits in a stationary block-fading channel with coherence time T_c. The PT uses a Gaussian codebook and its activity is assumed to follow a block static model with the duration of a block equal to T_c time epochs. Furthermore, the PU's interference and the additive noise at the SR, are assumed to be zero-mean Gaussian random variables with variances, δ_p^2 and δ_n^2, respectively.

In the spectrum-sharing system under consideration, the ST is equipped with a spectrum-sensing detector which enables evaluating the frequency band used by primary transmissions. In the case that the primary transmission strategy is unknown, energy detection technique is the most suitable method [46]. In this method, using the received signals from the PU, the ST detector calculates a single sensing metric, ξ, based on which the detector has to do a hypothesis test between the noise hypothesis H_0 (PU's activity being in OFF state), and hypothesis H_1 on the joint presence of the primary signal and noise (PU's activity being in ON state). Under the two aforementioned hypotheses, ξ can mathematically be expressed as follows:

$$\xi = \begin{cases} \sum_{n=1}^{N} \left(z[n] \right)^2, & H_0, \\ \sum_{n=1}^{N} \left(\sqrt{\gamma[n]} x[n] + z[n] \right)^2, & H_1, \end{cases} \tag{2.31}$$

where N is the number of observation samples, $\sqrt{\gamma[n]}$ is the channel gain between PT and ST and modeled according to a Rayleigh distribution with unit variance, $x[n]$ denotes the

PT's signal, $z[n]$ indicates the white Gaussian noise with unit variance at the detector, and n is the time sample index. As formulated in the above expression, we consider fast channel fading, i.e., the channel coefficients change at every sample (n). We define the PDF of ξ given that the PT is in OFF or ON states by $f_0(\xi)$ and $f_1(\xi)$, respectively. We assume that these PDFs are available at the ST and modeled as Gaussian distribution functions as detailed in Section 2.2.2. Hence, we choose $f_1(\xi) \sim \mathcal{N}(\mu_1, \delta_1)$ and $f_0(\xi) \sim \mathcal{N}(\mu_0, \delta_0)$ where (μ_1, δ_1^2) are given by $\mu_1 = N(S_p + 1)$ and $\delta_1^2 = 2N(S_p + 1)^2$, and ($\mu_0$, δ_0^2) are given by N and $2N$, respectively, where S_p denotes as the primary average transmit power.

The hypotheses on the activity of the PU imply that PT remains active (H_1) with probability $\Pr(H_1)$, or inactive (H_0) with probability $\Pr(H_0) = 1 - \Pr(H_1)$, in T_c time periods. On the other hand, it has been shown in Section 2.2.2 that the soft variation of the sensing parameter may be used by the ST to adaptively adjust its transmission power and rate. As shown in Section 2.2.2, the effect of sensing information may be reflected through the ratio of sensing PDFs, i.e., $f_0(\xi)/f_1(\xi)$. In this case, the false alarm and detection probabilities can be obtained as follows:

$$P_F(\xi) = \Pr(\eta(\xi) < \varepsilon \,|H_0) , \qquad (2.32)$$

$$P_D(\xi) = \Pr(\eta(\xi) < \varepsilon \,|H_1) , \qquad (2.33)$$

where $\eta(\xi) \triangleq f_0(\xi)/f_1(\xi)$ and ε is the decision threshold. It is worth noting that for the case with soft-sensing detection technique, there is no existing closed-form expressions known for probabilities $P_F(\xi)$ and $P_D(\xi)$, however herein, to present numerical results, we need to consider a specific function for these probability parameters. Hence, in the numerical results section, we assume that $P_F(\xi)$ and $P_D(\xi)$ are varied according to exponential functions, i.e., $P_F(\xi) = \exp(-\eta(\xi))$ and $P_D(\xi) = \exp(-\eta(\xi))$.

In the following, we obtain the optimal power allocation policy that maximizes the ergodic capacity of the spectrum-sharing system under imperfect spectrum sensing.

2.2.2 Ergodic Capacity

Herein, we assume that the CSI and the soft-sensing information (SSI) are available at the ST and SR. The ergodic capacity of a single-user in a time-varying channel is studied in [41]. By considering average transmit power constraint, the ergodic capacity of a

fading channel with CSI at both the transmitter and the receiver is obtained in [40]. The corresponding optimal power allocation is a water-filling strategy over the fading states.

In our case, the ST uses the CSI of the secondary link, h, and the SSI in order to achieve optimum channel capacity under average interference constraint at the PR. Adopting an approach similar to that used in [40], the channel capacity can be shown to be achieved through optimal utilization of the transmit power over time, such that the interference constraint is satisfied. Therefore, considering the aforementioned hypotheses on the activity of the PT, the ergodic capacity (C) in this case represents the solution to the following problem:

$$\frac{C}{B} = \max_{h,\xi} \left\{ \mathrm{E}_{h,\xi} \left[\Pr\left(\eta\left(\xi \right) < \varepsilon, H_1 \right) C_{\mathrm{ON}} \right] + \mathrm{E}_{h,\xi} \left[\Pr\left(\eta\left(\xi \right) > \varepsilon, H_0 \right) C_{\mathrm{OFF}} \right] \right\} \quad (2.34)$$

$$\text{s.t. } \mathrm{E}_{h,\xi,\gamma_{\mathrm{p}}|H_1} \left[\Pr\left(\eta\left(\xi \right) < \varepsilon, H_1 \right) S\left(h,\,\xi \right) g \right] \leq W, \quad (2.35)$$

where C_{ON} and C_{OFF} are defined as

$$C_{\mathrm{ON}} \triangleq \log\left(1 + \frac{S\left(h,\,\xi \right) h}{\delta_{\mathrm{n}}^2 + \delta_{\mathrm{p}}^2} \right), \quad C_{\mathrm{OFF}} \triangleq \log\left(1 + \frac{S\left(h,\,\xi \right) h}{\delta_{\mathrm{n}}^2} \right). \quad (2.36)$$

Please note that in (2.34), $\Pr\left(\eta\left(\xi \right) < \varepsilon, H_1 \right)$ denotes the probability of PT being active and also detected as ON by the sensing detector, and $\Pr\left(\eta\left(\xi \right) > \varepsilon, H_0 \right)$ is the probability of PT being inactive and detected as OFF. Now, from the Bayes' theorem [57], we can express $\Pr\left(\eta\left(\xi \right) < \varepsilon, H_1 \right)$ in terms of the detection probability as

$$\Pr\left(\eta\left(\xi \right) < \varepsilon, H_1 \right) = \Pr\left(\eta\left(\xi \right) < \varepsilon \,|H_1 \right) \Pr\left(H_1 \right)$$
$$= P_{\mathrm{D}}\left(\xi \right) \Pr\left(H_1 \right). \quad (2.37)$$

Then, for the probability $\Pr\left(\eta\left(\xi \right) > \varepsilon, H_0 \right)$, considering the fact that

$$\Pr\left(\eta\left(\xi \right) > \varepsilon \,|H_0 \right) = 1 - \Pr\left(\eta\left(\xi \right) < \varepsilon \,|H_0 \right), \quad (2.38)$$

we can present this probability in terms of the false-alarm probability as follows:

$$\Pr\left(\eta\left(\xi \right) > \varepsilon, H_0 \right) = \Pr\left(\eta\left(\xi \right) > \varepsilon \,|H_0 \right) \Pr\left(H_0 \right)$$
$$= \left(1 - P_{\mathrm{F}}\left(\xi \right) \right) \Pr\left(H_0 \right). \quad (2.39)$$

Thus, the capacity problem in (2.34) can be rewritten as

$$
\frac{C}{B} = \max_{h,\xi} \left\{ \Pr\left(H_1\right) \mathrm{E}_{h,\xi} \left[P_{\mathrm{D}}\left(\xi\right) \log\left(1 + \frac{S\left(h,\,\xi\right)h}{\delta_{\mathrm{n}}^2 + \delta_{\mathrm{p}}^2}\right) \right] \right.
$$
$$
\left. + \Pr\left(H_0\right) \mathrm{E}_{h,\xi} \left[\left(1 - P_{\mathrm{F}}\left(\xi\right)\right) \log\left(1 + \frac{S\left(h,\,\xi\right)h}{\delta_{\mathrm{n}}^2}\right) \right] \right\}, \tag{2.40}
$$

and the constraint in (2.35) becomes

$$
\mathrm{E}_{h,\xi|H_1} \left[\Pr\left(H_1\right) P_{\mathrm{D}}\left(\xi\right) S\left(h,\,\xi\right) \right] \leq W', \tag{2.41}
$$

where $W' = W d_{\mathrm{p}}^2$.

To find the optimal power allocation, $S\left(h,\,\xi\right)$, we adopt the Lagrangian optimization technique [52]. First, we form the Lagrangian objective function, $J(S\left(h,\,\xi\right),\lambda)$, for the optimization problem defined in (2.40) subject to constraint in (2.41), whose derivative with respect to $S\left(h,\,\xi\right)$ can be obtained as

$$
\frac{\partial J(S\left(h,\,\xi\right),\lambda)}{\partial S\left(h,\,\xi\right)} = \frac{\Pr\left(H_1\right) P_{\mathrm{D}}\left(\xi\right) h}{\delta_{\mathrm{n}}^2 + \delta_{\mathrm{p}}^2 + S\left(h,\,\xi\right) h} f_1\left(\xi\right) + \frac{\Pr\left(H_0\right)\left(1 - P_{\mathrm{F}}\left(\xi\right)\right) h}{\delta_{\mathrm{n}}^2 + S\left(h,\,\xi\right) h} f_0\left(\xi\right)
$$
$$
- \lambda \Pr\left(H_1\right) P_{\mathrm{D}}\left(\xi\right) f_1\left(\xi\right), \tag{2.42}
$$

where λ denotes the Lagrangian multiplier. For the optimization problem defined in (2.40), the first order KKT conditions are necessary and sufficient for optimality as explained in [52]. Thus, the optimal power allocation policy should satisfy $\partial J(S\left(h,\,\xi\right),\lambda)/\partial S\left(h,\,\xi\right) = 0$ with the constraint $S(h,\xi) > 0$, which yields:

$$
S\left(h,\,\xi\right) = \left(\frac{\psi^+\left(\xi\right)}{2\lambda} - \frac{\left(2\delta_{\mathrm{n}}^2 + \delta_{\mathrm{p}}^2\right)}{2h} + \frac{1}{2\lambda h} \sqrt{\left(\delta_{\mathrm{p}}^2 \lambda\right)^2 + 2\delta_{\mathrm{p}}^2 \lambda \psi^-\left(\xi\right) h + \left(\psi^+\left(\xi\right) h\right)^2} \right)^+, \tag{2.43}
$$

where $(\cdot)^+$ denotes $\max\{\cdot, 0\}$ and $\psi^{\pm}\left(\xi\right)$ is defined as

$$
\psi^{\pm}\left(\xi\right) \triangleq 1 \pm \frac{\Pr\left(H_0\right)\left(1 - P_{\mathrm{F}}\left(\xi\right)\right)}{\Pr\left(H_1\right) P_{\mathrm{D}}\left(\xi\right)} \eta\left(\xi\right). \tag{2.44}
$$

Finally, substituting the power allocation policy (2.43) into (2.40) yields the ergodic capac-

ity formula pertaining to the SU's link. It is worth to note that the parameter λ is determined such that the average received interference constraint in (2.41) is set to equality.

2.2.3 Quantized Sensing Information

It has been shown that the variation of the sensing parameter, ξ, can be utilized at the ST to adaptively adjust the transmission resources to better manage the transmission power budget and control the interference generated at the PU. However, it is difficult in practice to continuously change the transmission power according to the instantaneous variation of calculated sensing information. Moreover, in collaborative sensing techniques between the secondary nodes [58], significant overhead is needed for the information exchange feedback between the SUs. Thus, in the following, we propose using the discrete sensing technique where only discrete levels of the sensing information are considered.

As shown in (2.43), the effect of SSI is reflected through parameter $\eta(\xi)$. We will show that such quantization may be applied to parameter $\eta(\xi)$ which is simply the ratio of the sensing PDFs provided at the sensing detector. It is easy to show that $\eta(\xi) = 1$ is a threshold value that indicates the transition between higher and lower PU activity levels determined by the detection mechanism (See Section 2.1.4). This threshold can be considered as a decision criterion for the PU's activity between ON and OFF states.

So, we may restrict the parameter $\eta(\xi)$ to L discrete levels $\bar{\eta}[l]$ with $l = 1, 2, \cdots, L$, when it falls into the interval Ω_ξ defined by

$$\Omega_\xi : \left\{ \frac{l-1}{L}\eta_{\max} < \eta(\xi) \le \frac{l}{L}\eta_{\max}, \ \forall\, l = 1, \cdots, L \right\}, \tag{2.45}$$

where $\eta_{\max}$ denotes the maximum value of $\eta(\xi)$. Now, without loss of generality, considering the L-ary uniform quantization level of $\eta(\xi)$ [59], it can be shown that the l-th discrete level $\bar{\eta}[l]$ can be calculated according to $\bar{\eta}[l] = (2l - 1/2L)\eta_{\max}, \ \forall\, l = 1, \cdots, L$; if $\eta(\xi) \in \Omega_\xi$. In this context, the false-alarm and detection probabilities may be redefined as $\bar{P}_{\mathrm{F}}[l] = \mathrm{Pr}\left(\bar{\eta}[l] < \varepsilon\,|H_0\right)$ and $\bar{P}_{\mathrm{D}}[l] = \mathrm{Pr}\left(\bar{\eta}[l] < \varepsilon\,|H_1\right)$, respectively.

By substituting $\bar{\eta}[l]$ into (2.43), we obtain the power allocation policy under discrete

sensing information as,

$$
\bar{S}_h\left[l\right] = \left(\frac{\bar{\psi}^+\left[l\right]}{2\lambda} - \frac{\left(2\delta_{\mathrm{l}}^2 + \delta_{\mathrm{p}}^2\right)}{2h} + \frac{1}{2\lambda h}\sqrt{\left(\delta_{\mathrm{p}}^2\lambda\right)^2 + 2\delta_{\mathrm{p}}^2\lambda\bar{\psi}^-\left[l\right]h + \left(\bar{\psi}^+\left[l\right]h\right)^2} \right)^+,
$$

$$(2.46)$$

where $\bar{\psi}^\pm\left[l\right]$ is given by

$$
\bar{\psi}^\pm\left[l\right] \triangleq 1 \pm \frac{\Pr\left(H_0\right)\left(1 - \bar{P}_{\mathrm{F}}\left[l\right]\right)}{\Pr\left(H_1\right)\bar{P}_{\mathrm{D}}\left[l\right]}\bar{\eta}\left[l\right].
$$

$$(2.47)$$

In the power allocation policy shown in (2.46), the lagrangian parameter λ must satisfy the average interference constraint at equality, as follows:

$$
W' = \Pr\left(H_1\right) \times \mathrm{E}_h\left[\sum_{l\in\Theta}\beta\left[l\right]\bar{P}_{\mathrm{D}}\left[l\right]\bar{S}_h\left[l\right]\right],
$$

$$(2.48)$$

where $\Theta = \{l \,|\, \bar{\eta}\left[l\right] \leq 1,\, l = 1, 2, \cdots, L\}$, and $\beta[l]$ is the discrete PDF corresponding to the l-th level of the discrete sensing information which must satisfy $\sum_{1\leq l\leq L}\beta\left[l\right] = 1$.

Finally, the achievable capacity under the discrete sensing assumption can be obtained by rewriting (2.40) as

$$
\begin{aligned}
\frac{\bar{C}}{B} &= \Pr\left(H_1\right) \times \mathrm{E}_h\left[\sum_{1\leq l\leq L}\beta\left[l\right]\bar{P}_{\mathrm{D}}\left[l\right]\log\left(1 + \frac{\bar{S}_h\left[l\right]h}{\delta_{\mathrm{n}}^2 + \delta_{\mathrm{p}}^2}\right)\right] \\
&\quad + \Pr\left(H_0\right) \times \mathrm{E}_h\left[\sum_{1\leq l\leq L}\beta\left[l\right]\left(1 - \bar{P}_{\mathrm{F}}\left[l\right]\right)\log\left(1 + \frac{\bar{S}_h\left[l\right]h}{\delta_{\mathrm{n}}^2}\right)\right].
\end{aligned}
$$

$$(2.49)$$

2.2.4   Numerical Results

We now present numerical results for the ergodic capacity of the SU's channel and the corresponding power allocation policy under the constraint on the average received interference at the PR. In our simulations, we assume that the primary and secondary transmitters and receivers are located such that $d_h = d_g = 1$. We further assume that the probability of the PU remaining active is $\Pr(H_1) = 0.5$. As shown in Fig. 2.12, we consider the sensing PDFs to be Gaussian with mean and variances presented in Section 2.2.1 in terms of the

PU's transmit power, S_p, and the number of sensing samples, N. In Fig. 2.12, by setting $S_\mathrm{p} = 1$ and $N = 30$, we also plot the variation of the parameter $\eta(\xi)$ which is defined as the ratio of the sensing PDFs. In this regard, in Fig. 2.13, we model the variation of the false-alarm probability, $P_\mathrm{F}(\xi)$, and investigate the effect of the parameters S_p and N on the false-alarm probability. From Fig. 2.13-a, we observe that when S_p has unit value, the false-alarm probability decreases as long as the number of sensing samples, N, increases and that for different values of ξ. On the other hand, in Fig. 2.13-b, we observe that when we set $N = 30$, higher values of S_p provide a better resolution at the SU about the activity of the PU in the same spectrum band. Please note that in all the results presented hereafter, we assume $\delta_\mathrm{n}^2 = 1$ and $\delta_\mathrm{p}^2 = 0.5$.

In Fig. 2.14, we illustrate the variations of the instantaneous received-SNR at the SR and received-interference at the PR, for $W = -2$ dB, $N = 30$ and $S_\mathrm{p} = 1$. We observe that using CSI and SSI at the ST, the SU's transmit power can be adjusted adaptively according to the variation of $\eta(\xi)$ and h, such that the average received-interference at the PR remains under a specific limit. As observed from Fig. 2.14, the instantaneous SNR and interference at the SR and PR, respectively, increase as the parameter $\eta(\xi)$ has ascensional behavior and vice-versa. At the other dimension of Fig. 2.14, the effect of channel gain variation is shown. It is clear that in weak CSI the secondary transmitter prefers to be silent, whereas in strong CSI conditions its power increases, unless the interference constraint is more stringent than the transmit power.

Fig. 2.15 plots the achievable capacity in bits/s/Hz under $L = 8$ levels of quantization, versus the number of sensing samples N and for different values of W and S_p. We observe that the achievable capacity increases as the number of sensing samples increases. Also, for a fixed number of N, the capacity has an increasing behavior as the interference limit (W) and the transmit power S_p increase.

Fig. 2.16 investigates the achievable capacity of the spectrum-sharing system under consideration as a function of the average interference constraint, W. Specifically, we set $N = 30$ and $S_\mathrm{p} = 1$ and plot the achievable capacity in bits/sec/Hz for different levels of quantization, L. As observed, the achievable capacity increases as the interference limit at the PR increases. Moreover, for a fixed value of W, we observe that the quantized sensing approach reduces the achievable capacity of the SU as the number of levels L decreases.
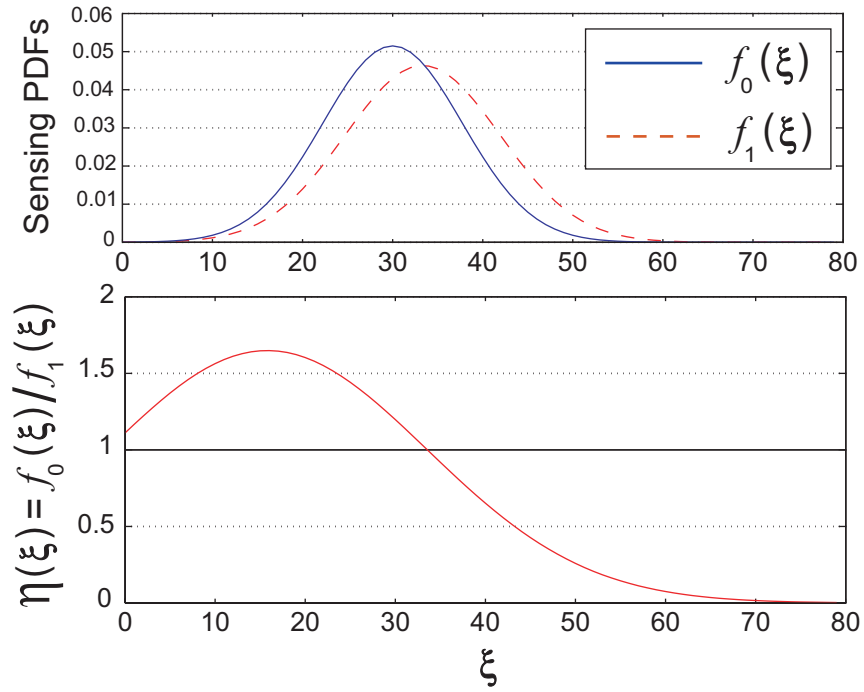
Figure 2.12: Sensing PDFs and variations of $\eta(\xi)$ for $S_{\mathrm{p}} = 1$ and $N = 30$.
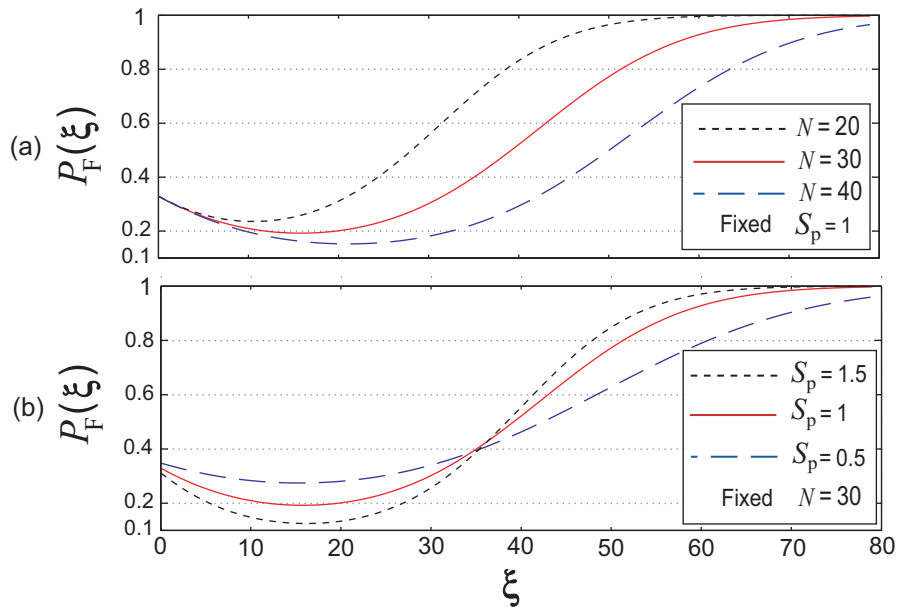
Figure 2.13: False-alarm probability variations for different levels of N and S_{p}.
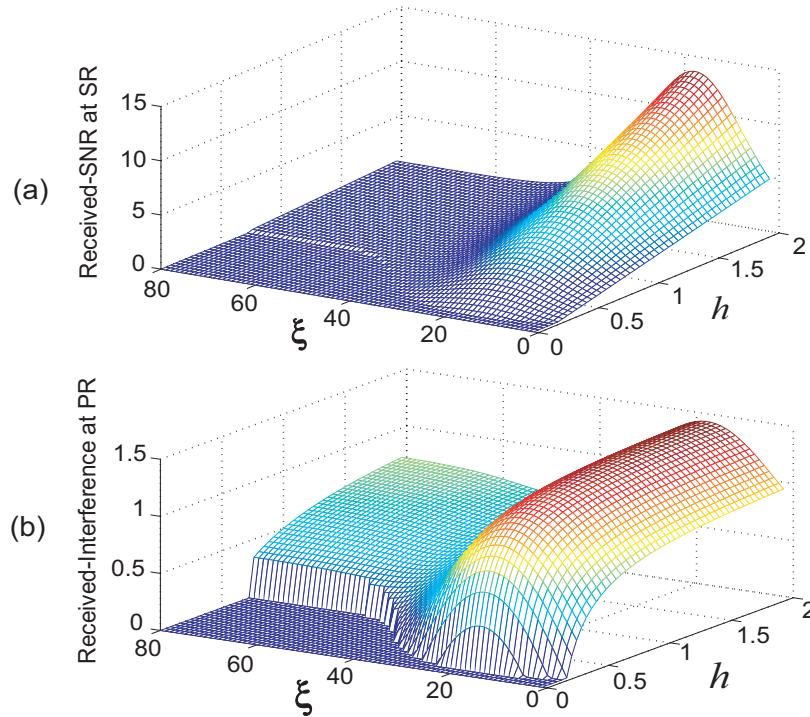
Figure 2.14: (a) Instantaneous received-SNR at the SR and (b) instantaneous received-interference at the PR, for $W = -2$ dB.

2.2.5 Summary

In this section, we considered a spectrum-sharing system where the SU's transmit power can be adjusted based on the soft-sensing information of the PU's activity. We characterized the uncertainty of the sensing information calculated at the sensing detector by taking into account predetermined false-alarm and detection probabilities in the system model. The CR system was limited by appropriate constraint on the average received-interference at the primary receiver. In this context, closed-form expression for the optimal power transmission has been derived in terms of false-alarm and detection probabilities such that the achievable capacity of the SU channel is maximized. Furthermore, in order to reduce the overall system complexity at the SU, we restricted the soft-sensing information about the PU's activity to limited activity levels. Numerical results and comparisons illustrated the performance of the CR system under imperfect sensing information. The investigated results have shown an improvement in the SU's performance as the uncertainty about the sensing information increases.

In the next chapter, we investigate different capacity notions in CR systems where the
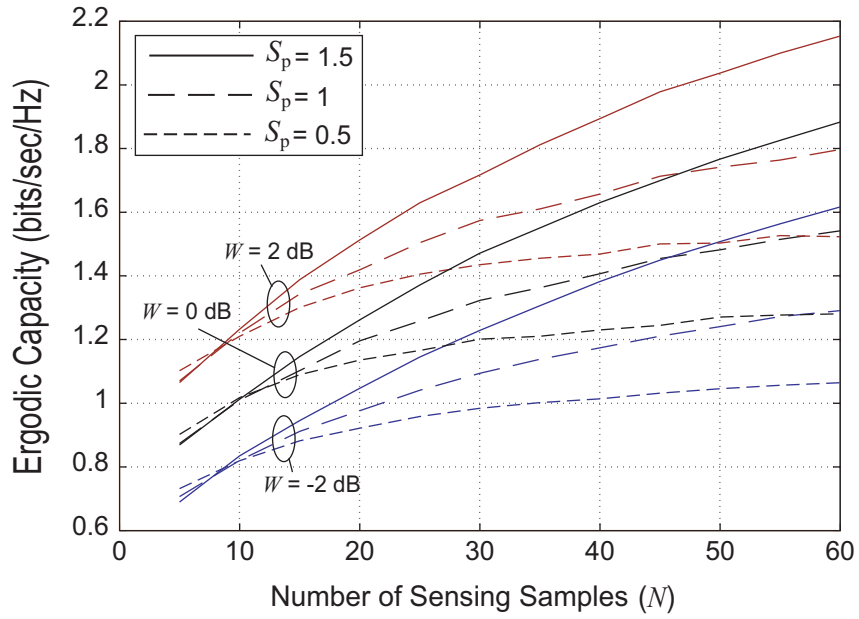
Figure 2.15: Achievable capacity of spectrum-sharing system with $L = 8$ quantization levels versus the number of sensing samples for different values of W and S_{p}.
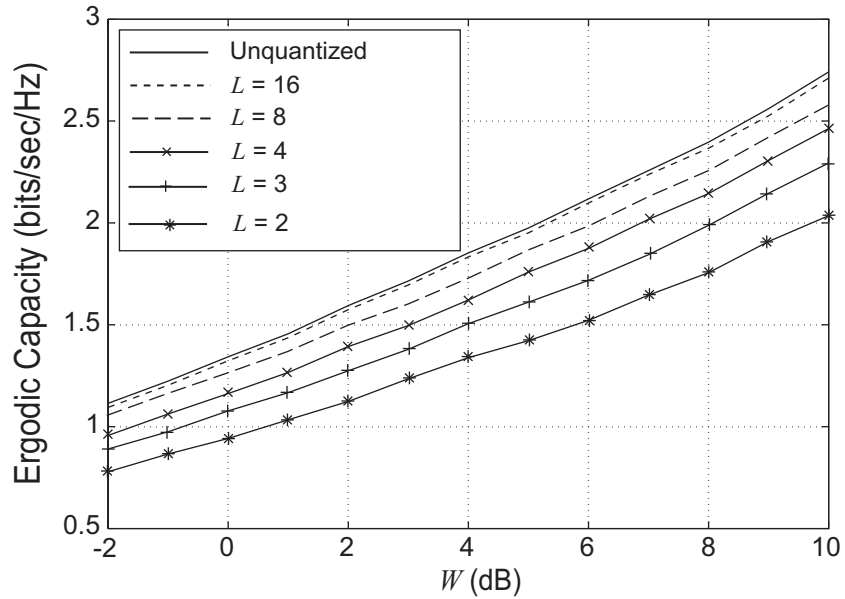
Figure 2.16: Achievable capacity of spectrum-sharing system as a function of W for different quantization levels, L.

transmission parameters of the cognitive users are adaptively changed based on the avail-ability of CSI pertaining to the SU link, and soft-sensing information about the activity of the licensed-band PU. Assuming the above considerations in a CR system operating under average received-interference and peak transmit-power constraints, we study three capacity notions of spectrum-sharing fading channels – namely, *ergodic*, *delay-limited* and *service-rate* with/without *outage* – and obtain the corresponding power allocation policies.

Chapter 3

Service-Oriented Capacity of Spectrum Sharing CR Systems[1]

3.1 Introduction

Reusing the licensed spectrum by unlicensed users is the main idea in CR technology to make use of the under-utilized spectrum bands in wireless communication systems [60]. A typical CR scenario includes several cognitive users (secondary users) that communicate over the same spectrum band originally assigned to existing licensed users (primary users). In this scenario, two important issues must be considered to avoid performance degradation for the PUs and maximize the throughput performance of SUs: (*i*) the aggregate interference at the primary receivers (PRs) [14], and (*ii*) the activity level of PUs in the shared spectrum band [9, 14].

As mentioned earlier in Chapter 1.1.3, using the appropriate capacity metric for performance analysis and design of CR systems is of great importance. Usually, ergodic capacity is used as a long-term throughput measure in these systems [20]. The ergodic capacity is the maximum average achievable rate over all fading states without any constraint on delay. Hence, the achievable transmission rate under an ergodic capacity transmission strategy could be very low or even zero in severe fading conditions. However, in CR systems, by imposing constraints on the interference generated by the cognitive users while adhering

---

[1]Parts of this chapter were accepted for publication at *IET Communications, Special Issue on: Cognitive Communications*, pp. 1 – 13, May 2011.

to the PUs' activity levels, it is obvious that some percentage of outage is unavoidable, whereas in many non-cognitive communication systems some level of outage can be tolerated [50]. Hence, for delay-sensitive applications, delay-limited capacity (also referred to as zero-outage capacity) [21], is a more appropriate metric. In delay-limited capacity, using *channel inversion* technique [40], the SU can transmit at higher power levels in weak channel states to guarantee a constant rate at the receiver all the time. In this regard, the delay-limited capacity of spectrum-sharing systems under different types of power constraints, was investigated in [22] and [23], considering availability of the CSI pertaining to the SU link and the one corresponding to the interference channel between the secondary transmitter (ST) and PR, both at the ST. Numerical results presented in the latter work, have shown that the delay-limited throughput does not guarantee reliable communication.

On the other hand, in many real-time applications, the required rate is not necessarily constant. For example, in wireless systems where a specific rate is needed for voice communication, any excess rate can be used for other applications. Motivated by this fact, the service-rate based capacity notion was proposed in [24, 25]. In particular, in CR systems where the transmission is limited by the PUs' activity, it is desirable for the SUs to fully utilize the radio resources while they have access to the shared spectrum band. In this regard, in [22], the service-rate capacity is investigated in a spectrum-sharing system considering availability of the secondary CSI and information about the interference channel (between ST and PR), at the ST. It is noteworthy that said availability of the CSI pertaining to the interference channel may not always be a practical assumption for CR systems. For instance, in the CR WRAN standard, namely IEEE 802.22 [3], the TV broadcast channels provide the transmission medium for CR applications [43]. Hence, in this standard, knowledge about the interference channel between the ST and the PR, i.e., TV receivers, is hard to obtain by the secondary party.

Furthermore, CR has the ability of sensing the environment in which it operates and consequently adapts the transmission parameters such as rate, power, etc., according to the radio resource variations in time and space [14]. Specifically, this capability can be utilized in CR networks such as wireless regional area network (WRAN) [3]. The sensing ability is provided by the sensing detector, mounted at the SU's equipment, which scans the spectrum band for a specific time. Then, the activity statistics of the PU's signal in the shared spectrum band is calculated [8]. According to this soft-sensing information, if

the presence of PU is not probable, this will imply a safe opportunity for SUs to occupy the licensed spectrum band. Indeed, the sensing metric can be used by the ST to adjust its transmission parameters for a better management of its power resources and the generated interference, as described in this work[2]. In this context, soft-sensing information about the PU activity has been utilized in Chapter 2 and [8] to adaptively control the transmission power at the SU transmitter. Specifically, using soft-sensing information about the PU's activity states and also CSI of the secondary link, the outage capacity lower-bound of the SU in Rayleigh fading channels, is investigated in [8], under received-interference and peak transmit-power constraints. Note that, in order to facilitate the investigation of the effects of sensing information on the CR power transmission policy, the interference caused at the secondary receiver due to the PU transmission, was assumed to be negligible in Chapter 2 and [8].

In this chapter, we consider a CR wireless communication system where the power of the ST is controlled based on *soft-sensing information* (SSI) about the PU's activity states, and CSI pertaining to the secondary link. It is worth noting that a specific distribution to model the primary link interference at the SU receiver is considered in this chapter. The considered system is subject to constraints on the average interference at the PR (hereafter referred to as interference constraint) and on the peak transmit power of the ST. Considering these two constraints, we first study the ergodic capacity of the SU's link in fading environments and derive the associated optimal power allocation policy. Then, we obtain the power allocation policy under outage probability constraint, and investigate the achievable capacity with such transmission policy in fading environments. Finally, we propose the service-rate capacity as a service-based capacity notion for CR networks that not only provides a minimum constant rate for cognitive users, but also increases the average long-term achievable rate of the secondary communication link through utilization of the available excess power. Note that in this chapter, the service-rate capacity with and without outage constraint, are both addressed.

In the following, the spectrum-sharing system and channel models are described in section 3.2. Then, the ergodic capacity of the SU's fading channel is presented in section 3.3. In section 3.4, we investigate the delay-limited capacity of fading channels under the above-mentioned system considerations and resource constraints. The service-rate based

---

[2]More details about the soft spectrum sensing technique will be provided later in the manuscript.

capacity of fading channels for the system under study is then provided in section 3.5. Numerical results followed by concluding remarks and summary are presented in sections 3.6 and 3.7, respectively.

3.2   Spectrum-Sharing System and Channel Models

We consider a spectrum-sharing system with a pair of primary/secondary transceivers, namely, (PT, PR) and (ST, SR), as shown in Fig. 3.1. The SU is allowed to use the spectrum occupied by the PU as long as it adheres to the predefined interference limit at the PR. The link between ST and SR is assumed to be a discrete-time flat fading channel with instantaneous gain $\sqrt{\gamma_s}$. Herein, we assume that perfect knowledge of $\sqrt{\gamma_s}$ is available at the SR and provided to the ST through a no-delay error-free feedback channel. The channel gain between ST and PR is defined by $\sqrt{\gamma_p}$, and the one between PT and ST by $\sqrt{\gamma_m}$. Channel power gains, γ_s, γ_p and γ_m are independent. We assume γ_s has unit-mean distribution[3], and consider exponential distributions for γ_p and γ_m with means that depend on the distances between the associated nodes ($\frac{1}{d_p^2}$ for γ_p and $\frac{1}{d_m^2}$ for γ_m). Moreover, the PU's interference and the additive noise at the SR, are considered as two zero-mean Gaussian random variables with different variances, δ_p^2 and δ_n^2, respectively.

As for the PU's link, we consider a stationary block-fading channel with coherence time T_c. It is also assumed that the PT uses a Gaussian codebook with average transmit power P_t, and that the PU's activity follows a block-static model with T_c block period[4]. This implies that the PT remains inactive (OFF state) with probability α or active (ON state) with probability $\bar{\alpha} = 1 - \alpha$, in T_c time periods.

A spectrum sensing detector (Fig. 3.1) is mounted on the ST to assess the PU's activity state in the shared spectrum band. The sensing detector scans the frequency band originally assigned to the PU, and calculates a single sensing metric, ξ[5]. We consider that the statistics of ξ conditioned on the PU's activity being in ON or OFF state, are known a priori to the SU's transmitter. We define the PDF of ξ given that the PT is ON or OFF by $f_1(\xi)$ and

---

[3]The expressions derived hereafter can be applied for any fading distribution. In the numerical results section, however, we will assume $\sqrt{\gamma_s}$ to be distributed according to Rayleigh, Nakagami and Lognormal functions.

[4]As detailed in Chapter 2.1.1.1, the importance of the PU block activity period is for the sensing mechanism.

[5]See Appendix A.1.
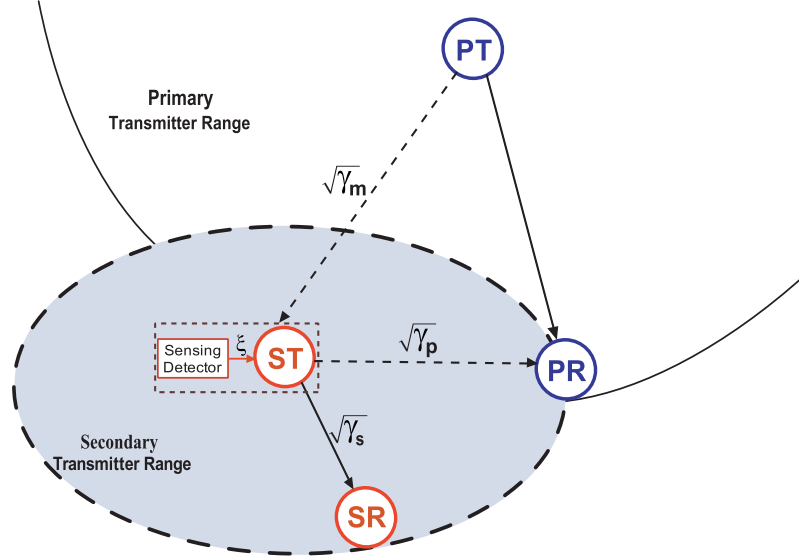
Figure 3.1: Spectrum-sharing system model.

$f_0(\xi)$, respectively.

Notice that conditioned on the PT being ON or OFF, ξ is a sum of i.i.d. random variables and distributed according to Chi-square PDF with N degrees of freedom, where N is the number of observation samples in each sensing interval [45]. Accordingly, under "PU is ON" condition, ξ follows a noncentral Chi-square distribution with variance $\delta^2 = 1$ and non-centrality parameter μ [6] [61]:

$$f_1(\xi) = \frac{1}{2}\left(\frac{\xi}{\mu}\right)^{\frac{N-2}{4}} e^{-\frac{\mu+\xi}{2}} I_{N/2-1}\left(\sqrt{\mu\xi}\right), \qquad (3.1)$$

where $I_\nu(\cdot)$ is the νth-order modified Bessel function of the first kind [51]. Similarly, under the "PU is OFF" condition, ξ will be distributed according to central Chi-square PDF given by:

$$f_0(\xi) = \frac{1}{2^{N/2}\Gamma(N/2)}\xi^{N/2-1}e^{-\frac{\xi}{2}}, \qquad (3.2)$$

where $\Gamma(\cdot)$ is the Gamma function [51]. These sensing statistics can be used by the ST to optimally adjust its transmit power while satisfying the interference constraint at the PR. Given that transmission pertaining to the SU should not harm the communication process

---

[6]Note that μ can be obtained in terms of the ratio of PT's signal energy to noise spectral density, as detailed in [45].

of the PU, we impose constraints on (i) the average interference-power inflicted at the PU's receiver when the PU is ON, and (ii) the peak transmit-power of the SU. These constraints are defined as

$$\mathrm{E}_{\gamma_{\mathrm{s}}, \xi, \gamma_{\mathrm{p}}} \left[S(\gamma_{\mathrm{s}}, \xi)\gamma_{\mathrm{p}} \middle| \mathrm{PU\ is\ ON} \right] \leq Q_{\mathrm{inter}}, \tag{3.3}$$

$$S(\gamma_{\mathrm{s}}, \xi) \leq Q_{\mathrm{peak}}, \quad \{\forall\ \gamma_{\mathrm{s}}, \gamma_{\mathrm{p}}, \xi\}, \tag{3.4}$$

where $S(\gamma_{\mathrm{s}}, \xi)$ is the transmit power of the SU, and Q_{inter}, Q_{peak} denote the interference and peak power limit values, respectively. Furthermore, $\mathrm{E}_{\gamma_{\mathrm{s}}, \xi, \gamma_{\mathrm{p}}}[\cdot]$ defines the expectation over the joint PDF of random variables γ_{s}, ξ and γ_{p}.

Hereafter, we investigate the ergodic capacity (C_{er}), delay-limited capacity (C_{out}) and service-rate capacity (C_{ser}) of the SU's fading channel taking into account the above presented resource constraints.

3.3 Ergodic Capacity

The ergodic capacity of single-user time-varying channel is studied in [41]. Considering the average transmit power to be constrained, the ergodic capacity of a fading channel with CSI at both the transmitter and the receiver is obtained in [40]. The corresponding optimal power allocation is a water-filling strategy over the fading states. Using water-filling, the capacity of fading channels subject to peak and average transmit power constraints is derived in [42], which shows that a multiplexed Gaussian codebook with optimally allocated power in time, such that both constraints are satisfied, can achieve the ergodic capacity.

The capacity of fading channels in a spectrum-sharing system is limited by the interference and transmit power constraints in a dedicated channel bandwidth. In our case, the secondary transmitter uses the CSI of the secondary link and soft-sensing information in order to achieve optimum channel capacity under interference (3.3) and peak transmit-power (3.4) constraints. Considering availability of SSI about the PU's activity and CSI pertaining to the secondary link at the ST, the ergodic capacity of the SU's link in fading environment under interference and peak transmit power constraints represents the solution

to the following problem:

$$\frac{C_{\text{er}}}{B} = \max_{S(\gamma_{\text{s}},\xi)} \left\{ \mathrm{E}_{\gamma_{\text{s}},\xi} \left[\alpha \log \left(1 + \frac{S\left(\gamma_{\text{s}},\,\xi\right)\gamma_{\text{s}}}{\delta_{\text{n}}^2} \right) \right] + \mathrm{E}_{\gamma_{\text{s}},\xi} \left[\overline{\alpha} \log \left(1 + \frac{S\left(\gamma_{\text{s}},\,\xi\right)\gamma_{\text{s}}}{\delta_{\text{n}}^2 + \delta_{\text{p}}^2} \right) \right] \right\},$$
$$\text{s.t.} \ (3.3) \text{ and } (3.4),$$

(3.5)

where $\max_{S(\gamma_{\text{s}},\xi)} \{\cdot\}$ denotes maximization over the secondary transmit power $S\left(\gamma_{\text{s}},\,\xi\right)$.

To find the optimal power allocation under the constraints in (3.3) and (3.4), we adopt the Lagrangian optimization approach presented in [52]. Thus, the Lagrangian objective function, L_{C}, of the maximization problem in (3.5) can be expressed according to (3.6), where λ_1^{er}, $\lambda_2^{\text{er}}(\gamma_{\text{s}},\xi)$ and $\lambda_3^{\text{er}}(\gamma_{\text{s}},\xi)$ are the Lagrangian parameters.

$$
\begin{aligned}
L_{\text{C}} \left[S\left(\gamma_{\text{s}},\xi\right), \lambda_1^{\text{er}}, \lambda_2^{\text{er}}\left(\gamma_{\text{s}},\xi\right), \lambda_3^{\text{er}}\left(\gamma_{\text{s}},\xi\right) \right] &= \mathcal{E}_{\gamma_{\text{s}},\xi} \left[\alpha \log \left(1 + \frac{S\left(\gamma_{\text{s}},\,\xi\right)\gamma_{\text{s}}}{\delta_n^2} \right) \right] \\
&+ \mathrm{E}_{\gamma_{\text{s}},\xi} \left[\overline{\alpha} \log \left(1 + \frac{S\left(\gamma_{\text{s}},\,\xi\right)\gamma_{\text{s}}}{\delta_{\text{n}}^2 + \delta_{\text{p}}^2} \right) \right] \\
&- \lambda_1^{\text{er}} \left(\mathrm{E}_{\gamma_{\text{s}},\xi|\text{PU is ON}} \left[S\left(\gamma_{\text{s}},\,\xi\right) - Q_{\text{inter}} d_{\text{p}}^2 \right] \right) \\
&+ \int_0^\infty \!\!\! \int_0^\infty \lambda_2^{\text{er}}\left(\gamma_{\text{s}},\,\xi\right) S\left(\gamma_{\text{s}},\,\xi\right) d\gamma_{\text{s}} d\xi \\
&- \int_0^\infty \!\!\! \int_0^\infty \lambda_3^{\text{er}}\left(\gamma_{\text{s}},\,\xi\right) \left(S\left(\gamma_{\text{s}},\,\xi\right) - Q_{\text{peak}} \right) d\gamma_{\text{s}} d\xi.
\end{aligned}
$$

(3.6)

It is easy to show that L_{C} is a concave function of $S(\gamma_{\text{s}},\xi)$ and that the interference constraint (3.3) is convex. Taking the derivative of L_{C} with respect to $S(\gamma_{\text{s}},\xi)$ and setting it to zero yields (3.7) under the necessary KKT conditions (corresponding to the resource

constraints (3.3) and (3.4)) given by (3.8)-(3.10).

$$\left(\alpha \frac{\gamma_{\mathrm{s}} f_0 \left(\xi \right)}{\delta_{\mathrm{n}}^2 + S \left(\gamma_{\mathrm{s}}, \xi \right) \gamma_{\mathrm{s}}} + \bar{\alpha} \frac{\gamma_{\mathrm{s}} f_1 \left(\xi \right)}{\delta_{\mathrm{n}}^2 + \delta_{\mathrm{p}}^2 + S \left(\gamma_{\mathrm{s}}, \xi \right) \gamma_{\mathrm{s}}} - \lambda_1^{\mathrm{er}} f_1 \left(\xi \right) \right) f_{\gamma_{\mathrm{s}}} \left(\gamma_{\mathrm{s}} \right)$$

$$+ \lambda_2^{\mathrm{er}} \left(\gamma_{\mathrm{s}}, \xi \right) - \lambda_3^{\mathrm{er}} \left(\gamma_{\mathrm{s}}, \xi \right) = 0. \quad (3.7)$$

$$\lambda_1^{\mathrm{er}} \left(\mathrm{E}_{\gamma_{\mathrm{s}}, \xi | \mathrm{PU \ is \ ON}} \left[S \left(\gamma_{\mathrm{s}}, \xi \right) - Q_{\mathrm{inter}} d_{\mathrm{p}}^2 \right] \right) = 0. \quad (3.8)$$

$$\lambda_2^{\mathrm{er}} S \left(\gamma_{\mathrm{s}}, \xi \right) = 0. \quad (3.9)$$

$$\lambda_3^{\mathrm{er}} \left(S \left(\gamma_{\mathrm{s}}, \xi \right) - Q_{\mathrm{peak}} \right) = 0. \quad (3.10)$$

The optimal transmit power $S \left(\gamma_{\mathrm{s}}, \xi \right)$ can take values 0, Q_{peak}, or the open interval $\left(0, Q_{\mathrm{peak}} \right)$.

1) $S(\gamma_{\mathrm{s}}, \xi) = 0$: Let the transmit power be 0 for some γ_{s} and ξ. In this case, equation (3.10) requires that $\lambda_3^{\mathrm{er}} = 0$ and (3.9) implies $\lambda_2^{\mathrm{er}} \geq 0$. Substituting these conditions into (3.7) yields

$$\alpha \frac{\gamma_{\mathrm{s}} f_0 \left(\xi \right)}{\delta_{\mathrm{n}}^2} + \bar{\alpha} \frac{\gamma_{\mathrm{s}} f_1 \left(\xi \right)}{\delta_{\mathrm{n}}^2 + \delta_{\mathrm{p}}^2} - \lambda_1^{\mathrm{er}} f_1 \left(\xi \right) < 0,$$

which, after further manipulation, simplifies to

$$\gamma_{\mathrm{s}} \leq A \left(\lambda_1^{\mathrm{er}}, \xi, \delta_{\mathrm{n}}^2 \right), \quad (3.11)$$

where the function $A \left(\lambda, \xi, \delta^2 \right)$ defined as

$$A \left(\lambda, \xi, \delta^2 \right) \triangleq \frac{\lambda \delta^2 \left(\delta^2 + \delta_{\mathrm{p}}^2 \right) f_1 \left(\xi \right)}{\bar{\alpha} \delta^2 f_1 \left(\xi \right) + \alpha \left(\delta^2 + \delta_{\mathrm{p}}^2 \right) f_0 \left(\xi \right)}. \quad (3.12)$$

2) $S(\gamma_{\mathrm{s}}, \xi) = Q_{\mathrm{peak}}$: In this case, (3.9) requires that $\lambda_2^{\mathrm{er}} = 0$ and (3.10) implies that $\lambda_3^{\mathrm{er}} \geq 0$, which when substituted into (3.7) yield

$$\alpha \frac{\gamma_{\mathrm{s}} f_0 \left(\xi \right)}{\delta_{\mathrm{n}}^2 + Q_{\mathrm{peak}} \gamma_{\mathrm{s}}} + \bar{\alpha} \frac{\gamma_{\mathrm{s}} f_1 \left(\xi \right)}{\delta_{\mathrm{n}}^2 + \delta_{\mathrm{p}}^2 + Q_{\mathrm{peak}} \gamma_{\mathrm{s}}} - \lambda_1^{\mathrm{er}} f_1 \left(\xi \right) > 0,$$

which can further be simplified according to

$$\gamma_{\mathrm{s}} \geq B \left(Q_{\mathrm{peak}}, \lambda_1^{\mathrm{er}}, \xi, \delta_{\mathrm{n}}^2 \right), \quad (3.13)$$

where the function $B\left(Q,\lambda,\xi,\delta^2\right)$ defined as

$$B\left(Q,\lambda,\xi,\delta^2\right) \triangleq \frac{\left(Q\lambda\left(2\delta^2+\delta_{\mathrm{p}}^2\right)-\bar{\alpha}\delta^2\right)f_1\left(\xi\right)-\alpha\left(\delta^2+\delta_{\mathrm{p}}^2\right)f_0\left(\xi\right)}{2Q\left(f_1\left(\xi\right)\left(\bar{\alpha}-Q\lambda\right)+\alpha f_0\left(\xi\right)\right)}$$
$$+\frac{\sqrt{\left(\alpha\left(\delta^2+\delta_{\mathrm{p}}^2\right)f_0\left(\xi\right)+\left(\bar{\alpha}\delta^2-Q\lambda\delta_{\mathrm{p}}^2\right)f_1\left(\xi\right)\right)^2+4\bar{\alpha}Q\lambda\delta^2\delta_{\mathrm{p}}^2\left(f_1\left(\xi\right)\right)^2}}{2Q\left(f_1\left(\xi\right)\left(\bar{\alpha}-Q\lambda\right)+\alpha f_0\left(\xi\right)\right)}.$$

$$(3.14)$$

3) $0 < S(\gamma_{\mathrm{s}},\xi) < Q_{\mathrm{peak}}$: For such interval $S(\gamma_{\mathrm{s}},\xi)$, from the conditions in (3.9) and (3.10), it follows that $\lambda_2^{\mathrm{er}} = \lambda_3^{\mathrm{er}} = 0$. Substituting these conditions into (3.7) yields

$$\alpha\frac{\gamma_{\mathrm{s}}f_0\left(\xi\right)}{\delta_{\mathrm{n}}^2+S\left(\gamma_{\mathrm{s}},\xi\right)\gamma_{\mathrm{s}}}+\bar{\alpha}\frac{\gamma_{\mathrm{s}}f_1\left(\xi\right)}{\delta_{\mathrm{n}}^2+\delta_{\mathrm{p}}^2+S\left(\gamma_{\mathrm{s}},\xi\right)\gamma_{\mathrm{s}}}-\lambda_1^{\mathrm{er}}f_1\left(\xi\right)=0.$$

Then after simple manipulation, the optimal power adaptation policy for $0 < S(\gamma_{\mathrm{s}},\xi) < Q_{\mathrm{peak}}$ can be expressed as,

$$S\left(\gamma_{\mathrm{s}},\xi\right)=\mathcal{P}\left(\gamma_{\mathrm{s}},\xi,\lambda_1^{\mathrm{er}},\delta_{\mathrm{n}}^2\right),\qquad(3.15)$$

where the power function $\mathcal{P}\left(\gamma_{\mathrm{s}},\xi,\lambda,\delta^2\right)$ defined as

$$\mathcal{P}\left(\gamma_{\mathrm{s}},\xi,\lambda,\delta^2\right)\triangleq\frac{\alpha f_0\left(\xi\right)+\bar{\alpha}f_1\left(\xi\right)}{2\lambda f_1\left(\xi\right)}-\frac{\left(2\delta^2+\delta_{\mathrm{p}}^2\right)}{2\gamma_{\mathrm{s}}}$$
$$+\frac{\sqrt{\left(\left(\delta_{\mathrm{p}}^2\lambda-\bar{\alpha}\gamma_{\mathrm{s}}\right)f_1\left(\xi\right)+\alpha\gamma_{\mathrm{s}}f_0\left(\xi\right)\right)^2+4\alpha\bar{\alpha}f_0\left(\xi\right)f_1\left(\xi\right)\gamma_{\mathrm{s}}^2}}{2\lambda f_1\left(\xi\right)\gamma_{\mathrm{s}}}.$$

$$(3.16)$$

According to the results in (3.11), (3.13) and (3.15), the optimal allocation policy for the SU's transmit power, i.e., the one which maximizes the capacity expression in (3.5), can be expressed according to (3.17), where the value of λ_1^{er} is such that both constraints in (3.5) are satisfied.

$$S\left(\gamma_{\mathrm{s}},\xi\right)=\begin{cases}Q_{\mathrm{peak}}, & \gamma_{\mathrm{s}}>B\left(Q_{\mathrm{peak}},\lambda_1^{\mathrm{er}},\xi,\delta_{\mathrm{n}}^2\right)\\\mathcal{P}\left(\gamma_{\mathrm{s}},\xi,\lambda_1^{\mathrm{er}},\delta_{\mathrm{n}}^2\right), & A\left(\lambda_1^{\mathrm{er}},\xi,\delta_{\mathrm{n}}^2\right)\leq\gamma_{\mathrm{s}}\leq B\left(Q_{\mathrm{peak}},\lambda_1^{\mathrm{er}},\xi,\delta_{\mathrm{n}}^2\right)\\0. & \gamma_{\mathrm{s}}<A\left(\lambda_1^{\mathrm{er}},\xi,\delta_{\mathrm{n}}^2\right)\end{cases}\qquad(3.17)$$
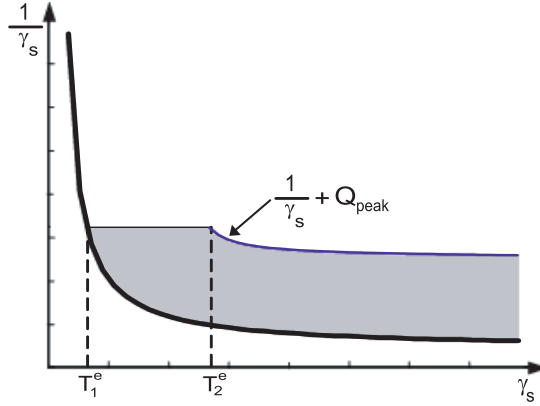
Figure 3.2: Schematic illustration of the optimal power adaption policies in ergodic capacity.

As observed, the optimal power allocation, in (3.17), is partitioned into three regions depending on the variation of the SU channel state. In the first region, we do not use the channel as long as γ_s is below the threshold $T_1^e = A\left(\lambda_1^{er}, \xi, \delta_n^2\right)$. In other words, transmission is suspended when the secondary channel is weak compared to threshold T_1^e. The second region is defined by the range $A\left(\lambda_1^{er}, \xi, \delta_n^2\right) \leq \gamma_s \leq B\left(Q_{peak}, \lambda_1^{er}, \xi, \delta_n^2\right)$, where the power allocation is related to the water-filing approach [62]. Finally, a constant power equal to Q_{peak} is considered for the third region which corresponds to $\gamma_s > T_2^e = B\left(Q_{peak}, \lambda_1^{er}, \xi, \delta_n^2\right)$. The threshold values of the power allocation policy, T_1^e and T_2^e, are determined such that the interference constraint (3.3) is satisfied. Fig. 3.2 plots the schematic location of these thresholds. Indeed, in the above transmission policy, the SU transmits with higher power levels in strong CSI, whereas it remains silent in weak CSI. Moreover, the SSI about the activity of the PU is reflected in the power transmission $\mathcal{P}\left(\gamma_s, \xi, \lambda_1^{er}, \delta_n^2\right)$ defined in (3.16), through the sensing metric distributions, i.e., $f_0(\xi)$ and $f_1(\xi)$.

According to the power allocation in (3.17), the ergodic capacity expression of the secondary link under interference and peak transmit-power constraints can be expressed as follows:

$$\frac{C_{er}}{B} = \mathop{\mathrm{E}}_{\substack{\gamma_s, \xi \\ T_1^e \leq \gamma_s \leq T_2^e}} \left[\alpha \log\left(1 + \frac{\mathcal{P}\left(\gamma_s, \xi, \lambda_1^{er}, \delta_n^2\right)\gamma_s}{\delta_n^2}\right) + \overline{\alpha}\log\left(1 + \frac{\mathcal{P}\left(\gamma_s, \xi, \lambda_1^{er}, \delta_n^2\right)\gamma_s}{\delta_n^2 + \delta_p^2}\right)\right]$$

$$+ \mathop{\mathrm{E}}_{\substack{\gamma_s, \xi \\ \gamma_s \geq T_2^e}} \left[\alpha \log\left(1 + \frac{Q_{peak}\gamma_s}{\delta_n^2}\right) + \overline{\alpha}\log\left(1 + \frac{Q_{peak}\gamma_s}{\delta_n^2 + \delta_p^2}\right)\right]. \qquad (3.18)$$

3.4   Delay-Limited Capacity

The ergodic capacity is the maximum long-term achievable rate over all possible rate and power allocation policies, with no delay constraints. In contrast to the ergodic capacity concept, in delay-sensitive applications, a constant transmission rate is needed in all channel states. For such applications, delay-limited capacity [63], also referred to as zero-outage capacity [40], is a more appropriate capacity notion. In delay-limited capacity, the transmission rate is kept constant in all channel states by using channel inversion [40], [63]. The latter technique inverts the channel fading to maintain a constant received power at the SU receiver.

Using channel inversion, the delay of the transmission link is independent of the channel variations. However, in some fading channels, e.g., Rayleigh, the delay-limited capacity is zero because of the severe fading conditions. Accordingly, by allowing some percentage of outage in deep fading states, called outage probability, we can achieve nonzero constant rate at the receiver. This nonzero outage capacity is referred to as truncated channel inversion with fixed-rate (*tifr*) capacity [8]. The *tifr* technique maintains a constant received-power for channel fades above a given cutoff depth. Moreover, the constant-rate that can be achieved with an outage probability less than a certain threshold is called outage capacity [41].

In CR spectrum-sharing systems, the activity state of the PU can also yield outage onto the SU. Indeed, while the spectrum is occupied by the PU, the secondary transmission must be suspended and, consequently, outage is experienced at the SU communication link. Hence, the available information about the PU's activity can be used at the ST to control its transmit power such that a constant-rate with an outage probability less than a given threshold is provided at the SU receiver. In this context, using SSI about the PU activity and CSI of the secondary link in an independent manner, the outage capacity lower-bound of Rayleigh fading channel in spectrum-sharing system was derived in [8]. Herein, the delay-limited capacity of the SU when using available CSI and SSI at the ST is investigated. We consider a *tifr* policy that only suspends transmission when γ_s is less than a certain cutoff threshold: $\gamma_s < A\left(\lambda^{\text{out}}, \xi, \delta_n^2\right)$. Accordingly, we express the power allocation policy as
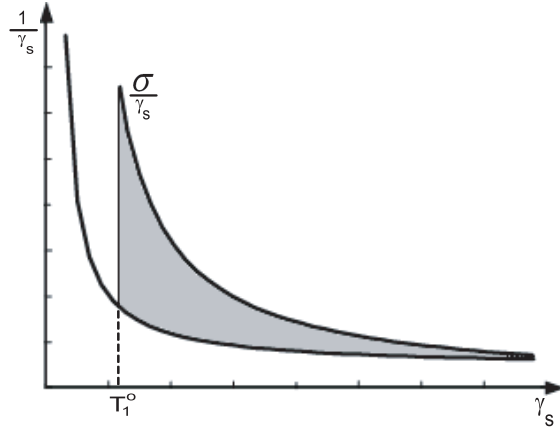
Figure 3.3: Schematic illustration of the optimal power adaption policies in delay-limited capacity.

follows:

$$S\left(\gamma_{s},\,\xi\right) = \begin{cases} 0, & \gamma_{s} < A\left(\lambda^{\mathrm{out}}, \xi, \delta_{n}^{2}\right) \\ \dfrac{\sigma}{\gamma_{s}}, & \gamma_{s} \geq A\left(\lambda^{\mathrm{out}}, \xi, \delta_{n}^{2}\right) \end{cases} \tag{3.19}$$

where λ^{out} and σ must satisfy the interference and peak transmit power constraints, (3.3) and (3.4), at equality:

$$Q'_{\mathrm{inter}} = \iint\limits_{\gamma_{s} \geq A(\lambda^{\mathrm{out}}, \xi, \delta_{n}^{2})} \frac{\sigma}{\gamma_{s}} f_{\gamma_{s}}\left(\gamma_{s}\right) f_{1}\left(\xi\right) d\gamma_{s} d\xi, \tag{3.20}$$

$$\frac{\sigma}{\gamma_{s}} \leq Q_{\mathrm{peak}}, \quad \forall\,\gamma_{s}: \quad \gamma_{s} \geq A\left(\lambda^{\mathrm{out}}, \xi, \delta_{n}^{2}\right), \tag{3.21}$$

where $Q'_{\mathrm{inter}} = Q_{\mathrm{inter}}\, d_{p}^{2}$, with d_{p} denoting the distance between the ST and the PR. More-over, from (3.21), the inequality $\sigma \leq Q_{\mathrm{peak}} A\left(\lambda^{\mathrm{out}}, \xi, \delta_{n}^{2}\right)$ must hold true.

In (3.19), the ST is allowed to transmit as long as γ_{s} exceeds a cutoff threshold $T_{1}^{o} = A\left(\lambda^{\mathrm{out}}, \xi, \delta_{n}^{2}\right)$. The schematic illustration of T_{1}^{o} is shown in Fig. 3.3. As observed in (3.19), the SU uses a higher power level in weak channel conditions, whereas in (3.17), the higher power strength is used in strong channel conditions.

The capacity under *tifr* transmission policy can be obtained by solving the following

maximization problem over all possible λ^{out} and ξ:

$$
\frac{C_{\text{tifr}}}{B} = \max_{\lambda^{\text{out}},\xi} \left\{ \left(\alpha \log \left(1 + \frac{\min\left\{\sigma,\, Q_{\text{peak}} T_1^{\text{o}}\right\}}{\delta_{\text{n}}^2} \right) + \overline{\alpha} \log \left(1 + \frac{\min\left\{\sigma,\, Q_{\text{peak}} T_1^{\text{o}}\right\}}{\delta_{\text{n}}^2 + \delta_{\text{p}}^2} \right) \right) \right.
$$
$$
\left. \times \Pr\left\{\gamma_{\text{s}} \geq T_1^{\text{o}}\right\} \right\}. \tag{3.22}
$$

In (3.22), $\Pr\left\{\gamma_{\text{s}} \geq T_1^{\text{o}}\right\}$ is defined as $(1 - P_0)$, where P_0 denotes the percentage of time that the transmission remains in outage condition and is called outage probability. Using (3.19), the outage probability expression can be obtained as follows:

$$
P_0 = 1 - \Pr\left\{\gamma_{\text{s}} \geq T_1^{\text{o}}\right\}
$$
$$
= 1 - \iint\limits_{\gamma_{\text{s}} \geq T_1^{\text{o}}} f_{\gamma_{\text{s}}}\left(\gamma_{\text{s}}\right) f_1\left(\xi\right) d\gamma_{\text{s}} d\xi. \tag{3.23}
$$

On the other hand, to find the achievable capacity for a fixed P_0, the cutoff value λ^{out} must be determined so as to satisfy (3.23) and, consequently, the capacity in the case with P_0 probability of outage can be obtained by maximizing over all possible ξ and λ^{out}:

$$
\frac{C_{\text{out}}}{B} = \max_{\lambda^{\text{out}},\xi} \left\{ \left(\alpha \log \left(1 + \frac{\min\left\{\sigma,\, Q_{\text{peak}} T_1^{\text{o}}\right\}}{\delta_{\text{n}}^2} \right) + \overline{\alpha} \log \left(1 + \frac{\min\left\{\sigma,\, Q_{\text{peak}} T_1^{\text{o}}\right\}}{\delta_{\text{n}}^2 + \delta_{\text{p}}^2} \right) \right) \right.
$$
$$
\left. \times (1 - P_0) \right\}. \tag{3.24}
$$

3.5 Service-Rate Capacity

In CR systems where the transmission is constrained by the PUs' activity, any excess rate would be desirable for cognitive users while they opportunistically access the shared spectrum band. Accordingly, besides the fact that a basic constant rate is needed to guarantee the minimum-rate requirement (cf. delay-limited capacity), variable-rate transmission is also used (cf. ergodic capacity) to provide different service-rate levels. The capacity under such a transmission strategy is called service-rate capacity or minimum-rate capacity [25]. Specifically, service-rate capacity (C_{ser}) is the maximum long-term average mutual information, subject to guaranteeing a minimum service-rate r_0 all the time. Thus, in service-rate capacity, some power is used to provide the minimum required rate, r_0, and the excess power is used to increase the average achievable rate over all fading states.

Herein, the service-rate capacity of the SU link is investigated subject to joint constraints on the average interference at the PR and peak-transmit power at the ST. Moreover, the problem of service-rate capacity with outage is also addressed. Indeed, in pure service-rate capacity (without outage), the ergodic capacity is maximized subject to guaranteeing the minimum-rate constraint all the time. In contrast, when transmission is allowed during outage, the minimum-rate constraint is loosened slightly and satisfied only for a tolerable percentage of time [24]. Accordingly, the service-rate capacity without outage can be considered as the combination of ergodic and zero-outage capacities, whereas the service-rate capacity with outage is the combination of ergodic and outage capacities. In this section, we first investigate the service-rate capacity of spectrum-sharing systems without outage under the considered resource constraints. Then, we find the service-rate capacity of the secondary link subject to an allowable outage probability.

3.5.1   Service-Rate Capacity without Outage

Using SSI about the PU activity and secondary CSI at the ST, the service-rate capacity, C_{ser}, under the constraints on received interference and peak transmit-power can be formulated as follows:

$$\frac{C_{\mathrm{ser}}}{B} = \max_{S(\gamma_{\mathrm{s}}, \xi)} \left\{ \mathrm{E}_{\gamma_{\mathrm{s}}, \xi} \left[\alpha \log \left(1 + \frac{S\left(\gamma_{\mathrm{s}}, \xi\right) \gamma_{\mathrm{s}}}{\delta_{\mathrm{n}}^2} \right) \right] + \mathrm{E}_{\gamma_{\mathrm{s}}, \xi} \left[\overline{\alpha} \log \left(1 + \frac{S\left(\gamma_{\mathrm{s}}, \xi\right) \gamma_{\mathrm{s}}}{\delta_{\mathrm{n}}^2 + \delta_{\mathrm{p}}^2} \right) \right] \right\}$$

$$(3.25\mathrm{a})$$

$$\text{s.t.} \ \ (3.3) \text{ and } (3.4), \tag{3.25b}$$

$$\alpha \log \left(1 + \frac{S\left(\gamma_{\mathrm{s}}, \xi\right) \gamma_{\mathrm{s}}}{\delta_{\mathrm{n}}^2} \right) + \overline{\alpha} \log \left(1 + \frac{S\left(\gamma_{\mathrm{s}}, \xi\right) \gamma_{\mathrm{s}}}{\delta_{\mathrm{n}}^2 + \delta_{\mathrm{p}}^2} \right) \geq r_0. \tag{3.25c}$$

As previously mentioned, we have two strategies in service-rate capacity. At first, we have to provide the minimum service-rate. Then using water-filling approach, we employ the excess power to increase the average achievable rate over all fading and PU activity states. In this context, the minimum achievable capacity for a minimum service-rate r_0 is obtained by using zero-outage capacity transmission policy[7]. Using this policy subject to the constraints (3.3) and (3.4), the minimum transmit-power required to guarantee r_0 all the time, can be obtained as $S_{\min}\left(\gamma_{\mathrm{s}}, \xi\right) = \dfrac{\sigma_{\min}}{\gamma_{\mathrm{s}}}$, where $\sigma_{\min}$ may be calculated using (3.25c)

---

[7]This capacity was investigated in section 3.4.

at equality as follows:

$$\alpha \log \left(1 + \frac{\sigma_{\min}}{\delta_{\mathrm{n}}^2} \right) + \overline{\alpha} \log \left(1 + \frac{\sigma_{\min}}{\delta_{\mathrm{n}}^2 + \delta_{\mathrm{p}}^2} \right) = r_0. \tag{3.26}$$

Now, using (3.3) and (3.4), the minimum values of the average received-power and peak transmit-power limitations, $Q_{\mathrm{inter}}^{\min}$ and $Q_{\mathrm{peak}}^{\min}$, can be calculated according to the following expressions:

$$Q_{\mathrm{inter}}^{\min} d_{\mathrm{p}}^2 = \mathrm{E}_{\gamma_{\mathrm{s}}, \xi | \mathrm{PU\ is\ ON}} \left[\frac{\sigma_{\min}}{\gamma_{\mathrm{s}}} \right], \tag{3.27}$$

$$Q_{\mathrm{peak}}^{\min} = \frac{\sigma_{\min}}{A \left(\lambda^{\mathrm{out}}, \xi, \delta_{\mathrm{n}}^2 \right)}, \tag{3.28}$$

where λ^{out} must satisfy the outage probability expression in (3.23).

It is worth noting that if either of the average interference or peak transmit-power values, is less than the minimum required, $Q_{\mathrm{inter}}^{\min}$ or $Q_{\mathrm{peak}}^{\min}$, respectively, the SU's transmission is suspended and no feasible power allocation exists.

Now, denote $S_{\mathrm{exc}}(\gamma_{\mathrm{s}}, \xi)$ as the excess power allocated to maximize the average achievable rate. Then, the service-rate capacity, (3.25a), can be expressed as

$$\begin{aligned} \frac{C_{\mathrm{ser}}}{B} = \mathrm{E}_{\gamma_{\mathrm{s}}, \xi} & \left[\alpha \log \left(1 + \frac{S_{\min}(\gamma_{\mathrm{s}}, \xi) \gamma_{\mathrm{s}}}{\delta_{\mathrm{n}}^2} + \frac{S_{\mathrm{exc}}(\gamma_{\mathrm{s}}, \xi) \gamma_{\mathrm{s}}}{\delta_{\mathrm{n}}^2} \right) \right. \\ & \left. + \overline{\alpha} \log \left(1 + \frac{S_{\min}(\gamma_{\mathrm{s}}, \xi) \gamma_{\mathrm{s}}}{\delta_{\mathrm{n}}^2 + \delta_{\mathrm{p}}^2} + \frac{S_{\mathrm{exc}}(\gamma_{\mathrm{s}}, \xi) \gamma_{\mathrm{s}}}{\delta_{\mathrm{n}}^2 + \delta_{\mathrm{p}}^2} \right) \right]. \end{aligned} \tag{3.29}$$

By splitting the capacity expression in (3.29)[8], and after some manipulation, the above expression simplifies to

$$\frac{C_{\mathrm{ser}}}{B} = r_0 + C_{\mathrm{exc}}, \tag{3.30}$$

where C_{exc} is the capacity achieved with the excess power $S_{\mathrm{exc}}(\gamma_{\mathrm{s}}, \xi)$, and can be expressed as

$$C_{\mathrm{exc}} = \mathrm{E}_{\gamma_{\mathrm{s}}, \xi} \left[\alpha \log \left(1 + \frac{S_{\mathrm{exc}}(\gamma_{\mathrm{s}}, \xi) \gamma_{\mathrm{s}}}{\delta_{\mathrm{n}}^2 + S_{\min}(\gamma_{\mathrm{s}}, \xi) \gamma_{\mathrm{s}}} \right) + \overline{\alpha} \log \left(1 + \frac{S_{\mathrm{exc}}(\gamma_{\mathrm{s}}, \xi) \gamma_{\mathrm{s}}}{\delta_{\mathrm{n}}^2 + \delta_{\mathrm{p}}^2 + S_{\min}(\gamma_{\mathrm{s}}, \xi) \gamma_{\mathrm{s}}} \right) \right]. \tag{3.31}$$

---

[8]i.e., $\log \left(1 + \frac{S_1}{N} + \frac{S_2}{N} \right) = \log \left(1 + \frac{S_1}{N} \right) + \log \left(1 + \frac{S_2}{S_1 + N} \right).$

After substitution of $S_{\min}(\gamma_s, \xi) = \dfrac{\sigma_{\min}}{\gamma_s}$, the excess capacity may be simplified further as

$$C_{\text{exc}} = \text{E}_{\gamma_s, \xi} \left[\alpha \log \left(1 + \frac{S_{\text{exc}}(\gamma_s, \xi)\gamma_s}{\delta_n^2 + \sigma_{\min}} \right) + \overline{\alpha} \log \left(1 + \frac{S_{\text{exc}}(\gamma_s, \xi)\gamma_s}{\delta_n^2 + \delta_p^2 + \sigma_{\min}} \right) \right], \quad (3.32)$$

under the excess average received-interference limit, $Q_{\text{inter}}^{\text{exc}} = Q_{\text{inter}} - Q_{\text{inter}}^{\min}$, and excess peak transmit-power limit, $Q_{\text{peak}}^{\text{exc}} = Q_{\text{peak}} - \dfrac{\sigma_{\min}}{\gamma_s}$, whereby the constraints are given by

$$\text{E}_{\gamma_s, \xi | \text{PU is ON}} \left[S_{\text{exc}}(\gamma_s, \xi) \right] \leq Q_{\text{inter}}^{\text{exc}} d_p^2 \qquad (3.33)$$

and

$$S_{\text{exc}}(\gamma_s, \xi) \leq Q_{\text{peak}}^{\text{exc}}, \qquad (3.34)$$

respectively.

To find the optimal excess power allocation under the constraints in (3.33) and (3.34), we adopt the Lagrangian optimization approach presented in section 3.3. Following the Lagrangian approach, to obtain the optimal power adaptation for $S_{\text{exc}}(\gamma_s, \xi)$, we can consider the following three cases:

1) $S_{\text{exc}}(\gamma_s, \xi) = 0$: Letting $S_{\text{exc}}(\gamma_s, \xi)$ be 0 for some γ_s and ξ, we have:

$$\gamma_s \leq A \left(\lambda_1^{\text{exc}}, \xi, \widehat{\delta_n^2} \right), \qquad (3.35)$$

where $\widehat{\delta_n^2} \triangleq \delta_n^2 + \sigma_{\min}$.

2) $S_{\text{exc}}(\gamma_s, \xi) = Q_{\text{peak}}^{\text{exc}}$: In this case, we obtain:

$$\gamma_s \geq B \left(Q_{\text{peak}}^{\text{exc}}, \lambda_1^{\text{exc}}, \xi, \widehat{\delta_n^2} \right). \qquad (3.36)$$

3) $0 < S_{\text{exc}}(\gamma_s, \xi) < Q_{\text{peak}}^{\text{exc}}$: Finally, in this case, after simple manipulation, the optimal power adaptation policy for $0 < S_{\text{exc}}(\gamma_s, \xi) < Q_{\text{peak}}^{\text{exc}}$ can be expressed as,

$$S_{\text{exc}}(\gamma_s, \xi) = \mathcal{P} \left(\gamma_s, \xi, \lambda_1^{\text{exc}}, \widehat{\delta_n^2} \right), \qquad (3.37)$$

where the function $\mathcal{P}(\cdot, \cdot, \cdot, \cdot)$ is defined in (3.16).
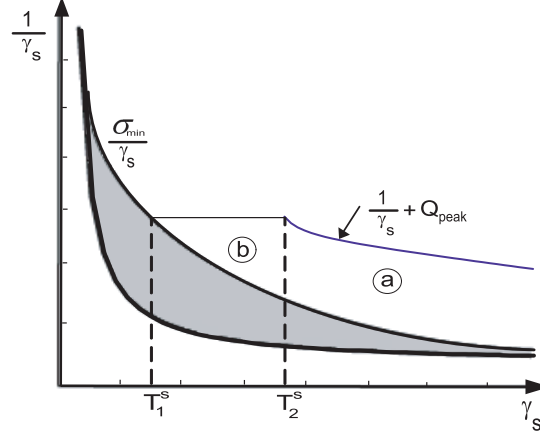
Figure 3.4: Schematic illustration of the optimal power adaption policies in service-rate (without outage) capacity.

According to the results in (3.35), (3.36) and (3.37), the optimal excess power allocation policy to maximize the excess capacity under the constraints in (3.32) and (3.33), can be expressed as shown in (3.38), where the value of λ_1^{exc} is such that these constraints are satisfied.

$$
S_{\text{exc}}\left(\gamma_{\text{s}},\,\xi\right) =
\begin{cases}
Q_{\text{peak}} - \dfrac{\sigma_{\min}}{\gamma_{\text{s}}}, & \gamma_{\text{s}} > B\left(Q_{\text{peak}}^{\text{exc}}, \lambda_1^{\text{exc}}, \xi, \widehat{\delta_{\text{n}}^2}\right) \\[2mm]
\mathcal{P}\left(\gamma_{\text{s}}, \xi, \lambda_1^{\text{exc}}, \widehat{\delta_{\text{n}}^2}\right), & A\left(\lambda_1^{\text{exc}}, \xi, \widehat{\delta_{\text{n}}^2}\right) \leq \gamma_{\text{s}} \leq B\left(Q_{\text{peak}}^{\text{exc}}, \lambda_1^{\text{exc}}, \xi, \widehat{\delta_{\text{n}}^2}\right) \\[2mm]
0. & \gamma_{\text{s}} < A\left(\lambda_1^{\text{exc}}, \xi, \widehat{\delta_{\text{n}}^2}\right)
\end{cases}
$$

$$(3.38)$$

It has been shown that the service-rate based transmission policy is a combination of two power transmission strategies. At first, the channel inversion technique was adopted to achieve basic service-rate (Fig. 3.4 – the region shown in gray). Then using water-filling approach, the excess power was spent to increase the average achievable rate over all SU channel states (Fig. 3.4 – regions a and b). In Fig. 3.4, T_1^{s} and T_2^{s} are the transmission thresholds defined as $T_1^{\text{s}} = A\left(\lambda_1^{\text{exc}}, \xi, \widehat{\delta_{\text{n}}^2}\right)$ and $T_2^{\text{s}} = B\left(Q_{\text{peak}}^{\text{exc}}, \lambda_1^{\text{exc}}, \xi, \widehat{\delta_{\text{n}}^2}\right)$, respectively.

Now, substituting (3.38) into (3.32) yields the formula for C_{exc} when $Q_{\text{inter}} > Q_{\text{inter}}^{\min}$

and $Q_{\text{peak}} > Q_{\text{peak}}^{\min}$, as follows:

$$
\begin{aligned}
C_{\text{exc}} = \underset{T_1^{\text{s}} \leq \gamma_{\text{s}} \leq T_2^{\text{s}}}{\mathrm{E}_{\gamma_{\text{s}}, \xi}} & \left[\alpha \log \left(1 + \frac{\mathcal{P}\left(\gamma_{\text{s}}, \xi, \lambda_1^{\text{exc}}, \widehat{\delta_{\text{n}}^2}\right) \gamma_{\text{s}}}{\widehat{\delta_{\text{n}}^2}} \right) + \overline{\alpha} \log \left(1 + \frac{\mathcal{P}\left(\gamma_{\text{s}}, \xi, \lambda_1^{\text{exc}}, \widehat{\delta_{\text{n}}^2}\right) \gamma_{\text{s}}}{\widehat{\delta_{\text{n}}^2} + \delta_{\text{p}}^2} \right) \right] \\
+ \underset{\gamma_{\text{s}} > T_2^{\text{s}}}{\mathrm{E}_{\gamma_{\text{s}}, \xi}} & \left[\alpha \log \left(\frac{\delta_{\text{n}}^2 + Q_{\text{peak}} \gamma_{\text{s}}}{\widehat{\delta_{\text{n}}^2}} \right) + \overline{\alpha} \log \left(\frac{\delta_{\text{n}}^2 + \delta_{\text{p}}^2 + Q_{\text{peak}} \gamma_{\text{s}}}{\widehat{\delta_{\text{n}}^2} + \delta_{\text{p}}^2} \right) \right].
\end{aligned}
\tag{3.39}
$$

Finally, the service-rate capacity expression of fading channels under average received-interference and peak transmit-power constraints with r_0 dedicated service-rate, can be expressed as

$$
\frac{C_{\text{ser}}}{B} = \begin{cases} \text{Not Feasible} & \text{if } Q_{\text{inter}} < Q_{\text{inter}}^{\min} \text{ or } Q_{\text{peak}} < Q_{\text{peak}}^{\min}, \\ r_0 & \text{if } Q_{\text{inter}} = Q_{\text{inter}}^{\min} \text{ or } Q_{\text{peak}} = Q_{\text{peak}}^{\min}, \\ r_0 + C_{\text{exc}} & \text{if } Q_{\text{inter}} > Q_{\text{inter}}^{\min} \text{ and } Q_{\text{peak}} > Q_{\text{peak}}^{\min}. \end{cases}
\tag{3.40}
$$

In (3.40), it is worth noting that if $Q_{\text{inter}} \gg Q_{\text{inter}}^{\min}$ and $Q_{\text{peak}} \gg Q_{\text{peak}}^{\min}$, this implies that Q_{inter} and Q_{peak} are high enough to guarantee the required service-rate r_0, over all fading and PU activity states. It is easy to show that in this case, the service-rate capacity is equal to the ergodic capacity and can be obtained from (3.18).

3.5.2 Service-Rate Capacity with Outage

In this part, we investigate the service-rate capacity with outage, $C_{\text{ser}}^{\text{out}}$, subject to the constraints on received-interference and peak transmit-power. In this regard, $C_{\text{ser}}^{\text{out}}$ can be obtained according to the following maximization problem:

$$
\frac{C_{\text{ser}}^{\text{out}}}{B} = \max_{S(\gamma_{\text{s}}, \xi)} \left\{ \mathrm{E}_{\gamma_{\text{s}}, \xi} \left[\alpha \log \left(1 + \frac{S\left(\gamma_{\text{s}}, \xi\right) \gamma_{\text{s}}}{\delta_{\text{n}}^2} \right) \right] + \mathrm{E}_{\gamma_{\text{s}}, \xi} \left[\overline{\alpha} \log \left(1 + \frac{S\left(\gamma_{\text{s}}, \xi\right) \gamma_{\text{s}}}{\delta_{\text{n}}^2 + \delta_{\text{p}}^2} \right) \right] \right\}
\tag{3.41a}
$$

$$
\text{Subject to (3.3) and (3.4),}
\tag{3.41b}
$$

$$
\mathrm{Pr} \left\{ \alpha \log \left(1 + \frac{S\left(\gamma_{\text{s}}, \xi\right) \gamma_{\text{s}}}{\delta_{\text{n}}^2} \right) + \overline{\alpha} \log \left(1 + \frac{S\left(\gamma_{\text{s}}, \xi\right) \gamma_{\text{s}}}{\delta_{\text{n}}^2 + \delta_{\text{p}}^2} \right) < r_0 \right\} \leq P_0.
\tag{3.41c}
$$

To find the service-rate outage capacity, we apply the same approach used for the service-rate capacity (without outage) in section 3.5.1. We first provide the minimum service-rate with outage probability less than $(1 - P_0)$, and then use the excess power based on water-filling approach to increase the average achievable rate over all fading and PU activity states.

Using (3.24), the minimum achievable capacity for a minimum service-rate of r_0 and an outage probability of P_0 is obtained as, $\dfrac{C_{\min}^{\text{out}}}{B} = r_0 (1 - P_0)$. Accordingly, using (3.20) and (3.21), the minimum values of the average received-power and peak transmit-power limitations, $Q_{\text{inter}}^{\min}$ and $Q_{\text{peak}}^{\min}$, can be calculated according to the following expressions[9]:

$$Q_{\text{inter}}^{\min} d_{\text{p}}^2 = \iint\limits_{\gamma_{\text{s}} \geq A\left(\lambda_{\min}^{\text{out}}, \xi, \delta_{\text{n}}^2\right)} \frac{\sigma_{\min}}{\gamma_{\text{s}}} f_{\gamma_{\text{s}}} (\gamma_{\text{s}}) f_1 (\xi) \, d\gamma_{\text{s}} d\xi, \tag{3.42}$$

$$Q_{\text{peak}}^{\min} = \frac{\sigma_{\min}}{A \left(\lambda_{\min}^{\text{out}}, \xi, \delta_{\text{n}}^2\right)}, \tag{3.43}$$

where $\sigma_{\min}$ is calculated using (3.26), and $\lambda_{\min}^{\text{out}}$ must satisfy the minimum allowable outage probability expression in (3.23) according to:

$$\iint\limits_{\gamma_{\text{s}} \geq A\left(\lambda_{\min}^{\text{out}}, \xi, \delta_{\text{n}}^2\right)} f_{\gamma_{\text{s}}} (\gamma_{\text{s}}) f_1 (\xi) \, d\gamma_{\text{s}} d\xi = 1 - P_0. \tag{3.44}$$

Considering (3.19), the minimum power required at each channel state to provide r_0 for $1 - P_0$ percentage of time can be obtained as

$$S_{\min}^{\text{out}} (\gamma_{\text{s}}, \xi) = \begin{cases} 0, & \gamma_{\text{s}} < A \left(\lambda_{\min}^{\text{out}}, \xi, \delta_{\text{n}}^2\right) \\ \dfrac{\sigma_{\min}}{\gamma_{\text{s}}} & \gamma_{\text{s}} \geq A \left(\lambda_{\min}^{\text{out}}, \xi, \delta_{\text{n}}^2\right) \end{cases} \tag{3.45}$$

Now, let $S_{\text{exc}}^{\text{out}}(\gamma_{\text{s}}, \xi)$ be the excess power allocated to maximize the average achievable rate. Then, the service-outage based capacity, (3.41a), can be expressed as

$$\frac{C_{\text{ser}}^{\text{out}}}{B} = r_0 (1 - P_0) + C_{\text{exc}}^{\text{out}}, \tag{3.46}$$

---

[9] It is worth noting that if $Q_{\text{inter}} < Q_{\text{inter}}^{\min}$ or $Q_{\text{peak}} < Q_{\text{peak}}^{\min}$, then the SU's transmission is suspended and no feasible power allocation policy exists.

where $C_{\text{exc}}^{\text{out}}$ is the capacity achieved with the excess power and can be expressed as

$$C_{\text{exc}}^{\text{out}} = \text{E}_{\gamma_{\text{s}},\xi} \left[\alpha \log \left(1 + \frac{S_{\text{exc}}^{\text{out}} (\gamma_{\text{s}}, \xi) \gamma_{\text{s}}}{\delta_{\text{n}}^2 + S_{\text{min}}^{\text{out}} (\gamma_{\text{s}}, \xi) \gamma_{\text{s}}} \right) + \overline{\alpha} \log \left(1 + \frac{S_{\text{exc}}^{\text{out}} (\gamma_{\text{s}}, \xi) \gamma_{\text{s}}}{\delta_{\text{n}}^2 + \delta_{\text{p}}^2 + S_{\text{min}}^{\text{out}} (\gamma_{\text{s}}, \xi) \gamma_{\text{s}}} \right) \right].$$

$$(3.47)$$

After substituting (3.45) into (3.47), the excess capacity can be obtained by considering two conditions:

$$C_{\text{exc}}^{\text{out}} = \begin{cases} \text{E}_{\gamma_{\text{s}},\xi} \left[\alpha \log \left(1 + \frac{S_{\text{exc}}^{\text{out}} (\gamma_{\text{s}}, \xi) \gamma_{\text{s}}}{\delta_{\text{n}}^2} \right) \right. \\ \qquad \left. + \overline{\alpha} \log \left(1 + \frac{S_{\text{exc}}^{\text{out}} (\gamma_{\text{s}}, \xi) \gamma_{\text{s}}}{\delta_{\text{n}}^2 + \delta_{\text{p}}^2} \right) \right], & \gamma_{\text{s}} < A \left(\lambda_{\text{min}}^{\text{out}}, \xi, \delta_{\text{n}}^2 \right) \\[2mm] \text{E}_{\gamma_{\text{s}},\xi} \left[\alpha \log \left(1 + \frac{S_{\text{exc}}^{\text{out}} (\gamma_{\text{s}}, \xi) \gamma_{\text{s}}}{\delta_{\text{n}}^2 + \sigma_{\text{min}}} \right) \right. \\ \qquad \left. + \overline{\alpha} \log \left(1 + \frac{S_{\text{exc}}^{\text{out}} (\gamma_{\text{s}}, \xi) \gamma_{\text{s}}}{\delta_{\text{n}}^2 + \delta_{\text{p}}^2 + \sigma_{\text{min}}} \right) \right], & \gamma_{\text{s}} \geq A \left(\lambda_{\text{min}}^{\text{out}}, \xi, \delta_{\text{n}}^2 \right) \end{cases}$$

$$(3.48)$$

under the excess average received-interference limit, $Q_{\text{inter}}^{\text{exc}}$, and excess peak transmit-power limit, $Q_{\text{peak}}^{\text{exc}}$.

Using the Lagrangian optimization technique, we can obtain the optimal power adaptation policy for $S_{\text{exc}}^{\text{out}}(\gamma_{\text{s}}, \xi)$ that maximizes the excess capacity, $C_{\text{exc}}^{\text{out}}$, by following the approach in section 3.3. Considering the conditions for the excess capacity expression in (3.48) and under the appropriate KKT conditions, the following cases are considered:

1) $S_{\text{exc}}^{\text{out}}(\gamma_{\text{s}}, \xi) = 0$: In this case, we obtain

$$\begin{aligned} \gamma_{\text{s}} &< A \left(\lambda_1^{\text{exc}}, \xi, \delta_{\text{n}}^2 \right) & \text{if } \gamma_{\text{s}} < A \left(\lambda_{\text{min}}^{\text{out}}, \xi, \delta_{\text{n}}^2 \right), \\ \gamma_{\text{s}} &< A \left(\lambda_1^{\text{exc}}, \xi, \widehat{\delta_{\text{n}}^2} \right) & \text{if } \gamma_{\text{s}} \geq A \left(\lambda_{\text{min}}^{\text{out}}, \xi, \delta_{\text{n}}^2 \right). \end{aligned}$$

$$(3.49)$$

2) $S_{\text{exc}}^{\text{out}}(\gamma_{\text{s}}, \xi) = Q_{\text{peak}}^{\text{exc}}$: The condition $\gamma_{\text{s}} \geq A \left(\lambda_{\text{min}}^{\text{out}}, \xi, \delta_{\text{n}}^2 \right)$ is always valid in this case, thus yielding

$$\gamma_{\text{s}} \geq B \left(Q_{\text{peak}}^{\text{exc}}, \lambda_1^{\text{exc}}, \xi, \widehat{\delta_{\text{n}}^2} \right).$$

$$(3.50)$$

3) $0 < S_{\text{exc}}^{\text{out}}(\gamma_{\text{s}}, \xi) < Q_{\text{peak}}^{\text{exc}}$: Finally, considering the thresholds in (3.48), we obtain two

possible power levels as follows

$$S_{\text{exc}}^{\text{out}}\left(\gamma_{\text{s}},\,\xi\right) = \begin{cases} \mathcal{P}\left(\gamma_{\text{s}},\xi,\lambda_1^{\text{exc}},\delta_{\text{n}}^2\right), & \text{if}: \gamma_{\text{s}} < A\left(\lambda_{\min}^{\text{out}},\xi,\delta_{\text{n}}^2\right) \\ \mathcal{P}\left(\gamma_{\text{s}},\xi,\lambda_1^{\text{exc}},\widehat{\delta_{\text{n}}^2}\right). & \text{if}: \gamma_{\text{s}} \geq A\left(\lambda_{\min}^{\text{out}},\xi,\delta_{\text{n}}^2\right) \end{cases} \tag{3.51}$$

According to the results in (3.49), (3.50) and (3.51), the optimal excess power allocation policy to maximize the excess capacity under the constraints in (3.41b) and (3.41c), can be expressed as shown in (3.52), where the value of λ_1^{exc} is such that these constraints are satisfied.

$$S_{\text{exc}}^{\text{out}}\left(\gamma_{\text{s}},\,\xi\right) = \begin{cases} Q_{\text{peak}} - \dfrac{\sigma_{\min}}{\gamma_{\text{s}}}, & \gamma_{\text{s}} > B\left(Q_{\text{peak}}^{\text{exc}},\lambda_1^{\text{exc}},\xi,\widehat{\delta_{\text{n}}^2}\right) \\ \mathcal{P}\left(\gamma_{\text{s}},\xi,\lambda_1^{\text{exc}},\widehat{\delta_{\text{n}}^2}\right), & A\left(\lambda_1^{\text{exc}},\xi,\widehat{\delta_{\text{n}}^2}\right) \leq \gamma_{\text{s}} \leq B\left(Q_{\text{peak}}^{\text{exc}},\lambda_1^{\text{exc}},\xi,\widehat{\delta_{\text{n}}^2}\right) \\ 0, & A\left(\lambda_{\min}^{\text{out}},\xi,\delta_{\text{n}}^2\right) \leq \gamma_{\text{s}} < A\left(\lambda_1^{\text{exc}},\xi,\widehat{\delta_{\text{n}}^2}\right) \\ \mathcal{P}\left(\gamma_{\text{s}},\xi,\lambda_1^{\text{exc}},\delta_{\text{n}}^2\right), & A\left(\lambda_1^{\text{exc}},\xi,\delta_{\text{n}}^2\right) \leq \gamma_{\text{s}} < A\left(\lambda_{\min}^{\text{out}},\xi,\delta_{\text{n}}^2\right) \\ 0, & \gamma_{\text{s}} < A\left(\lambda_1^{\text{exc}},\xi,\delta_{\text{n}}^2\right) \end{cases} \tag{3.52}$$

where $\mathcal{P}\left(\cdot,\cdot,\cdot,\cdot\right)$ is previously defined in (3.16).

By comparing the service-rate based transmission policy with outage in (3.52) and the one without outage in (3.38), it has been shown that the additional outage constraint restricts the set of feasible SU transmission policies more tightly than in the case without outage constraint (Fig. 3.5). In Fig. 3.5, the thresholds are defined according to $T_1^{\text{so}} = A\left(\lambda_1^{\text{exc}},\xi,\delta_{\text{n}}^2\right)$, $T_2^{\text{so}} = A\left(\lambda_{\min}^{\text{out}},\xi,\delta_{\text{n}}^2\right)$, $T_3^{\text{so}} = A\left(\lambda_1^{\text{exc}},\xi,\widehat{\delta_{\text{n}}^2}\right)$ and $T_4^{\text{so}} = B\left(Q_{\text{peak}}^{\text{exc}},\lambda_1^{\text{exc}},\xi,\widehat{\delta_{\text{n}}^2}\right)$. Furthermore, in (3.52), it is worth noting that if $T_3^{\text{so}} \leq T_2^{\text{so}}$, then $S_{\text{exc}}^{\text{out}}\left(\gamma_{\text{s}},\,\xi\right) > 0$ for all $\gamma_{\text{s}} \geq T_2^{\text{so}}$. This implies that Q_{inter} is high enough to guarantee the required service-rate, r_0, for $1 - P_0$ percentage of time. In this case, the service-rate outage capacity can be obtained from (3.18).

Now, substituting (3.52) and (3.48) into the excess capacity expression in (3.47) yields the formula for $C_{\text{exc}}^{\text{out}}$ when $T_1^{\text{so}} < T_2^{\text{so}} < T_3^{\text{so}}$, as follows:

$$C_{\text{exc}}^{\text{out}} = C_{\text{exc1}}^{\text{out}} + C_{\text{exc2}}^{\text{out}}, \tag{3.53}$$
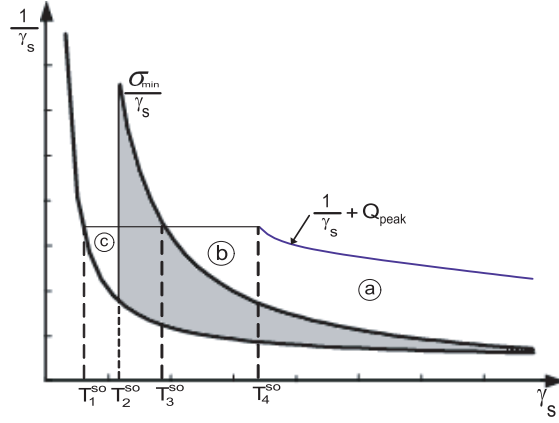
Figure 3.5: Schematic illustration of the optimal power adaption policies in service-rate (with outage) capacity.

where

$$
C_{\text{exc1}}^{\text{out}} = \underset{T_1^{\text{so}} \leq \gamma_{\text{s}} < T_2^{\text{so}}}{\text{E}_{\gamma_{\text{s}}, \xi}} \left[\alpha \log \left(1 + \frac{\mathcal{P}\left(\gamma_{\text{s}}, \xi, \lambda_1^{\text{exc}}, \delta_{\text{n}}^2\right) \gamma_{\text{s}}}{\delta_{\text{n}}^2} \right) + \overline{\alpha} \log \left(1 + \frac{\mathcal{P}\left(\gamma_{\text{s}}, \xi, \lambda_1^{\text{exc}}, \delta_{\text{n}}^2\right) \gamma_{\text{s}}}{\delta_{\text{n}}^2 + \delta_{\text{p}}^2} \right) \right],
$$

(3.54)

and

$$
C_{\text{exc2}}^{\text{out}} = \underset{T_3^{\text{so}} \leq \gamma_{\text{s}} \leq T_4^{\text{so}}}{\text{E}_{\gamma_{\text{s}}, \xi}} \left[\alpha \log \left(1 + \frac{\mathcal{P}\left(\gamma_{\text{s}}, \xi, \lambda_1^{\text{exc}}, \widehat{\delta_{\text{n}}^2}\right) \gamma_{\text{s}}}{\widehat{\delta_{\text{n}}^2}} \right) + \overline{\alpha} \log \left(1 + \frac{\mathcal{P}\left(\gamma_{\text{s}}, \xi, \lambda_1^{\text{exc}}, \widehat{\delta_{\text{n}}^2}\right) \gamma_{\text{s}}}{\widehat{\delta_{\text{n}}^2} + \delta_{\text{p}}^2} \right) \right]
$$

$$
+ \underset{\gamma_{\text{s}} > T_4^{\text{so}}}{\text{E}_{\gamma_{\text{s}}, \xi}} \left[\alpha \log \left(\frac{\delta_{\text{n}}^2 + Q_{\text{peak}} \gamma_{\text{s}}}{\widehat{\delta_{\text{n}}^2}} \right) + \overline{\alpha} \log \left(\frac{\delta_{\text{n}}^2 + \delta_{\text{p}}^2 + Q_{\text{peak}} \gamma_{\text{s}}}{\widehat{\delta_{\text{n}}^2} + \delta_{\text{p}}^2} \right) \right].
$$

(3.55)

Finally, the service-rate outage capacity expression of fading channels under average received-interference and peak transmit-power constraints with r_0 service-rate and P_0 probability of outage, can be expressed as shown in (3.56), where λ_1^{exc} is computed by substi-

tuting (3.52) into the interference constraint in (3.41b), for different values of $\lambda_{\min}^{\text{out}}$.

$$
\frac{C_{\text{ser}}^{\text{out}}}{B} = \begin{cases}
\text{Not Feasible} & \text{if } Q_{\text{inter}} < Q_{\text{inter}}^{\min} \text{ or } Q_{\text{peak}} < Q_{\text{peak}}^{\min}, \\
r_0 \left(1 - P_0 \right) & \text{otherwise if } Q_{\text{inter}} = Q_{\text{inter}}^{\min} \text{ or } Q_{\text{peak}} = Q_{\text{peak}}^{\min}, \\
r_0 \left(1 - P_0 \right) + C_{\text{exc2}}^{\text{out}} & \text{otherwise if } T_1^{\text{so}} \geq T_2^{\text{so}}, \\
r_0 \left(1 - P_0 \right) + C_{\text{exc2}}^{\text{out}} + C_{\text{exc1}}^{\text{out}} & \text{otherwise if } T_1^{\text{so}} < T_2^{\text{so}} \,\&\, T_3^{\text{so}} > T_2^{\text{so}}, \\
\dfrac{C_{\text{er}}}{B} & \text{otherwise if } T_3^{\text{so}} \leq T_2^{\text{so}}.
\end{cases}
$$

(3.56)

3.6   Numerical Results

In this section, we provide numerical results for the different capacity notions investigated in this chapter, namely, ergodic, *tifr*, outage and service-rate with/without outage, under constraints on the average received-interference and peak transmit-power for different fading channel distributions. The SU channel variations are modeled through Nakagami (nak) with unit-mean and fading parameter $m = 2$, Rayleigh (ray) with unit-mean, and Log-normal (log) with several values for the standard deviation: $\mathcal{K} = 4,\, 6,\, 8$ dB. We assume the CSI of the secondary link to be available at the ST, through an error-free feedback channel. The interference channel gain $\sqrt{\gamma_{\text{p}}}$ is also distributed according to Rayleigh PDF with unit variance, $d_{\text{p}} = 1$. Furthermore, the sensing detector is assumed to calculate the sensing information metric in an observation time $N = 30$, and the non-centrality parameter in $f_1(\xi)$ is set to unity ($\mu = 1$). About the PU's activity, we consider that the PU remains active 50% of the time ($\alpha = 0.5$), and set the PU's transmit power to $P_t = 1$. In the following, we assume $\delta_{\text{p}}^2 = 0.5$ and $\delta_{\text{n}}^2 = 1$.

In Figs. 3.6-3.8, we plot the ergodic, *tifr* and outage capacities (formulae (3.18), (3.22) and (3.24), respectively) as a function of the average interference limit, Q_{inter}, with $\rho = 1.5$, where $\rho = \frac{Q_{\text{peak}}}{Q_{\text{inter}}}$. In Fig. 3.8, the outage probability is given by $P_0 = 0.2$. By comparing the capacity plots in Figs. 3.6-3.8, we provide the following remarks and observations.

Considering Rayleigh and Nakagami ($m = 2$) fading channels, the capacity difference between these fading channels grows more in the *tifr* and outage capacities in comparison with the ergodic capacity. This implies that as the fading severity decreases (goes from Rayleigh to Nakagami), the capacity of the channel shows more improvement compared
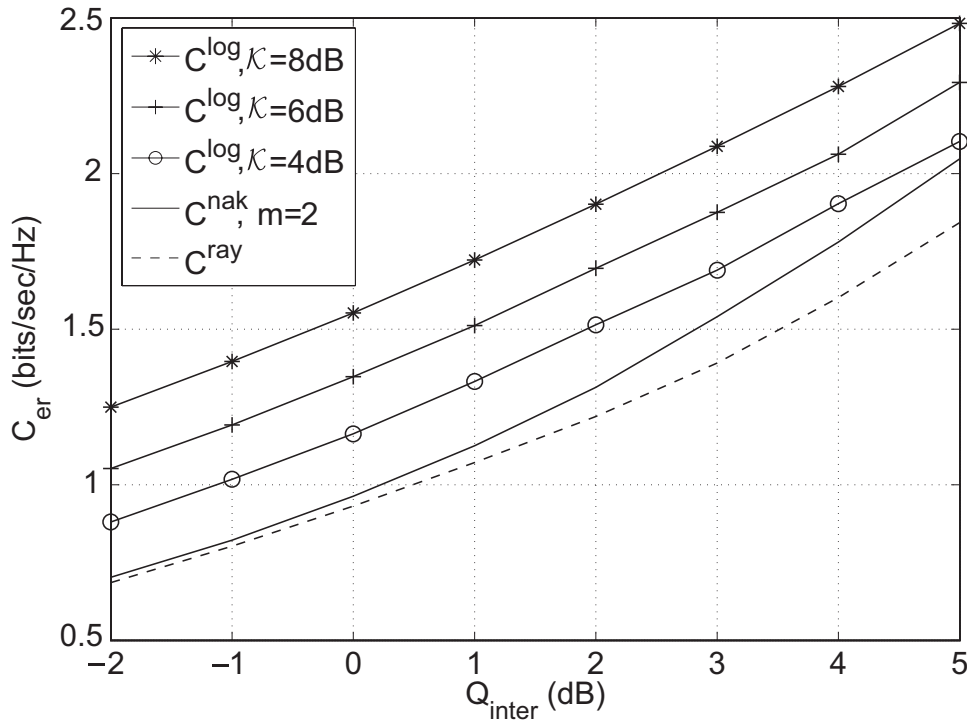
Figure 3.6: Ergodic capacity in different fading channel environments for $\rho = 1.5$.

to adaptive channel transmission policies, i.e., *tifr* and outage. On the other hand, for the Log-normal fading case, as the standard deviation increases, the probability of being in deep fading states also increases, and consequently results in a large amount of capacity penalty for Log-normal fading channels with high $\mathcal{K}$ under *tifr* and outage transmission strategies.

The service-rate capacity of fading channels: Rayleigh, Nakagami with $m = 2$ and Log-normal with standard deviation values of $\mathcal{K} = 6,\ 8$ dB, are shown in Figs. 3.9-3.10, as a function of the average interference limit Q_{inter} for several values of r_0. In these figures, we fix $\rho = 1.3$ and investigate the service-rate capacity with and without outage constraint. For the service-rate capacity with outage, we fix $P_0 = 0.2$, and for comparison purposes, we also plot the associated ergodic, outage and zero-outage capacities. As investigated in Section 3.5, the service-rate capacity varies between the outage and ergodic capacity results for different values of r_0. Furthermore, we observe that this capacity gradually increases from $r_0 (1 - P_0)$ in the outage capacity curve and converges to the ergodic capacity as Q_{inter} increases.
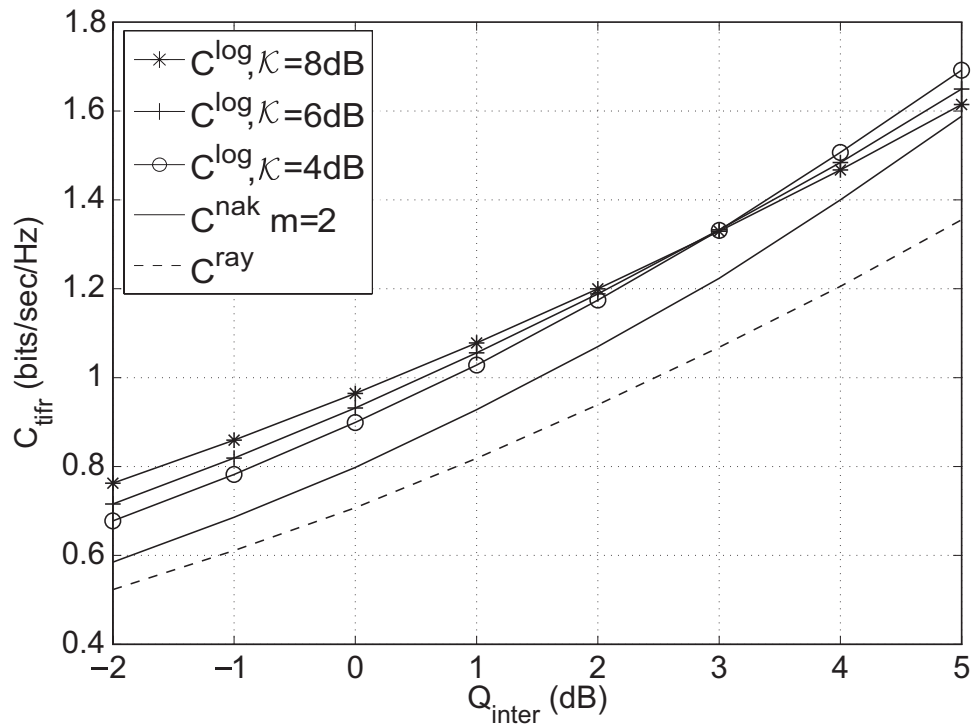
Figure 3.7: Truncated channel inversion with fixed-rate (*tifr*) capacity in different fading channel environments for $\rho = 1.5$.
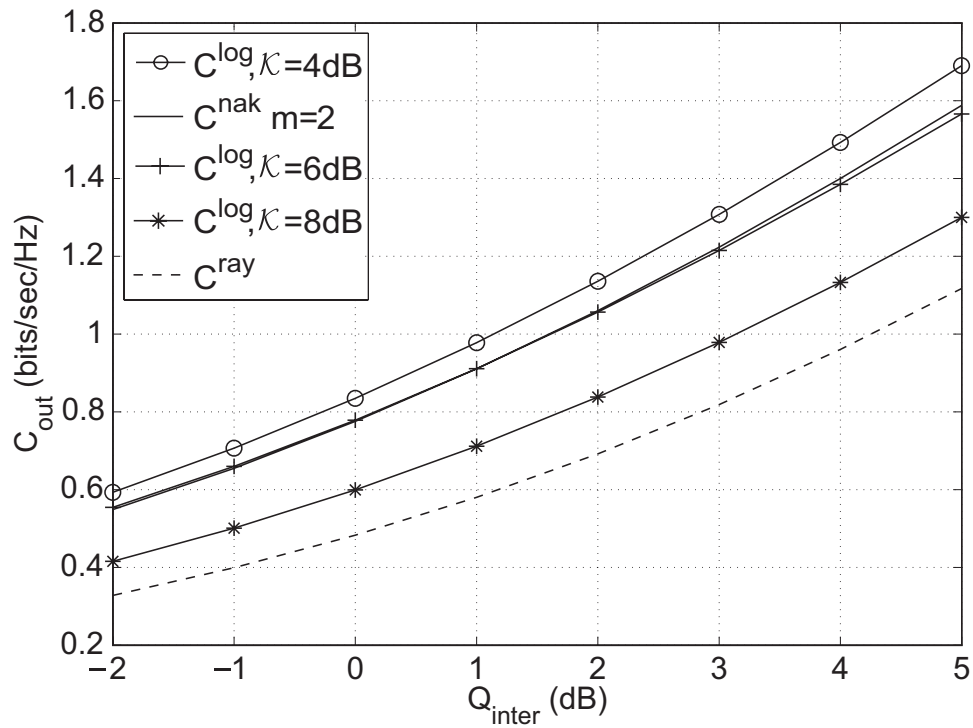
Figure 3.8: Outage capacity in different fading channel environments for $\rho = 1.5$ and $P_0 = 0.2$.
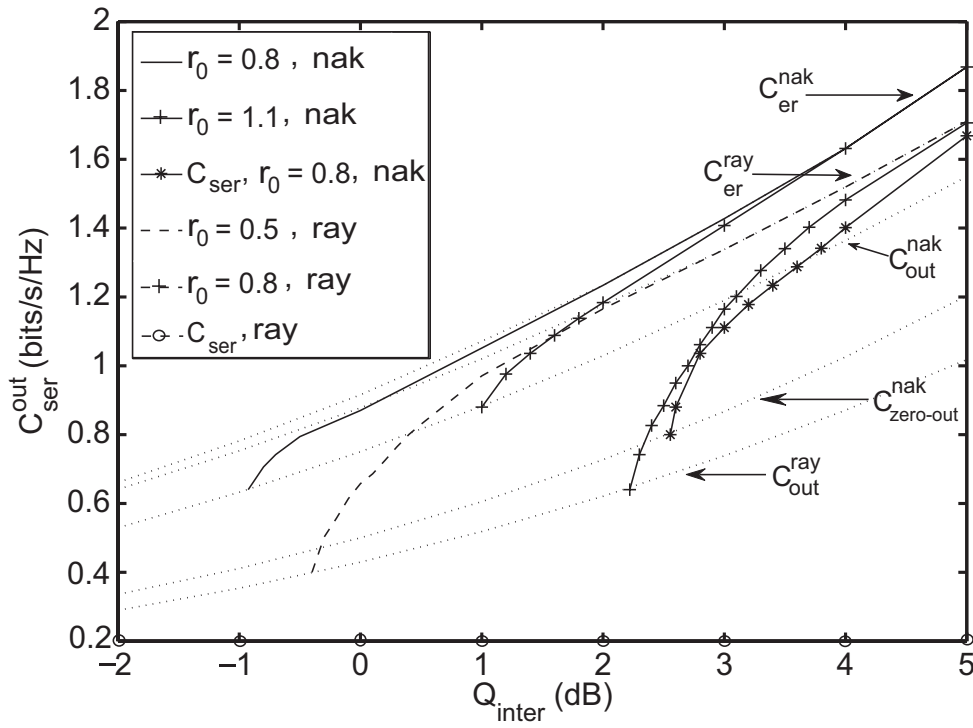
Figure 3.9: Service-rate capacity with/without outage in Rayleigh and Nakagami ($m = 2$) channel environments for $\rho = 1.3$, $P_0 = 0.2$, and $r_0 = 0.5$, 0.8 or 1.1 bits/sec/Hz.
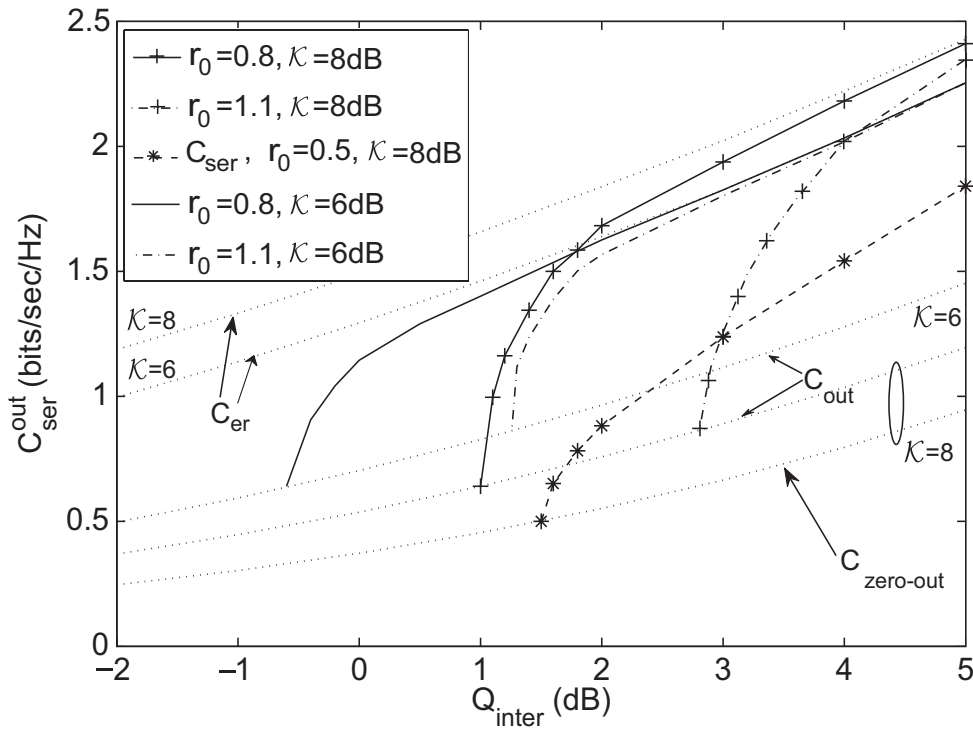
Figure 3.10: Service-rate capacity with/without outage in Log-normal channel environment with $\mathcal{K} = 6$, 8dB for $\rho = 1.3$, $P_0 = 0.2$, and $r_0 = 0.5$, 0.8 or 1.1 bits/sec/Hz.

3.7 Summary

In this chapter, we studied three capacity notions, namely, ergodic, delay-limited and service-rate (with and without outage), for CR spectrum-sharing systems operating under constraints on the average received-interference and peak transmit-power. We assumed that the transmission power of the SUs can be adapted based on availability of the SU's channel state information, and soft-sensing information about the PU's activity provided by the energy-based sensing detector at the SU transmitter. Specifically, we investigated the benefits of using different transmission policies pertaining to the three aforementioned capacity notions in CR communication systems.

Theoretical analysis besides numerical results and comparisons for different fading environments, have shown that each capacity notion has some features that can be used according to different system requirements. In particular, in this chapter, the service-rate capacity has been proposed as an appropriate capacity metric in CR networks which combines the advantages of the short- and long-term transmission strategies. In other words, we showed that the service-rate capacity not only guarantees the minimum required service-rate, but also allows using the excess power to increase the long-term achievable rate of CR users.

In the next chapter, we consider a primary/secondary spectrum-sharing system and study adaptive resource management in CR fading broadcast channels (BC). Specifically, we propose utilizing spectrum sensing information about the primary's activity at the secondary base station for an efficient allocation of the resources, namely, transmission time and power, to the SUs.

Chapter 4

Resource Management in CR Broadcast Channels[1]

4.1 Introduction

As mentioned earlier in Chapter 1.1.1, CR technology offers tremendous potential to improve the radio spectrum usage by efficiently reusing and sharing licensed spectrum bands while adhering to the interference limitations of their primary users. In this context, two main tasks in CR systems are considered as *spectrum sensing* and *spectrum access*.

Spectrum sensing consists of observing the radio spectrum band and processing observations in order to acquire information about the licensed-transmission in the shared spectrum band. Various spectrum sensing problems have been observed in the literature as presented in Chapters 2 and 3, and references [5–8]. In this regard, it has been shown in [6], that a conventional energy detector cannot guarantee accurate detection of primary signals because of the *hidden-terminal* problem. To alleviate this problem, a cooperative spectrum-sensing approach was proposed in [6] and [7] based on spectrum-aware sensor networking. In this technique, the CR network is designed such that the spectrum sensing devices are separated from the secondary users[2].

Spectrum access, on the other hand, consists of providing efficient allocation and man-

---

[1]Parts of this chapter were presented at the *IEEE Transactions on Communications*, vol. 59, no. 5, pp. 1446 – 1457, May 2011, and in Proc. *IEEE International Conference on Communications* (ICC'10), Cape Town, South Africa, May. 2010, pp. 1 – 5.

[2]More details about this technique will be provided later in this chapter.

agement of the available resources among the secondary users. Chief among the challenges in opportunistic CR networks is spectrum access [9]. Indeed, how to efficiently and fairly allocate the radio resources between secondary users in a CR network, is a fundamental problem (see e.g. [10–13]). This issue is similar to the broadcast channel (BC) problem in current wireless communication systems. In BC systems, typically and traditionally, CSI has been utilized to adaptively allocate the transmission resources such as time, power, bandwidth and rate, among users [26]. In particular, considering perfect CSI at the base station and receivers, the optimal time and power allocation policies that maximize the ergodic capacity of fading BCs was investigated in [26] under time division multiple access (TDMA). In spectrum-sharing CR networks, the problem of fair resource allocation among secondary users was investigated in [12, 13] subject to quality of service constraints at the secondary users and interference constraints at the primary receivers. In [64] and [65], the authors proposed resource adaptation schemes for users in a CR network equipped with multiple antennas under given interference constraints at the primary receivers. In the latter works, CSI is the only information based on which the base station decides how to distribute the resources between users.

In the cognitive radio broadcast channel (CR-BC) scenario presented in the WRAN standard [3], rather than channel information, the secondary (CR) base station may employ its observations about the surrounding environment to optimally allocate its resources, such as transmission time and power, between secondary users. In this chapter, while focusing on the capability of CR systems to sense the environment in which they operate, our objective is to obtain an optimal resource-sharing policy for CR-BC systems, based on local observations about the primary system activity around each secondary receiver. Our approach is novel relative to utilizing local soft-sensing information in order to determine which secondary user should have access to the shared spectrum band at each sensing state. The CR-BC network is limited by appropriate constraints on the average received-interference at the primary receiver and on the peak transmit-power at the secondary transmitter. We also implement a discrete sensing mechanism in order to limit the overall system complexity, without compromising the system performance significantly. In this scheme, we consider only restricted levels of primary activity for the sensing observations.

In detailing these contributions, the remainder of this chapter is organized as follows. In the next section, we present the CR-BC system under study along with the channel

model used. In Section 4.3, using soft-sensing information about the primary user activity, we obtain the optimal time-sharing and transmit power allocation policies for the CR-BC network. The discrete sensing mechanism is proposed in Section 4.4. Finally, numerical results followed by concluding remarks and a summary are presented in Sections 4.5 and 4.6, respectively. Throughout the chapter, boldface letters are used for vector notation, and $\mathrm{E}_x[\cdot]$ denotes the expectation of random variable x.

4.2 System and Channel Models

A classical broadcast channel (BC) scenario is considered for a spectrum-sharing CR network with one secondary transmitter (ST) as base station (BS) and K secondary receivers (SRs), as shown in Fig. 4.1. It is considered that the secondary BS is allowed to use the spectrum band originally assigned to a pair of primary transmitter and receiver (PT and PR), as long as it adheres to the PU activity level and satisfies predefined constraint on the average received-interference at the PR. In practice, the transmit power of the BS needs to be limited according to the operation range of power amplifiers. Thus, in addition to the aforementioned constraint, we limit the BS transmission policy by a peak transmit power constraint as well.

We assume a discrete-time flat-fading channel with perfect CSI at the secondary BS and receivers. Indeed, we assume that each SR is equipped with a channel estimator, as shown in Fig. 4.2, whose output is an estimate of the channel power gain associated with the corresponding BS-SR link. Furthermore, the CSI is assumed to be fed back to the BS for adaptive allocation purposes of the resources, namely, transmission time and power, among the SUs in the CR-BC network. We define the channel gain between the BS and the k-th SR by $\sqrt{h_k[i]}$, where $k = 1, \cdots, K$ and i denotes the time index. In the CR-BC network, mathematically, the received signal for the k-th user, $\mathrm{y}_k[i]$, depends on the transmitted signal $\mathrm{x}[i]$ as follows:

$$\mathrm{y}_k[i] = \sqrt{h_k[i]}\mathrm{x}[i] + \mathrm{n}_k[i], \ \ \forall k = 1, 2, \cdots, K,$$

where $\mathrm{n}_k[i]$ denotes the additive Gaussian noise at the k-th SR. Channel knowledge is needed by the SRs for coherent detection of the transmitted signal. We consider that the variations of $\sqrt{h_k[i]}$ follow Rayleigh fading distribution with mean $\mathrm{E}[h_k]$.
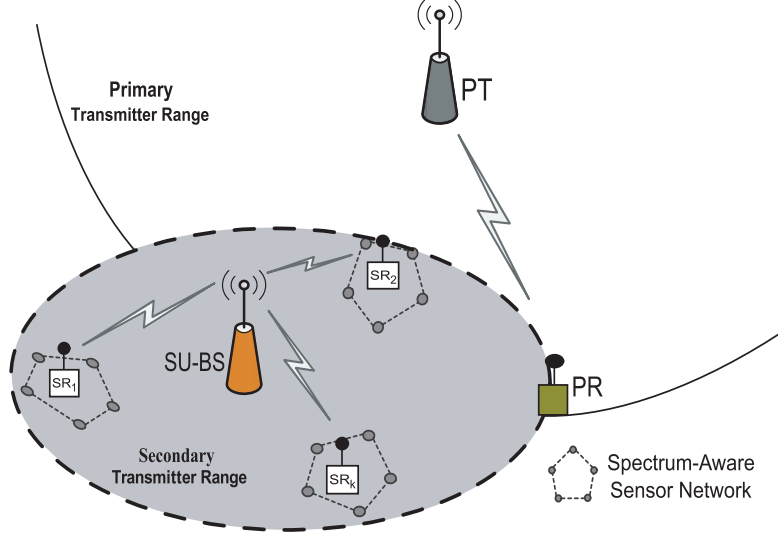
Figure 4.1: Spectrum-sharing system configuration.

We define the channel gain between the secondary BS and the PR by $\sqrt{q[i]}$, which we also use to refer to the interference channel. We consider that all the channel power gains, i.e., $\mathbf{h} = [h_1, h_2, \cdots, h_K]$[3] and q, are independent. We also consider that q is modeled by a Rayleigh fading distribution[4] with a variance that depends on the distance between the secondary BS and the PR, i.e., $(1/d_q)^2$. Channel gains are assumed to be stationary, ergodic and mutually independent from the noise. We further assume that the additive noise at each SR (including interference from the PU link) is modeled as zero-mean Gaussian random variable with equal variance of N_0B, where N_0 and B denote the noise power spectral density and the signal bandwidth, respectively.

The PU's link is modeled as a stationary block-fading channel with coherence time T_c. As such, the channel power gain (square of the channel gain absolute value) remains constant over T_c time epochs, after which it takes a new independent value. We assume a block-static model for the activity of the PT, with a coherence interval of T_c. In other words, for a period of T_c channel uses (one block), the activity state of the PT remains unchanged. Based on this model, it is assumed the PT remains active (ON state) with probability α, or inactive (OFF state) with probability $\bar{\alpha} = 1 - \alpha$, in T_c time periods.

---

[3]Hereafter, we omit the time index as it is clear from the context.

[4]Note that we just select a fading PDF and this does not mean that we have perfect knowledge of q at the ST.
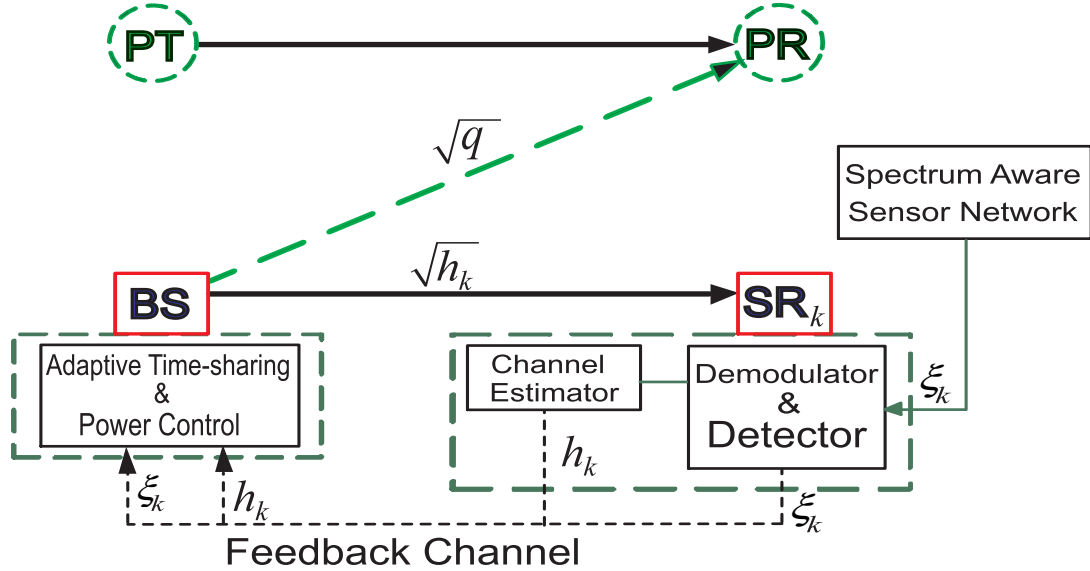
Figure 4.2: System model: elements and building blocks.

It is assumed that statistical information about the PT's activity is available at the secondary BS and SRs. As shown in Fig. 4.2, each SR communicates with a spectrum-aware sensor network (SASN) whose function is to determine the activity of the PT in its neighboring area. The SASN acts as a dedicated sensor network which is separated from the SUs and built by the secondary service provider to perform the sensing about the PT activity [6]. More specifically, each SASN is composed of a set of sensors distributed in the desired area, with the ability to sense the PT's activity in said area, and to report the sensing information to a sink node [58]. The latter can further process the information received from all sensors to calculate a single sensing metric, ξ, and then pass it to the SR[5]. We consider that the statistics of ξ, conditioned on the PT's activity being in ON or OFF states, which is called *sensing information*, are known a priori to the SRs. We define the probability density functions (PDF) of ξ_k, $k = 1, \cdots, K$, given that the PT is ON or OFF, by $f_k^{\mathrm{on}}(\xi)$ and $f_k^{\mathrm{off}}(\xi)$ respectively. The sensing information provided at each SR is assumed to be fed back to the BS[6]. This information can be utilized for adaptive time and power adaptation

---

[5]Details about the detection mechanism adopted by the SASN nodes are beyond the scope of this thesis. However, the readers are referred to [6] and [7] for further details. The impact of spectrum sensing errors on the performance of CR systems can be studied in terms of the probabilities of *mis-detection* and *false alarm*, which can further affect the estimation of the PT status, i.e., the ON or OFF states, as considered in [55].

[6]This information may be sent back to the BS through the available feedback channel for the CSI knowledge.

purposes at the secondary BS in order to improve the performance of the CR-BC network, which is the main contribution of this work.

At the sensors, we adopt the conventional energy-detection technique which was previously proven to be more energy-efficient and practical in sensor networking applications [7]. Let $\mathfrak{F}$ denote the vector of sensing observations pertaining to the K SRs, i.e., $\mathfrak{F} = [\xi_1, \xi_2, \cdots, \xi_K]$. Now, conditioned on the PT being ON or OFF, the components of $\mathfrak{F}$ are calculated based on the sum of i.i.d. Gaussian random variables and, consequently, are distributed according to Chi-square PDFs, each with M degrees of freedom, where M is the number of observation samples in each sensing interval [45]. Accordingly, under "PT is ON" condition, ξ_k has a noncentral Chi-square distribution with variance $\sigma_k^2 = 1$ and non-centrality parameter μ_k[7] [61]. Similarly, under "PT is OFF" condition, ξ_k will be distributed according to central Chi-square PDF. Thus, we define

$$
\begin{cases}
f_k^{\text{on}}(\xi) = \dfrac{1}{2} \left(\dfrac{\xi_k}{\mu_k} \right)^{\frac{M-2}{4}} e^{-\frac{\mu_k + \xi_k}{2}} I_{\frac{M}{2}-1} \left(\sqrt{\mu_k \xi_k} \right), & \text{PU is ON} \\[3mm]
f_k^{\text{off}}(\xi) = \dfrac{\xi_k^{\frac{M}{2}-1}}{2^{\frac{M}{2}} \Gamma \left(\dfrac{M}{2} \right)} \, e^{-\frac{\xi_k}{2}}, & \text{PU is OFF}
\end{cases}
\tag{4.1}
$$

where $I_\nu(\cdot)$ is the νth-order modified Bessel function of the first kind, and $\Gamma(\cdot)$ is the Gamma function [51]. We consider the above PDFs as the soft-sensing information (SSI) about the PT activity, which is periodically updated during each sensing period.

4.3   Ergodic Capacity of Cognitive Radio Broadcast Channels

In this section, considering that the secondary BS and receivers have perfect CSI and SSI pertaining to the PT's activity, the ergodic capacity of CR fading BC and the associated optimal power and time allocation policies are investigated assuming time division (TD) multiple access. At a given time slot, the network state is defined by a pair $(\mathbf{h}, \mathfrak{F})$, where $\mathbf{h}$ and $\mathfrak{F}$ denote the channel gain and sensing observation vectors corresponding to the

---

[7]The non-centrality parameter, μ_k, can be obtained in terms of the ratio of PT's signal energy to the noise spectral density, as detailed in [45].

K secondary users, respectively. Under a TD strategy and in a given network state, a fraction of time, $\tau_k^{h,\xi}$, is assigned for transmission to the k-th SR subject to the constraint $\sum_{k=1}^{K} \tau_k^{h,\xi} = 1$ with $0 \leq \tau_k^{h,\xi} \leq 1$. As mentioned before, the secondary transmission is constrained by limitations on the average-interference at the PR and peak transmit-power at the secondary BS, formulated by

$$\mathbb{F} \triangleq \begin{cases} \mathrm{E}_{\mathbf{h},q,\mathfrak{F}|\mathrm{PT\,is\,ON}} \left[\sum_{k=1}^{K} \tau_k^{h,\xi} S_k^{h,\xi} q \right] \leq Q^{\mathrm{I}}, \\ S_k^{h,\xi} \leq Q^{\mathrm{P}}, \quad \forall\, k = 1, 2, \cdots, K, \end{cases} \tag{4.2}$$

where $S_k^{h,\xi}$ is the transmit power allocated to user k ($k = 1, 2, \cdots, K$) for channel state, h, and sensing information, ξ, and Q^{I}, Q^{P} denote the interference and peak power limit values, respectively. Now, let $\mathcal{S}$ be the set of all possible power and time allocation policies satisfying $\mathbb{F}$. Then, the ergodic capacity of the CR-BC network under the above-defined resource constraints can be expressed as follows (see e.g., [26]):

$$C^{\mathrm{BC}} = \max_{\mathcal{S} \in \mathbb{F}} \left\{ C\left(\mathcal{S}\right) \right\}, \tag{4.3}$$

where

$$C\left(\mathcal{S}\right) = \left\{ \mathbf{R} : \ R_k \leq \mathrm{E}_{\mathbf{h},\mathfrak{F}} \left[\tau_k^{h,\xi} B \log_2 \left(1 + \frac{S_k^{h,\xi} h_k}{N_0 B} \right) \right], \forall\, 1 \leq k \leq K \right\}. \tag{4.4}$$

It is easy to show that the capacity expression in (4.4) is a convex function[8]. Thus, for optimal transmission, we decompose the above maximization problem with respect to the capacity expression in (4.4) and the constraint set $\mathbb{F}$. We first assume that the total transmit power $S^{h,\xi}$ at the BS which is assigned to the K users, is distributed between these users according to the time allocation $\mathbf{T}^{h,\xi} = \left[\tau_1^{h,\xi}, \tau_2^{h,\xi}, \cdots, \tau_k^{h,\xi} \right]$, i.e., $S^{h,\xi} = \sum_{k=1}^{K} \tau_k^{h,\xi} S_k^{h,\xi}$ for a given power vector $\mathbf{S}^{h,\xi} = \left[S_1^{h,\xi}, S_2^{h,\xi}, \cdots, S_K^{h,\xi} \right]$. Then, due to the convexity of the capacity region, we determine the optimum time-sharing coefficient set $\mathbf{T}^{h,\xi}$ that maximizes the total rate in a given network state defined by the channel and sensing vectors $(\mathbf{h}, \mathfrak{F})$[9]. For this purpose, we define the following optimization problem in

---

[8]Convexity of the capacity region can be easily proved for this case by following the approach in [26, Appendix-Sec. B].

[9]Note that whereas in [26] the fading variation was investigated in broadcast channels, in this chapter we investigate the variation of the sensing metric while the channel state is fixed. In addition, our results also

(4.5):

$$\mathfrak{J}^1_{\mathrm{BC}}\left(\mathbf{S}^{h,\xi}\right) = \max_{\mathbf{T}^{h,\xi}} \sum_{k=1}^{K} \tau_k^{h,\xi}\left(\alpha f_k^{\mathrm{on}}(\xi)\log_2\left(1+\frac{S_k^{h,\xi}h_k}{N_0 B}\right) + \bar{\alpha} f_k^{\mathrm{off}}(\xi)\log_2\left(1+\frac{S_k^{h,\xi}h_k}{N_0 B}\right)\right).$$
$$\text{s.t.} \begin{cases} \sum_{k=1}^{K}\tau_k^{h,\xi}S_k^{h,\xi} = S^{h,\xi} \\ \sum_{k=1}^{K}\tau_k^{h,\xi} = 1 \end{cases}$$
$$\tag{4.5}$$

In the next step, we apply the Lagrangian optimization technique to maximize $\mathfrak{J}^1_{\mathrm{BC}}\left(\mathbf{S}^{h,\xi}\right)$ over all channel states and sensing values, subject to the constraints in $\mathbb{F}$. For this purpose, we adopt the Lagrangian decomposition method proposed in [66]. Notice that the maximization problem in (4.3) has decoupled constraints. Therefore, we separate the problem into two parts. At first, we arrange the Lagrangian objective function considering the interference constraint as shown in (4.6), where λ denotes the Lagrangian multiplier.

$$\mathfrak{J}^2_{\mathrm{BC}}\left(\mathbf{S}^{h,\xi},\lambda\right) = \mathrm{E}_{\mathbf{h},\mathfrak{F}}\left[\mathfrak{J}^1_{\mathrm{BC}}\left(\mathbf{S}^{h,\xi}\right)\right] - \lambda\left(\mathrm{E}_{\mathbf{h},q,\mathfrak{F}|\mathrm{PT\,is\,ON}}\left[\sum_{k=1}^{K}\tau_k^{h,\xi}S_k^{h,\xi}q\right] - Q^{\mathrm{I}}\right). \quad (4.6)$$

Then, applying the decomposition method, we perform the maximization subject to the peak transmit-power constraint, according to:

$$\Lambda\left(\lambda\right) = \max_{\mathbf{S}^{h,\xi}} \mathfrak{J}^2_{\mathrm{BC}}\left(\mathbf{S}^{h,\xi},\,\lambda\right)$$
$$\text{s.t.} \begin{cases} S_k^{h,\xi} \le Q^{\mathrm{P}}, \\ S_k^{h,\xi} \ge 0, \end{cases} \quad \forall\, k = 1,\cdots,K. \tag{4.7}$$

Finally, the optimal power allocation policy that maximizes the total transmission rate in TD cognitive radio broadcast channels can be obtained by applying the necessary KKT conditions.

Next, we apply the above procedure to obtain the optimal power and time allocation policies in the scenario with two SRs. Then, we generalize our results for the case with $K > 2$ SRs.

---

deal with the joint variations of the fading channel and the sensing metric.

4.3.1 System with $K = 2$ SRs

Consider a two-user CR-BC system with a total transmit power $S^{h,\xi}$. We assume that the optimal time-sharing policy between cognitive users is given by $\tau_1^{h,\xi} S_1^{h,\xi} + \tau_2^{h,\xi} S_2^{h,\xi} = S^{h,\xi}$, where $\tau_1^{h,\xi} = \tau^{h,\xi}$, $\tau_2^{h,\xi} = 1 - \tau^{h,\xi}$, and $S_1^{h,\xi}$ and $S_2^{h,\xi}$ are the powers used for transmission to *user-1* and *user-2*, respectively. In order to obtain the optimal time-sharing policy in (4.5) which maximizes the total achievable rate, we assume assignment of more time resources to the user that can yield a higher transmission rate under the available transmit power budget. Indeed, for given values of h_k and ξ_k, $k = 1, 2, \cdots, K$, the user that yields a higher rate has priority to be serviced in these channel and sensing states. Mathematically, define the instantaneous achievable rate function for the k-th user as[10]

$$r_k\left(\cdot\right) \triangleq \gamma_k\left(\xi\right) \log_2\left(1 + \frac{S_k h_k}{N_0 B}\right), \tag{4.8}$$

where $\gamma_k\left(\xi\right) = \alpha f_k^{\mathrm{on}}(\xi) + \bar{\alpha} f_k^{\mathrm{off}}(\xi)$ and $0 \leq \gamma_k\left(\xi\right) \leq 1$. Furthermore, let $\Delta\left(S\right) \triangleq r_1\left(S\right) - r_2\left(S\right)$, whose derivative with respect to S can be obtained as,

$$\begin{aligned}
\frac{\partial \Delta\left(S\right)}{\partial S} &= \frac{\partial r_1\left(S\right)}{\partial S} - \frac{\partial r_2\left(S\right)}{\partial S} \\
&= \frac{\gamma_1\left(\xi\right) h_1}{N_0 B + h_1 S} - \frac{\gamma_2\left(\xi\right) h_2}{N_0 B + h_2 S} \\
&= \frac{\left(\gamma_1\left(\xi\right) h_1 - \gamma_2\left(\xi\right) h_2\right) N_0 B + \left(\gamma_1\left(\xi\right) - \gamma_2\left(\xi\right)\right) h_1 h_2 S}{\left(N_0 B + h_1 S\right)\left(N_0 B + h_2 S\right)}.
\end{aligned} \tag{4.9}$$

Now, supposing that $h_2 > h_1$ and based on the variation of sensing parameters $\gamma_1\left(\xi\right)$ and $\gamma_2\left(\xi\right)$, the following conditions are distinguished.

1) When $\gamma_1\left(\xi\right) h_1 \geq \gamma_2\left(\xi\right) h_2$ for some values of $\left(h_1, \xi_1\right)$ and $\left(h_2, \xi_2\right)$, then considering that $h_2 > h_1$, it is easy to show that $\gamma_1\left(\xi\right) > \gamma_2\left(\xi\right)$. As such, substituting these conditions into (4.9), we obtain

$$\frac{\partial \Delta\left(S\right)}{\partial S} = \frac{\partial r_1\left(S\right)}{\partial S} - \frac{\partial r_2\left(S\right)}{\partial S} > 0, \tag{4.10}$$

i.e., $\frac{\partial r_1\left(S\right)}{\partial S} > \frac{\partial r_2\left(S\right)}{\partial S}$. Since $r_1\left(S\right)$ and $r_2\left(S\right)$ are both increasing functions of S, it follows that $r_1\left(S\right) > r_2\left(S\right)$ for $S > 0$. Accordingly, *user-1* is selected for the

---

[10]Hereafter and for simplicity, we omit the random variables h and ξ whenever it is clear from the context.

transmission and (4.5) reduces to

$$\mathfrak{J}_{\mathrm{BC}}^1\left(\mathbf{S}\right) = r_1\left(S\right). \tag{4.11}$$

It is worth nothing that, in this case, despite the fact that h_2 is stronger than h_1, *user-1* is selected for the transmission because of the lower PT's activity in its adjacent area, i.e., $\gamma_1\left(\xi\right) \geq \gamma_2\left(\xi\right)$. Finally, the optimal time and power allocation policy in this case can be expressed as

$$\begin{cases} \tau_1^{h,\xi} = 1, & \tau_2^{h,\xi} = 0, \\ S_1^{h,\xi} = S^{h,\xi}, & S_2^{h,\xi} = 0. \end{cases} \tag{4.12}$$

2) When $\gamma_1\left(\xi\right) h_1 \;<\; \gamma_2\left(\xi\right) h_2$ for some values of (h_1, ξ_1) and (h_2, ξ_2), substituting this condition into (4.9), the solution to the maximization problem in (4.5) can be characterized by the following cases:

Case a: Assume that $\gamma_1\left(\xi\right) \;>\; \gamma_2\left(\xi\right)$ for some values of ξ_1 and ξ_2. Using (4.9), it is easy to show that for S high enough, $\dfrac{\partial \Delta\left(S\right)}{\partial S} > 0$, i.e., $\dfrac{\partial r_1\left(S\right)}{\partial S} > \dfrac{\partial r_2\left(S\right)}{\partial S}$, and since $r_1\left(S\right)$ and $r_2\left(S\right)$ are increasing functions of S, we have $r_1\left(S\right) > r_2\left(S\right)$. Accordingly, *user-1* is selected for the transmission and $\mathfrak{J}_{\mathrm{BC}}^1\left(\mathbf{S}\right) = r_1\left(S\right)$. Then, the optimal time and power allocation policy can be illustrated by

$$\begin{cases} \tau_1^{h,\xi} = 1, & \tau_2^{h,\xi} = 0, \\ S_1^{h,\xi} = S^{h,\xi}, & S_2^{h,\xi} = 0. \end{cases} \tag{4.13}$$

Case b: When $\gamma_1\left(\xi\right) < \gamma_2\left(\xi\right)$ for some values of ξ_1 and ξ_2, similar to Case a, substituting this condition into (4.9), we obtain $\dfrac{\partial \Delta\left(S\right)}{\partial S} < 0$, i.e., $\dfrac{\partial r_2\left(S\right)}{\partial S} > \dfrac{\partial r_1\left(S\right)}{\partial S}$. Accordingly, $r_2\left(S\right) > r_1\left(S\right)$ and, thus, *user-2* is selected for the transmission at the BS. Finally, it is easy to show that $\mathfrak{J}_{\mathrm{BC}}^1\left(\mathbf{S}\right) = r_2\left(S\right)$, and the optimal allocation policy can be expressed as

$$\begin{cases} \tau_1^{h,\xi} = 0, & \tau_2^{h,\xi} = 1, \\ S_1^{h,\xi} = 0, & S_2^{h,\xi} = S^{h,\xi}. \end{cases} \tag{4.14}$$

Case c: Other than the above cases, assume that at some power values, we have

$\frac{\partial r_1\left(S_b\right)}{\partial S} = \frac{\partial r_2\left(S_a\right)}{\partial S} = \Psi^{11}$, where $S_a, S_b > 0$. By appropriate substitution into (4.9), we have

$$
\begin{cases}
\Psi = \dfrac{\partial r_1\left(S_b\right)}{\partial S} = \dfrac{\gamma_1\left(\xi\right)h_1}{N_0 B + h_1 S_b}, \\[3mm]
\Psi = \dfrac{\partial r_2\left(S_a\right)}{\partial S} = \dfrac{\gamma_2\left(\xi\right)h_2}{N_0 B + h_2 S_a},
\end{cases}
\tag{4.15}
$$

which, after simple manipulation, yields

$$
\begin{cases}
S_a = \dfrac{\gamma_2\left(\xi\right)}{\Psi} - \dfrac{N_0 B}{h_2}, \\[3mm]
S_b = \dfrac{\gamma_1\left(\xi\right)}{\Psi} - \dfrac{N_0 B}{h_1},
\end{cases}
\tag{4.16}
$$

where Ψ is the slope of the straight line between the pairs $\left(r_1\left(S_b\right), S_b\right)$ and $\left(r_2\left(S_a\right), S_a\right)$, i.e.,

$$
\Psi = \frac{r_2\left(S_a\right) - r_1\left(S_b\right)}{S_a - S_b}.
\tag{4.17}
$$

It is worth noting that Ψ is calculated by substituting (4.16) into (4.17). Furthermore, it is easy to show that for power values satisfying $S_a < S < S_b$, the maximum total transmission rate increases linearly, as $\mathfrak{J}^1_{\mathrm{BC}}\left(\mathbf{S}\right) = \Psi\left(S - S_a\right) + r_2\left(S_a\right)$. Accordingly, in this case, making use of the time-sharing approach, both users are selected in the transmission process with the power levels obtained in (4.16), i.e., $\tau S_b + \left(1 - \tau\right)S_a = S$, where τ is given by $\tau = \dfrac{S_a - S}{S_a - S_b}$. Finally, the optimal time and power allocation policy can be expressed as:

$$
\begin{cases}
\tau_1^{h,\xi} = \dfrac{S_a^{h,\xi} - S^{h,\xi}}{S_a^{h,\xi} - S_b^{h,\xi}}, \quad \tau_2^{h,\xi} = \dfrac{S^{h,\xi} - S_b^{h,\xi}}{S_a^{h,\xi} - S_b^{h,\xi}}, \\[3mm]
S_1^{h,\xi} = S_b^{h,\xi}, \qquad\qquad S_2^{h,\xi} = S_a^{h,\xi}.
\end{cases}
\tag{4.18}
$$

Now, using the results obtained in Cases *a*, *b* and *c*, we can express the solution to

---

[11]$\dfrac{\partial \Delta\left(S\right)}{\partial S} = 0.$

the maximization problem in (4.5) when $\gamma_1 \left(\xi \right) h_1 < \gamma_2 \left(\xi \right) h_2$, as follows:

$$\mathfrak{J}_{\mathrm{BC}}^1 \left(\mathbf{S}^{h,\xi} \right) = \begin{cases} r_2 \left(S^{h,\xi} \right), & 0 < S^{h,\xi} \leq S_a^{h,\xi}, \\ \Psi \left(S^{h,\xi} - S_a^{h,\xi} \right) + r_2 \left(S_a^{h,\xi} \right), & S_a^{h,\xi} < S^{h,\xi} < S_b^{h,\xi}, \\ r_1 \left(S^{h,\xi} \right), & S^{h,\xi} \geq S_b^{h,\xi}. \end{cases} \qquad (4.19)$$

As shown in this case, if $S_a < S < S_b$, using time-sharing, both users will have contribution in the transmission process and $\mathfrak{J}_{\mathrm{BC}}^1 \left(\mathbf{S}^{h,\xi} \right)$ can achieve the values between $r_2 \left(S^{h,\xi} \right)$ and $r_1 \left(S^{h,\xi} \right)$ on the straight line. But, for $0 < S < S_a$ or $S \geq S_b$, $\mathfrak{J}_{\mathrm{BC}}^1 \left(\mathbf{S}^{h,\xi} \right)$ is simply $r_2 \left(S^{h,\xi} \right)$ or $r_1 \left(S^{h,\xi} \right)$, respectively.

In the following, we solve the maximization problem in (4.7) in order to obtain the optimal power allocation policy pertaining to *user-1* and *user-2* at the secondary BS, under average received-interference and peak transmit-power constraints (4.2). Specifically, using the previously explained decomposition method, we obtain the optimal power allocation policy for each of the solutions in (4.11) and (4.19), such that the achievable rate of the CR-BC network is maximized.

1) $\gamma_1 \left(\xi \right) h_1 \geq \gamma_2 \left(\xi \right) h_2$: In this case, $\mathfrak{J}_{\mathrm{BC}}^1 \left(\mathbf{S}^{h,\xi} \right) = r_1 \left(S^{h,\xi} \right)$. In order to solve the maximization problem in (4.7), the dual objective function $\Lambda \left(\lambda \right)$ for any h and ξ states can be rewritten as

$$\begin{aligned} \Lambda \left(\lambda \right) = \max_{S_1^{h,\xi}} \Bigg\{ & \mathrm{E}_{\mathbf{h},\,\mathfrak{F}} \left[\gamma_1 \left(\xi \right) \log_2 \left(1 + \frac{S_1^{h,\xi} h_1}{N_0 B} \right) \right] \\ & - \lambda \left(\mathrm{E}_{\mathbf{h},\mathfrak{F}|\mathrm{PT\,is\,ON}} \left[S_1^{h,\xi} \left(\frac{1}{d_q} \right)^2 \right] - Q^{\mathrm{I}} \right) \Bigg\}, \qquad (4.20) \\ \mathrm{s.t.}\ & S_1^{h,\xi} \leq Q^{\mathrm{P}}, \\ & S_1^{h,\xi} \geq 0. \end{aligned}$$

To solve the maximization problem in (4.20), adopting the Lagrangian optimization technique presented in [52], the necessary KKT conditions corresponding to the in-

terference and power constraints in $\mathbb{F}$ can be obtained as follows:

$$\frac{\gamma_1\left(\xi\right)h_1}{N_0 B + S_1^{h,\xi}h_1} - \lambda\left(\frac{1}{d_q}\right)^2 f_1^{\mathrm{on}}(\xi) + \lambda_1' - \lambda_1'' = 0, \qquad (4.21\mathrm{a})$$

$$\lambda_1' S_1^{h,\xi} = 0, \qquad (4.21\mathrm{b})$$

$$\lambda_1''\left(S_1^{h,\xi} - Q^{\mathrm{P}}\right) = 0, \qquad (4.21\mathrm{c})$$

where λ_1' and λ_1'' are the Lagrangian multipliers.

The optimal secondary transmit power can take values satisfying $0 \leq S_1^{h,\xi} \leq Q^{\mathrm{P}}$. First, assume that $S_1^{h,\xi} = 0$. Then, equations (4.21b) and (4.21c) require that $\lambda_1' \geq 0$ and $\lambda_1'' = 0$, respectively. Substituting these conditions into (4.21a) implies the following condition:

$$\frac{N_0 B}{h_1} > \chi_1\left(\xi\right), \qquad (4.22)$$

where $\chi_i\left(\xi\right)$, $i = 1, 2, \cdots, K$, is defined as

$$\chi_i\left(\xi\right) \triangleq \frac{d_q^2 \gamma_i\left(\xi\right)}{\lambda f_i^{\mathrm{on}}(\xi)} \qquad (4.23\mathrm{a})$$

$$= \frac{d_q^2}{\lambda}\left(\alpha + \bar{\alpha}\frac{f_i^{\mathrm{off}}(\xi)}{f_i^{\mathrm{on}}(\xi)}\right). \qquad (4.23\mathrm{b})$$

Assume that $S_1^{h,\xi} = Q^{\mathrm{P}}$. In this case, the conditions presented in (4.21b) and (4.21c) imply $\lambda_1' = 0$ and $\lambda_1'' \geq 0$, respectively. Further, substitution into (4.21a) yields:

$$\frac{N_0 B}{h_1} < \chi_1\left(\xi\right) - Q^{\mathrm{P}}. \qquad (4.24)$$

Finally, suppose that $0 < S_1^{h,\xi} < Q^{\mathrm{P}}$. Then, (4.21b) and (4.21c) imply that $\lambda_1' = \lambda_1'' = 0$, which according to (4.21a) and after simple manipulation yield the optimal transmit power given by:

$$S_1^{h,\xi} = \chi_1\left(\xi\right) - \frac{N_0 B}{h_1}. \qquad (4.25)$$

Hence, according to the results presented in (4.22), (4.24) and (4.25), the optimal power allocation policy pertaining to the secondary BS given that $\gamma_1\left(\xi\right)h_1 \geq \gamma_2\left(\xi\right)h_2$,

is expressed as:

$$S_1^{h,\xi} = \begin{cases} Q^{\mathrm{P}}, & \dfrac{N_0 B}{h_1} < \chi_1(\xi) - Q^{\mathrm{P}}, \\[2mm] \chi_1(\xi) - \dfrac{N_0 B}{h_1}, & \chi_1(\xi) - Q^{\mathrm{P}} \leq \dfrac{N_0 B}{h_1} \leq \chi_1(\xi), \\[2mm] 0, & \dfrac{N_0 B}{h_1} > \chi_1(\xi), \end{cases} \qquad (4.26)$$

where parameter $\chi_1(\xi)$ must satisfy the interference constraint at equality, according to:

$$\begin{aligned} Q^{\mathrm{I}} &= \mathrm{E}_{\mathbf{h},\mathfrak{F}|\mathrm{PT\,is\,ON}}\left[S_1^{h,\xi}\left(\frac{1}{d_q}\right)^2 \right] \\ &= \underset{\chi_1(\xi)-Q^{\mathrm{P}} \leq \frac{N_0 B}{h_1} \leq \chi_1(\xi)}{\mathrm{E}_{\mathbf{h},\mathfrak{F}|\mathrm{PT\,is\,ON}}}\left[\frac{\chi_1(\xi)}{d_q^2} - \frac{N_0 B}{d_q^2 h_1} \right] + \underset{\frac{N_0 B}{h_1} < \chi_1(\xi)-Q^{\mathrm{P}}}{\mathrm{E}_{\mathbf{h},\mathfrak{F}|\mathrm{PT\,is\,ON}}}\left[\frac{Q^{\mathrm{P}}}{d_q^2} \right]. \qquad (4.27) \end{aligned}$$

2) $\gamma_1(\xi) h_1 < \gamma_2(\xi) h_2$: To determine the optimal power allocation policy in this case, we recall our previous result in (4.19). Accordingly, we characterize the transmission policy while $\gamma_1(\xi) h_1 < \gamma_2(\xi) h_2$ by the following cases:

Case a: $\mathfrak{J}_{\mathrm{BC}}^1\left(\mathbf{S}^{h,\xi}\right) = r_2\left(S^{h,\xi}\right)$. In this case, to solve the maximization problem in (4.7), the dual objective function $\Lambda(\lambda)$ for any h and ξ states is rewritten as

$$\begin{aligned} \Lambda(\lambda) = \max_{S_2^{h,\xi}} &\left\{ \mathrm{E}_{\mathbf{h},\mathfrak{F}}\left[\gamma_2(\xi) \log_2\left(1 + \frac{S_2^{h,\xi} h_2}{N_0 B}\right) \right] \right. \\ &\left. - \lambda\left(\mathrm{E}_{\mathbf{h},\mathfrak{F}|\mathrm{PT\,is\,ON}}\left[S_2^{h,\xi}\left(\frac{1}{d_q}\right)^2 \right] - Q^{\mathrm{I}} \right) \right\}, \qquad (4.28) \\ \text{s.t.}\ \ &S_2^{h,\xi} \leq Q^{\mathrm{P}}, \\ &S_2^{h,\xi} \geq 0. \end{aligned}$$

Again, we apply the Lagrangian optimization technique for the above problem. The corresponding KKT conditions for the maximization problem in (4.28) can be ex-

pressed as:

$$\frac{\gamma_2\left(\xi\right)h_2}{N_0 B + S_2^{h,\xi}h_2} - \lambda \left(\frac{1}{d_q}\right)^2 f_2^{\mathrm{on}}(\xi) + \lambda_2' - \lambda_2'' = 0, \qquad (4.29\mathrm{a})$$

$$\lambda_2' S_2^{h,\xi} = 0, \qquad (4.29\mathrm{b})$$

$$\lambda_2'' \left(S_2^{h,\xi} - Q^{\mathrm{P}}\right) = 0, \qquad (4.29\mathrm{c})$$

where λ_2' and λ_2'' are the Lagrangian multipliers.

Then, following the approach used for the case when $\gamma_1\left(\xi\right)h_1 \geq \gamma_2\left(\xi\right)h_2$, it is easy to show that the optimal power allocation policy pertaining to the secondary BS when $\gamma_1\left(\xi\right)h_1 < \gamma_2\left(\xi\right)h_2$, given that $0 \leq S^{h,\xi} \leq S_a^{h,\xi}$, can be formulated as:

$$S_2^{h,\xi} = \begin{cases} Q^{\mathrm{P}}, & \frac{N_0 B}{h_2} < \chi_2\left(\xi\right) - Q^{\mathrm{P}}, \\ \chi_2\left(\xi\right) - \frac{N_0 B}{h_2}, & \chi_2\left(\xi\right) - Q^{\mathrm{P}} \leq \frac{N_0 B}{h_2} \leq \chi_2\left(\xi\right), \\ 0, & \frac{N_0 B}{h_2} > \chi_2\left(\xi\right). \end{cases} \qquad (4.30)$$

Note that parameter $\chi_2\left(\xi\right)$ must be such that it satisfies the interference constraint at equality, according to:

$$Q^{\mathrm{I}} = \mathrm{E}_{\mathbf{h},\mathfrak{F}|\mathrm{PT\ is\ ON}} \left[S_2^{h,\xi} \left(\frac{1}{d_q}\right)^2 \right]$$

$$= \underset{\chi_2(\xi) - Q^{\mathrm{P}} \leq \frac{N_0 B}{h_2} \leq \chi_2(\xi)}{\mathrm{E}_{\mathbf{h},\mathfrak{F}|\mathrm{PT\ is\ ON}}} \left[\frac{\chi_2\left(\xi\right)}{d_q^2} - \frac{N_0 B}{d_q^2 h_2} \right] + \underset{\frac{N_0 B}{h_2} < \chi_2(\xi) - Q^{\mathrm{P}}}{\mathrm{E}_{\mathbf{h},\mathfrak{F}|\mathrm{PT\ is\ ON}}} \left[\frac{Q^{\mathrm{P}}}{d_q^2} \right]. \qquad (4.31)$$

Case b: $\mathfrak{J}_{\mathrm{BC}}^1\left(\mathbf{S}^{h,\xi}\right) = r_1\left(S^{h,\xi}\right)$. Here, using the results obtained for the case with $\gamma_1\left(\xi\right)h_1 \geq \gamma_2\left(\xi\right)h_2$, it is easy to show that the optimal transmit power pertaining to the secondary BS for $\gamma_1\left(\xi\right)h_1 < \gamma_2\left(\xi\right)h_2$, given that $S^{h,\xi} \geq S_b^{h,\xi}$, is expressed by the allocation policy shown in (4.26).

Case c: $\mathfrak{J}_{\mathrm{BC}}^1\left(\mathbf{S}^{h,\xi}\right) = \Psi\left(S^{h,\xi} - S_a^{h,\xi}\right) + r_2\left(S_a^{h,\xi}\right)$ for $S_a^{h,\xi} < S^{h,\xi} < S_b^{h,\xi}$. In this case, both users are selected for the transmission. Hence, using the allocation policy obtained in (4.18), the total transmit power $S^{h,\xi}$ is allocated between these

users using

$$S^{h,\xi} = \tau^{h,\xi} S_1^{h,\xi} + (1 - \tau^{h,\xi}) S_2^{h,\xi}, \tag{4.32}$$

where $0 \leq \tau^{h,\xi} \leq 1$, and the transmission policies pertaining to $S_1^{h,\xi}$ and $S_2^{h,\xi}$ are illustrated in (4.30) and (4.26), respectively. Note that the total transmit power $S^{h,\xi}$ must always satisfy the interference constraint at equality:

$$Q^{\mathrm{I}} = \mathrm{E}_{\mathbf{h},\mathfrak{F}|\mathrm{PT\,is\,ON}} \left[\frac{\tau^{h,\xi} S_1^{h,\xi} + (1 - \tau^{h,\xi}) S_2^{h,\xi}}{d_q^2} \right]. \tag{4.33}$$

Finally, two cases remain to be considered: $h_1 > h_2$ and $h_1 = h_2$. When $h_1 > h_2$, the optimum power and time allocation policy can be obtained by applying the approach used when $h_2 > h_1$. For the case when $h_1 = h_2$, since *user-1* and *user-2* are both in the same channel state, the decision will be made based only on the sensing information available at the BS. Accordingly, the optimal power and time allocation policy is given by: *i)* for $\gamma_1 (\xi) > \gamma_2 (\xi)$: $S^{h,\xi} = S_1^{h,\xi}$ and *user-2* is silent, *ii)* for $\gamma_1 (\xi) < \gamma_2 (\xi)$: $S^{h,\xi} = S_2^{h,\xi}$ and *user-1* is silent. Note that $S_1^{h,\xi}$ and $S_2^{h,\xi}$ are defined in (4.30) and (4.26), respectively.

4.3.2   System with $K > 2$ SRs

Consider a CR-BC system with $K > 2$ users, operating under average interference and peak-transmit power constraints as given in $\mathbb{F}$. It is supposed that the SU with better channel and primary activity conditions obtains higher priority to access the shared spectrum. Note that the aforementioned required information (CSI and SSI) are provided by each SU and are available to the BS through the feedback channel. Herein, we generalize the approach considered for two users in part A, in order to investigate the optimal power and time-sharing allocation policies for multiple SUs. In this regard, without loss of generality, we first assume that $\vartheta (\cdot)$ defines the permutation of K SRs such that $h_{\vartheta(1)} < h_{\vartheta(2)} < \cdots < h_{\vartheta(K)}$. Then, we can consider the following cases:

Case a: $\gamma_{\vartheta(i)} (\xi) h_{\vartheta(i)} \geq \gamma_{\vartheta(j)} (\xi) h_{\vartheta(j)}$, $\forall i < j$ for any $i, j = 1, 2, \cdots, K$. Using the results in part A for the two-user case, we can show that $r_{\vartheta(1)} \left(S^{h,\xi} \right) > \left\{ r_{\vartheta(j)} \left(S^{h,\xi} \right) \right\}_{j=2}^{K}$ and, consequently, the solution to (4.5) is given by $\mathfrak{J}_{\mathrm{BC}}^1 \left(\mathbf{S}^{h,\xi} \right) = r_{\vartheta(1)} \left(S^{h,\xi} \right)$. Thus, in this case, the optimal power allocation policy can be expressed

as

$$
S_{\vartheta(1)}^{h,\xi} = \begin{cases} Q^{\mathrm{P}}, & \dfrac{N_0 B}{h_{\vartheta(1)}} < \chi_{\vartheta(1)}\left(\xi\right) - Q^{\mathrm{P}}, \\[2ex] \chi_{\vartheta(1)}\left(\xi\right) - \dfrac{N_0 B}{h_{\vartheta(1)}}, & \chi_{\vartheta(1)}\left(\xi\right) - Q^{\mathrm{P}} \leq \dfrac{N_0 B}{h_{\vartheta(1)}} \leq \chi_{\vartheta(1)}\left(\xi\right), \\[2ex] 0, & \dfrac{N_0 B}{h_{\vartheta(1)}} > \chi_{\vartheta(1)}\left(\xi\right). \end{cases} \tag{4.34}
$$

Case b: $\gamma_{\vartheta(i)}\left(\xi\right) h_{\vartheta(i)} < \gamma_{\vartheta(j)}\left(\xi\right) h_{\vartheta(j)}$, $\forall i < j$ for any $i, j = 1, 2, \cdots, K$. In this case, based on the results provided in part A, $r_{\vartheta(i)}\left(S^{h,\xi}\right)$ and $r_{\vartheta(j)}\left(S^{h,\xi}\right)$ will intersect at some value of $S^{h,\xi}$. Accordingly, we can define $J_{\mathrm{BC}}^1\left(\mathbf{S}^{h,\xi}\right)$ by

$$
J_{\mathrm{BC}}^1\left(\mathbf{S}^{h,\xi}\right) = \begin{cases} r_{\vartheta(\omega_i)}\left(S^{h,\xi}\right), & S_{b_{i-1}}^{h,\xi} \leq S^{h,\xi} < S_{a_i}^{h,\xi} \\[1ex] \Psi_{\vartheta(\omega_i)}\left(S^{h,\xi} - S_{a_i}^{h,\xi}\right) + r_{\vartheta(\omega_i)}\left(S_{a_i}^{h,\xi}\right), & S_{a_i}^{h,\xi} \leq S^{h,\xi} < S_{b_i}^{h,\xi} \end{cases} \tag{4.35}
$$

where $\Psi_{\vartheta(\omega_i)}$, $S_{a_i}^{h,\xi}$ and $S_{b_i}^{h,\xi}$ are given by[12]:

$$
\Psi_{\vartheta(\omega_i)} = \frac{r_{\vartheta(\omega_i)}\left(S_{a_i}^{h,\xi}\right) - r_{\vartheta(\omega_{i+1})}\left(S_{b_i}^{h,\xi}\right)}{S_{a_i}^{h,\xi} - S_{b_i}^{h,\xi}}, \tag{4.36}
$$

and

$$
\begin{cases} S_{a_i}^{h,\xi} = \dfrac{\gamma_{\vartheta(\omega_i)}\left(\xi\right)}{\Psi_{\vartheta(\omega_i)}} - \dfrac{N_0 B}{h_{\vartheta(\omega_i)}}, \\[2ex] S_{b_i}^{h,\xi} = \dfrac{\gamma_{\vartheta(\omega_{i+1})}\left(\xi\right)}{\Psi_{\vartheta(\omega_i)}} - \dfrac{N_0 B}{h_{\vartheta(\omega_{i+1})}}. \end{cases} \tag{4.37}
$$

It is worth noting that $\omega_i \triangleq K + 1 - i$, where i is given by $i = \arg \max_j \{\Psi_{\vartheta(\omega_j)} \Big| j = 1, 2, \cdots, K\}$ for different values of $S^{h,\xi}$. This implies that for any value of $S^{h,\xi}$, the user with a higher value of Ψ will have a contribution in the functional $J_{\mathrm{BC}}^1\left(\mathbf{S}^{h,\xi}\right)$.

The optimal power and time-sharing allocation policy in this case, can be illustrated as:

---

[12]Note that $S_{b_0}^{h,\xi} = 0$.

1) $J_{\mathrm{BC}}^1 \left(\mathbf{S}^{h,\xi} \right) = r_{\vartheta(\omega_i)} \left(S^{h,\xi} \right)$ for $S_{b_{i-1}}^{h,\xi} \leq S^{h,\xi} < S_{a_i}^{h,\xi}$:

$$
S_{\vartheta(\omega_i)}^{h,\xi} = \begin{cases} Q^{\mathrm{P}}, & \dfrac{N_0 B}{h_{\vartheta(\omega_i)}} < \chi_{\vartheta(\omega_i)}\left(\xi\right) - Q^{\mathrm{P}}, \\[2ex] \chi_{\vartheta(\omega_i)}\left(\xi\right) - \dfrac{N_0 B}{h_{\vartheta(\omega_i)}}, & \chi_{\vartheta(\omega_i)}\left(\xi\right) - Q^{\mathrm{P}} \leq \dfrac{N_0 B}{h_{\vartheta(\omega_i)}} \leq \chi_{\vartheta(\omega_i)}\left(\xi\right) \\[2ex] 0, & \dfrac{N_0 B}{h_{\vartheta(\omega_i)}} > \chi_{\vartheta(\omega_i)}\left(\xi\right). \end{cases}
\tag{4.38}
$$

2) $J_{\mathrm{BC}}^1 \left(\mathbf{S}^{h,\xi} \right) = \Psi_{\vartheta(\omega_i)} \left(S^{h,\xi} - S_{a_i}^{h,\xi} \right) + r_{\vartheta(\omega_i)} \left(S_{a_i}^{h,\xi} \right)$ for $S_{a_i}^{h,\xi} \leq S^{h,\xi} < S_{b_i}^{h,\xi}$:

$$
S^{h,\xi} = \tau_{\vartheta(\omega_i)}^{h,\xi} S_{\vartheta(\omega_i)}^{h,\xi} + \tau_{\vartheta(\omega_{i+1})}^{h,\xi} S_{\vartheta(\omega_{i+1})}^{h,\xi},
\tag{4.39}
$$

which, after further manipulation and since $\tau_{\vartheta(\omega_i)}^{h,\xi} + \tau_{\vartheta(\omega_{i+1})}^{h,\xi} = 1$, yields:

$$
\begin{cases} \tau_{\vartheta(\omega_i)}^{h,\xi} = \dfrac{S_{a_i}^{h,\xi} - S^{h,\xi}}{S_{a_i}^{h,\xi} - S_{b_i}^{h,\xi}}, \\[2ex] \tau_{\vartheta(\omega_{i+1})}^{h,\xi} = 1 - \tau_{\vartheta(\omega_i)}^{h,\xi}. \end{cases}
\tag{4.40}
$$

In the power allocation policies shown in (4.34) and (4.38), the water-filling level $\chi\left(\xi\right)$ must satisfy the aggregate interference constraint (4.2) at equality, as follows:

$$
Q^{\mathrm{I}} = \mathrm{E}_{\mathbf{h}, \mathfrak{F} | \mathrm{PT\,is\,ON}} \left[\sum_{k=1}^{K} \frac{\tau_{\vartheta(\omega_k)}^{h,\xi} S_{\vartheta(\omega_k)}^{h,\xi}}{d_q^2} \right].
\tag{4.41}
$$

It has been shown that the soft variation of the sensing parameter may be used by the secondary BS to adaptively adjust its resources for a better management of the transmission time and power among the CR users and, consequently, the generated interference at the primary user of the spectrum band. However, in a collaborative sensing mechanism between the BS and SRs, significant overhead is required to feedback observations between each SR and the BS. Moreover, it is difficult in practice to continuously adapt the transmission time and power to the soft-sensing parameters given by $\gamma_k\left(\xi\right)$, $k = 1, 2, \cdots, K$. In contrast, the conventional hard decision scheme requires only one bit of overhead, but has worse performance because of information loss caused by local hard decisions. Thus, in the following section, we propose using discrete sensing technique where only discrete levels of the sensing information are considered, which achieves a good tradeoff between perfor-

mance and complexity. Note that this yields a suboptimal spectral efficiency. However, as we will show in Section 4.5, this cost is not significant.

4.4 Transmission Policy under Discrete Sensing Information

In this part, we restrict ourselves to quantized levels of SSI calculated at the SASN nodes, and present the power allocation policy and the achievable rate of the CR-BC system operating under the constraints given in (4.2). As shown in (4.23b), the effect of SSI is reflected through parameters $\eta_k(\xi) := \alpha + \bar{\alpha} f_k^{\text{off}}(\xi) / f_k^{\text{on}}(\xi)$. We will show that such quantization may be applied to parameter $\eta_k(\xi)$ which is directly related to the sensing PDFs provided at each SR. It has been shown in Chapter 2.1.4 that as long as the probability that the PT is ON increases, $\eta_k(\xi)$ has a descending behavior. This behavior is illustrated in Fig. 4.3 for $K = 3$ users operating in the same channel conditions, but with different SSI knowledge given by the parameters $\mu_1 < \mu_2 < \mu_3$. Based on the results presented in Chapter 2.1.4, $\eta_k(\xi) = 1$ is a threshold value that indicates the transition between higher and lower PU activity levels determined by the detection mechanism. This threshold can be considered as a decision criterion for the PT activity between ON and OFF states.

In this context, $\eta_k(\xi)$ is restricted to N discrete levels $\overline{\eta}_k[n]$; $n = 1, 2, \cdots, N$, if it falls into the interval $\Im_k$ given by

$$\Im_k : \left\{ \frac{n-1}{N} \eta_k^{\text{max}} < \eta_k(\xi) \leq \frac{n}{N} \eta_k^{\text{max}} \right\}, \tag{4.42}$$

where η_k^{max} denotes the maximum value of $\eta_k(\xi)$ for $k = 1, 2, \cdots, K$. Herein, without loss of generality, we use uniform quantization, one of the most common quantization techniques [59]. Assuming N-ary uniform quantization of $\eta_k(\xi)$, it can be shown that the n-th discrete level $\overline{\eta}_k[n]$ can be calculated according to

$$\overline{\eta}_k[n] = \frac{2n-1}{2N} \eta_k^{\text{max}}; \quad k = 1, 2, \cdots, K. \tag{4.43}$$

Hence, considering the decision intervals in (4.42) and the quantization levels presented in
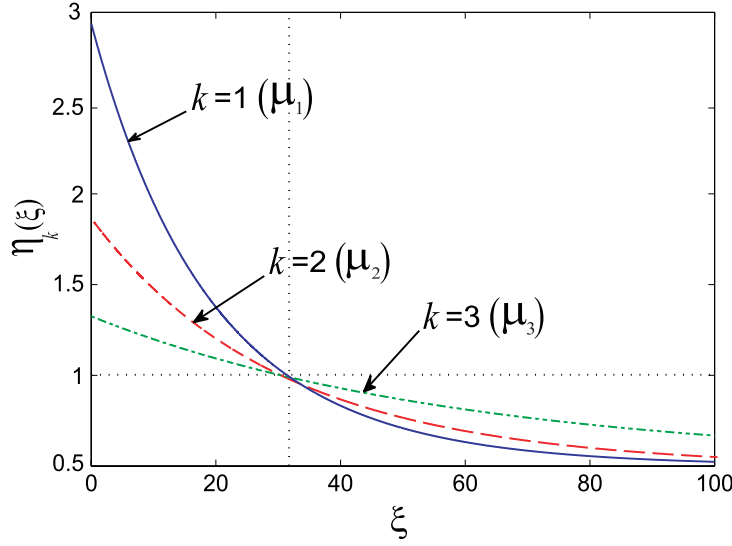
Figure 4.3: Variation of parameter $\eta_k(\xi) := \alpha + \bar{\alpha} f_k^{\text{off}}(\xi)/f_k^{\text{on}}(\xi)$, as a function of ξ for users $k = 1, 2, 3$.

(4.43), the quantization rule can be illustrated as

$$\overline{\eta}_k[n] = \frac{2n-1}{2N}\eta_k^{\max} \quad \text{if} \quad \eta_k(\xi) \in \Im_k. \tag{4.44}$$

By substituting $\overline{\eta}_k[n]$ into (4.34) and (4.38), we obtain the power allocation policy under discrete sensing information as,

$$S_{\vartheta(\omega_k)}^h[n] = \begin{cases} Q^{\mathrm{P}}, & \dfrac{N_0 B}{h_{\vartheta(\omega_k)}} < \overline{\chi}_{\vartheta(\omega_k)}[n] - Q^{\mathrm{P}}, \\[2ex] \overline{\chi}_{\vartheta(\omega_k)}[n] - \dfrac{N_0 B}{h_{\vartheta(\omega_k)}}, & \overline{\chi}_{\vartheta(\omega_k)}[n] - Q^{\mathrm{P}} \leq \dfrac{N_0 B}{h_{\vartheta(\omega_k)}} \leq \overline{\chi}_{\vartheta(\omega_k)}[n] \\[2ex] 0, & \dfrac{N_0 B}{h_{\vartheta(\omega_k)}} > \overline{\chi}_{\vartheta(\omega_k)}[n], \end{cases} \tag{4.45}$$

where $k \in \{1, 2, \cdots, K\}$, $n \in \{1, 2, \cdots, N\}$, and $\overline{\chi}_{\vartheta(\omega_k)}[n]$ is given by

$$\overline{\chi}_{\vartheta(\omega_k)}[n] = \frac{\overline{\eta}_{\vartheta(\omega_k)}[n] d_q^2}{\lambda}. \tag{4.46}$$

Considering the power allocation policy given in (4.45), the interference constraint in this

case can be expressed as

$$Q^{\mathrm{I}} \geq \mathrm{E}_{\mathbf{h}} \left[\sum_{k=1}^{K} \sum_{n \in \phi} \beta_k [n] \left(\frac{\tau_{\vartheta(\omega_k)}^{h} [n] \, S_{\vartheta(\omega_k)}^{h} [n]}{d_q^2} \right) \right],$$ (4.47)

where $\phi = \left\{ n \, \middle| \, \overline{\eta}_{\vartheta(\omega_k)}[n] \leq 1, \; n = 1, 2, \cdots, N \right\}$, and $\beta_k[n]$ is the discrete PDF corresponding to the n-th level of the discrete sensing information which must verify $\sum_{1 \leq n \leq N} \beta_k[n] = 1$, for $k = 1, 2, \cdots, K$.

Finally, the capacity of CR-BC with perfect CSI and discrete sensing information at the secondary BS and SRs, under the constraints on the average interference and peak transmit-power, can be obtained by rewriting (4.4) as follows:

$$\overline{C}(\mathcal{S}) = \left\{ \mathbf{R} : R_k \leq \sum_{1 \leq n \leq N} \beta_k [n] \, \mathrm{E}_{\mathbf{h}} \left[\tau_k^h [n] \, B \log_2 \left(1 + \frac{S_k^h [n] \, h_k}{N_0 B} \right) \right], \forall \, 1 \leq k \leq K \right\}.$$ (4.48)

4.5 Numerical Results

In this section, we numerically illustrate the performance of the proposed CR-BC system in terms of the ergodic capacity under predefined constraints on the average interference generated by the secondary network at the PR and peak transmit-power at the secondary BS. Moreover, we investigate the capacity penalty of the proposed quantized sensing approach for the system under consideration. In our simulations, we assume a secondary BS and two SRs communicating in a TD multiple access fashion while sharing the spectrum band with the primary user link[13]. To provide SSI about the PU's activity, it is assumed that the number of observation samples at the sensing detectors is 30, i.e., $M = 30$ in (4.1). We also assume perfect knowledge at the BS of the channels between the secondary transmitter and receivers and also of the SSI, through no-delay error-free feedback. In our simulations, the fading channels pertaining to the SUs are modeled according to Rayleigh PDFs, with $\mathrm{E}[h_1] = 0$ dB and $\mathrm{E}[h_2] = 2$ dB for *user-1* and *user-2*, respectively. As for the PT's activity model, we suppose that the PT remains active 50% of the time ($\alpha = 0.5$). Furthermore, we assume that $N_0 B = 1$.

---

[13]For simplicity of presentation, herein, we focus on CR-BC system with two users, but we recall that our theoretical analysis applies to higher numbers of SUs.
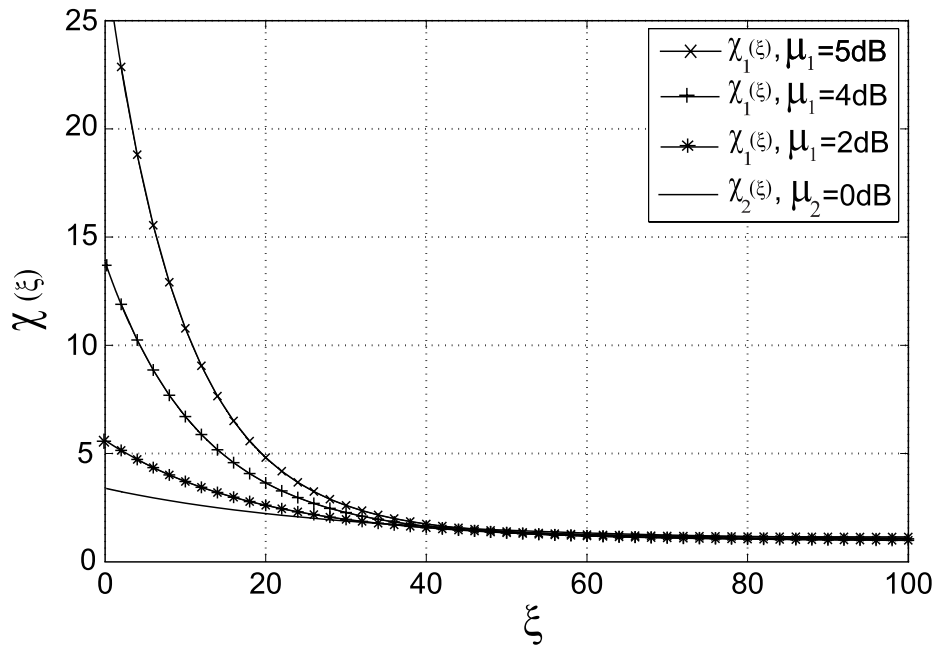
Figure 4.4: Variation of parameter $\chi_k(\xi)$ as a function of ξ for *user-1* and *user-2* and different values of non-centrality parameter μ_1 and $\mu_2 = 0$ dB ($Q^{\mathrm{I}} = -5$ dB, $Q^{\mathrm{P}} = -2$ dB).
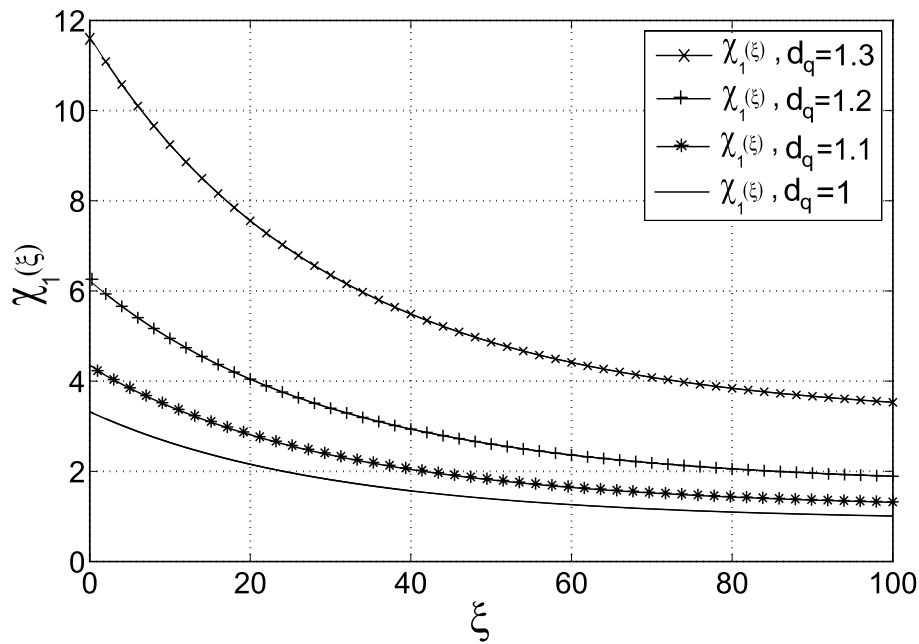

Figure 4.5: Variation of parameter $\chi_1(\xi)$ versus ξ for *user-1* and different values of d_q ($Q^{\mathrm{I}} = -5$ dB, $Q^{\mathrm{P}} = -2$ dB).

We start by analyzing the parameter $\chi(\xi)$ as a function of the sensing metric ξ. We set the interference and peak power limits to $Q^{\mathrm{I}} = -5$ dB and $Q^{\mathrm{P}} = -2$ dB. The variation of $\chi_k(\xi) \ \forall k = 1, 2$, is illustrated in Figs. 4.4 and 4.5, for certain non-centrality values of the sensing distributions, μ_1 and μ_2, and different values for the distance between the BS and the PR, d_q, respectively. From Fig. 4.4, we observe that when $\mu_2 = 0$ dB and d_q has unit value, $\chi_1(\xi) \geq \chi_2(\xi)$ as long as $\mu_1 \geq \mu_2$, and that for different values of ξ. It is worth noting that for higher values of ξ, in which case "PT being ON" is more probable, $\chi_1(\xi)$ and $\chi_2(\xi)$ have descensional behaviors. On the other hand, setting $\mu_1 = 0$ dB in Fig. 4.5, we observe that $\chi_1(\xi)$ increases as d_q increases, while it still has a decreasing behavior as a function of ξ ($Q^{\mathrm{I}} = -5$ dB, $Q^{\mathrm{P}} = -2$ dB).

Referring to Fig. 4.6, the achievable capacity regions for the Rayleigh fading CR-BC pertaining to *user-1* and *user-2* is shown for different values of (μ_1, μ_2). In these plots, the average interference limit $Q^{\mathrm{I}} = 5$ dB and we consider $B = 100$kHz. In Fig. 4.6, the variation of μ_1 and μ_2 are investigated when the peak transmit-power limit is fixed at $Q^{\mathrm{P}} = 5.5$ dB. We observe that the SU which senses a lower PU's activity level, i.e., lower values of μ, will have more contribution in the transmission rate, and vice-versa. On the other hand, in Fig. 4.7, we set $\mu_1 = 7$ dB and $\mu_2 = -3$ dB, and illustrate the effect of the peak power limit on the transmission rate achieved by the SUs. It is observed that higher Q^{P} yields an increase in the transmission rate achieved by the SUs.

In the broadcast channels under study, it is customary to consider the maximum sum-capacity of SUs as a figure-of-merit. This metric can be defined as, $\max \left\{ \sum_{k=1}^{K} R_k \right\}$ subject to satisfying the resource constraints in $\mathbb{F}$. In this regard, the sum-capacity of two users in CR-BC versus the average interference limit Q^{I} is investigated in Figs. 4.8 and 4.9, for $\rho = 2$, where $\rho = \dfrac{Q^{\mathrm{P}}}{Q^{\mathrm{I}}}$. In Fig. 4.8, we set $d_q = 1$ and $\mu_2 = 0$ dB. As observed, the sum-capacity increases as parameter μ_1 decreases. These results are reasonable since according to the sensing PDFs given in (4.1), as μ_1 increases, the probability of "PT being ON" also increases and, consequently, this diminishes the chance of *user-1* to be selected by the BS. In Fig. 4.9, setting $\mu_1 = 0$ dB and $\mu_2 = 2$ dB, the sum-capacity of two-user CR-BC is plotted for different values of d_q. The plots show how when the distance between the secondary BS and the PR increases, i.e. d_q, the capacity of CR-BC increases. It is worth noting that for higher values of d_q, the capacity converges towards that of a system where no Q^{I} constraint is considered. Furthermore, regarding the above figures, we observe that
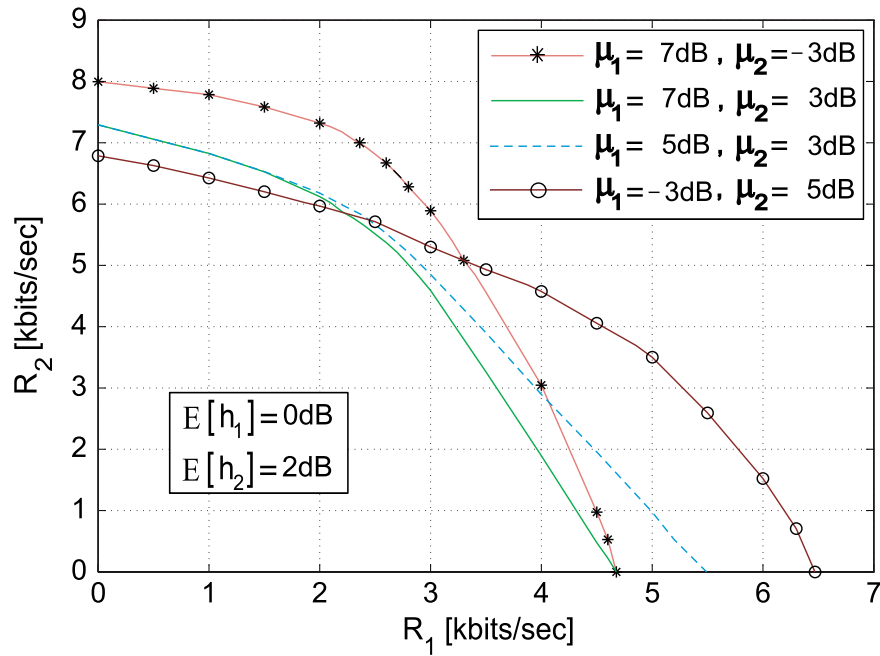
Figure 4.6: Two-SU ergodic capacity region: comparisons when $Q^{\mathrm{I}} = 5$ dB and $Q^{\mathrm{P}} = 5.5$ dB.
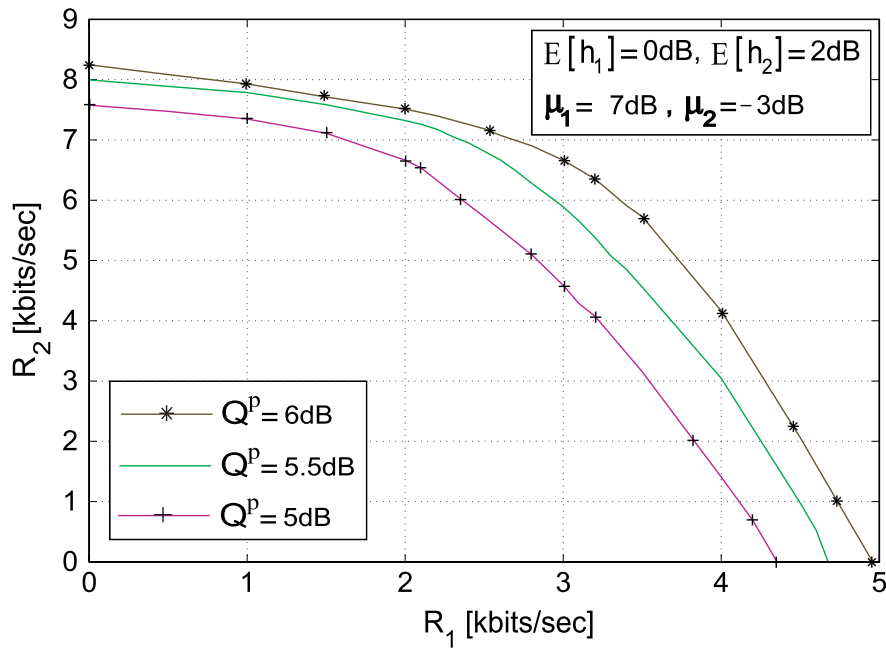
Figure 4.7: Two-SU ergodic capacity region: comparisons when $Q^{\mathrm{I}} = 5$ dB, $\mu_1 = 7$ dB and $\mu_2 = -3$ dB.
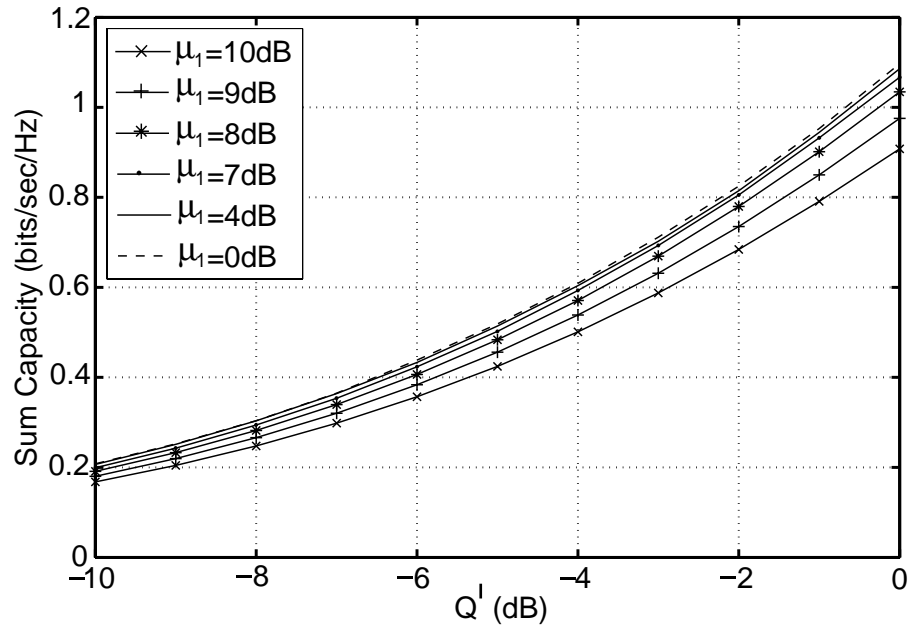
Figure 4.8: Sum-capacity of CR Rayleigh fading BC versus Q^{I} for various values of non-centrality parameter μ_1 ($\rho = 2$).
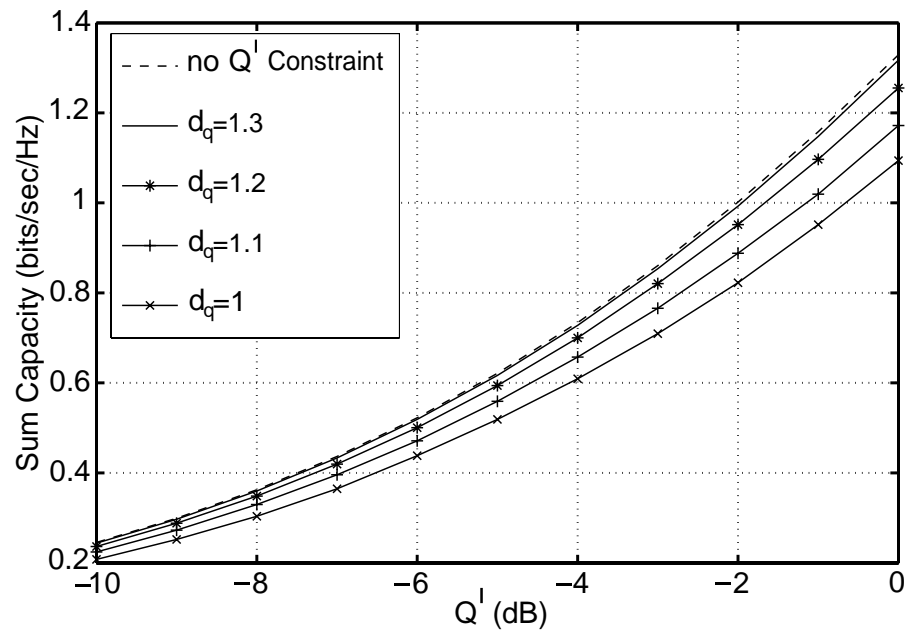
Figure 4.9: Sum-capacity of CR Rayleigh fading BC versus Q^{I} for various values of d_q ($\rho = 2$).
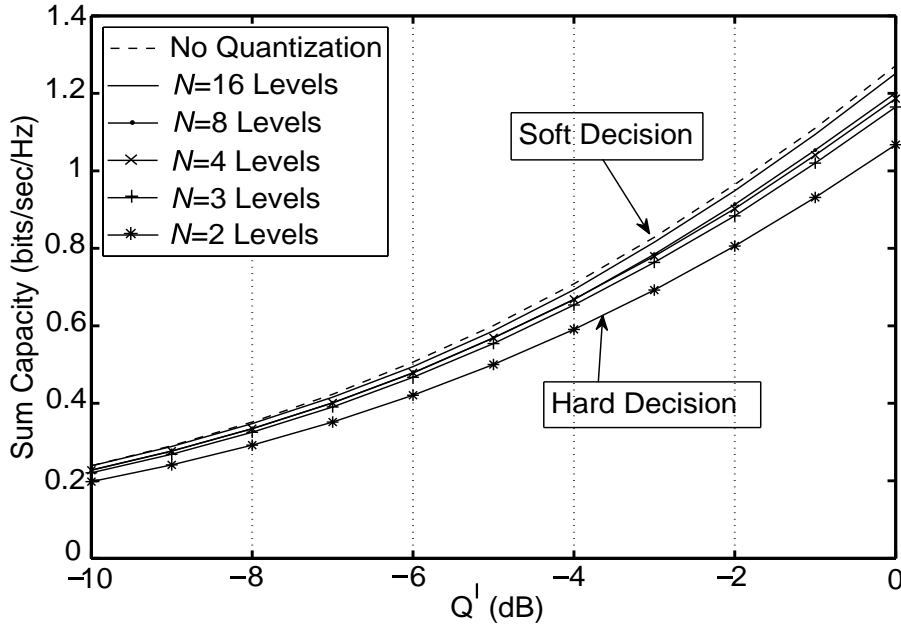
Figure 4.10: Sum-capacity with quantized sensing scheme ($\rho = 2$).

as the limit on the average received-interference Q^{I} increases, the sum-capacity of the BC channels increases as well.

The performance analysis of the proposed discrete sensing scheme in terms of the maximum sum-capacity of a two-user Rayleigh fading broadcast channel, is investigated in Fig. 4.10 versus Q^{I}, for several numbers of discrete sensing levels. In this figure, we assume that $\beta_k[n]$ is distributed according to a Poisson PDF with mean ϵ_k, i.e., $\sum\limits_{1 \leq n \leq N} \beta_k[n] = \sum_{n=1}^{N} \frac{(\epsilon_k)^n}{n!} e^{-\epsilon_k} = 1$, for different numbers of discrete levels N. Furthermore, to illustrate the effect of the discrete sensing approach on the achievable capacity of the system, we fix $\mu_1 = 0$ dB, $\mu_2 = 2$ dB and $d_q = 1$. As shown in Fig. 4.10, the discrete sensing approach pulls down the achievable capacity of the SUs as the number of levels N decreases[14]. In this figure, the performance with soft-decision ($N > 16$) and hard-decision ($N = 2$ levels) schemes is illustrated. As observed, performances with other discrete levels are laid within the soft-decision and hard-decision results. Furthermore, as expected, the sum-capacity plots have ascensional behavior when Q^{I} increases.

---

[14]Note that for comparison purposes in our numerical results, ϵ_k is considered such that the $\beta_k[n]$'s distribution follows the same curve as its equivalent continuous distribution function using sensing PDFs given in (4.1).

4.6   Summary

In this chapter, we investigated adaptive resource sharing in CR fading broadcast channels when spectrum-sensing information is utilized at the base station of the secondary network to more effectively and efficiently use the shared-spectrum resources. In particular, considering TD multiple access, we proposed using soft-sensing information about the primary system activity at the secondary base station to fairly allocate the resources, namely, transmission time and power, among users, under appropriate constraints on the average interference at the primary receiver and peak transmit-power at the secondary transmitter. The sensing was performed by assuming a spectrum-aware sensor networking approach in the secondary network. Based on the sensing information attained, an optimal time-sharing and transmit power allocation policy was investigated such that the achievable capacity of fading CR broadcast channels is maximized. Furthermore, we considered a quantized spectrum sensing mechanism in order to reduce the overall system complexity, where only limited activity levels are used for the sensing observations.

Theoretical analysis besides numerical results and comparisons have shown that soft-sensing information about the primary system activity allows for an efficient management of the time and power resources between the SUs and, consequently, the resulting interference onto the primary system. Specifically, in the scenario with two SUs, it has been shown that as the primary system activity decreases in an area, more transmission time and power can be allocated to a SU located in that area and vice-versa.

Next, as mentioned in Chapter 1, we propose to adopt relaying in spectrum-sharing CR networks to more efficiently utilize the available resources at the secondary communication and decrease the interference at the PRs. In the next chapter and as an initial step, we consider a source/destination transmission link and investigate the performance evaluation of single- and multi-hop relaying communication systems by using the MGF-based approach. In particular, at first, considering a generalized fading scenario in a classical communication system, we investigate the performance analysis of typical communication system in terms of the average symbol error probability (SEP) of arbitrary M-ary QAM constellations in maximal-ratio combining (MRC) schemes over non-identical correlated channels. Thereafter, we investigate the performance analysis of cooperative relaying networks in terms of the average SEP, ergodic capacity and outage probability performance subject to independent and non-identically distributed Nakagami-m fading.

Chapter 5

Performance Analysis of Cooperative Communications[1]

5.1 Symbol Error Probability of MRC Systems with Correlated η-μ Fading Channels

In wireless communications, accurate modeling of the propagation channel is of extreme importance for a successful system design. Due to this, over the years a great number of channel models (e.g., Rayleigh, Nakagami-*m*, and Hoyt) were proposed with the aim to provide a good statistical characterization of the fading signal. In addition, efforts have also been made to extend the existing fading models in order to obtain more flexible and generalized models [67]. Recently, a new fading distribution, namely η-μ distribution, which includes as special cases Nakagami-*m* and Hoyt was proposed in [68]. Its flexibility renders it more adaptable to situations in which neither of these two distributions yields a good fit [68], particularly at the tail portion, where several distributions fail to follow the true statistics. However, because of the fact that the η-μ distribution has one degree of freedom more than the Hoyt and Nakagami-*m* distributions, analytical studies regarding system performance subject to η-μ fading are even more intricate given that the analytical complexity is substantially increased during the calculus. Therefore, although the investi-

---

[1] Parts of this chapter were presented at the *IEEE Transactions on Vehicular Technology*, vol. 59, no. 3, pp. 1497 – 1503, Mar. 2010, and in Proc. *IEEE Wireless Communications and Networking Conference (WCNC'10)*, Sydney, Australia, April, 2010, pp. 1 – 6, and submitted to *IEEE Transactions on Communications*, Jan. 2011.

gation of generalized fading scenarios is important to acquire a more realistic behavior of wireless systems, there are very few works in the open literature reporting the performance of wireless communication systems over η-μ fading channels.

As mentioned in Chapter 1.1.5, among the performance metrics usually employed to describe wireless diversity systems, symbol error probability (SEP) of *M*-ary modulations has been considered of major importance [69]. This metric has been investigated for some fading scenarios under different assumptions (see [70], [71], [72], and references therein). In [70], a useful integral representing the average over Rayleigh fading of the product of two Gaussian Q-functions is derived and the average SEP for a single reception scheme is calculated. For multichannel diversity reception, the average SEP of rectangular quadrature amplitude modulation (QAM) over independent but not-necessarily identically distributed Nakagami-*m* fading channels, is investigated in [71]. Regarding η-μ fading channels, in [73], accurate closed-form approximations for the error probability of several diversity schemes were provided assuming independent and identically distributed (i.i.d.) channels. More recently, considering single channel reception scheme, an exact closed-form expression for the SEP of rectangular QAM constellations was derived in [72]. In this section, we generalize the latter work by focusing on the derivation of the average SEP of *M*-ary rectangular QAM over correlated channels with non-identical fading parameters and employing multichannel reception[2]. First, a general closed-form expression for the moment generating function (MGF) of the signal-to-noise ratio (SNR) at the combiner output is derived by rearranging the Gaussian components used to model the correlation between the diversity branches [74]. Second, adopting the MGF-based approach, the SEP of rectangular QAM with maximal-ratio combining (MRC) at the receiver is derived in closed-form in terms of multivariate Lauricella hypergeometric functions [75].

The remainder of Section 5.1 is organized as follows. In Section 5.1.1, the η-μ fading model is revisited. Section 5.1.2 derives a general closed-expression for the MGF of multichannel diversity schemes over arbitrary correlated η-μ fading channels. Based on this result, the average SEP of rectangular QAM constellations is derived in Section 5.1.3, in which some special cases are also presented and discussed. Numerical results are provided in Section 5.1.4 along with insightful discussions. Finally, concluding remarks and

---

[2]Note that whereas in [72] a single reception scheme was considered, in this section we consider a multichannel reception subject to arbitrary correlated η-μ fading channels. In addition, our results allow for different fading parameters among the input diversity branches.

summary are drawn in Section 5.1.5.

5.1.1 The η-μ Fading Model - A Brief Overview

The η-μ distribution [68] is a general model that describes the short-term variation of the fading signal and embraces as special cases other important distributions, such as Hoyt (Nakagami-q) and Nakagami-m. Such distribution may appear in two different formats, namely Format 1 and Format 2, for which two fading models are associated[3]. Regarding the former, its fading model considers that the in-phase and quadrature components within each multipath cluster are independent from each other and have different powers. In this case, the ratio between these powers is given by the parameter η, whereas the parameter μ is related to the number of multipath clusters.

By considering a diversity scenario, let R_i be the η-μ envelope of the i-th branch, $i = 1, ..., L$. From the respective η-μ fading model, R_i can be written in terms of the in-phase and quadrature components of each one of the n_i clusters of the fading signal as

$$R_i^2 = \sum_{j=1}^{n_i}(X_{i,j}^2 + Y_{i,j}^2),\tag{5.1}$$

where $X_{i,j}$ and $Y_{i,j}$ are mutually independent Gaussian random variables with zero-mean, i.e, $\mathrm{E}\left[X_{i,j}\right] = \mathrm{E}\left[Y_{i,j}\right] = 0$, and non-identical variances given by $\mathrm{E}\left[X_{i,j}^2\right] = \delta_{X_i}^2$ and $\mathrm{E}\left[Y_{i,j}^2\right] = \delta_{Y_i}^2$ ($\mathrm{E}\left[\cdot\right]$ denotes statistical average). By expressing the instantaneous SNR per symbol over each branch as $\gamma_i \triangleq R_i^2 E_\mathrm{s}/N_0$, where E_s/N_0 stands for the ratio of the average symbol energy and noise power spectral density, it follows that the PDF of γ_i can be written as

$$f_{\gamma_i}\left(x, \mu_i, \eta_i, \bar{\gamma}_i\right) = \frac{2\sqrt{\pi}h_i^{\mu_i}x^{\mu_i-\frac{1}{2}}}{\Gamma\left(\mu_i\right)H_i^{\mu_i-\frac{1}{2}}}\left(\frac{\mu_i}{\bar{\gamma}_i}\right)^{\mu_i+\frac{1}{2}}\exp\left(-\frac{2\mu_i h_i}{\bar{\gamma}_i}x\right)I_{\mu_i-\frac{1}{2}}\left(\frac{2\mu_i H_i}{\bar{\gamma}_i}x\right), \quad \forall x \geq 0,\tag{5.2}$$

whereby $\bar{\gamma}_i = \mathrm{E}[R_i^2]E_\mathrm{s}/N_0 = \Omega_i E_\mathrm{s}/N_0$, $I_\nu[\cdot]$ is the modified Bessel function of the first kind and arbitrary order ν [51, Eq. 9.6.20], $\Gamma(\cdot)$ is the Gamma function [51, Eq. 6.1.1], $h_i = (2 + \eta_i^{-1} + \eta_i)/4$, $H_i = (\eta_i^{-1} - \eta_i)/4$, $\eta_i = \delta_{X_i}^2/\delta_{Y_i}^2$, and μ_i is the real extension of

---

[3]In this section, only Format 1 is considered. However, as shown in [68], one format can be converted into the other by means of a simple bilinear transformation. Hence, the results provided in this section can also be used to investigate Format 2 of such a fading model.

$n_i/2$. From [68], it can be shown that $\delta^2_{X_i} = \eta_i\Omega_i/(2\mu_i(1+\eta_i))$ and $\delta^2_{Y_i} = \Omega_i/(2\mu_i(1+\eta_i))$.

Analyzing briefly the particular cases of the η-μ distribution, we can mention that the Hoyt distribution can be obtained in an exact manner from it by setting $\mu_i = 0.5$ with the Hoyt parameter $b_i = (\eta_i - 1)/(\eta_i + 1)$. In addition, for $\mu_i = m_i/2$ and $\eta_i \to 1$, the η-μ distribution reduces to the Nakagami-*m* one. For further details, the readers may refer to [68].

5.1.2   Moment Generating Function of the Output SNR

Consider a digital communication system implementing MRC of L diversity correlated branches. Accordingly, the effective SNR at the output of the MRC scheme, $\gamma^{(L)}$, is given by the summation of the instantaneous SNRs of the input branches, i.e.,

$$\gamma^{(L)} = \sum_{i=1}^{L} \gamma_i. \tag{5.3}$$

Based on (5.3), in the sequel we derive a new, elegant, closed-form expression for the MGF of $\gamma^{(L)}$, denoted as $M_{\gamma^{(L)}}(s) \triangleq \mathrm{E}\left[e^{s\gamma^{(L)}}\right]$. Such expression will be useful for the calculation of the average SEP of rectangular QAM constellations, performed posteriorly in Section 5.1.3. We will follow several steps as described below.

Firstly, since we are concerned with multichannel reception techniques, the input envelopes at the branches can be structured in the following manner

$$
\begin{aligned}
R_1 \to &\begin{cases} X_1 = [X_{1,1}\, X_{1,2} \cdots X_{1,2\mu_1}] \\ Y_1 = [Y_{1,1}\, Y_{1,2} \cdots Y_{1,2\mu_1}] \end{cases}, \\[4pt]
R_2 \to &\begin{cases} X_2 = [X_{2,1}\, X_{2,2} \cdots X_{2,2\mu_2}] \\ Y_2 = [Y_{2,1}\, Y_{2,2} \cdots Y_{2,2\mu_2}] \end{cases}, \\
&\qquad\qquad \vdots \\
R_L \to &\begin{cases} X_L = [X_{L,1}\, X_{L,2} \cdots X_{L,2\mu_L}] \\ Y_L = [Y_{L,1}\, Y_{L,2} \cdots Y_{L,2\mu_L}] \end{cases},
\end{aligned}
\tag{5.4}
$$

so that the envelope at the combiner output can be obtained from $RR^{\mathrm{T}} = XX^{\mathrm{T}} + YY^{\mathrm{T}}$, where $R = [R_1, \cdots, R_L]$ is written in terms of the components $X \triangleq [X_1, X_2, \cdots, X_L]$ and $Y \triangleq [Y_1, Y_2, \cdots, Y_L]$. Without loss of generality, we assume that the elements of X_i and

Y_i are such that $\mu_1 \le \mu_2 \le \cdots \le \mu_L$. Also, note that X_i and Y_i correspond, respectively, to the in-phase and quadrature components of the fading signal at the i-th branch and, in turn, they can be decomposed into the in-phase and quadrature components of each multipath cluster. Such decomposition is illustrated below:

$$
\begin{array}{llll}
R_1 \rightarrow & X_{1,1}, Y_{1,1} & X_{1,2}, Y_{1,2} \cdots & X_{1,2\mu_1}, Y_{1,2\mu_1} \\
R_2 \rightarrow & X_{2,1}, Y_{2,1} & X_{2,2}, Y_{2,2} & \cdots \quad X_{2,2\mu_2}, Y_{2,2\mu_2} \\
\vdots & \vdots & \vdots & \cdots \quad \ddots \\
R_{L-1} \rightarrow & X_{L-1,1}, Y_{L-1,1} & X_{L-1,2}, Y_{L-1,2} \cdots & \cdots \quad X_{L-1,2\mu_{L-1}}, Y_{L-1,2\mu_{L-1}} \\
R_L \rightarrow & X_{L,1}, Y_{L,1} & X_{L,2}, Y_{L,2} & \cdots \quad \cdots \quad X_{L,2\mu_{L-1}}, Y_{L,2\mu_{L-1}} \quad X_{L,2\mu_L}, Y_{L,2\mu_L}
\end{array}
$$
(5.5)

Under these considerations, we can now relate the statistical dependency among the L correlated branches, R_i, to the statistical dependency between the Υ elements $(X_{i,j}, Y_{i,j})$, $j = 1, \cdots, 2\mu_i$, with $\Upsilon = \sum_{i=1}^{L} 2\mu_i$. Considering that there is only second-order dependency, three cases can be distinguished for the covariance coefficients between the elements $X_{i,j}$ and $Y_{i,j}$, denoted by $\text{cov}(X_{i,k}, X_{j,t})$ and $\text{cov}(Y_{i,k}, Y_{j,t})$ respectively, and are given by the following:

case a: for $i = j$, $k = t$,

$$\text{cov}(X_{i,k}, X_{j,t}) = \delta_{X_i}^2, \quad \text{cov}(Y_{i,k}, Y_{j,t}) = \delta_{Y_i}^2, \tag{5.6a}$$

case b: for $i \ne j$ and $k = t = 1, \cdots, 2\min\{\mu_i, \mu_j\}$,

$$\text{cov}(X_{i,k}, X_{j,t}) = \delta_{X_i}\delta_{X_j}\rho_{i,j}, \quad \text{cov}(Y_{i,k}, Y_{j,t}) = \delta_{Y_i}\delta_{Y_j}\rho_{i,j}, \tag{5.6b}$$

case c: Otherwise of the above constraints,

$$\text{cov}(X_{i,k}, X_{j,t}) = 0, \quad \text{cov}(Y_{i,k}, Y_{j,t}) = 0, \tag{5.6c}$$

where $\rho_{i,j}$ stands for the correlation coefficients between the associated signal elements $(X_{i,k}, X_{j,t})$ and $(Y_{i,k}, Y_{j,t})$ [76, Sec. II].

Our next step is to define the covariance matrices of X and Y given by $K_X = \text{cov}(X^{\mathrm{T}}, X) = \mathrm{E}\left[X^{\mathrm{T}}X\right]$ and $K_Y = \text{cov}(Y^{\mathrm{T}}, Y) = \mathrm{E}\left[Y^{\mathrm{T}}Y\right]$, respectively. Consider λ_v^X and λ_v^Y ($v = 1, 2, \cdots, V$) as two sets of V distinct eigenvalues of K_X and K_Y with algebraic multiplic-

ities ξ_v^X and ξ_v^Y, respectively, such that $\frac{1}{2}\sum_{i=1}^{V}\left(\xi_i^X+\xi_i^Y\right)=\Upsilon$ [77]. Then, using the Karhunen-Loève (KL) orthogonal series expansion of X and Y as in [77, 78][4], we obtain that the envelope at the combiner output can be written in terms of V orthogonal virtual branch components as $\sum_{l=1}^{L}\left(X_lX_l^{\mathrm{T}}+Y_lY_l^{\mathrm{T}}\right)\stackrel{\mathrm{r}}{=}\sum_{v=1}^{V}\left(\lambda_v^X U_v^X+\lambda_v^Y W_v^Y\right)$, where "$\stackrel{\mathrm{r}}{=}$" denotes "*equal in their respective distributions*", and $\left\{U_v^X, W_v^Y\right\}_{v=1}^{V}$ are the virtual branch variables pertaining to the in-phase and quadrature components defined as

$$U_v^X\triangleq\sum_{i=1}^{\xi_v^X}\left(U_{v,i}^X\right)^2,\quad W_v^Y\triangleq\sum_{i=1}^{\xi_v^Y}\left(W_{v,i}^Y\right)^2.\tag{5.7}$$

Finally, the total received-SNR at the MRC output can be expressed according to

$$\gamma^{(L)}\stackrel{\mathrm{r}}{=}\sum_{v=1}^{V}\left(\lambda_v^X U_v^X+\lambda_v^Y W_v^Y\right).\tag{5.8}$$

Note that $\left\{U_{v,i}^X\right\}_{i=1}^{\xi_v^X}$ and $\left\{W_{v,i}^Y\right\}_{i=1}^{\xi_v^Y}$ are two sets of independent zero-mean unity-variance Gaussian random variables. Consequently, U_v^X and W_v^Y are distributed according to Chi-square PDF with degrees of freedom ξ_v^X and ξ_v^Y, respectively. The associated characteristic functions pertaining to U_v^X and W_v^Y, are calculated according to [57]

$$\begin{aligned}\Phi_{U_v^X}\left(s\right)&\triangleq\mathrm{E}[e^{s\lambda_v^X U_v^X}]=\left(1-2\lambda_v^X s\right)^{-\frac{\xi_v^X}{2}},\\ \Phi_{W_v^Y}\left(s\right)&\triangleq\mathrm{E}[e^{s\lambda_v^Y W_v^Y}]=\left(1-2\lambda_v^Y s\right)^{-\frac{\xi_v^Y}{2}}.\end{aligned}\tag{5.9}$$

Using expression (5.8), the MGF of $\gamma^{(L)}$ can be written as

$$M_{\gamma^{(L)}}\left(s\right)\triangleq\mathrm{E}\left[e^{s\gamma^{(L)}}\right]=\mathrm{E}\left[e^{s\sum_{v=1}^{V}\left(\lambda_v^X U_v^X+\lambda_v^Y W_v^Y\right)}\right].\tag{5.10}$$

Now, knowing that the in-phase and quadrature components within each multipath cluster are independent, (5.10) can be rewritten as

$$M_{\gamma^{(L)}}\left(s\right)=\prod_{v=1}^{V}\mathrm{E}\left[e^{s\lambda_v^X U_v^X}e^{s\lambda_v^Y W_v^Y}\right]=\prod_{v=1}^{V}\left(\Phi_{U_v^X}\left(s\right)\Phi_{W_v^Y}\left(s\right)\right).\tag{5.11}$$

---

[4]For further details about the KL series expansion, we refer the readers to [79, Sections III and VI.B.2].

Substituting (5.9) into (5.11), the MGF expression in (5.11) may then be expressed as

$$M_{\gamma^{(L)}}\left(s\right) = \prod_{v=1}^{V}\left(1 - 2\lambda_v^X s\right)^{-\frac{\xi_v^X}{2}}\left(1 - 2\lambda_v^Y s\right)^{-\frac{\xi_v^Y}{2}}, \qquad \forall\, s \geq 0. \qquad (5.12)$$

Now, it remains to calculate the eigenvalues, λ_v^X and λ_v^Y, and their respective algebraic multiplicities, ξ_v^X and ξ_v^Y, which are required in (5.12). This will be performed in the next section for the general case, i.e., for non-identical correlated channels, as well as for some particular cases obtained from our formulations. To conclude this section, we would like to emphasize that (5.12) allows for arbitrary η_i and $\bar{\gamma}_i$ parameters, assuming not necessarily the same values among the diversity branches. Concerning the values of μ_i, although they may be different among the branches, they are multiple integers of 0.5, in order to comply with the analytical derivations. To the best of the authors' knowledge, (5.12) has not been reported yet in the literature.

5.1.3   Average Symbol Error Probability

In order to derive the average SEP of rectangular *M*-QAM constellations undergoing η-μ fading, we resort to the well-known MGF-based approach [69], which has proved over the years to be a simple and efficient method for error probability analysis.

For *M*-ary rectangular QAM with coherent MRC multichannel reception, according to the statistical independence between the in-phase and quadrature parts of the additive Gaussian noise at the receiver [71], the *M*-QAM ($M = I \times J$) constellation is treated as two independent square pulse amplitude modulation (PAM) signal constellations, *I*-ary and *J*-ary, with square quadrature to in-phase distance ratio given by $\beta \triangleq d_J^2/d_I^2$. Hence, the instantaneous SEP conditioned on $\gamma^{(L)}$ for the $I \times J$ rectangular QAM, can be expressed as

$$\begin{aligned}
P_{\mathrm{s}}^{\mathrm{MRC}}\left(e\,\middle|\,\gamma^{(L)}\right) = {}& 2q_I Q\left(\sqrt{2g_{\mathrm{Q}}\left(I, J; \beta\right)\gamma^{(L)}}\right) + 2q_J Q\left(\sqrt{2g_{\mathrm{Q}}\left(I, J; \beta\right)\beta\gamma^{(L)}}\right) \\
& -4q_I q_J Q\left(\sqrt{2g_{\mathrm{Q}}\left(I, J; \beta\right)\gamma^{(L)}}\right) Q\left(\sqrt{2g_{\mathrm{Q}}\left(I, J; \beta\right)\beta\gamma^{(L)}}\right),
\end{aligned}$$
$$(5.13)$$

where $q_x \triangleq 1 - 1/x$, $Q\left(x\right) \triangleq \frac{1}{\sqrt{2\pi}}\int_0^{\infty}\exp(-t^2/2)\,dt$ and $g_{\mathrm{Q}}\left(I, J; \beta\right) \triangleq 3/[(I^2 - 1) + (J^2 - 1)\beta]$.

Averaging (5.13) over the SNR distribution, $f_{\gamma^{(L)}}(\gamma)$, a general expression for the cal-

culation of the average SEP of arbitrary rectangular QAM is given by

$$
\begin{aligned}
\bar{P}_{\mathrm{s}}^{\mathrm{MRC}}(e) &= \int_0^{+\infty} P_{\mathrm{s}}^{\mathrm{MRC}}\left(e \left| \gamma^{(L)} = \gamma\right.\right) f_{\gamma^{(L)}}(\gamma)\, d\gamma \\
&= 2q_I I_1\left(g_{\mathrm{Q}}(I, J; \beta)\right) + 2q_J I_1\left(g_{\mathrm{Q}}(I, J; \beta)\,\beta\right) \\
&\quad - 4q_I q_J I_2\left(g_{\mathrm{Q}}(I, J; \beta),\, g_{\mathrm{Q}}(I, J; \beta)\,\beta\right),
\end{aligned}
\tag{5.14}
$$

where

$$
I_1(g) \triangleq \int_0^{+\infty} Q\left(\sqrt{2g\gamma}\right) f_{\gamma^{(L)}}(\gamma)\, d\gamma,
\tag{5.15}
$$

and

$$
I_2(g_1, g_2) \triangleq \int_0^{+\infty} Q\left(\sqrt{2g_1\gamma}\right) Q\left(\sqrt{2g_2\gamma}\right) f_{\gamma^{(L)}}(\gamma)\, d\gamma.
\tag{5.16}
$$

Now, using the alternative form of the Gaussian Q-function [69, Eq. 4.2], we can rearrange (5.15) as

$$
I_1(g) = \frac{1}{\pi} \int_0^{\pi/2} M_{\gamma^{(L)}}\left(\frac{-g}{\sin^2\theta}\right) d\theta = \frac{1}{\pi} \int_0^{\pi/2} \prod_{v=1}^{V} \left(1 + \frac{2\lambda_v^X g}{\sin^2\theta}\right)^{-\frac{\xi_v^X}{2}} \left(1 + \frac{2\lambda_v^Y g}{\sin^2\theta}\right)^{-\frac{\xi_v^Y}{2}} d\theta.
\tag{5.17}
$$

Then making the change of variables $t = \cos^2(\theta)$, (5.17) can be simplified to:

$$
I_1(g) = \frac{M_{\gamma^{(L)}}(-g)}{2\pi} \int_0^1 t^{-\frac{1}{2}} (1-t)^{\mu_\Sigma - \frac{1}{2}} \prod_{v=1}^{V} \left(1 - \frac{t}{1 + 2\lambda_v^X g}\right)^{-\frac{\xi_v^X}{2}} \left(1 - \frac{t}{1 + 2\lambda_v^Y g}\right)^{-\frac{\xi_v^Y}{2}} dt,
\tag{5.18}
$$

where $\mu_\Sigma \triangleq \sum_{i=1}^{V} \left(\xi_i^X + \xi_i^Y\right)$. Finally, after some algebraic manipulations, (5.18) can be expressed as

$$
I_1(g) = \frac{B\left(\frac{1}{2}, \frac{1}{2} + \mu_\Sigma\right)}{2\pi} M_{\gamma^{(L)}}(-g) \times F_D^{(2V)} \left(\begin{array}{c} \frac{1}{2}, \xi_1^X, \xi_1^Y, \cdots, \xi_V^X, \xi_V^Y; 1 + \mu_\Sigma \\ ; \dfrac{1}{1 + 2\lambda_1^X g}, \cdots, \dfrac{1}{1 + 2\lambda_L^X g}, \dfrac{1}{1 + 2\lambda_V^X g} \end{array}\right),
\tag{5.19}
$$

where $B(a, b) \triangleq \Gamma(a)\Gamma(b)/\Gamma(a+b)$ represents the Beta function and $F_D^{(V)}(a, b_1, \cdots, b_V$ $; c; x_1, \cdots, x_V)$ denotes the integral representation of the multivariate Lauricella hypergeometric function of V variables, $c > \{b_i\}_{i=1}^{V} > 0$ [75, eq. (2.3.6)].

In order to solve the integral in (5.16), making use of the product of two Gaussian

functions as provided in [72, eq. (9)], (5.16) can be expressed as

$$
I_2\left(g_1, g_2\right) = \frac{1}{2\pi} \sum_{(k_1, k_2)} \int_0^{\tan^{-1}\left(\sqrt{\frac{g_{k_2}}{g_{k_1}}}\right)} M_{\gamma^{(V)}}\left(\frac{-g_{k_2}}{\sin^2\theta}\right) d\theta
$$

$$
= \frac{1}{2\pi} \sum_{(K_1, K_2)} \int_0^{\tan^{-1}\left(\sqrt{\frac{g_{K_2}}{g_{K_1}}}\right)} \prod_{v=1}^{V}\left(1 + \frac{2\lambda_v^X g_{K_2}}{\sin^2\theta}\right)^{-\xi_v^X}\left(1 + \frac{2\lambda_v^Y g_{K_2}}{\sin^2\theta}\right)^{-\xi_v^Y} d\theta,
$$

(5.20)

where the summation is over the two permutations $\{(1,2),(2,1)\}$. Then using the same approach applied for the derivation of $I_1(g)$, $I_2(g_1, g_2)$ can be expressed in terms of the multivariate Lauricella hypergeometric function as:

$$
I_2\left(g_1, g_2\right) = \frac{M_{\gamma^{(L)}}\left(-(g_1 + g_2)\right)}{4\pi\left(\frac{1}{2} + \mu_\Sigma\right)\left(\sqrt{\frac{g_1}{g_2}} + \sqrt{\frac{g_2}{g_1}}\right)}
$$

$$
\times \sum_{(K_1, K_2)} F_D^{2V+1}\left(\begin{array}{c} 1, \xi_1^X, \xi_1^Y, \cdots, \xi_V^X, \xi_V^Y, 1; \mu_\Sigma + \frac{3}{2}; \dfrac{1 + 2\lambda_1^X g_{K_2}}{1 + 2\left(g_1 + g_2\right)\lambda_1^X}, \dfrac{1 + 2\lambda_1^Y g_{K_2}}{1 + 2\left(g_1 + g_2\right)\lambda_1^Y} \\[2ex] , \cdots, \dfrac{1 + 2\lambda_V^X g_{K_2}}{1 + 2\left(g_1 + g_2\right)\lambda_V^X}, \dfrac{1 + 2\lambda_V^Y g_{K_2}}{1 + 2\left(g_1 + g_2\right)\lambda_V^Y}, \dfrac{1}{1 + \frac{g_{K_1}}{g_{K_2}}} \end{array}\right).
$$

(5.21)

It is noteworthy that the necessary requirements for the validation of the Lauricella functions in (5.19) and (5.21) are easily satisfied, i.e., $g, g_1, g_2, \{\lambda_i, \mu_i, \eta_i\}_{i=1}^{V} > 0$.

Finally, substituting (5.19) and (5.21) into (5.14), yields a closed-form expression for the average SEP of general rectangular QAM with MRC diversity over correlated general-

ized η-μ fading channels as shown in (5.22).

$$
\begin{aligned}
\bar{P}_{\mathrm{s}}^{\mathrm{MRC}}(e) &= \frac{q_I M_{\gamma^{(L)}}\left(-g_{\mathrm{QAM}}^{\mathrm{R}}(I,J;\beta)\right)}{\pi\left\{B\left(\frac{1}{2},\frac{1}{2}+\mu_\Sigma\right)\right\}^{-1}} \\
&\times F_D^{2V}\left(
\begin{array}{c}
\frac{1}{2},\xi_1^X,\xi_1^Y,\cdots,\xi_V^X,\xi_V^Y;1+\mu_\Sigma;\frac{1}{1+2\lambda_1^X g_{\mathrm{QAM}}^{\mathrm{R}}(I,J;\beta)}, \\
\frac{1}{1+2\lambda_1^Y g_{\mathrm{QAM}}^{\mathrm{R}}(I,J;\beta)},\cdots,\frac{1}{1+2\lambda_V^X g_{\mathrm{QAM}}^{\mathrm{R}}(I,J;\beta)},\frac{1}{1+2\lambda_V^Y g_{\mathrm{QAM}}^{\mathrm{R}}(I,J;\beta)}
\end{array}
\right) \\
&+ \frac{q_J M_{\gamma^{(L)}}\left(-\beta g_{\mathrm{QAM}}^{\mathrm{R}}(I,J;\beta)\right)}{\pi\left\{B\left(\frac{1}{2},\frac{1}{2}+\mu_\Sigma\right)\right\}^{-1}} \\
&\times F_D^{2V}\left(
\begin{array}{c}
\frac{1}{2},\xi_1^X,\xi_1^Y,\cdots,\xi_V^X,\xi_V^Y;1+\mu_\Sigma;\frac{1}{1+2\beta\lambda_1^X g_{\mathrm{QAM}}^{\mathrm{R}}(I,J;\beta)},\frac{1}{1+2\beta\lambda_1^Y g_{\mathrm{QAM}}^{\mathrm{R}}(I,J;\beta)}, \\
\cdots,\frac{1}{1+2\beta\lambda_V^X g_{\mathrm{QAM}}^{\mathrm{R}}(I,J;\beta)},\frac{1}{1+2\beta\lambda_V^Y g_{\mathrm{QAM}}^{\mathrm{R}}(I,J;\beta)}
\end{array}
\right) \\
&- \frac{q_I q_J M_{\gamma^{(L)}}\left(-(1+\beta)g_{\mathrm{QAM}}^{\mathrm{R}}(I,J;\beta)\right)}{\pi\left(\frac{1}{2}+\mu_\Sigma\right)\left(\sqrt{\beta}+\frac{1}{\sqrt{\beta}}\right)}\times\sum_{(K_1,K_2)} \\
&\times F_D^{2V+1}\left(
\begin{array}{c}
1,\xi_1^X,\xi_1^Y,\cdots,\xi_V^X,\xi_V^Y,1;\mu_\Sigma+\frac{3}{2};\frac{1+2\beta^{K_2-1}g_{\mathrm{QAM}}^{\mathrm{R}}(I,J;\beta)\lambda_1^X}{1+2(1+\beta)g_{\mathrm{QAM}}^{\mathrm{R}}(I,J;\beta)\lambda_1^X},\frac{1+2\beta^{K_2-1}g_{\mathrm{QAM}}^{\mathrm{R}}(I,J;\beta)\lambda_1^Y}{1+2(1+\beta)g_{\mathrm{QAM}}^{\mathrm{R}}(I,J;\beta)\lambda_1^Y}, \\
\cdots,\frac{1+2\beta^{K_2-1}g_{\mathrm{QAM}}^{\mathrm{R}}(I,J;\beta)\lambda_V^X}{1+2(1+\beta)g_{\mathrm{QAM}}^{\mathrm{R}}(I,J;\beta)\lambda_V^X},\frac{1+2\beta^{K_2-1}g_{\mathrm{QAM}}^{\mathrm{R}}(I,J;\beta)\lambda_V^Y}{1+2(1+\beta)g_{\mathrm{QAM}}^{\mathrm{R}}(I,J;\beta)\lambda_V^Y},\frac{1}{1+\beta^{K_1-K_2}}
\end{array}
\right).
\end{aligned}
$$

$$(5.22)$$

In particular, when the in-phase and quadrature decision distances d_I and d_J are equal ($\beta = 1$), (5.22) specializes to the following expression

$$
\begin{aligned}
\bar{P}_{\mathrm{s}}^{\mathrm{MRC}}(e) &= \frac{(q_I+q_J)M_{\gamma^{(L)}}\left(-g_{\mathrm{QAM}}^{\mathrm{R}}(I,J)\right)}{\pi\left\{B\left(\frac{1}{2},\frac{1}{2}+\mu_\Sigma\right)\right\}^{-1}} \\
&\times F_D^{2V}\left(
\begin{array}{c}
\frac{1}{2},\xi_1^X,\xi_1^Y,\cdots,\xi_V^X,\xi_V^Y;1+\mu_\Sigma; \\
\frac{1}{1+2\lambda_1^X g_{\mathrm{QAM}}^{\mathrm{R}}(I,J)},\frac{1}{1+2\lambda_1^Y g_{\mathrm{QAM}}^{\mathrm{R}}(I,J)}, \\
\cdots,\frac{1}{1+2\lambda_V^X g_{\mathrm{QAM}}^{\mathrm{R}}(I,J)},\frac{1}{1+2\lambda_V^Y g_{\mathrm{QAM}}^{\mathrm{R}}(I,J)}
\end{array}
\right) \\
&- \frac{q_I q_J M_{\gamma^{(L)}}\left(-2g_{\mathrm{QAM}}^{\mathrm{R}}(I,J)\right)}{\pi\left(\frac{1}{2}+\mu_\Sigma\right)} \\
&\times \sum_{(K_1,K_2)} F_D^{2V+1}\left(
\begin{array}{c}
1,\xi_1^X,\xi_1^Y,\cdots,\xi_V^X,\xi_V^Y,1;\mu_\Sigma+\frac{3}{2};\frac{1+2g_{\mathrm{QAM}}^{\mathrm{R}}(I,J)\lambda_1^X}{1+4g_{\mathrm{QAM}}^{\mathrm{R}}(I,J)\lambda_1^X}, \\
\frac{1+2g_{\mathrm{QAM}}^{\mathrm{R}}(I,J)\lambda_1^Y}{1+4g_{\mathrm{QAM}}^{\mathrm{R}}(I,J)\lambda_1^Y},\cdots,\frac{1+2g_{\mathrm{QAM}}^{\mathrm{R}}(I,J)\lambda_V^X}{1+4g_{\mathrm{QAM}}^{\mathrm{R}}(I,J)\lambda_V^X},\frac{1+2g_{\mathrm{QAM}}^{\mathrm{R}}(I,J)\lambda_V^Y}{1+4g_{\mathrm{QAM}}^{\mathrm{R}}(I,J)\lambda_V^Y},\frac{1}{2}
\end{array}
\right),
\end{aligned}
$$

$$(5.23)$$

where $g_{\mathrm{QAM}}^{\mathrm{R}}(I,J) \triangleq g_{\mathrm{QAM}}^{\mathrm{R}}(I,J,1)$.

To finalize, the eigenvalues, λ_v^X and λ_v^Y, and their respective algebraic multiplicities, ξ_v^X and ξ_v^Y, which are required in the above formulations will be derived. As the L diversity branches may assume different fading parameters (μ_i, η_i) and arbitrary correlation coefficients $\rho_{i,j}$, the covariance matrix pertaining to the in-phase and quadrature components X and Y can be obtained by calculating K_X and K_Y. Now, substituting K_X and K_Y in $\left| K_Z - \lambda^Z I \right| = 0$ ($Z = X$ or $Z = Y$) and solving the required determinant, the eigenvalues and their respective multiplicities are obtained.

5.1.3.1 Special Cases

Here, we study some special cases of the above results. For each case, we determine the eigenvalues and their corresponding multiplicities, which are used in (5.22) in order to evaluate the average SEP of rectangular QAM schemes undergoing η-μ fading.

5.1.3.2 Single Reception

For single-branch reception ($L = 1$), each covariance coefficient pertaining to the components X and Y has only one eigenvalue ($V = 1$) given, respectively, by

$$\lambda_1^X = \mathrm{E}\left[X_{1,j}^2 \right] = \frac{\eta_1 \Omega_1}{2\mu_1(1 + \eta_1)}, \quad \lambda_1^Y = \mathrm{E}\left[Y_{1,j}^2 \right] = \frac{\Omega_1}{2\mu_1(1 + \eta_1)}, \quad \forall j = 1, \cdots, 2\mu_1,$$

(5.24)

with the same multiplicity: $\xi_1^X = \xi_1^Y = 2\mu_1$. Substituting these values into the MGF expression (5.12), we have

$$M_{\gamma^{(1)}}(s) = \left(1 - \frac{\eta_1 \Omega_1}{\mu_1 (1 + \eta_1)} s \right)^{-\mu_1} \left(1 - \frac{\Omega_1}{\mu_1 (1 + \eta_1)} s \right)^{-\mu_1},$$

(5.25)

which after simple manipulation can be expressed as

$$M_{\gamma^{(1)}}(s) = \left(\frac{\mu_1^2 (1 + \eta_1)^2}{(\mu_1 (1 + \eta_1) - \eta_1 \Omega_1 s)(\mu_1 (1 + \eta_1) - \Omega_1 s)} \right)^{\mu_1},$$

(5.26)

thus yielding in the same formula reported in [72, Eq. 5].

5.1.3.3   Independent Multi-Channel Diversity

Here, it is considered that the L diversity branches are mutually independent. In this case, the covariance matrices K_X and K_Y have L distinct eigenvalues ($V = L$) given by

$$\lambda_v^X = \mathrm{E}\left[X_{v,j}^2\right] = \frac{\eta_v \Omega_v}{2\mu_v(1 + \eta_v)}, \quad \lambda_v^Y = \mathrm{E}\left[Y_{v,j}^2\right] = \frac{\Omega_v}{2\mu_v(1 + \eta_v)},$$

$$\forall j = 1, \cdots, 2\mu_v, \ v = 1, \cdots, V, \quad (5.27)$$

with multiplicities given by $\xi_v^X = \xi_v^Y = 2\mu_v$. Then, the MGF (5.12) can be expressed as

$$M_{\gamma^{(L)}}(s) = \prod_{v=1}^{L} \left(1 - \frac{\eta_v \Omega_v}{\mu_v(1 + \eta_v)}s\right)^{-\mu_v} \left(1 - \frac{\Omega_v}{\mu_v(1 + \eta_v)}s\right)^{-\mu_v}. \quad (5.28)$$

5.1.3.4   Dual-Branch Correlated Diversity

Consider now a dual-branch correlated MRC system with fading parameters (μ_1, η_1) and (μ_2, η_2), and correlation coefficient $\rho_{1,2}$. The corresponding X and Y vectors are defined according to (5.4), from which the covariance matrices K_X and K_Y can be easily calculated. Then, substituting K_X and K_Y into $\left|K_Z - \lambda^Z I\right| = 0$ ($Z = X$ or $Z = Y$), the eigenvalues can be derived as

$$\lambda_{1,2}^X = \frac{1}{2}\left[\frac{\Omega_{X_1}}{2\mu_1} + \frac{\Omega_{X_2}}{2\mu_2} \pm \sqrt{\left(\frac{\Omega_{X_1}}{2\mu_1} + \frac{\Omega_{X_2}}{2\mu_2}\right)^2 - \frac{\Omega_{X_1}\Omega_{X_2}}{\mu_1\mu_2}\left(1 - \rho_{1,2}^2\right)}\right],$$

$$\lambda_{1,2}^Y = \frac{1}{2}\left[\frac{\Omega_{Y_1}}{2\mu_1} + \frac{\Omega_{Y_2}}{2\mu_2} \pm \sqrt{\left(\frac{\Omega_{Y_1}}{2\mu_1} + \frac{\Omega_{Y_2}}{2\mu_2}\right)^2 - \frac{\Omega_{Y_1}\Omega_{Y_2}}{\mu_1\mu_2}\left(1 - \rho_{1,2}^2\right)}\right], \quad (5.29)$$

$$\lambda_3^X = \eta_2 \lambda_3^Y = \frac{\Omega_{X_2}}{2\mu_2},$$

where $\Omega_{X_i} = \eta_i \Omega_{Y_i} = \eta_i \Omega_i/(1 + \eta_i)$, and their respective multiplicities are given by $\xi_{1,2}^X = \xi_{1,2}^Y = 2\mu_1$ and $\xi_3^X = \xi_3^Y = 2(\mu_2 - \mu_1)$. Finally, substituting these values in (5.12), a general MGF expression for dual-branch correlated schemes is attained.
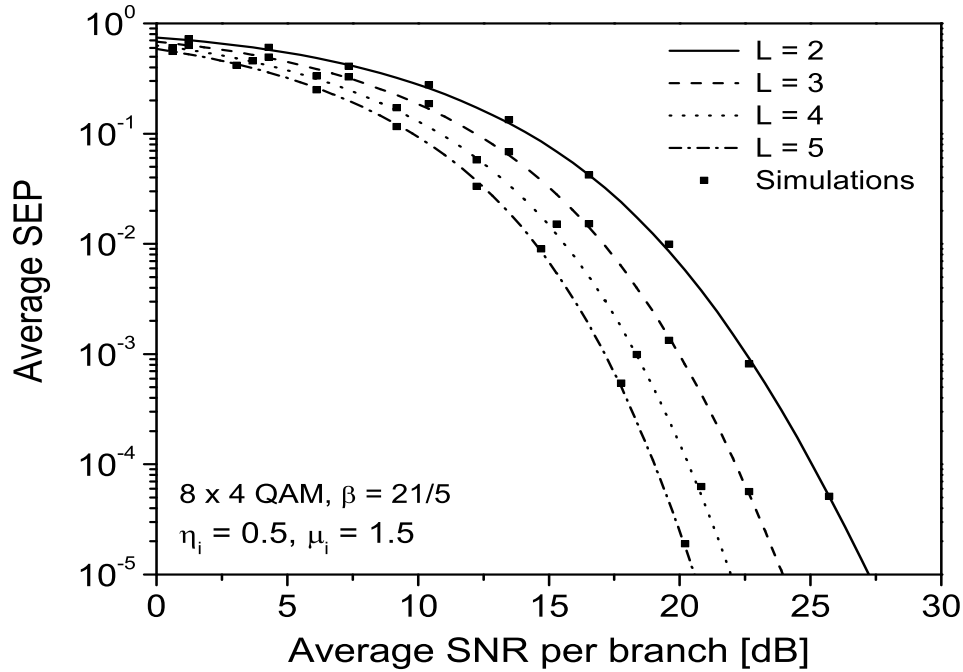
Figure 5.1: Average SEP for a 8×4 QAM constellation over independent η-μ fading channels ($\eta_i = 0.5$, $\mu_i = 1.5$ and $\beta = 21/5$).

5.1.4 Numerical Results and Discussions

In this Section, we illustrate with some representative examples the analytical expressions derived previously. Simulations results are also provided and, as will be seen, an excellent agreement is attested between the analytical and simulated curves. In our plots, the effect of the fading parameters as well as the variation of L on the system performance is investigated, and insightful discussions are provided. Note that since η-μ fading model is flexible and comprises Hoyt ($\mu_i = 0.5$), Nakagami-*m* ($\eta_i = 1$), and Rayleigh ($\mu_i = 0.5$, $\eta_i = 1$) as special cases, a myriad of interesting cases can be analyzed from our proposed expressions. For example, assuming $L = 2$, a possible fading-setting that can be analyzed in future works is: first branch $\rightarrow$ Hoyt fading; second branch $\rightarrow$ Nakagami-*m* fading.

Figs. 5.1, 5.2 and 5.3 plot the average SEP as a function of the average SNR per branch, $\bar{\gamma}_i$, for independent η-μ fading channels. All the input branches are assumed to have the same average SNR. In Fig. 5.1, the influence of L on the SEP performance is shown for a 8×4 QAM constellation and assuming the following parameters: $\eta_i = 0.5$, $\mu_i = 1.5$
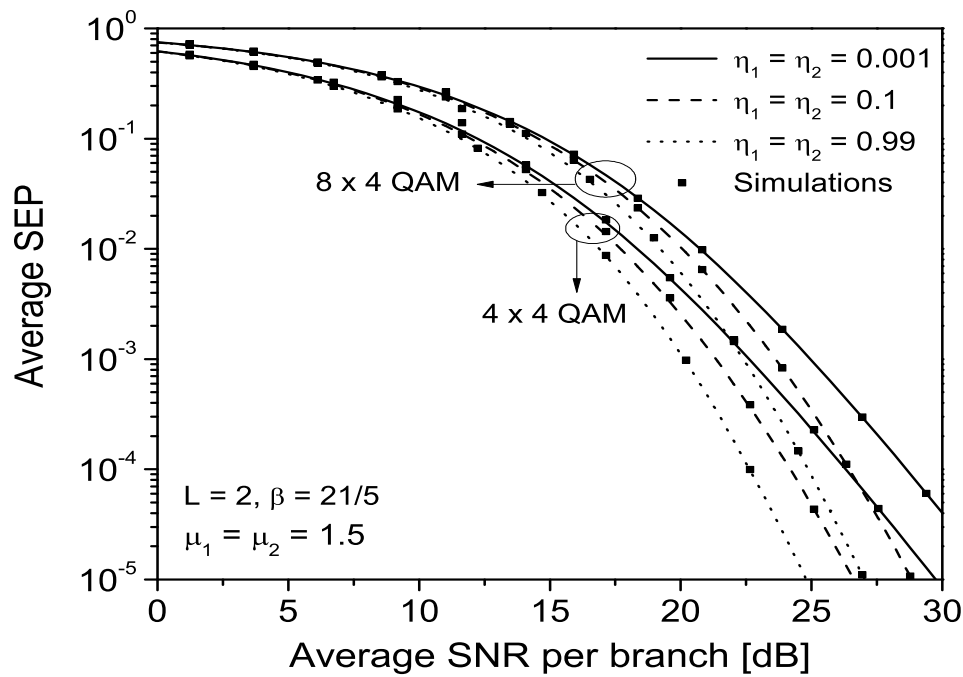
Figure 5.2: Average SEP for 8×4 and 4×4 QAM constellations over two independent η-μ fading channels ($\mu_1 = \mu_2 = 1.5$ and $\beta = 21/5$).
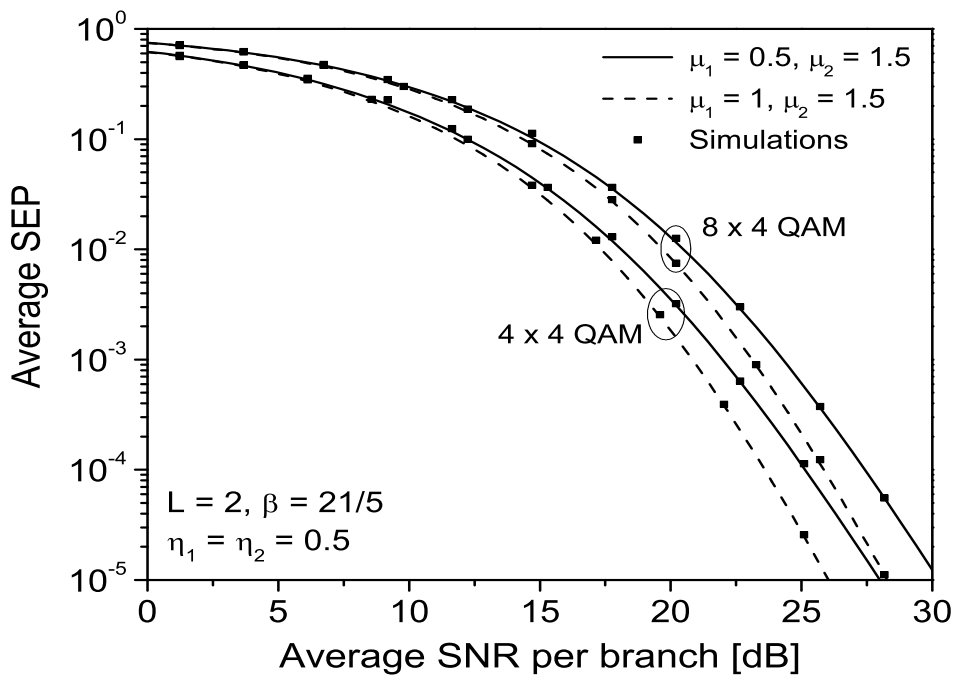
Figure 5.3: Average SEP for 8×4 and 4×4 QAM constellations over two independent η-μ fading channels ($\eta_1 = \eta_2 = 0.5$ and $\beta = 21/5$).

and $\beta = 21/5$. As expected, when L increases the system performance improves. Fig. 5.2 investigates the effect of the power imbalance, defined by the parameter η_i, between the in-phase and quadrature components of the fading signal. Two QAM constellations are considered and we assume the following parameters: $\mu_1 = \mu_2 = 1.5$, $\beta = 21/5$ and $L = 2$. For the same type of modulation, the SEP performance improves as the channel model approaches the Nakagami-m model (i.e., $\eta_i \to 1$). This leads us to conclude that the power imbalance is harmful for the system performance, specially at high SNRs. In addition, when the constellation enlarges (i.e., goes from 4×4 QAM to 8×4 QAM), the performance degrades. Such behavior has been reported in the technical literature [69] and is confirmed here as well. Finally, Fig. 5.3 examines the effect of the parameter μ_i on the SEP performance by considering two independent η-μ fading channels ($L = 2$) and employing 8×4 and 4×4 QAM constellations with $\beta = 21/5$. For both input branches, we consider the same value for η_i, i.e, $\eta_1 = \eta_2 = 0.5$. Since higher values of μ_i imply a higher number of multipath clusters at the receiver, the performance is improved given that the received signals tend to be more deterministic than the ones composed by few multipath clusters.

Figs. 5.4 and 5.5 analyze the average SEP as a function of $\bar{\gamma}_i$ for correlated η-μ fading channels over a 8×4 QAM constellation. In order to make the figures clearer, simulation data have been omitted. Actually, they are practically coincident with the analytical curves. In Fig. 5.4, two input branches are considered and we assume the following parameters: $\eta_1 = \eta_2 = 0.5$, $\mu_1 = 0.5$ and $\mu_2 = 1.5$. Note that in the high SNR range, increasing the parameter β degrades the average SEP reasonably. This can be justified from (5.13) which shows that the instantaneous SEP increases for high values of β. On the other hand, in the low SNR region, β does not play a crucial role in the system performance given that (5.13) is practically the same regardless of the value. These facts were also attested in [70] for the independent case and they are confirmed here for the correlated scenario as well. The effect of L on the SEP performance is illustrated in Fig. 5.5 by setting $\eta_i = 0.5$, $\mu_{i \neq L} = 0.5$, $\mu_L = 1$, $\beta = 1$, and $\rho_{i,j} = \rho$. Finally, as observed, in both figures, when the correlation coefficient $\rho_{i,j} = \rho$ increases, the system performance decreases, consequently.
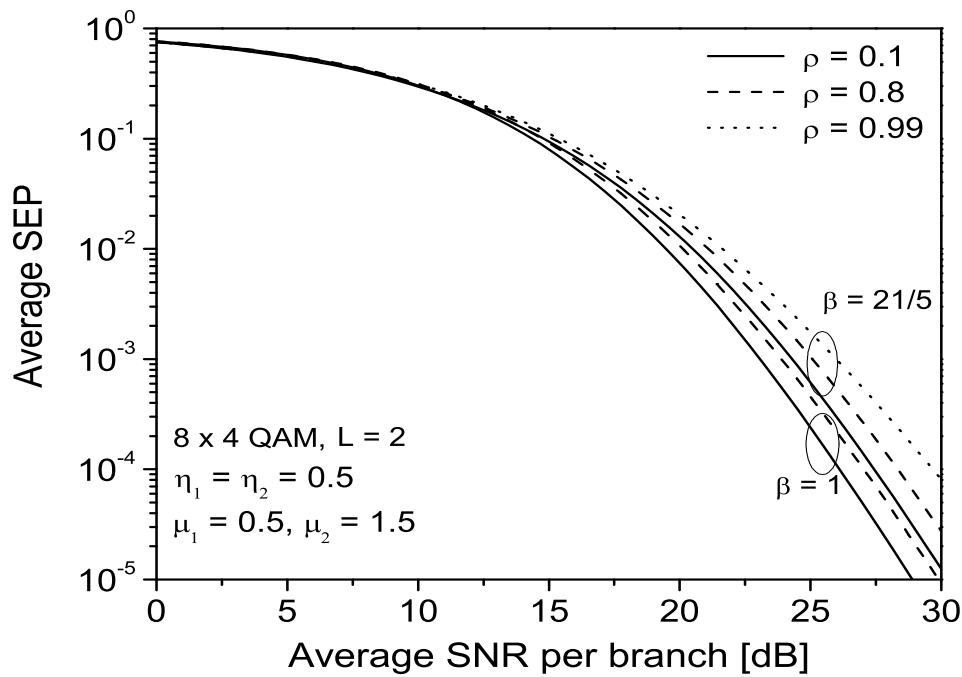
Figure 5.4: Average SEP for a 8×4 QAM constellation over two correlated η-μ fading channels ($\eta_1 = \eta_2 = 0.5$, $\mu_1 = 0.5$, $\mu_2 = 1.5$ and $\rho_{1,2} = \rho$).
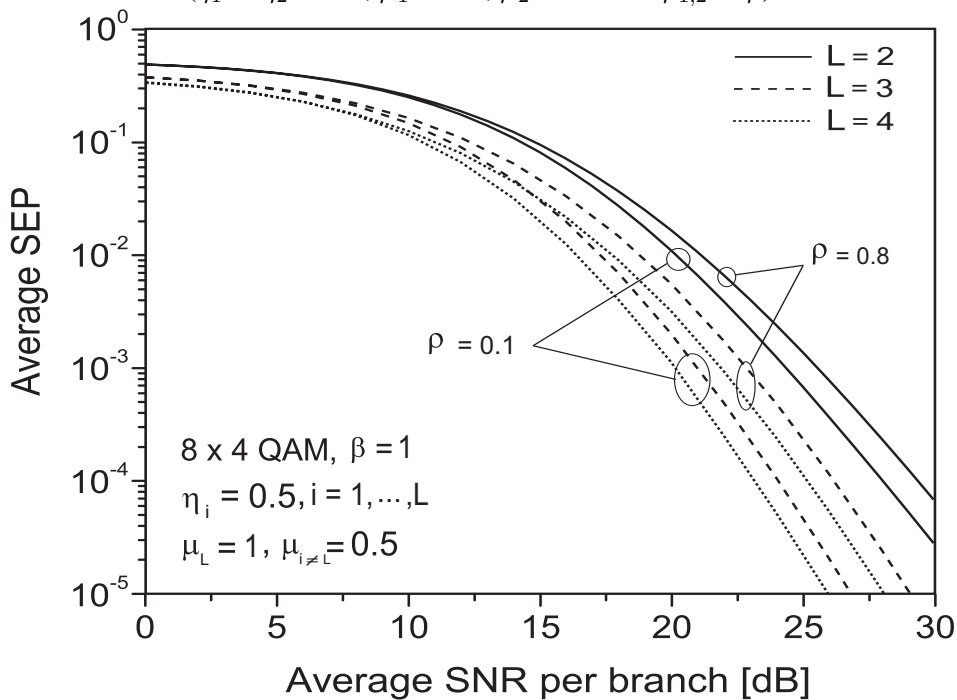
Figure 5.5: Average SEP for a 8×4 QAM constellation over $L = 2, 3, 4$ correlated η-μ fading channels ($\eta_i = 0.5$, $\mu_L = 1$, $\mu_{i \neq L} = 0.5$ and $\rho_{i,j} = \rho$).

5.1.5   Summary

In this section, a general closed-form expression for the average SEP in M-ary rectangular QAM constellations was derived assuming multichannel reception over η-μ correlated fading channels. For such, we reorganized appropriately the input diversity branch components in order to obtain the MGF of the instantaneous SNR at the combiner output. Based on this result and applying the MGF-based method, the average SEP was then attained in terms of the distinct eigenvalues of the Gaussian components and their associated algebraic multiplicities. The approach has been applied for some special cases, such as the dual-branch correlated and the independent multichannel case, and agreements with previously reported results were verified. Furthermore, although the analysis focused on rectangular QAM constellations, the proposed approach can be easily extended to other M-ary modulation schemes.

In the next section, we consider a multi-hop relaying system and derive closed-form expressions for the average SEP of arbitrary M-ary rectangular QAM constellations, when the links between the K successive nodes forming the multi-hop cooperation chain follow Nakagami-m fading distributions.

5.2   Symbol Error Probability Analysis for Multihop Relaying Channels

In the context of cooperative communications, as mentioned earlier in Chapter 1.1.5, cooperative relaying transmission has emerged as a powerful tool to increase the spectral efficiency and coverage of wireless networks. In particular, multihop transmissions enable two nodes, one source and one destination, to reach one another through a set of cooperating relays, the aim of which is to propagate the signal from the source to the destination in order to enhance coverage and increase the achievable throughput between the end nodes. This communication paradigm, also known as multihop relaying, has received much attention of late [27–31]. Roughly speaking, there are two main types of signal processing at the relay in multihop transmissions: Amplify-and-forward (AF) relaying whereby the relay simply amplifies the received signal without any sort of decoding and forwards the amplified version to the next hop, which is the most straightforward and practical option,

and decode-and-forward (DF) relaying whereby the relay decodes the received signal and then re-encodes it before forwarding it to the next hop. DF is known to outperform AF in small to medium signal-to-noise ratios (SNRs) whereas the two schemes yield relatively the same performance in the high SNR regime. Owing to its low-complexity and straight-forward implementation, AF probably remains the most popular option, at least from a practicality standpoint.

The performance of the DF scheme over fading channels was investigated in [80, 81]. Moreover, the work in [30] has studied the end-to-end performance of a dual-hop semi-blind nonregenerative relaying system with partial relay selection. Nonetheless, and de-spite the recent appearance in the literature of exact as well as tight approximate results for the SEP of $I \times J$-ary QAM constellations over fading channels as obtained in Section 5.1 and [71, 82] for systems with or without spatial diversity, the SEP performance of rectangular QAM is yet to be investigated for multihop relaying systems with either DF or AF transmission schemes. The aim of this section is to derive closed-form expressions for the SEP of arbitrary rectangular QAM for multihop AF relaying systems over independent but not-necessarily identically distributed (i.n.i.d.) Nakagami-m fading channels characterized by an arbitrary set $\{m_k, \bar{\gamma}_k\}_{k=1}^K$ of real-valued Nakagami indexes and average power levels, where K is the number of multihop links, m_k is the Nakagami index and $\bar{\gamma}_k$ is the average SNR associated with the k-th multihop link, respectively. Our results can be seen as a nat-ural extension of the dual-hop results provided in [30] to the case of a multihop relaying system.

The remainder of Section 5.2 is organized as follows. First, Section 5.2.1 briefly in-troduces the system model and formulates the problem. Next, Section 5.2.2 presents the end-to-end performance analysis for rectangular QAM over i.n.i.d. Nakagami-m fading channels in multihop AF relaying systems along with the newly derived rectangular QAM average SEP closed-from expression. Numerical and simulation results are presented in Section 5.2.3, and a conclusion summarizing the contributions of this work is provided in Section 5.2.4.

5.2.1   System and Channel Models

We consider the system model illustrated in Fig. 5.6, where a set of $K - 1$ intermediate (nonregenerative) relays $\{R_k\}_{k=1}^{K-1}$ amplify and forward the signal to be transmitted from a
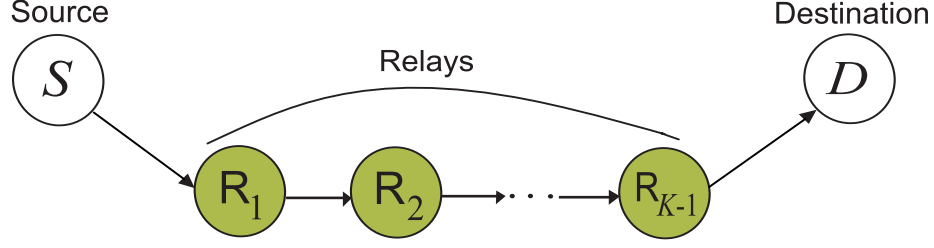
Figure 5.6: Multi-hop cooperative relaying system.

source S to a destination D, thereby cooperating to create a K-hop AF transmission system with no direct line-of-sight between the source and the destination nodes. The received signal at the k-th terminal can be expressed in baseband notation as

$$y_k = \alpha_k x_{k-1} + n_k, \ \ \forall\, k = 1, \cdots, K, \tag{5.30}$$

where α_k is the channel gain associated with the k-th hop, x_{k-1} is the signal forwarded from the previous node (x_0 being the signal at the source) and n_k is the additive white noise at node k, independent from the signals x_k, and modeled as a zero-mean complex circularly symmetric Gaussian random variable with variance $N_{0,k}$. For convenience, let y_K and n_K denote the received signal and noise at the destination, respectively. Furthermore, one could also write $y_k = \alpha_k x_k$. Then, we have

$$y_K = \alpha_K \prod_{i=1}^{K-1} v_i \alpha_i x_0 + \sum_{i=1}^{K-1} \prod_{j=i}^{K-1} v_j \alpha_{j+1} n_i + n_K, \tag{5.31}$$

where $\{v_i\}_{i=1}^{K-1}$ denote the amplification factors associated with the $K-1$ relay terminals. Usually, the amplification factor v_k at relay k, $k = 1, \ldots, K-1$ is set to $v_k = \sqrt{\frac{E_s}{E_s \alpha_k^2 + N_{0,k}}}$, where E_s is the average energy per symbol, in order to satisfy an average power constraint as in [83]. However, for the sake of simplicity and mathematical tractability, we set $v_k = \frac{1}{\alpha_k}$, i.e. the relay inverts the channel of the previous hop regardless of the fading state of that hop, which leads to the following expression for the end-to-end SNR as given by [33]

$$\gamma_{\text{eq}} = \left[\sum_{k=1}^{K} \frac{1}{\gamma_k} \right]^{-1}, \tag{5.32}$$

where $\gamma_k := E_s \alpha_k^2 / N_{0,k}$. Since we are concerned with independent fading between the different hops, then the moment generating function (MGF) of γ_{eq}^{-1}, i.e., $M_{\gamma_{\text{eq}}^{-1}}(s) :=$ $\mathrm{E}\left[e^{-s\gamma_{\text{eq}}^{-1}}\right]$ where $\mathrm{E}[\cdot]$ stands for mathematical expectation, can be expressed as the product of the individual MGFs pertaining to the K hops, thus implying

$$
\begin{aligned}
M_{\gamma_{\text{eq}}^{-1}}(s) &= \int_0^{+\infty} p_{\gamma_{\text{eq}}^{-1}}(\gamma) \, e^{-s\gamma} d\gamma \\
&= \prod_{k=1}^{K} M_{\gamma_k^{-1}}(s),
\end{aligned}
\tag{5.33}
$$

where $p_x(\cdot)$ denotes the probability distribution function (PDF) of random variable x. For Nakagami-m fading, the MGF of γ_k^{-1} can be expressed as [28]

$$
M_{\gamma_k^{-1}}(s) = \frac{2}{\Gamma(m_k)} \left(\frac{m_k s}{\bar{\gamma}_k}\right)^{\frac{m_k}{2}} \mathrm{K}_{m_k}\left(2\sqrt{\frac{m_k s}{\bar{\gamma}_k}}\right),
\tag{5.34}
$$

where $\Gamma(\cdot)$ denotes the Gamma function [51], $\mathrm{K}_\nu(\cdot)$ is the modified Bessel function of the second kind with order ν and $\bar{\gamma}_k := E_s \mathrm{E}\left[\alpha_k^2\right]/N_{0,k}$. Accordingly,

$$
M_{\gamma_{\text{eq}}^{-1}}(s) = \prod_{k=1}^{K} \frac{2}{\Gamma(m_k)} \left(\frac{m_k}{\bar{\gamma}_k}\right)^{\frac{m_k}{2}} s^{\frac{m_\Sigma}{2}} \prod_{k=1}^{K} \mathrm{K}_{m_k}\left(2\sqrt{\frac{m_k s}{\bar{\gamma}_k}}\right),
\tag{5.35}
$$

where $m_\Sigma := \sum_{k=1}^{K} m_k$.

In order to evaluate $M_{\gamma_{\text{eq}}}(s)$, we consider the MGF inversion formula provided in [28, theorem 1] along with an appropriate change of variable, leading up to the following MGF expression:

$$
M_{\gamma_{\text{eq}}}(s) = 1 - 2\sqrt{s} \int_0^{\infty} J_1\left(2\beta\sqrt{s}\right) M_{\gamma^{-1}}\left(\beta^2\right) d\beta,
\tag{5.36}
$$

where $J_1(\cdot)$ represents the first-order Bessel function of the first kind [51].

Upon substitution of (5.35) into (5.36), one obtains

$$
\begin{aligned}
M_{\gamma_{\text{eq}}}(s) = 1 - 2\sqrt{s} &\left(\prod_{k=1}^{K} \frac{2}{\Gamma(m_k)} \left(\frac{m_k}{\bar{\gamma}_k}\right)^{\frac{m_k}{2}}\right) \\
&\times \int_0^{\infty} J_1\left(2\beta\sqrt{s}\right) \beta^{m_\Sigma} \prod_{k=1}^{K} \mathrm{K}_{m_k}\left(2\beta\sqrt{\frac{m_k}{\bar{\gamma}_k}}\right) d\beta.
\end{aligned}
\tag{5.37}
$$

Hereafter, using the above MGF expression, we investigate the average SEP performance of rectangular QAM for the multihop relaying system under consideration.

5.2.2   End-to-End Average Symbol Error Probability

The average SEP of rectangular QAM for multi-hop relaying (MHR) is given by

$$\bar{P}_{\mathrm{s}}^{\mathrm{MHR}}(E) = \int_0^{+\infty} P_{\mathrm{s}}^{\mathrm{MHR}}(E\,|\gamma)\, p_{\gamma_{\mathrm{eq}}}(\gamma)\, d\gamma, \tag{5.38}$$

where $P_{\mathrm{s}}^{\mathrm{MHR}}(E\,|\gamma)$ is the instantaneous SEP conditioned on the received SNR γ. According to the statistical independency between the constituent parts of the additive Gaussian noise at the receiver, in-phase and quadrature, the M-QAM ($M = I \times J$) constellation is treated as two independent square pulse amplitude modulation (PAM) signal constellations, I-ary and J-ary, with square quadrature to in-phase distances ratio of $\xi \triangleq d_J^2/d_I^2$. Hence, the instantaneous SEP conditioned on γ for the $I \times J$ rectangular QAM, can be expressed as

$$\begin{aligned}
P_{\mathrm{s}}^{\mathrm{MHR}}(E\,|\gamma) = {}& 2h(I)\, Q\left(\sqrt{2g_{\mathrm{QAM}}^{\mathrm{R}}(I,J;\xi)\,\gamma}\right) + 2h(J)\, Q\left(\sqrt{2g_{\mathrm{QAM}}^{\mathrm{R}}(I,J;\xi)\,\xi\gamma}\right) \\
& - 4h(I)\,h(J)\, Q\left(\sqrt{2g_{\mathrm{QAM}}^{\mathrm{R}}(I,J;\xi)\,\gamma}\right) \times Q\left(\sqrt{2g_{\mathrm{QAM}}^{\mathrm{R}}(I,J;\xi)\,\xi\gamma}\right),
\end{aligned} \tag{5.39}$$

where $h(x) \triangleq 1 - x^{-1}$, and $g_{\mathrm{QAM}}^{\mathrm{R}}(I,J;\xi)$ and $Q(x)$ are defined as

$$g_{\mathrm{QAM}}^{\mathrm{R}}(I,J;\xi) \triangleq 3\big/\left[\left(I^2 - 1\right) + \left(J^2 - 1\right)\xi\right], \tag{5.40}$$

$$Q(x) \triangleq \frac{1}{\sqrt{2\pi}} \int_0^\infty \exp(-t^2/2)\, dt. \tag{5.41}$$

The average SEP can then be obtained by substituting the latter conditional SEP expression into (5.38), as

$$\begin{aligned}
\bar{P}_{\mathrm{s}}^{\mathrm{MHR}}(E) = {}& 2h(I)\, I_1\left(g_{\mathrm{QAM}}^{\mathrm{R}}(I,J;\xi)\right) \\
& + 2h(J)\, I_1\left(g_{\mathrm{QAM}}^{\mathrm{R}}(I,J;\xi)\,\xi\right) \\
& - 4h(I)\,h(J)\, I_2\left(g_{\mathrm{QAM}}^{\mathrm{R}}(I,J;\xi),\, g_{\mathrm{QAM}}^{\mathrm{R}}(I,J;\xi)\,\xi\right),
\end{aligned} \tag{5.42}$$

where

$$I_1(g) \triangleq \int_0^{+\infty} Q\left(\sqrt{2g\gamma}\right) p_{\gamma_{eq}}(\gamma)\, d\gamma, \quad \forall\, g > 0 \tag{5.43}$$

and

$$I_2(g_1, g_2) \triangleq \int_0^{+\infty} Q\left(\sqrt{2g_1\gamma}\right) Q\left(\sqrt{2g_2\gamma}\right) p_{\gamma_{eq}}(\gamma)\, d\gamma, \quad \forall\, g_1, g_2 > 0. \tag{5.44}$$

We now have to solve for both integrals in 5.43 and 5.44 in order to derive the average SEP expression of rectangular QAM for the multihop cooperative relaying system under consideration.

Starting with $I_1(g)$, and using the alternate form of the Gaussian Q-function [69, eq. 4.2], we have

$$
\begin{aligned}
I_1(g) &= \frac{1}{\pi} \int_0^{\pi/2} M_{\gamma_{eq}}\left(\frac{g}{\sin^2 \theta}\right) d\theta = \frac{1}{2} - \frac{2\sqrt{g}}{\pi}\left(\prod_{k=1}^{K} \frac{2}{\Gamma(m_k)}\left(\frac{m_k}{\bar{\gamma}_k}\right)^{\frac{m_k}{2}}\right) \\
&\quad \times \int_0^{\infty} \beta^{m_\Sigma} \prod_{k=1}^{K} \mathrm{K}_{m_k}\left(2\beta\sqrt{\frac{m_k}{\bar{\gamma}_k}}\right) \int_0^{\pi/2} \frac{1}{\sin\theta} J_1\left(\frac{2\beta\sqrt{g}}{\sin\theta}\right) d\theta\, d\beta.
\end{aligned}
\tag{5.45}
$$

Then, employing the change of variable $t = \sin^{-1}\theta$ in 5.45, we obtain

$$
\begin{aligned}
I_1(g) &= \frac{1}{2} - \frac{2\sqrt{g}}{\pi}\left(\prod_{k=1}^{K} \frac{2}{\Gamma(m_k)}\left(\frac{m_k}{\bar{\gamma}_k}\right)^{\frac{m_k}{2}}\right) \\
&\quad \times \int_0^{\infty} \beta^{m_\Sigma} \prod_{k=1}^{K} \mathrm{K}_{m_k}\left(2\beta\sqrt{\frac{m_k}{\bar{\gamma}_k}}\right) \int_1^{\infty} \frac{J_1\left(2\beta\sqrt{g}t\right)}{\sqrt{t^2-1}} dt\, d\beta.
\end{aligned}
\tag{5.46}
$$

Using [84, Eq.s 6.552.6, 8.464.1, 8.469.1], we have

$$\int_1^{\infty} J_1\left(2\beta\sqrt{g}t\right)\Big/\sqrt{t^2-1}\, dt = \sin\left(2\beta\sqrt{g}\right)/2\beta\sqrt{g}. \tag{5.47}$$

Accordingly,

$$I_1(g) = \frac{1}{2} - \frac{2\sqrt{g}}{\pi}\left(\prod_{k=1}^{K} \frac{2}{\Gamma(m_k)}\left(\frac{m_k}{\bar{\gamma}_k}\right)^{\frac{m_k}{2}}\right) \int_0^{\infty} \beta^{m_\Sigma} \frac{\sin\left(2\beta\sqrt{g}\right)}{2\beta\sqrt{g}} \prod_{k=1}^{K} \mathrm{K}_{m_k}\left(2\beta\sqrt{\frac{m_k}{\bar{\gamma}_k}}\right) d\beta. \tag{5.48}$$

Now, recognizing that the Bessel function can be represented in terms of the confluent Hypergeometric function $_1F_1(a; b, c)$ [75, Eq. 1.1.2.2], as [85]

$$
\begin{aligned}
\mathrm{K}_v(z) = {} & 2^{v-1}\Gamma(v)\, e^{-v} z^{-v} {}_1F_1\left(\frac{1}{2} - v; 1 - 2v, 2z\right) \\
& + 2^{-v-1}\Gamma(-v)\, e^{-v} z^v {}_1F_1\left(\frac{1}{2} + v; 1 + 2v, 2z\right).
\end{aligned}
\tag{5.49}
$$

Note that (5.49) is valid only for non-integer values of v. However, this representation can easily be extended to encompass integer values of v by inducing a small perturbation to the actual integer values of v, i.e., $v = \lim_{\epsilon \to 0}(v + \epsilon)$. Simulation results provided in Sec. 5.2.3 prove that this has no actual bearing on the final SEP results. Likewise, the function $\sin(x)$ can be expressed in terms of $_1F_1(a; b, c)$ [51, Eq. (13.6.13)]

$$
\sin(x) = x\, e^{-ix} {}_1F_1(1; 2, 2ix),
\tag{5.50}
$$

where $i^2 = -1$. As a result, $I_1(g)$ can be expressed as

$$
\begin{aligned}
I_1(g) = {} & \frac{1}{2} - \frac{4\sqrt{g}}{\pi}\left(\prod_{k=1}^{K}\frac{1}{\Gamma(m_k)}\left(\frac{m_k}{\bar{\gamma}_k}\right)^{\frac{m_k}{2}}\right) \\
& \times \int_0^{\infty} \beta^{m_\Sigma} e^{-2i\beta\sqrt{g}} {}_1F_1(1; 2, 4i\beta\sqrt{g})\prod_{k=1}^{K}(X_k + Y_k)d\beta,
\end{aligned}
\tag{5.51}
$$

where

$$
X_k = \Gamma(m_k)\, e^{-m_k}\left(2\beta\sqrt{\frac{m_k}{\bar{\gamma}_k}}\right)^{-m_k} {}_1F_1\left(\frac{1}{2} - m_k; 1 - 2m_k, 4\sqrt{\frac{m_k}{\bar{\gamma}_k}}\beta\right),
\tag{5.52}
$$

and

$$
Y_k = \Gamma(-m_k)\, e^{-m_k}\left(2\beta\sqrt{\frac{m_k}{\bar{\gamma}_k}}\right)^{m_k} {}_1F_1\left(\frac{1}{2} + m_k; 1 + 2m_k, 4\sqrt{\frac{m_k}{\bar{\gamma}_k}}\beta\right).
\tag{5.53}
$$

Next, we make use of the following alternate expression for the product involved in (5.51):

$$
\prod_{k=1}^{K}(X_k + Y_k) = \sum_{\kappa \in \mathcal{P}_K}\prod_{k=1}^{K} X_k^{\kappa_k} Y_k^{1-\kappa_k},
\tag{5.54}
$$

where $\mathcal{P}_K := \{\kappa = (\kappa_1, \kappa_2, \ldots, \kappa_K) : \kappa \in \{0, 1\}^K\}$. Upon substituting (5.54) into (5.51), the latter becomes

$$I_1(g) = \frac{1}{2} - \frac{4\sqrt{g}}{\pi} \left(\prod_{k=1}^{K} \frac{1}{\Gamma(m_k)} \left(\frac{m_k}{\bar{\gamma}_k}\right)^{\frac{m_k}{2}}\right) \int_0^{\infty} \beta^{m_\Sigma} e^{-2i\beta\sqrt{g}} {}_1F_1(1; 2, 4i\beta\sqrt{g})$$

$$\times \sum_{\kappa \in \mathcal{P}_K} \prod_{k=1}^{K} X_k^{\kappa_k} Y_k^{1-\kappa_k} d\beta, \qquad (5.55)$$

which after some manipulations, simplifies into

$$I_1(g) = \frac{1}{2} - \frac{4\sqrt{g}}{\pi} \left(\prod_{k=1}^{K} \frac{1}{\Gamma(m_k)} \left(\frac{m_k}{\bar{\gamma}_k}\right)^{\frac{m_k}{2}}\right)$$
$$\times \sum_{\kappa \in \mathcal{P}_K} \left(\prod_{k=1}^{K} \left(\frac{4m_k}{\bar{\gamma}_k}\right)^{-m_k\kappa_k} e^{-m_k} \Gamma(m_k)^{\kappa_k} \Gamma(-m_k)^{1-\kappa_k}\right) I_1^{\kappa}, \qquad (5.56)$$

where

$$I_1^{\kappa} = \int_0^{\infty} \beta^{\Omega(\kappa)} e^{-2i\beta\sqrt{g}} {}_1F_1(1; 2, 4i\beta\sqrt{g}) \prod_{k=1}^{K} \left[{}_1F_1\left(\frac{1}{2} - m_k; 1 - 2m_k, 4\sqrt{\frac{m_k}{\bar{\gamma}_k}}\beta\right)\right]^{\kappa_k}$$
$$\times \left[{}_1F_1\left(\frac{1}{2} + m_k; 1 + 2m_k, 4\sqrt{\frac{m_k}{\bar{\gamma}_k}}\beta\right)\right]^{1-\kappa_k} d\beta, \qquad (5.57)$$

and $\Omega(\kappa) = 2m_\Sigma - 2\sum_{k=1}^{K} m_k\kappa_k$. Now, using a slightly modified version of [75, Eq. (6.4.1)] given by

$$\int_0^{\infty} e^{-\nu t} t^{a-1} \prod_{i=1}^{L} {}_1F_1(b_i; c_i; x_i t) \, dt = \frac{\Gamma(a)}{\nu^a} F_A^{(L)}\left(a; b_1, \cdots, b_L; c_1, \cdots, c_L; \frac{x_1}{\nu}, \cdots, \frac{x_L}{\nu}\right)$$

$$(5.58)$$

where $F_A^{(L)}(a; b_1, \cdots, b_L; c_1, \cdots, c_L; x_1, \cdots, x_L)$ denotes the first Lauricella hypergeo-

metric function of L variables, 5.57 can be expressed as

$$
I_1^\kappa = \frac{\Gamma\left(1 + \Omega\left(\kappa\right)\right)}{\left(2i\sqrt{g}\right)^{\Omega(\kappa)+1}} \times F_A^{(K+1)} \left(
\begin{array}{l}
1 + \Omega\left(\kappa\right); 1, \dfrac{1}{2} - \delta_1 m_1, \cdots, \dfrac{1}{2} - \delta_K m_K; \\[2mm]
2, 1 - 2\delta_1 m_1, \cdots, 1 - 2\delta_K m_K; \\[2mm]
2, -2i\sqrt{\dfrac{m_1}{g\bar{\gamma}_1}}, \cdots, -2i\sqrt{\dfrac{m_K}{g\bar{\gamma}_K}}
\end{array}
\right),
$$
(5.59)

where $\delta_k = sgn(\kappa_k - 1/2), \forall k = 1, \ldots, K$ and sgn denotes the standard sign function. The multivariable Lauricella function $F_A^{(L)}(\cdot; \cdot; \cdot; \cdot)$ is usually defined via its series representation given by [75, eq. (2.1.1)], and its convergence is assured whenever $\sum_{i=1}^{L} |x_i| < 1$. Note that one can always modify the arguments x_i in 5.59 in order for this convergence condition be satisfied, by making use of the following Euler integral transformation [75, Eq. (4.2.2)]:

$$
F_A^{(L)}\left(a; b_1, \cdots, b_L; c_1, \cdots, c_L; x_1, \cdots, x_L\right) = \Delta^{-a}
$$
$$
F_A^{(L)}\left(a; c_1 - b_1, \cdots, c_L - b_L; c_1, \cdots, c_L; -\frac{x_1}{\Delta}, \cdots, -\frac{x_L}{\Delta}\right)
$$
(5.60)

where $\Delta := 1 - \sum_{i=1}^{L} x_i$. Accordingly, substituting (5.59) into (5.56), $I_1(g)$ can be expressed as

$$
I_1\left(g\right) = \frac{1}{2} - \frac{2\sqrt{g}}{\pi} \left(\prod_{k=1}^{K} \frac{1}{\Gamma\left(m_k\right)} \left(\frac{m_k}{\bar{\gamma}_k}\right)^{\frac{m_k}{2}}\right)
$$
$$
\times \sum_{\kappa \in \mathcal{P}_K} \left(\prod_{k=1}^{K} \left(\frac{4m_k}{\bar{\gamma}_k}\right)^{-m_k \kappa_k} \frac{e^{-m_k} \Gamma\left(m_k\right)^{-\kappa_k} \Gamma\left(-m_k\right)^{1-\kappa_k}}{\left(2i\sqrt{g}\right)^{\Omega(\kappa)+1} \Gamma^{-1}\left(1 + \Omega\left(\kappa\right)\right)}\right)
$$
$$
\times F_A^{(K+1)} \left(
\begin{array}{l}
1 + \Omega\left(\kappa\right); 1, \dfrac{1}{2} - \delta_1 m_1, \cdots, \dfrac{1}{2} - \delta_K m_K; \\[2mm]
2, 1 - 2\delta_1 m_1, \cdots, 1 - 2\delta_K m_K; \\[2mm]
2, -2i\sqrt{\dfrac{m_1}{g\bar{\gamma}_1}}, \cdots, -2i\sqrt{\dfrac{m_K}{g\bar{\gamma}_K}}
\end{array}
\right).
$$
(5.61)

As for solving the second integral form (5.44), we resort to the accurate approximation for the product of two Gaussian Q-functions presented in [82, Eq. 14], thus yielding

$$
Q\left(\sqrt{2g_1\gamma}\right) Q\left(\sqrt{2g_2\gamma}\right) \simeq \sum_{i=1}^{2} a_i e^{-2\gamma(b_i g_1 + c_i g_2)},
$$
(5.62)

where $(a_1, a_2) = (1/9, 1/3)$, $(b_1, b_2) = (1, 4/3)$ and $(c_1, c_2) = (4/3, 1)$. The accuracy of the above tight upper bound was discussed in [82], where the authors mentioned its good agreement with the error complementary function defined by $\mathrm{erfc}(x)$ for $x > 0.5$. Therefore, by using (5.62), we can approximate $I_2(g_1, g_2)$ as

$$I_2 (g_1, g_2) \simeq \sum_{i=1}^{2} a_i M_{\gamma_{\mathrm{eq}}} (2\gamma (b_i g_1 + c_i g_2)). \tag{5.63}$$

Substituting (5.37) into (5.63), and after some manipulations, we have

$$I_2 (g_1, g_2) \simeq \frac{4}{9} - 2 \left(\prod_{k=1}^{K} \frac{2}{\Gamma(m_k)} \left(\frac{m_k}{\bar{\gamma}_k} \right)^{\frac{m_k}{2}} \right) \sum_{i=1}^{2} a_i \sqrt{2 (b_i g_1 + c_i g_2)}$$
$$\times \int_0^{\infty} \beta^{m_\Sigma} J_1 \left(2\beta \sqrt{2 (b_i g_1 + c_i g_2)} \right) \prod_{k=1}^{K} \mathrm{K}_{m_k} \left(2\beta \sqrt{\frac{m_k}{\bar{\gamma}_k}} \right) d\beta. \tag{5.64}$$

Now, considering the approach presented to obtain $I_1(g)$ and using the equivalent expression for the Bessel function $J_1(z)$ in terms of the confluent hypergeometric function as [51, Eq. (9.1.69)]

$$J_1 (x) = \frac{xe^{-ix}}{2} {}_1F_1 \left(\frac{3}{2}; 3, 2ix \right), \tag{5.65}$$

$I_2(g_1, g_2)$ in (5.64) can be reexpressed as

$$I_2 (g_1, g_2) \simeq \frac{4}{9} - 2 \left(\prod_{k=1}^{K} \frac{2}{\Gamma(m_k)} \left(\frac{m_k}{\bar{\gamma}_k} \right)^{\frac{m_k}{2}} \right) \sum_{i=1}^{2} 2a_i (b_i g_1 + c_i g_2)$$
$$\times \sum_{\kappa \in \mathcal{P}_K} \left(\prod_{k=1}^{K} \left(\frac{4m_k}{\bar{\gamma}_k} \right)^{-m_k \kappa_k} e^{-m_k} \Gamma(m_k)^{\kappa_k} \Gamma(-m_k)^{1-\kappa_k} \right) I_2^{\kappa}, \tag{5.66}$$

where

$$I_2^{\kappa} = \int_0^{\infty} \beta^{\Omega(\kappa)+1} e^{-i\sqrt{8(b_i g_1 + c_i g_2)}\beta} {}_1F_1 \left(3/2; 3, +i\sqrt{32 (b_i g_1 + c_i g_2)}\beta \right)$$
$$\times \prod_{k=1}^{K} \left[{}_1F_1 \left(\frac{1}{2} - m_k; 1 - 2m_k, 4\sqrt{\frac{m_k}{\bar{\gamma}_k}}\beta \right) \right]^{\kappa_k} \left[{}_1F_1 \left(\frac{1}{2} + m_k; 1 + 2m_k, 4\sqrt{\frac{m_k}{\bar{\gamma}_k}}\beta \right) \right]^{1-\kappa_k} d\beta. \tag{5.67}$$

Then, by recognizing the integral representation of the first Lauricella hypergeometric function 5.58 and following the same approach used to evaluate $I_1(g)$, we find out that (5.67)

can be expressed as shown in (5.68).

$$I_2\left(g_1, g_2\right) \simeq \frac{4}{9} - 2 \left(\prod_{k=1}^{K} \frac{2}{\Gamma\left(m_k\right)} \left(\frac{m_k}{\bar{\gamma}_k}\right)^{\frac{m_k}{2}}\right) \sum_{i=1}^{2} 2a_i \left(b_i g_1 + c_i g_2\right) \sum_{\kappa \in \mathcal{P}_K} \left(\prod_{k=1}^{K} \left(\frac{4m_k}{\bar{\gamma}_k}\right)^{-m_k \kappa_k}\right)$$

$$\times \left(\frac{2\, e^{-m_k} \Gamma\left(m_k\right)^{-\kappa_k} \Gamma\left(-m_k\right)^{1-\kappa_k}}{\left(\sqrt{8i\left(b_i g_1 + c_i g_2\right)}\right)^{\Omega(\kappa)+2} \Gamma^{-1}\left(2 + \Omega\left(\kappa\right)\right)}\right)$$

$$\times F_A^{(K+1)} \left(\begin{array}{c} 2 + \Omega\left(\kappa\right); \frac{3}{2}, \frac{1}{2} - \delta_1 m_1, \cdots, \frac{1}{2} - \delta_K m_K; 3, 1 - 2\delta_1 m_1, \\ \cdots, 1 - 2\delta_K m_K; 2, -\sqrt{\frac{2m_1}{(b_i g_1 + c_i g_2)\bar{\gamma}_1}}i, \cdots, -\sqrt{\frac{2m_K}{(b_i g_1 + c_i g_2)\bar{\gamma}_K}}i \end{array}\right).$$

$$(5.68)$$

Again, the necessary convergence requirements for the Lauricella function in (5.68) can be met by making use of the Euler integral transformation (5.60). Finally, incorporating (5.61) and (5.68) into (5.42) yields a closed-form expression for the average SEP of general rectangular QAM with multihop relaying transmission.

5.2.3 Numerical and Simulation Results

In this section, we show illustrative numerical results for the average SEP expression derived in the previous section. In our plots, the impact of varying the Nakagami fading parameters as well as the number of cooperating relay nodes on the system performance are investigated, and insightful discussions are provided. In all the numerical calculations, we consider a rectangular QAM system with $\xi = 1$.

Figs. 5.7 and 5.8 plot the average SEP as a function of the average SNR per hop, $\bar{\gamma}_k$, for i.n.i.d. Nakagami-m fading channels. All the transmission hops are assumed to have the same average received SNR, i.e., $\{\bar{\gamma}_k\}_{k=1}^{K} = \bar{\gamma}$. In Fig. 5.7, assuming dual-hop transmission, the influence of m_k on the SEP performance is shown for 8×4 and 4×4 QAM constellations. As expected, for a given modulation format, the SEP performance improves with increasing values of m_k. On the other hand, Fig. 5.8 investigates the effects of the number of transmission hops, K, between the source and destination nodes. In this figure, an 8×4 QAM constellation is considered and we assume identical Nakagami fading channels: $\{m_k\}_{k=1}^{K} = m$. It is clear from this figure that the average SEP deteriorates whenever the number of hops, K, increases.
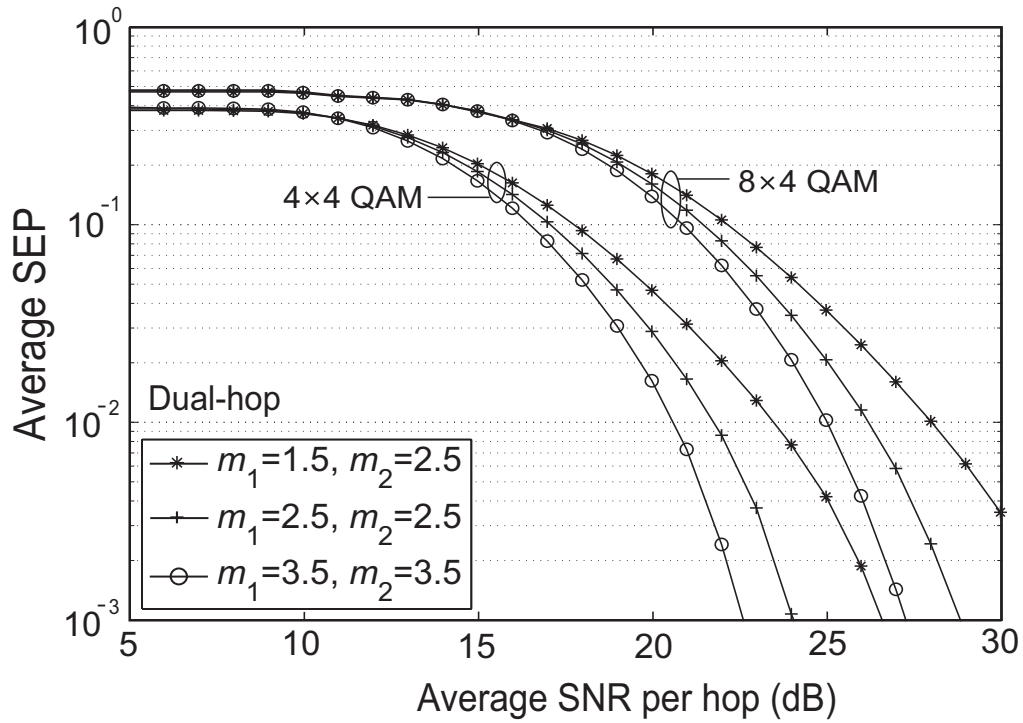
Figure 5.7: Average SEP of dual-hop transmission system employing AF relaying over independent Nakagami fading channels.
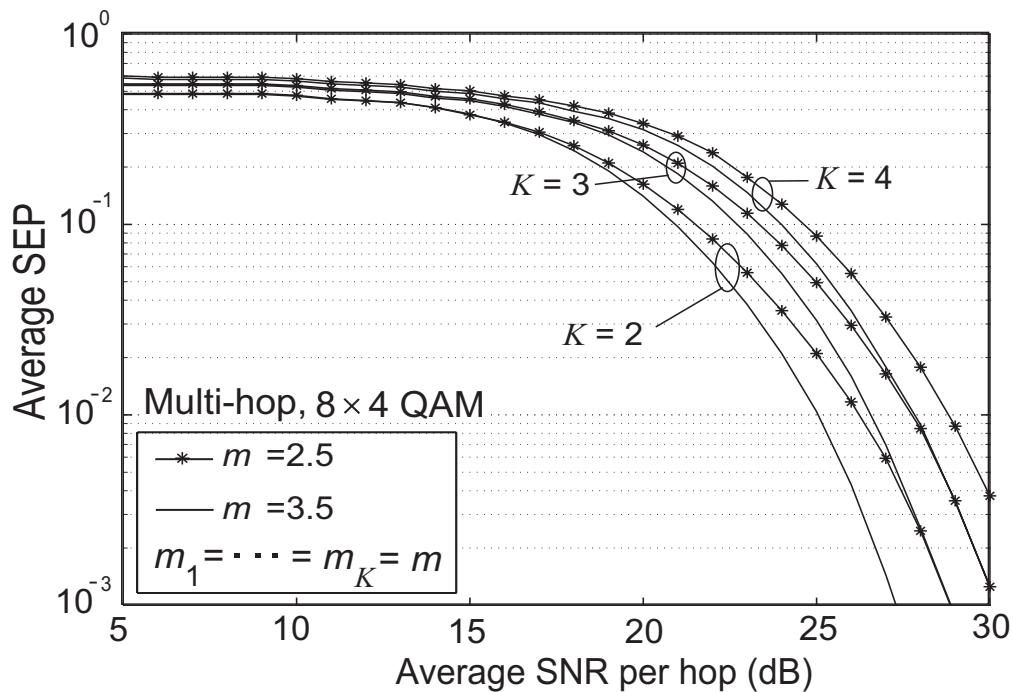
Figure 5.8: Average SEP of multi-hop transmission system employing AF relaying over independent Nakagami fading channels.

5.2.4 Summary

In the above part, we considered a multi-hop cooperative relaying system with AF transmission and no direct line-of-sight between the source and destination nodes, operating over i.n.i.d. Nakagami fading channels with arbitrary fading parameters, and derived a closed-form expression for the average symbol error probability of M-ary rectangular QAM. In particular, the SEP result was expressed in closed-form as a linear combination of multivariate Lauricella hypergeometric functions which can be easily implemented using standard numerical softwares. Numerical and simulation results corroborating our analysis were provided and the impact of several parameters such as the number of relaying nodes and Nakagami fading indexes were investigated for various rectangular QAM modulations. Although the analysis considered herein focused on QAM signals, the proposed approach can be easily extended to other M-ary modulation schemes.

Next, we investigate the ergodic capacity and outage probability performance of multi-hop cooperative relaying networks subject to independent non-identically distributed Nakagami-m fading. Particularly, we exploit an AF relaying system with an arbitrary number of cooperative relays and investigate the performance of the multihop relaying system by making use of MGF-based approach.

5.3 Performance Analysis for Multihop Relaying Channels

As mentioned in Chapter 1.1.5, multihop transmissions have been another outstanding topic of research in the recent years due to their ability of providing broader coverage without the need of high transmitting powers. In this case, communication between a source and destination nodes is performed through several intermediate relay nodes. Depending on the nature and complexity of the relaying technique, relay nodes can be broadly categorized as either non-regenerative or regenerative. In the former, the relays simply amplify and forward the received signal, while in the latter the relays decode, encode, and then forward the received signal to the destination. The amplify-and-forward (AF) mode puts less processing burden on the relays and, hence, is often preferable when complexity and/or latency are of importance.

In the open literature, several works investigating cooperative relaying communications are available, which are briefly discussed next. The performance evaluation of multi-branch multihop cooperative wireless systems has been investigated in [32] by proposing a unified framework which relies on the MGF-based approach. In [33], an analytical framework for the evaluation of the outage probability (OP) in multihop wireless channels with AF relays and subject to Nakagami-*m* fading was proposed. Boyer *et al.* in [86] presented an analysis for the physical layer of multihop networks, and introduced the concept of multihop diversity where each terminal receives signals from all the previous terminals along a single primary route. In [87–91], assuming AF relaying technique in different cooperative relaying transmissions scenarios such as multihop, multiple dualhop and dualhop, closed-form upper bounds were derived for the OP and average bit error probability (ABEP) of binary modulation schemes in identical and non-identical Nakagami-*m* fading channels. For instance in [87], by using the well-known inequality between harmonic and geometric means of positive random variables, the performance bound pertaining to the end-to-end SNR in multihop relayed communications was studied. Karagiannidis in [92] investigated the performance of multihop systems with non-regenerative blind relays undergoing Rice, Nakagami-*m* and Hoyt fading, where the OP and the ABEP for coherent and noncoherent modulation schemes were studied using the moment-based approach. In [93], the symbol error rate of multihop DF scheme over Rayleigh channels was analyzed by modeling the transmission line as a Markov chain. Recently, capacity of cooperative diversity systems with multiple parallel relays has been studied for both AF and DF protocols in [94], where an approximated expression for the ergodic capacity was derived based on the Taylor's expansion of $\ln(1 + x)$ function, and the fading was assumed to be Rayleigh. In [95], the authors examined the ergodic capacity of multihop transmission systems employing either AF or DF relays under Rayleigh fading channels. Two upper bounds were proposed based on the Jensen's inequality and the harmonic-geometric means inequality, however, the analysis was restricted to Rayleigh fading. In [32], by making use of the MGF-based approach, a simple lower bound for the outage capacity of multihop cooperative systems was obtained under different fading environments.

In this section, relying on the Jensen's inequality formulation and assuming AF relays, we provide a closed-form upper bound expression for the ergodic capacity of multihop cooperative relaying channels over independent non-identically distributed (i.n.i.d.)

Nakagami-*m* fading characterized by an arbitrary set $\{m_k, \overline{\gamma}_k\}_{k=1}^K$ of real-valued Nakagami indexes and average SNR levels, where K is the number of multihop links, m_k is the Nakagami index and $\overline{\gamma}_k$ is the average SNR associated with the k-th multihop link, respectively. For this purpose, firstly the MGF of the inverse of the end-to-end SNR is obtained in closed-form. Then, making use of this expression, an upper bound for the ergodic capacity is attained. We also investigate the end-to-end outage probability performance of the multihop AF relaying channels in Nakagami-*m* fading by making use of the above-mentioned MGF expression. Monte Carlo simulation results are provided to verify the accuracy of our mathematical formulations and to show the tightness of the proposed bounds. It is worthwhile to mention that closed-form upper bound expressions for the ergodic capacity of multihop AF relaying channels in Nakagami fading have never been reported in the open literature.

Briefly speaking, the remainder of this section is organized as follows. Section 5.3.1 details the system and channel models. In Section 5.3.2, a closed-form upper bound expression for the the ergodic capacity of multihop cooperative systems subject to i.n.i.d. Nakagami-*m* fading is derived. This general closed-form expression is also specialized to the dual-hop case, in which a very elegant and simple expression is achieved. The end-to-end outage probability performance is investigated in Section 5.3.4. Numerical and simulation results are provided in Section 5.3.5 and a very good tightness between them is observed. Finally, some concluding remarks and a summary are presented in Section 5.3.6.

5.3.1   System and Channel Models

We consider a K-hop wireless cooperative system composed by one source node S, one destination node D, and $K - 1$ non-regenerative half-duplex nodes $R_1, \ldots, R_{K-1}$, which act as intermediate relays from one hop to the next, as illustrated in Fig. 5.9. These intermediate nodes amplify and forward the received signal from the previous node without any sort of decoding. It is assumed that there is no direct link between S and D, and that each terminal communicates only with the closer node. Also, channel state information is assumed to be available only at the receiving terminals and all nodes are synchronized, i.e., no delay is incurred in the whole chain of transmission. The total communication time from node S to node D is divided into K time slots, where each transmitting terminal uses only one time slot to communicate with the next node. The cooperative links undergo i.n.i.d
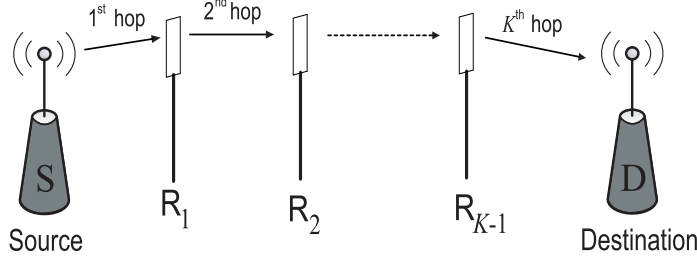
Figure 5.9: Multihop cooperative relaying system.

Nakagami-m fading with arbitrary fading parameters and arbitrary average SNR levels. Following the same procedure as presented in Section 5.2.1, the received signal y_K at the destination node can be written as

$$y_K = \alpha_K \prod_{k=1}^{K-1} v_k \alpha_k x_0 + \sum_{k=1}^{K-1} \prod_{j=k}^{K-1} v_j \alpha_{j+1} n_k + n_K, \qquad (5.69)$$

where α_k and n_k denote the channel amplitude and the additive white Gaussian noise (AWGN) of the k-th hop, respectively. Equivalently, α_K and n_K represent the channel amplitude and the AWGN of the link ending at node D, respectively, and x_0 stands for the signal transmitted by the source. The AWGN components are modeled as zero-mean complex circularly symmetric Gaussian random variables with variance $N_{0,k}$. Furthermore, $\{v_k\}_{k=1}^{K-1}$ denote the amplification gains associated with the $K-1$ relay terminals. In order to limit the output power at the relays, an average power constraint can be employed [96], in which v_k is given by $v_k = \sqrt{\frac{P_k}{P_{k-1}\alpha_k^2 + N_{0,k}}}$, with P_k representing the transmit power from the k-th terminal[5]. However, for the sake of simplicity and mathematical tractability, herein we set $v_k = \frac{1}{\alpha_k}$, which yields an extremely tight upper bound for the end-to-end SNR [35]. As mentioned in [35], this assumption serves as a benchmark for the design of practical relay systems. In this case, a relay just amplifies the incoming signal with the inverse of the channel of the previous hop, regardless of the noise level of that hop, leading to the following expression for the end-to-end SNR [33]

$$\gamma_{\text{eq}} = \left[\sum_{k=1}^{K} \frac{1}{\gamma_k} \right]^{-1}, \qquad (5.70)$$

---

[5]P_0 denotes the power transmitted by the source.

where $\gamma_k \triangleq \frac{P}{K N_{0,k}} \alpha_k^2$ represents the instantaneous SNR of the k-th hop[6], with P being the total available transmit power. As α_k is Nakagami-m distributed, the corresponding instantaneous SNR γ_k follows a Gamma distribution with PDF given by

$$f_{\gamma_k}(\gamma) = \frac{m_k^{m_k}}{\bar{\gamma}_k^{m_k} \Gamma(m_k)} \gamma^{m_k-1} \exp\left(-\frac{m_k \gamma}{\bar{\gamma}_k}\right), \tag{5.71}$$

where $\Gamma(\cdot)$ is the Gamma function [84, Eq. 8.310.1], $m_k \geq 1/2$ denotes the Nakagami-m parameter, which describes the fading severity of the k-th hop, and $\bar{\gamma}_k$ is the average SNR of the k-th hop, i.e., $\bar{\gamma}_k = \mathrm{E}[\gamma_k]$, with $\mathrm{E}[\cdot]$ denoting mathematical expectation.

5.3.2 Ergodic Capacity - Upper Bounds

Capacity analysis is of extreme importance in the design of wireless systems since it determines the maximum rates that can be attained. In this section, tight closed-form upper bounds for the ergodic capacity of multihop systems subject to i.n.i.d Nakagami-m fading are derived. Such a performance measure corresponds to the long-term average achievable rate over all states of the time-varying fading channel [41]. In a K-hop cooperative relaying system, the end-to-end ergodic capacity can be expressed as

$$C_{\mathrm{er}} = \frac{1}{K} \mathrm{E}\left[\log_2\left(1 + \gamma_{\mathrm{eq}}\right)\right], \tag{5.72}$$

in which the factor $1/K$ concerns the total number of time slots used in the transmission and is directly associated with the rate loss due to the half-duplex mode of operation. Knowing that $\log_2(x)$ is a concave function and making use of the Jensen's inequality [52, eq. (3.1.8)], an upper-bound for (5.72) can be written as

$$C_{\mathrm{er}} \leq \frac{1}{K} \log_2\left(1 + \mathrm{E}\left[\gamma_{\mathrm{eq}}\right]\right), \tag{5.73}$$

---

[6]Herein, it is assumed that the transmitted signals by the source are selected from an independent identically distributed Gaussian codebook with covariance matrix $\frac{P}{K} I_K$, where I_K stands for the identity matrix of size K.

where $\mathrm{E}\left[\gamma_{\mathrm{eq}}\right]$ is the average end-to-end SNR, defined as $\mathrm{E}\left[\gamma_{\mathrm{eq}}\right] \triangleq \int_0^\infty \gamma f_{\gamma_{\mathrm{eq}}}(\gamma)d\gamma$. An alternative definition for $\mathrm{E}\left[\gamma_{\mathrm{eq}}\right]$ can be attained using the MGF of the inverse of γ_{eq} as [95]

$$\mathrm{E}\left[\gamma_{\mathrm{eq}}\right] = \int_0^\infty M_X(s)ds, \tag{5.74}$$

where $X = 1/\gamma_{\mathrm{eq}}$. Since the cooperative links are statistically independent, the MGF of X can be expressed by the product of the corresponding marginal MGFs pertaining to the K hops so that

$$M_X(s) = \int_0^\infty f_X(\gamma)e^{-s/\gamma}d\gamma = \prod_{k=1}^K M_{Z_k}(s), \tag{5.75}$$

where $f_X(\cdot)$ denotes the PDF of X and $Z_k = 1/\gamma_k$. Performing the standard statistical procedure of transformation of variants, the PDF of Z_k can be easily obtained from (5.71) and, consequently, the corresponding MGF is achieved, being expressed by [33]

$$M_{Z_k}(s) = \frac{2}{\Gamma(m_k)}\left(\frac{m_k s}{\bar{\gamma}_k}\right)^{\frac{m_k}{2}} \mathrm{K}_{m_k}\left(2\sqrt{\frac{m_k s}{\bar{\gamma}_k}}\right), \tag{5.76}$$

in which $\mathrm{K}_\nu(\cdot)$ represents the modified Bessel function of the second kind with order ν [51, Eq. 9.6.22]. By substituting (5.76) in (5.75), it follows that

$$M_X(s) = \prod_{k=1}^K \frac{2}{\Gamma(m_k)}\left(\frac{m_k}{\bar{\gamma}_k}\right)^{\frac{m_k}{2}} s^{\frac{m_\Sigma}{2}} \prod_{k=1}^K \mathrm{K}_{m_k}\left(2\sqrt{\frac{m_k s}{\bar{\gamma}_k}}\right), \tag{5.77}$$

where $m_\Sigma \triangleq \sum_{k=1}^K m_k$. From (5.74) and (5.77), the average end-to-end SNR, as required into (5.73), can be mathematically formulated as

$$\mathrm{E}\left[\gamma_{\mathrm{eq}}\right] = \prod_{k=1}^K \frac{2}{\Gamma(m_k)}\left(\frac{m_k}{\bar{\gamma}_k}\right)^{\frac{m_k}{2}} \underbrace{\int_0^\infty s^{\frac{m_\Sigma}{2}} \prod_{k=1}^K \mathrm{K}_{m_k}\left(\sqrt{\frac{4m_k s}{\bar{\gamma}_k}}\right)ds}_{\mathbf{I}^{\mathrm{mh}}}, \tag{5.78}$$

in which the integral $\mathbf{I}^{\mathrm{mh}}$ can be expressed as

$$\mathbf{I}^{\mathrm{mh}} = \int_0^\infty s^{\frac{m_\Sigma}{2}} \mathrm{K}_{m_1}\left(\sqrt{\frac{4m_1 s}{\bar{\gamma}_1}}\right) \prod_{k=2}^K \mathrm{K}_{m_k}\left(\sqrt{\frac{4m_k s}{\bar{\gamma}_k}}\right)ds. \tag{5.79}$$

Next, a closed-form expression for (5.79) will be derived. With this aim, making use of [97], we start by representing the Bessel function in terms of the confluent Hypergeometric function $_0F_1\left(;b,c\right)$ [75]

$$\mathrm{K}_{m_k}\left(\sqrt{\frac{4m_ks}{\bar{\gamma}_k}}\right) = \frac{\Gamma\left(m_k\right)}{2}\left(\sqrt{\frac{m_ks}{\bar{\gamma}_k}}\right)^{-m_k} {}_0F_1\left(;1-m_k,\frac{m_ks}{\bar{\gamma}_k}\right)$$
$$+ \frac{\Gamma\left(-m_k\right)}{2}\left(\sqrt{\frac{m_ks}{\bar{\gamma}_k}}\right)^{m_k} {}_0F_1\left(;1+m_k,\frac{m_ks}{\bar{\gamma}_k}\right). \qquad (5.80)$$

Relying on the properties inherent to Gamma functions, note that (5.80) is valid only for non-integer values of m_k. However, this representation can easily be extended to encompass integer values of m_k by inducing a small perturbation to the integer values of m_k, i.e., $m_k = \lim_{\epsilon \to 0}(m_k + \epsilon)$. As will be seen from the simulation results provided in Sec. 5.3.5, this has no actual effect on the final capacity results.

Now, from (5.80) and (5.79), the latter can be expressed as

$$\mathbf{I}^{\mathrm{mh}} = \frac{1}{2^{K-1}}\int_0^\infty s^{\frac{m_\Sigma}{2}}\mathrm{K}_{m_1}\left(\sqrt{\frac{4m_1s}{\bar{\gamma}_1}}\right)\prod_{k=2}^K(X_k+Y_k)ds, \qquad (5.81)$$

where

$$X_k = \Gamma\left(m_k\right)\left(\sqrt{\frac{m_ks}{\bar{\gamma}_k}}\right)^{-m_k} {}_0F_1\left(;1-m_k,\frac{m_ks}{\bar{\gamma}_k}\right), \qquad (5.82)$$

and

$$Y_k = \Gamma\left(-m_k\right)\left(\sqrt{\frac{m_ks}{\bar{\gamma}_k}}\right)^{m_k} {}_0F_1\left(;1+m_k,\frac{m_ks}{\bar{\gamma}_k}\right). \qquad (5.83)$$

Using the following alternate expression for the product involved in (5.81), i.e.,

$$\prod_{k=2}^K(X_k+Y_k) = \sum_{l\in\mathcal{P}_K}\prod_{k=2}^K X_k^{l_k}Y_k^{1-l_k}, \qquad (5.84)$$

where $\mathcal{P}_K \triangleq \{l = (l_2, l_3, \ldots, l_K) : l \in \{0,1\}\}$, (5.81) can be rewritten as

$$\mathbf{I}^{\mathrm{mh}} = \frac{1}{2^{K-1}}\int_0^\infty s^{\frac{m_\Sigma}{2}}\mathrm{K}_{m_1}\left(\sqrt{\frac{4m_1s}{\bar{\gamma}_1}}\right)\sum_{l\in\mathcal{P}_K}\prod_{k=2}^K X_k^{l_k}Y_k^{1-l_k}ds. \qquad (5.85)$$

By substituting (5.82) and (5.83) into the above expression, and after some algebraic ma-

nipulations, (5.85) simplifies to

$$\mathbf{I}^{\mathrm{mh}} = \left(\prod_{k=2}^{K} \frac{1}{2} \left(\frac{m_k}{\bar{\gamma}_k} \right)^{\frac{m_k}{2}} \right) \sum_{l \in \mathcal{P}_K} \left(\prod_{k=2}^{K} \left(\frac{m_k}{\bar{\gamma}_k} \right)^{-m_k l_k} \Gamma(m_k)^{l_k} \Gamma(-m_k)^{1-l_k} \right)$$

$$\times \int_0^\infty s^{\Omega(l)} \, \mathrm{K}_{m_1} \left(\sqrt{\frac{4m_1 s}{\bar{\gamma}_1}} \right) \prod_{k=2}^{K} \left[{}_0F_1 \left(; 1 - m_k, \frac{m_k s}{\bar{\gamma}_k} \right) \right]^{l_k} \left[{}_0F_1 \left(; 1 + m_k, \frac{m_k s}{\bar{\gamma}_k} \right) \right]^{1-l_k} ds,$$

(5.86)

where $\Omega(l) = m_\Sigma - \frac{m_1}{2} - \sum_{k=2}^{K} m_k l_k$. Now, representing the modified Bessel function $\mathrm{K}_{m_1}(\cdot)$ in terms of Meijer's G-function as [85]

$$\mathrm{K}_{m_1} \left(\sqrt{\frac{4m_1 s}{\bar{\gamma}_1}} \right) = \frac{1}{2} G_{0,2}^{2,0} \left[\frac{m_1 s}{\bar{\gamma}_1} \middle| \frac{m_1}{2}, \frac{-m_1}{2} \right],$$

(5.87)

and substituting (5.87) into (5.86), we obtain

$$\mathbf{I}^{\mathrm{mh}} = \frac{1}{2^K} \left(\prod_{k=2}^{K} \left(\frac{m_k}{\bar{\gamma}_k} \right)^{\frac{m_k}{2}} \right) \sum_{l \in \mathcal{P}_K} \left(\prod_{k=2}^{K} \left(\frac{m_k}{\bar{\gamma}_k} \right)^{-m_k l_k} \Gamma(m_k)^{l_k} \Gamma(-m_k)^{1-l_k} \right)$$

$$\times \int_0^\infty s^{\Omega(l)} G_{0,2}^{2,0} \left[\frac{m_1 s}{\bar{\gamma}_1} \middle| \frac{m_1}{2}, \frac{-m_1}{2} \right]$$

$$\times \prod_{k=2}^{K} \left[{}_0F_1 \left(; 1 - m_k, \frac{m_k s}{\bar{\gamma}_k} \right) \right]^{l_k} \left[{}_0F_1 \left(; 1 + m_k, \frac{m_k s}{\bar{\gamma}_k} \right) \right]^{1-l_k} ds.$$

(5.88)

After a careful inspection, the modified version of the third Lauricella hypergeometric function [75], which is given by

$$F_C^{(L)} \left(a, b; c_1, \cdots, c_L; \frac{x_1}{x_0}, \cdots, \frac{x_L}{x_0} \right) = \frac{1}{\Gamma(a)\Gamma(b)} \int_0^\infty t^{-1} G_{0,2}^{2,0} \left[x_0 t \middle| a, b \right] \prod_{i=1}^{L} {}_0F_1 \left(; c_i; x_i t \right) dt,$$

(5.89)

can be applied to solve the integral in (5.88). Therefore, with the help of (5.89) and after

some mathematical manipulations, a closed-form expression for $\mathbf{I}^{\mathrm{mh}}$ is finally obtained as

$$
\begin{aligned}
\mathbf{I}^{\mathrm{mh}} = \frac{1}{2^K} & \left(\prod_{k=2}^{K} \left(\frac{m_k}{\bar{\gamma}_k} \right)^{\frac{m_k}{2}} \right) \sum_{l \in \mathcal{P}_K} \left(\prod_{k=2}^{K} \left(\frac{m_k}{\bar{\gamma}_k} \right)^{-m_k l_k} \Gamma \left(m_k \right)^{l_k} \Gamma \left(-m_k \right)^{1-l_k} \right) \\
& \times \Gamma \left(\Omega \left(l \right) + 1 + \frac{m_1}{2} \right) \Gamma \left(\Omega \left(l \right) + 1 - \frac{m_1}{2} \right) \left(\frac{\bar{\gamma}_1}{m_1} \right)^{1+\Omega(l)} \\
& \times F_C^{(K-1)} \left(\begin{array}{c} \Omega \left(l \right) + \frac{m_1}{2} + 1, \Omega \left(l \right) - \frac{m_1}{2} + 1; 1 - \delta_2 m_2, \\ \cdots, 1 - \delta_K m_K; \frac{\bar{\gamma}_1 m_2}{m_1 \bar{\gamma}_2}, \cdots, \frac{\bar{\gamma}_1 m_K}{m_1 \bar{\gamma}_K} \end{array} \right),
\end{aligned}
\tag{5.90}
$$

where $\delta_k = sgn(l_k - 0.5), \forall k = 2, \ldots, K$, and $sgn(\cdot)$ denotes the standard sign function.

Finally, from (5.90), (5.78) and (5.73), the proposed upper bound expression for the ergodic capacity of multihop relaying systems undergoing i.n.i.d Nakagami-*m* fading is derived in closed-form. To the best of the authors' knowledge, this result is new. In addition, it is worthwhile to mention that, even for the Rayleigh case, such closed-form upper bound was not presented in the technical literature before.

5.3.3 Special Case - Dual-Hop System

Our general expression can be reduced to some particular cases. Herein, we assume a dual-hop cooperative system ($K = 2$) with arbitrary Nakagami-*m* fading parameters and distinct average SNR levels. In this case, from (5.90), it follows that

$$
\begin{aligned}
\mathbf{I}^{\mathrm{dh}} = \frac{1}{4} & \left(\frac{m_2}{\bar{\gamma}_2} \right)^{\frac{m_2}{2}} \left(\frac{m_2}{\bar{\gamma}_2} \right)^{-m_2} \left(\frac{\bar{\gamma}_1}{m_1} \right)^{1+\frac{m_1}{2}} \Gamma \left(m_2 \right) \Gamma \left(1 + m_1 \right) F_C^{(1)} \left(1 + m_1, 1; 1 - m_2; \frac{\bar{\gamma}_1 m_2}{m_1 \bar{\gamma}_2} \right) \\
& + \frac{1}{4} \left(\frac{m_2}{\bar{\gamma}_2} \right)^{\frac{m_2}{2}} \left(\frac{\bar{\gamma}_1}{m_1} \right)^{1+m_2+\frac{m_1}{2}} \Gamma \left(-m_2 \right) \Gamma \left(m_2 + m_1 + 1 \right) \Gamma \left(m_2 + 1 \right) \\
& \times F_C^{(1)} \left(m_2 + m_1 + 1, m_2 + 1; 1 + m_2; \frac{\bar{\gamma}_1 m_2}{m_1 \bar{\gamma}_2} \right).
\end{aligned}
\tag{5.91}
$$

Then, considering that $F_C^{(1)} \left(a, b; x; y \right) = {}_2F_1 \left(a, b; x; y \right)$, with ${}_2F_1 \left(\cdot, \cdot; \cdot; \cdot \right)$ denoting the Gauss hypergeometric function [75], (5.91) can be further simplified after some mathemat-

ical manipulations as

$$\mathbf{I}^{\text{dh}} = \frac{(m_2 \bar{\gamma}_2)^{\frac{-m_2}{2}}}{4} \left(\frac{\bar{\gamma}_1}{m_1} \right)^{1 + \frac{m_1}{2}} \left[\left(\frac{m_2 \bar{\gamma}_1}{m_1} \right)^{m_2} \left(1 - \frac{m_2 \bar{\gamma}_1}{m_1 \bar{\gamma}_2} \right)^{-1 - m_1 - m_2} \right.$$

$$\times \Gamma\left(-m_2\right) \Gamma\left(1 + m_2\right) \Gamma\left(m_2 + m_1 + 1\right)$$

$$\left. + (\bar{\gamma}_2)^{m_2} \Gamma\left(1 + m_1\right) \Gamma\left(m_2\right) {}_2F_1 \left(1, 1 + m_1; 1 - m_2; \frac{m_2 \bar{\gamma}_1}{m_1 \bar{\gamma}_2} \right) \right].$$

$$(5.92)$$

Finally, from (5.92), (5.78) and (5.73), a closed-form upper bound expression for the ergodic capacity of dual-hop relaying systems with i.n.i.d. Nakagami-*m* fading links is achieved as

$$C_{\text{er}}^{\text{dh}} \leq \frac{1}{2} \log_2 \left(1 + \frac{4}{\Gamma\left(m_1\right) \Gamma\left(m_2\right)} \left(\frac{m_1}{\bar{\gamma}_1} \right)^{\frac{m_1}{2}} \left(\frac{m_2}{\bar{\gamma}_2} \right)^{\frac{m_2}{2}} \times \mathbf{I}^{\text{dh}} \right). \qquad (5.93)$$

5.3.4   Inverse MGF Application to the End-to-End Outage Probability

The outage probability of the end-to-end SNR is defined as the probability that the SNR falls below a predetermined threshold γ_{th}. For multihop relaying transmission, the outage probability is expressed in terms of $M_{\gamma_{\text{eq}}^{-1}}\left(s\right)$ as [98]

$$P_{\text{out}}\left(\gamma_{\text{th}}\right) = \Pr\left(\gamma_{\text{eq}} < \gamma_{\text{th}}\right) = \Pr\left(\frac{1}{\gamma_{\text{eq}}} > \frac{1}{\gamma_{\text{th}}} \right)$$

$$= 1 - \mathfrak{L}^{-1} \left\{ \frac{M_X\left(s\right)}{s} \right\} \Big|_{1_{/\gamma_{\text{th}}}} \qquad (5.94)$$

where $\mathfrak{L}^{-1}\{\cdot\}$ denotes the inverse Laplace transform and $M_X(s)$ is the MGF expression pertaining to γ_{eq}^{-1}. Substituting the inverse MGF expression given in (5.77) into (5.94), we can evaluate the outage probability using a numerical technique for the Laplace transform inversion. Herein, we employ the Euler numerical technique illustrated in [98] for the inverse Laplace transform. In this context, considering $\Phi_X\left(X\right) \triangleq \mathfrak{L}^{-1}\left\{M_X\left(s\right)/s\right\}$ and following the steps presented in [98], the end-to-end outage probability of multihop

relaying communication systems using AF relaying can be calculated according to

$$
\begin{aligned}
P_{\text{out}}\left(\gamma_{\text{th}}\right) &= 1 - \Phi_X\left(\frac{1}{\gamma_{\text{th}}}, A, N, Q\right) \\
&= 1 - \frac{\gamma_{\text{th}} e^{A/2}}{2^Q} \sum_{q=0}^{Q} \binom{Q}{q} \times \left[\sum_{n=0}^{N+q} \frac{(-1)^n}{\beta_n} \Re\left\{\frac{M_X\left(\frac{\gamma_{\text{th}}}{2}\left(A + 2\pi i n\right)\right)}{\frac{\gamma_{\text{th}}}{2}\left(A + 2\pi i n\right)}\right\}\right] \\
&\quad + E\left(A, N, Q\right),
\end{aligned}
$$
(5.95)

where $\Re\{\cdot\}$ denotes real part value, $\beta_0 = 2$, $\beta_{n|n\neq 0} = 1$, and $E\left(A, N, Q\right)$ is the overall discretization & truncation error term which can be approximately bounded by [98]

$$
\begin{aligned}
|E\left(A, N, Q\right)| &\simeq \frac{e^{-A}}{1 - e^{-A}} \\
&\quad + \left|\frac{\gamma_{\text{th}} e^{A/2}}{2^Q} \sum_{q=0}^{Q} (-1)^{N+1+q} \binom{Q}{q} \times \left[\Re\left\{\frac{M_X\left(\frac{\gamma_{\text{th}}}{2}\left(A + 2\pi i\left(N + q + 1\right)\right)\right)}{\frac{\gamma_{\text{th}}}{2}\left(A + 2\pi i\left(N + q + 1\right)\right)}\right\}\right]\right| .
\end{aligned}
$$
(5.96)

In our numerical results pertaining to the end-to-end outage probability of multihop relaying system, we assume the typical parameter values used in [98]. Accordingly, by considering $A = 10\ln(10)$, we guarantee a discretization error less than 10^{-10}. Furthermore, parameters Q and N are set at 15 and 21, respectively, to assure a resulting truncation error less than 10^{-10}. Finally, the overall resulting error is negligible compared to the actual outage probability value.

5.3.5 Numerical and Simulation Results

In order to show the tightness of the proposed upper bounds, illustrative numerical examples are presented and compared with Monte Carlo simulation results. In the plots, both i.i.d. and i.n.i.d. Nakagami-*m* fading scenarios are examined. As will be observed, the proposed bounds are very close to the simulated curves, rendering them very useful from a practical point of view in the design of multihop cooperative systems with AF relays and subject to Nakagami-*m* fading. It is noteworthy that a myriad of other examples were plotted and, in all of them, the good proximity between the curves was also attested[7].

The i.i.d. Nakagami-*m* fading case is analyzed in Fig. 5.10 for different number of hops.

---

[7]Note that there are some computational methods presented in [99, 100] that can be used to obtain the numerical results presented here involving the Lauricella hypergeometric function.
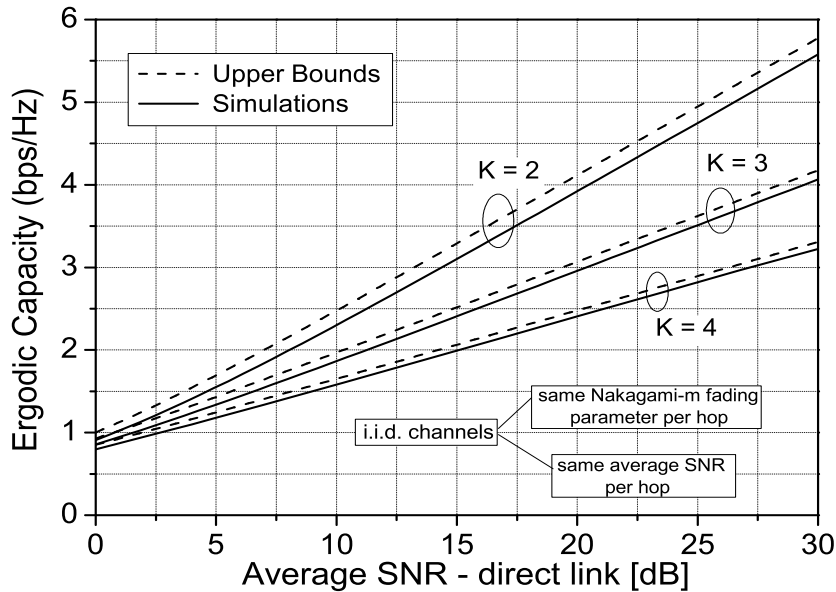
Figure 5.10: Ergodic capacity bounds of K-hop cooperative systems with AF relays in i.i.d. Nakagami-m channels ($m_k = 1.5$, $\delta = 4$).

In this case, all cooperative links have the same Nakagami-m fading parameter ($m_k = 1.5$) and the same average received SNR. Assuming that the total available transmitter power is P, the average individual link SNRs are obtained as $\bar{\gamma}_k = K^{\delta-1} \bar{\gamma}_0$, where δ denotes the path loss exponent and $\bar{\gamma}_0$ is the average received SNR over the direct link in a single hop network. We set $\delta = 4$ and plot the curves as a function of $\bar{\gamma}_0$. Note that when K increases, the ergodic capacity decreases. This is because of the rate loss inherent to multihop communications, described by the factor $1/K$ in (5.72). In addition, the accuracy of the bounds becomes even tighter when K increases, as opposed to the simulation efficiency which decreases given that the simulation time increases as the number of hops increases. Therefore, although the analytical bounds are useful for all the cases analyzed, the performance is even better for a large number of hops.

Fig. 5.11 analyzes the i.n.i.d. Nakagami-m fading case where the hops are assumed to have distinct Nakagami-m fading parameters and distinct average received SNR levels. Again, assuming a total transmit power P and using the Friis propagation formula, the average individual link SNRs are attained as $\bar{\gamma}_k = \frac{1}{K} \left(\frac{K(K+1)}{2k} \right)^{\delta} \bar{\gamma}_0$, $k = 1, \cdots, K$. Similarly to Fig. 5.10, we set $\delta = 4$ and depict the curves as a function of $\bar{\gamma}_0$. Note that the same
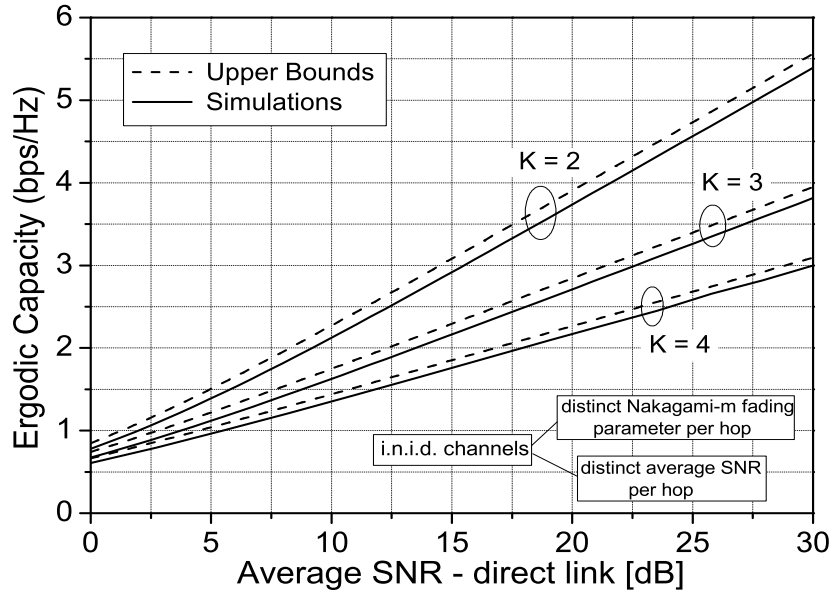
Figure 5.11: Ergodic capacity bounds of K-hop cooperative systems with AF relays in i.n.i.d. Nakagami-m channels ($m_1 = 2.5$, $m_2 = 2$, $m_3 = m_4 = 1.5$, $\delta = 4$).

conclusions as those observed for the i.i.d. case can also be extended for the i.n.i.d. one.

Figs. 5.12 and 5.13 illustrate the outage probability of end-to-end SNR for cooperative transmission versus the average SNR over the direct link for i.n.i.d. Nakagami-m fading channels. In Fig. 5.12, setting the path loss exponent $\delta = 4$, the results pertaining to the dualhop transmission are shown for different fading parameters and threshold values $\gamma_{th} = 3$ dB and 6 dB. It is observed that for a given threshold value, the performance improves with increasing values of m_k. On the other hand, the effect of power imbalance on the overall cooperative system performance is investigated in Fig. 5.13 for a threshold value of $\gamma_{th} = 3$ dB. In our numerical results, we consider the aforementioned Friis propagation formula. In this figure, it can be seen, as expected, that the power imbalance between the relaying links can be advantageous or disadvantageous. This figure also shows the effect of increasing the number of hops, K, on the outage probability performance.
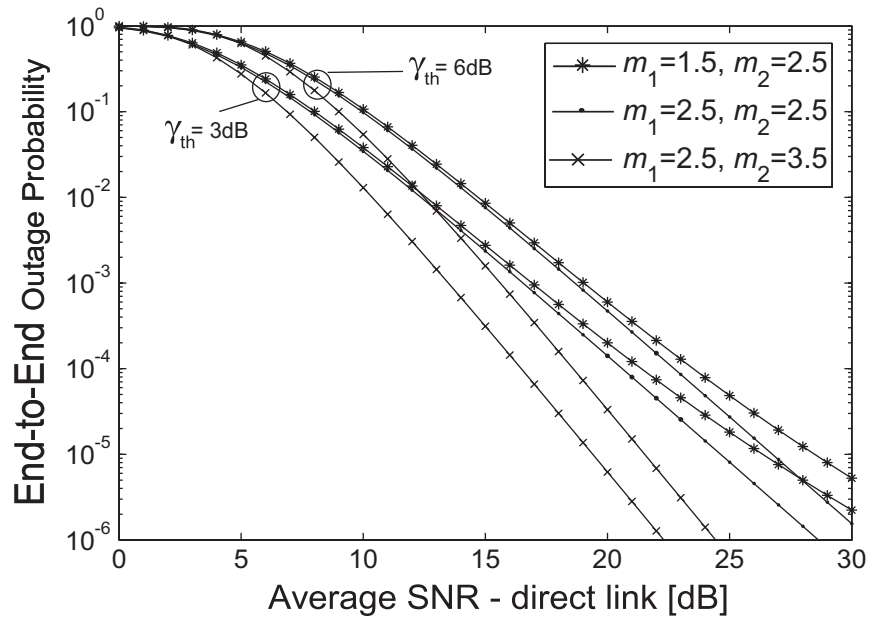
Figure 5.12: Outage probability of dualhop cooperative systems with AF relaying over independent Nakagami-m fading channels with $\delta = 4$.
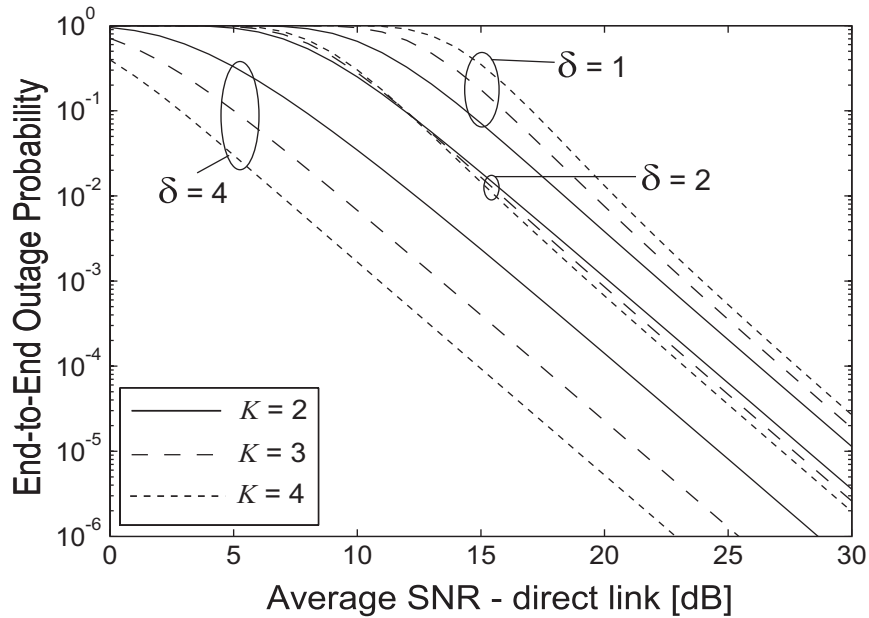
Figure 5.13: Outage probability of K-hop cooperative systems with AF relaying over independent Nakagami-m fading channels with $\gamma_{\text{th}} = 3$ dB and $m_k = 2.5$, $k = 1, \cdots, K$.

5.3.6   Summary

The ergodic capacity and outage probability performance of multihop cooperative AF relaying networks over i.n.i.d. Nakagami fading channels were investigated. More specifically, a tight closed-form upper bound expression for the ergodic capacity has been derived. For such, the MGF of the inverse of the end-to-end SNR was firstly attained in closed-form. Then, by making use of this MGF expression, we investigated the ergodic capacity and the outage probability performance of the multihop AF relaying systems. Simulation results were presented in order to confirm the tightness of the proposed bounds. Besides the fact that our results are analytically tractable and mathematically reducible to special cases such as the dual-hop scenario, they are of major importance for the design of multi-hop cooperative networks in practice.

In the next chapter, we propose adopting a cooperative relaying technique in spectrum-sharing CR systems to more effectively and efficiently utilize the available transmission resources, such as power, rate and bandwidth, while adhering to the QoS requirements of the PUs of the shared spectrum band. In particular, we first consider that the SU's communication is assisted by an intermediate relay that implements the DF technique into the SU's relayed signal in order to help the communication between the corresponding source and destination nodes. In this context, we propose a framework based on the first-order statistics approach to investigate the overall average BER, ergodic capacity and outage probability of the secondary's communication subject to appropriate constraints on the interference power at the PU receivers.

Chapter 6

Cooperative Relaying in CR Communications[1]

6.1 Performance of Cooperative Decode-and-Forward Relaying in Spectrum-Sharing Systems

Electromagnetic spectrum shortage is one of the main challenges in wireless communication systems [60]. Based on the frontier technology of CR, the concept of spectrum sharing was proposed as a solution to the inefficient utilization of the spectrum. Spectrum-sharing CR offers a tremendous potential to improve the spectral efficiency by allowing unlicensed (secondary) users to share the spectrum band originally allocated to the licensed (primary) users, as long as the generated interference aggregated at the primary receivers is below acceptable levels.

Generally, in spectrum-sharing systems, the secondary user's transmission is limited according to the maximum interference power inflicted on the primary receiver, in terms of average or peak values [48]. In this context, [101] investigated the capacity of a spectrum-sharing system considering either peak or average interference constraint at the primary receiver. Later in [22], the ergodic capacity and optimal power allocation policy of fading spectrum-sharing channels were studied considering joint constraints on the peak and

---

average interference powers at the primary receiver. In addition, in spectrum-sharing systems, the primary users having privileged access to the spectrum, any transmission by the secondary party should not affect their QoS, which necessitates proper management of the resources at the secondary users's transmitters. For instance, appropriate constraints on the secondary transmit power need to be imposed so that the primary's rate is guaranteed to remain higher than a target value for a given percentage of time.

Resource management is indeed of fundamental importance in spectrum-sharing systems, as explained in Chapter 2. However, when the available spectrum resources are not sufficient to guarantee reliable transmission at the secondary party, the resource allocation policy may not be able to fulfill the secondary users' requirements. In such cases, the secondary system has to implement sophisticated techniques to meet its performance requirements. One notable technique is cooperative communication which exploits the natural spatial diversity of multi-user systems. Indeed, cooperative transmission (communication using relay nodes) is a promising way to combat signal fading due to multipath radio propagation, and improve the system performance and coverage area [35].

A basic cooperative relay communication model consists of three terminals: a source, a relay and a destination. Relaying protocols mainly include DF [35,96], where the relay decodes the received signal and then re-encodes it before forwarding it to the destination, and AF [102], where the relay sends a scaled version of its received signal to the destination. Recently, different cooperative transmission models were analyzed in terms of outage and error probability performance. For instance, the bit error rate performance of dual-hop cooperative transmissions was analyzed in [35] considering DF relaying over Rayleigh fading channels. The effects of the interference generated by the relays in cooperative networks has also been addressed, e.g., in [103]. On the other hand, achievable capacities and power allocation for cooperative and relay channels, were investigated in [104]. The concept of relaying has also been applied in CR context to assist the transmission of secondary users and improve spectrum efficiency [36–39]. In particular, the effective capacity of CR relay channels has been investigated in [37] under a delay constraint at the secondary user transmission.

Using cooperative transmission in spectrum-sharing CR systems can indeed yield a higher efficiency in utilizing the spectrum resources. In this context, we herein adopt a cooperative relaying technique for the secondary transmission in a spectrum-sharing sys-

tem, to more effectively use the available spectrum resources and decrease the generated interference at the primary receivers. Specifically, we consider a dual-hop cooperative spectrum-sharing relaying system, and investigate its end-to-end performance when transmissions are limited by constraints on the tolerable interference by the primary user such that its transmission is supported with a constant-rate for a certain period of time. DF relays are employed in the communication between the secondary source (transmitter) and destination (receiver) nodes, and we obtain the average BER and ergodic capacity of the cooperative spectrum-sharing relaying system with an intermediate relay between the source and destination to help the secondary communication process. We further consider the scenario when a cluster of relays is available between the secondary source and destination nodes. In this case, using partial relay selection [30], we generalize the results presented here for the single-relay scenario, and obtain the average BER and the ergodic capacity of the cooperative system with a cluster of L available relays. Finally, we investigate the outage probability performance of the cooperative spectrum-sharing system under consideration for both, the single-relay and multiple-relay schemes.

In detailing these contributions, the remainder of Section 6.1 is organized as follows. Section 6.1.1 describes the system and channel models. In Section 6.1.2, we determine the power constraints that need to be satisfied by the secondary users to guarantee the QoS requirement at the primary user side is always met. Several relevant statistics corresponding to the instantaneous SNR of the first- and second-hop transmission channels are derived in Section 6.1.3. In Section 6.1.4, we obtain the average BER and the ergodic capacity of the spectrum-sharing cooperative systems under the above-mentioned power constraints. Thereafter, the system with a partial relay selection strategy is considered in Section 6.1.5. Section 6.1.6 presents numerical results and comparisons illustrating the performance of the secondary communication in terms of average BER, ergodic capacity and outage probability for the cases with and without relay selection. At the end, concluding remarks and summary are provided in Section 6.1.7.

6.1.1 System and Channel Models

Consider a spectrum-sharing CR system where DF relays are employed to help in the secondary user's communication process. More specifically, our system consists of a pair of secondary source and destination nodes (SS and SD) located in the vicinity of the primary

SS : Secondary Source   PR : Primary Receiver
SD : Secondary Destination R_S : Secondary Relay
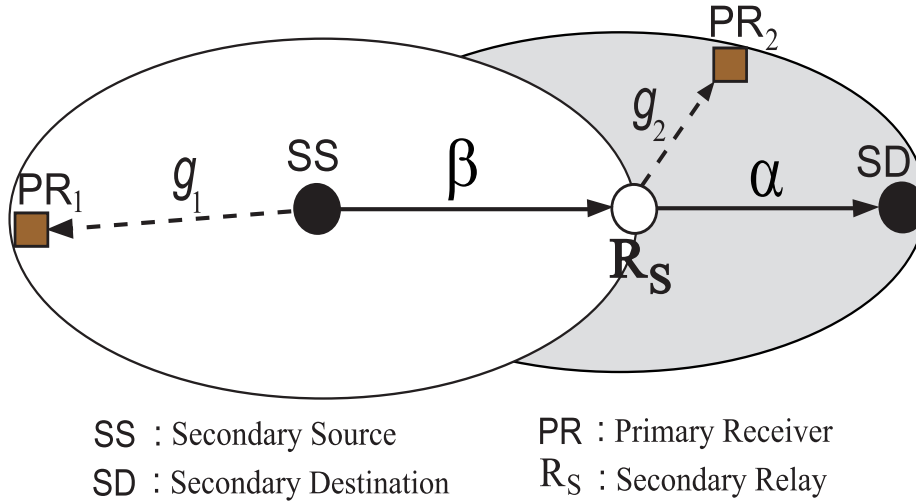
Figure 6.1: Dual-hop cooperative spectrum-sharing system.

receiver (PR), and a DF relay node $(R_s)^2$, as shown in Fig. 6.1. There is no direct link between the source and destination nodes, and the communication is established only via the relay in a dual-hop fashion. In this way, during the first hop, the SS communicates with the relay node, R_s. As the primary and secondary users share the same frequency band, the cognitive (secondary) user is allowed to operate in the licensee's spectrum as long as the primary QoS remains satisfied. For such, based on the interference channel state, g_1, the SS adjusts its transmit power under predefined resource constraints in order to assure the primary QoS is unaffected. Similar to the first-hop transmission, in the second-hop one, R_s node uses the same spectrum band originally assigned to the primary signals in order to communicate with SD. In the second hop, R_s makes use of the interference channel state, g_2, to adhere to the primary requirements. It is assumed that the first and second hops' transmissions are independent. It is also conjectured that SS and R_s have perfect knowledge of their respective interference channel gains. This can be obtained through a spectrum-band manager that mediates between the licensed and unlicensed users [105]. However, it is worth to note that, for certain scenarios, obtaining the interference channel power gains at the secondary network may be challenging. For these cases, our results serve as upper bounds for the performance of the considered spectrum-sharing relay channels and represent efficient system design tools.

We assume that all nodes transmit over discrete-time Rayleigh fading channels. The

---

[2]The scheme with multiple relays and partial relay selection is considered in Section 6.1.5.

channel power gain between SS and R_s is given by β with mean τ^f, and the one between R_s and SD by α with mean τ^s. The interference channel gains, g_1 and g_2, are mutually independent and exponentially distributed with unit mean. Perfect CSI is available at terminals SS, R_s and SD. Finally, we consider that the interference generated by the primary transmitter (PT) operating in the secondary transmission area, is modeled as additive zero-mean Gaussian noise at R_s and SD, with noise variance σ_1^2 and σ_2^2, respectively[3].

6.1.2 Spectrum-Sharing Constraints

The aim of this section is to define the QoS requirements pertaining to the the the primary users of the shared spectrum band, and present them in terms of resource constraints on the secondary transmission policy which are considered throughout this section. As briefly aforementioned, to control the interference power imposed on the primary receivers, the secondary transmitters must adjust their transmit powers so that the QoS requirements associated with the primary communication is maintained at a predefined required level. Herein, the primary's QoS is defined in terms of a minimum service-rate r_0 that should be satisfied with a certain outage probability P_p^{out}, according to

$$\Pr\left\{ E_{\beta,g_1}\left[\log_2\left(1 + \frac{S_p h_1}{S_{sr}(\beta, g_1) g_1 + \delta_1^2} \right) \right] < r_0 \right\} \leq P_p^{out}, \tag{6.1a}$$

$$\Pr\left\{ E_{\alpha,g_2}\left[\log_2\left(1 + \frac{S_p h_2}{S_{rd}(\alpha, g_2) g_2 + \delta_2^2} \right) \right] < r_0 \right\} \leq P_p^{out}, \tag{6.1b}$$

where $\Pr\{\cdot\}$ stands for probability, $E_X[\cdot]$ denotes statistical average with respect to X, h_1 and h_2 are the channel power gains pertaining to the links PT–PR$_1$ and PT–PR$_2$, respectively[4], and $S_{sr}(\beta, g_1)$ and $S_{rd}(\alpha, g_2)$ denote the secondary source-relay and relay-destination transmit powers[5], respectively, written as a function of (β,g_1) and (α,g_2). Furthermore, S_p denotes the average transmit power of the primary user, and δ_1^2 and δ_2^2 designate the variances of the additive Gaussian noise at nodes PR$_1$ and PR$_2$, respectively. In the following theory, we translate the primary QoS requirements into average interference constraints that should be accounted for in the secondary transmission policy.

---

[3] Validity of this assumption is sustained by the fact of considering the "*low-interference regime*" as studied in [106].

[4] We consider that h_1 and h_2 are independent and exponentially distributed with unit mean.

[5] Subscripts "sr" and "rd" denote the source-relay and relay-destination links, respectively.

Theorem 1: (Average Interference Constraints) In a primary/secondary cooperative spectrum-sharing system, where the secondary user's communication is performed through dual-hop relaying (cf. Fig. 6.1) and the primary QoS is defined by (1), the secondary user has to adhere to the following average interference constraints for the first and second hops, respectively,

$$E_{\beta, g_1} \left[S_{\text{sr}} \left(\beta, g_1 \right) g_1 \right] \leq W_1, \tag{6.2a}$$

$$E_{\alpha, g_2} \left[S_{\text{rd}} \left(\alpha, g_2 \right) g_2 \right] \leq W_2, \tag{6.2b}$$

where the power limits W_1 and W_2 are expressed in terms of the primary's minimum required rate r_0 and outage probability $P_{\text{p}}^{\text{out}}$, as

$$W_1 = \frac{\ln \left(1 - P_{\text{p}}^{\text{out}} \right)}{\eta} - \delta_1^2, \quad W_2 = \frac{\ln \left(1 - P_{\text{p}}^{\text{out}} \right)}{\eta} - \delta_2^2, \tag{6.3}$$

with $\eta = \dfrac{1 - 2^{r_0}}{S_{\text{p}}}$.

Proof 2 *See Appendix A.2.*

Furthermore, given that the primary receiver does not tolerate an interference higher than a certain threshold, in addition to the constraints in (6.2), we consider limitations on the peak-received power at the primary receivers, as follows:

$$S_{\text{sr}} \left(\beta, g_1 \right) g_1 \leq Q_1, \tag{6.4a}$$

$$S_{\text{rd}} \left(\alpha, g_2 \right) g_2 \leq Q_2, \tag{6.4b}$$

where Q_1 and Q_2 are the peak received-power limits pertaining to the first- and second-hop, respectively.

6.1.3 Main Statistics

In this section, based on the average and peak received power constraints at the primary receivers, we derive the PDF and CDF of the instantaneous SNR pertaining to each hop on the secondary link. As well-known, these statistics are two important metrics that can be used to study the performance of cooperative communication systems in general. In

our case, such statistics will be crucial in the analysis of the proposed spectrum-sharing cooperative relaying system (Fig. 6.1), where the relay, R_s, is utilized by the secondary user to enable communication between SS and SD.[6]

From the interference constraints given in (6.2a) and (6.4a), the optimal power transmission policy that maximizes the ergodic capacity of the secondary's first-hop link can be obtained as [22]

$$S_{\text{sr}}\left(\beta, g_1\right) = \begin{cases} \dfrac{Q_1}{g_1}, & \dfrac{\beta}{g_1} > \dfrac{\sigma_1^2}{\mu^{\text{f}}}, \\[2ex] \dfrac{\lambda^{\text{f}}}{g_1} - \dfrac{\sigma_1^2}{\beta}, & \dfrac{\sigma_1^2}{\lambda^{\text{f}}} \leq \dfrac{\beta}{g_1} \leq \dfrac{\sigma_1^2}{\mu^{\text{f}}}, \\[2ex] 0, & \dfrac{\beta}{g_1} < \dfrac{\sigma_1^2}{\lambda^{\text{f}}}, \end{cases} \tag{6.5}$$

where $\mu^{\text{f}} = \lambda^{\text{f}} - Q_1$ and the first-hop optimization parameters, namely λ^{f} and μ^{f}, are found by setting the power constraints in (6.2a) and (6.4a) at equality. These optimization parameters can be obtained using (6.6) and (6.7), where $\mathfrak{X} = \dfrac{\left(W_1 - Q_1\right)\tau^{\text{f}}}{\sigma_1^2}$.

$$\lambda^{\text{f}} = \frac{Q_1}{1 - \exp\left(\mathfrak{X}\right)} - \frac{\sigma_1^2}{\tau^{\text{f}}}. \tag{6.6}$$

$$\mu^{\text{f}} = \frac{Q_1}{\exp\left(\mathfrak{X}\right) - 1} - \frac{\sigma_1^2}{\tau^{\text{f}}}. \tag{6.7}$$

Details pertaining to the derivations of (6.6) and (6.7) are provided in Appendix A.3.

Accordingly, the instantaneous received SNR at the secondary relay (R_s) can be expressed as

$$\begin{aligned} \gamma_{\text{sr}}\left(\frac{\beta}{g_1}\right) &= \frac{S_{\text{sr}}\left(\beta, g_1\right)\beta}{\sigma_1^2} \\[2ex] &= \begin{cases} \dfrac{Q_1}{\sigma_1^2}\left(\dfrac{\beta}{g_1}\right), & \dfrac{\beta}{g_1} > \dfrac{\sigma_1^2}{\mu^{\text{f}}}, \\[2ex] \dfrac{\lambda^{\text{f}}}{\sigma_1^2}\left(\dfrac{\beta}{g_1}\right) - 1, & \dfrac{\sigma_1^2}{\lambda^{\text{f}}} \leq \dfrac{\beta}{g_1} \leq \dfrac{\sigma_1^2}{\mu^{\text{f}}}, \\[2ex] 0, & \dfrac{\beta}{g_1} < \dfrac{\sigma_1^2}{\lambda^{\text{f}}}. \end{cases} \end{aligned} \tag{6.8}$$

Now, since β and g_1 are independent exponential random variables, it is easy to show that the PDF of $Z = \beta/g_1$ is given by $f_Z\left(z\right) = \dfrac{\tau^{\text{f}}}{\left(\tau^{\text{f}} + z\right)^2}$ [107]. In addition, from Fig. 6.2, we observe two different slopes when sketching γ_{sr} in terms of Z. Hence, in order to

---

[6]Hereafter, for clarity, this relay is referred to as a secondary relay.
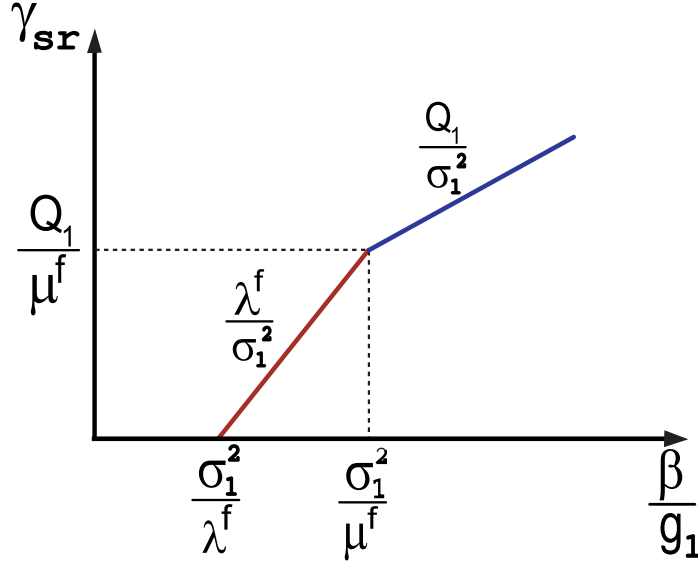
Figure 6.2: Schematic variation of the total received SNR at the secondary destination, SD.

find the required first-order statistics (PDF and CDF) of γ_{sr}, we have to take into account two ranges: $0 \leq \gamma_{\text{sr}} \leq \frac{Q_1}{\mu^{\text{f}}}$ and $\gamma_{\text{sr}} > \frac{Q_1}{\mu^{\text{f}}}$. For $0 \leq \gamma_{\text{sr}} \leq \frac{Q_1}{\mu^{\text{f}}}$, γ_{sr} increases by the order of $\frac{\lambda^{\text{f}}}{\sigma_1^2}$ and, hence, its PDF is given by

$$f_{\gamma_{\text{sr}}}\left(\gamma\right) = \left.\frac{\sigma_1^2}{\lambda^{\text{f}}} f_Z\left(z\right)\right|_{z=\frac{\sigma_1^2}{\lambda^{\text{f}}}(\gamma+1)}. \tag{6.9}$$

For the second range, i.e., when $\gamma_{\text{sr}} > \frac{Q_1}{\mu^{\text{f}}}$, the PDF of γ_{sr} can be obtained according to

$$f_{\gamma_{\text{sr}}}\left(\gamma\right) = \left.\frac{\sigma_1^2}{Q_1} f_Z\left(z\right)\right|_{z=\frac{\sigma_1^2}{Q_1}\gamma}. \tag{6.10}$$

Thus, combining (6.9) and (6.10) and after some mathematical manipulations[7], it follows that

$$f_{\gamma_{\text{sr}}}\left(\gamma\right) = \begin{cases} \dfrac{\sigma_1^2 \lambda^{\text{f}} \tau^{\text{f}}}{\left(\lambda^{\text{f}} \tau^{\text{f}} + \sigma_1^2 \gamma\right)^2}, & 0 \leq \gamma_{\text{sr}} \leq \dfrac{\lambda^{\text{f}}}{\mu^{\text{f}}}, \\[4mm] \dfrac{\sigma_1^2 Q_1 \tau^{\text{f}}}{\left(Q_1 \tau^{\text{f}} + \sigma_1^2 \left(\gamma - 1\right)\right)^2}, & \gamma_{\text{sr}} > \dfrac{\lambda^{\text{f}}}{\mu^{\text{f}}}. \end{cases} \tag{6.11}$$

---

[7]Note that $\lambda^{\text{f}} = \mu^{\text{f}} + Q_1$.

Subsequently, using $F_{\gamma_{\text{sr}}}(\gamma) = \int_0^{\gamma} f_{\gamma_{\text{sr}}}(x)\, dx$, the CDF of γ_{sr} can be expressed as

$$F_{\gamma_{\text{sr}}}(\gamma) = \begin{cases} \dfrac{\sigma_1^2 \gamma}{\lambda^{\text{f}} \tau^{\text{f}} + \sigma_1^2 \gamma}, & 0 \leq \gamma_{\text{sr}} \leq \dfrac{\lambda^{\text{f}}}{\mu^{\text{f}}}, \\[2ex] \dfrac{\sigma_1^2 (\gamma - 1)}{(Q_1 \tau^{\text{f}} + \sigma_1^2 (\gamma - 1))}, & \gamma_{\text{sr}} > \dfrac{\lambda^{\text{f}}}{\mu^{\text{f}}}. \end{cases} \tag{6.12}$$

Using the same rationale described above, the PDF of the instantaneous SNR associated with the second-hop transmission can be obtained as

$$f_{\gamma_{\text{rd}}}(\gamma) = \begin{cases} \dfrac{\sigma_2^2 \lambda^{\text{s}} \tau^{\text{s}}}{(\lambda^{\text{s}} \tau^{\text{s}} + \sigma_2^2 \gamma)^2}, & 0 \leq \gamma_{\text{rd}} \leq \dfrac{\lambda^{\text{s}}}{\mu^{\text{s}}}, \\[2ex] \dfrac{\sigma_2^2 Q_2 \tau^{\text{s}}}{(Q_2 \tau^{\text{s}} + \sigma_2^2 (\gamma - 1))^2}, & \gamma_{\text{rd}} > \dfrac{\lambda^{\text{s}}}{\mu^{\text{s}}}, \end{cases} \tag{6.13}$$

where λ^{s} and μ^{s} denote the second-hop optimization parameters, which can be obtained from (6.6) and (6.7) with the appropriate substitutions. Then, performing the integration of (6.13) with respect to γ, the CDF of γ_{rd} can be expressed as shown in (6.14).

$$F_{\gamma_{\text{rd}}}(\gamma) = \begin{cases} \dfrac{\sigma_2^2 \gamma}{\lambda^{\text{s}} \tau^{\text{s}} + \sigma_2^2 \gamma}, & 0 \leq \gamma_{\text{rd}} \leq \dfrac{\lambda^{\text{s}}}{\mu^{\text{s}}}, \\[2ex] \dfrac{\sigma_2^2 (\gamma - 1)}{(Q_2 \tau^{\text{s}} + \sigma_2^2 (\gamma - 1))}, & \gamma_{\text{rd}} > \dfrac{\lambda^{\text{s}}}{\mu^{\text{s}}}. \end{cases} \tag{6.14}$$

In the next section, using the derived statistics and focusing on the secondary communication through a single relay, we investigate the end-to-end performance of the spectrum-sharing cooperative system with DF relaying. More specifically, closed-form expressions for the average BER and ergodic capacity are provided under the resource constraints given in (6.2) and (6.4).

6.1.4   End-to-End Performance Analysis

6.1.4.1   Average Bit Error Rate

We now investigate the average BER of the spectrum-sharing cooperative system described in section 6.1.3. Considering DF as the relaying technique implemented at node

R_s, the average end-to-end (e2e) BER of the system under study is given by [35],

$$P_{\text{e2e}} = P_{\gamma_{\text{sr}}} + P_{\gamma_{\text{rd}}} - 2P_{\gamma_{\text{sr}}}P_{\gamma_{\text{rd}}}, \tag{6.15}$$

where $P_{\gamma_{\text{sr}}}$ and $P_{\gamma_{\text{rd}}}$ correspond to the average BER of the first- and second-hop, respectively, which can be calculated according to [108]

$$P_{\gamma_\tau} = \frac{1}{\sqrt{2\pi}} \int_0^\infty F_{\gamma_\tau}\left(\frac{\xi^2}{C}\right) \exp\left(-\frac{\xi^2}{2}\right) d\xi, \tag{6.16}$$

where $\tau \in \{\text{sr}, \text{rd}\}$ and C is a constant related to the modulation scheme, e.g., $C = 2$ for phase shift keying modulation. Substituting (6.12) in (6.16), the average BER for the first-hop transmission is given by,

$$P_{\gamma_{\text{sr}}} = \frac{1}{\sqrt{2\pi}} \left[\begin{array}{c} \int_0^{\sqrt{\frac{\lambda^f C}{\mu^f}}} \left(\frac{\sigma_1^2 \xi^2}{\lambda^f \tau^f C + \sigma_1^2 \xi^2}\right) \exp\left(-\frac{\xi^2}{2}\right) d\xi \\ + \int_{\sqrt{\frac{\lambda^f C}{\mu^f}}}^\infty \left(\frac{\sigma_1^2 (\xi^2 - C)}{(Q_1 C \tau^f + \sigma_1^2 (\xi^2 - C))}\right) \exp\left(-\frac{\xi^2}{2}\right) d\xi \end{array} \right], \tag{6.17}$$

which after simple manipulations, can be rewritten as

$$P_{\gamma_{\text{sr}}} = \frac{\sigma_1^2}{\sqrt{2\pi}} (I_1 + I_2), \tag{6.18}$$

where

$$I_1 \triangleq \int_0^{\sqrt{\frac{\lambda^f C}{\mu^f}}} \left(\frac{\xi^2}{\lambda^f \tau^f C + \sigma_1^2 \xi^2}\right) \exp\left(-\frac{\xi^2}{2}\right) d\xi, \tag{6.19a}$$

and

$$I_2 \triangleq \int_{\sqrt{\frac{\lambda^f C}{\mu^f}}}^\infty \left(\frac{(\xi^2 - C)}{(Q_1 C \tau^f + \sigma_1^2 (\xi^2 - C))}\right) \exp\left(-\frac{\xi^2}{2}\right) d\xi. \tag{6.19b}$$

In the sequel, we provide closed-form expressions for the integrals I_1 and I_2. For the first integral form (6.19a), we perform the change of variable $t = \dfrac{\mu^{\mathrm{f}}}{\lambda^{\mathrm{f}} C} \xi^2$, thus leading to

$$I_1 = \left(\frac{1}{\mu^{\mathrm{f}} \tau^{\mathrm{f}}} \sqrt{\frac{\lambda^{\mathrm{f}} C}{4 \mu^{\mathrm{f}}}} \right) \int_0^1 \exp\left(\frac{-\lambda^{\mathrm{f}} C}{2 \mu^{\mathrm{f}}} t \right) t^{\frac{1}{2}} \left(1 + \frac{\sigma_1^2}{\mu^{\mathrm{f}} \tau^{\mathrm{f}}} t \right)^{-1} dt, \qquad (6.20)$$

which can further be derived according to the following closed-form expression:

$$I_1 = \left(\frac{1}{3 \mu^{\mathrm{f}} \tau^{\mathrm{f}}} \sqrt{\frac{\lambda^{\mathrm{f}} C}{\mu^{\mathrm{f}}}} \right) \Phi_1 \left(\frac{3}{2}, -1; \frac{5}{2}; \frac{-\sigma_1^2}{\mu^{\mathrm{f}} \tau^{\mathrm{f}}}, \frac{-\lambda^{\mathrm{f}} C}{2 \mu^{\mathrm{f}}} \right), \qquad (6.21)$$

where $\Phi_1 (a, b_1, b_2; z; x_1, x_2, y)$ is the first-kind confluent hypergeometric function [109] defined by

$$\Phi_1 (a, b_1, \cdots, b_L; z; x_1, \cdots, x_L, y) = \frac{\Gamma(z)}{\Gamma(a) \Gamma(z - a)}$$

$$\times \int_0^1 \exp(yt) t^{a-1} (1 - t)^{z-a-1} \prod_{i=1}^L (1 - x_i t)^{-b_i} dt, \qquad (6.22)$$

with $\Gamma(\cdot)$ denoting the Gamma function [51].

Then, carrying out the change of variable $t = \dfrac{\mu^{\mathrm{f}}}{\lambda^{\mathrm{f}} C} \xi^2$ in the integral of (6.19b), and after further algebraic manipulations, we obtain

$$I_2 = \frac{\sqrt{\lambda^{\mathrm{f}} C}}{2 \sqrt{\mu^{\mathrm{f}}} (\sigma_1^2 - Q_1 \tau^{\mathrm{f}})} \int_1^\infty \exp\left(-\frac{\lambda^{\mathrm{f}} C}{2 \mu^{\mathrm{f}}} t \right) t^{-\frac{1}{2}} \left(1 - \frac{\lambda^{\mathrm{f}}}{\mu^{\mathrm{f}}} t \right)$$

$$\times \left(1 - \frac{\sigma_1^2 \lambda^{\mathrm{f}}}{\mu^{\mathrm{f}} (\sigma_1^2 - Q_1 \tau^{\mathrm{f}})} t \right)^{-1} dt. \qquad (6.23)$$

By considering the integral complementary characteristic, (6.23) can be reexpressed

$$I_2 = \frac{\sqrt{\lambda^{\mathrm{f}} C}}{2 \sqrt{\mu^{\mathrm{f}}} (\sigma_1^2 - Q_1 \tau^{\mathrm{f}})}$$

$$\times \left(\begin{array}{l} \displaystyle\int_0^\infty \exp\left(-\frac{\lambda^{\mathrm{f}} C}{2 \mu^{\mathrm{f}}} t \right) t^{-\frac{1}{2}} \left(1 - \frac{\lambda^{\mathrm{f}}}{\mu^{\mathrm{f}}} t \right) \left(1 - \frac{\sigma_1^2 \lambda^{\mathrm{f}}}{\mu^{\mathrm{f}} (\sigma_1^2 - Q_1 \tau^{\mathrm{f}})} t \right)^{-1} dt \\[2ex] -\displaystyle\int_0^1 \exp\left(-\frac{\lambda^{\mathrm{f}} C}{2 \mu^{\mathrm{f}}} t \right) t^{-\frac{1}{2}} \left(1 - \frac{\lambda^{\mathrm{f}}}{\mu^{\mathrm{f}}} t \right) \left(1 - \frac{\sigma_1^2 \lambda^{\mathrm{f}}}{\mu^{\mathrm{f}} (\sigma_1^2 - Q_1 \tau^{\mathrm{f}})} t \right)^{-1} dt \end{array} \right). \qquad (6.24)$$

In order to solve (6.24), first we present an integral representation for the second-kind confluent hypergeometric function, given by [75]

$$
\Phi_2\left(a, b_1, \cdots, b_K; z; x_1, \cdots, x_K, y\right) = \frac{1}{\Gamma(a)}
$$
$$
\times \int_0^\infty \exp\left(-yt\right) t^{a-1} \left(1+t\right)^{z-a-1} \prod_{i=1}^K \left(1+x_i t\right)^{-b_i} dt. \tag{6.25}
$$

Then, after careful observation, one can recognize that (6.24) can be expressed in terms of confluent hypergeometric functions of the first and second kinds as follows:

$$
I_2 = \frac{\sqrt{\lambda^{\mathrm{f}} C}}{2\sqrt{\mu^{\mathrm{f}}}\left(\sigma_1^2 - Q_1 \tau^{\mathrm{f}}\right)} \left(
\begin{array}{l}
\sqrt{\pi}\Phi_2\left(\frac{1}{2}, -1, 1; \frac{3}{2}; \frac{-\lambda^{\mathrm{f}}}{\mu^{\mathrm{f}}}, \frac{-\sigma_1^2 \lambda^{\mathrm{f}}}{\mu^{\mathrm{f}}\left(\sigma_1^2 - Q_1 \tau^{\mathrm{f}}\right)}, \frac{\lambda^{\mathrm{f}} C}{2\mu^{\mathrm{f}}}\right) \\
-2\Phi_1\left(\frac{1}{2}, -1, 1; \frac{3}{2}; \frac{\lambda^{\mathrm{f}}}{\mu^{\mathrm{f}}}, \frac{\sigma_1^2 \lambda^{\mathrm{f}}}{\mu^{\mathrm{f}}\left(\sigma_1^2 - Q_1 \tau^{\mathrm{f}}\right)}, \frac{-\lambda^{\mathrm{f}} C}{2\mu^{\mathrm{f}}}\right)
\end{array}
\right). \tag{6.26}
$$

Finally, incorporating the expressions in (6.21) and (6.26) into (6.18) yields a closed-form expression for the average BER of the first-hop link according to

$$
P_{\gamma_{\mathrm{sr}}} = \frac{\sigma_1^2 \sqrt{\lambda^{\mathrm{f}} C}}{3\mu^{\mathrm{f}} \tau^{\mathrm{f}} \sqrt{2\pi\mu^{\mathrm{f}}}} \Phi_1\left(\frac{3}{2}, -1; \frac{5}{2}; \frac{-\sigma_1^2}{\mu^{\mathrm{f}} \tau^{\mathrm{f}}}, \frac{-\lambda^{\mathrm{f}} C}{2\mu^{\mathrm{f}}}\right)
$$
$$
+ \frac{\sigma_1^2 \sqrt{\lambda^{\mathrm{f}} C}}{\sqrt{8\mu^{\mathrm{f}}}\left(\sigma_1^2 - Q_1 \tau^{\mathrm{f}}\right)} \Phi_2\left(\frac{1}{2}, -1, 1; \frac{3}{2}; \frac{-\lambda^{\mathrm{f}}}{\mu^{\mathrm{f}}}, \frac{-\sigma_1^2 \lambda^{\mathrm{f}}}{\mu^{\mathrm{f}}\left(\sigma_1^2 - Q_1 \tau^{\mathrm{f}}\right)}, \frac{\lambda^{\mathrm{f}} C}{2\mu^{\mathrm{f}}}\right)
$$
$$
- \frac{\sigma_1^2 \sqrt{\lambda^{\mathrm{f}} C}}{\sqrt{2\pi\mu^{\mathrm{f}}}\left(\sigma_1^2 - Q_1 \tau^{\mathrm{f}}\right)} \Phi_1\left(\frac{1}{2}, -1, 1; \frac{3}{2}; \frac{\lambda^{\mathrm{f}}}{\mu^{\mathrm{f}}}, \frac{\sigma_1^2 \lambda^{\mathrm{f}}}{\mu^{\mathrm{f}}\left(\sigma_1^2 - Q_1 \tau^{\mathrm{f}}\right)}, \frac{-\lambda^{\mathrm{f}} C}{2\mu^{\mathrm{f}}}\right). \tag{6.27}
$$

It is worth noting that applying the same approach for the second-hop transmission, $P_{\gamma_{\mathrm{rd}}}$ can be easily obtained by appropriate substitutions of the respective second-hop transmission parameters, namely, $(Q_1, \lambda^{\mathrm{f}}, \mu^{\mathrm{f}}, \tau^{\mathrm{f}}, \sigma_1^2) \rightarrow (Q_2, \lambda^{\mathrm{s}}, \mu^{\mathrm{s}}, \tau^{\mathrm{s}}, \sigma_2^2)$ respectively. Finally, by substituting $P_{\gamma_{\mathrm{sr}}}$ and $P_{\gamma_{\mathrm{rd}}}$ into (6.15), a closed-form expression for the average BER is attained.

6.1.4.2 Ergodic Capacity

Ergodic capacity is an important performance index for the system under study. In theory, ergodic capacity corresponds to the maximum long-term achievable rate over all

channel states of the time-varying fading channel. Herein, we obtain a closed-form expression for the ergodic capacity of the dual-hop cooperative spectrum-sharing relaying system under average and peak received-power constraints defined in section 6.1.2.

In dual-hop DF cooperative relaying transmission, based on the min-cut max-flow theorem presented in [110], the total system capacity cannot be larger than the capacity achieved by each individual relaying link. Mathematically speaking, the overall system capacity is the minimum of the individual capacity that can be achieved over the first and second hops [111]. Therefore, the ergodic capacity of dual-hop DF relaying channels is given by

$$C = \frac{1}{2} \min \left\{ C_{\gamma_{\mathrm{sr}}}, \, C_{\gamma_{\mathrm{rd}}} \right\}, \tag{6.28}$$

where $C_{\gamma_{\mathrm{sr}}}$ and $C_{\gamma_{\mathrm{rd}}}$ denote the capacity of the first- and second-hop, respectively, with C_γ ($\gamma \in \{\gamma_{\mathrm{sr}}, \gamma_{\mathrm{rd}}\}$) calculated according to $C_\gamma = \mathrm{E}_\gamma \left[\log_2 (1 + \gamma) \right]$. By substituting the obtained PDFs pertaining to the first- and second-hop transmissions expressed in (6.11) and (6.13), these terms can be expressed as

$$C_{\gamma_{\mathrm{sr}}} = \int_0^{\frac{\lambda^{\mathrm{f}}}{\mu^{\mathrm{f}}}} \log_2 (1 + \gamma) \, f_{\gamma_{\mathrm{sr}}} (\gamma) d\gamma + \int_{\frac{\lambda^{\mathrm{f}}}{\mu^{\mathrm{f}}}}^{\infty} \log_2 (1 + \gamma) \, f_{\gamma_{\mathrm{sr}}} (\gamma) d\gamma, \tag{6.29}$$

and

$$C_{\gamma_{\mathrm{rd}}} = \int_0^{\frac{\lambda^{\mathrm{s}}}{\mu^{\mathrm{s}}}} \log_2 (1 + \gamma) \, f_{\gamma_{\mathrm{rd}}} (\gamma) d\gamma + \int_{\frac{\lambda^{\mathrm{s}}}{\mu^{\mathrm{s}}}}^{\infty} \log_2 (1 + \gamma) \, f_{\gamma_{\mathrm{rd}}} (\gamma) d\gamma. \tag{6.30}$$

Then, evaluating the integrals in the above expressions and using some mathematical manipulation [84], the first- and second-hop capacity expressions are obtained as given in (6.31) and (6.32),

$$\begin{aligned} C_{\gamma_{\mathrm{sr}}} = {} & \frac{Q_1 \tau^{\mathrm{f}}}{2\sigma_1^2 - Q_1 \tau^{\mathrm{f}}} \log_2 \left(\frac{\sigma_1^2}{Q_1} \right) - \frac{\lambda^{\mathrm{f}} \tau^{\mathrm{f}}}{\sigma_1^2 - \lambda^{\mathrm{f}} \tau^{\mathrm{f}}} \log_2 \left(\tau^{\mathrm{f}} \right) \\ & + \frac{\sigma_1^2 \tau^{\mathrm{f}} \left(Q_1 - 2\lambda^{\mathrm{f}} \right)}{\left(2\sigma_1^2 - Q_1 \tau^{\mathrm{f}} \right) \left(\sigma_1^2 - \lambda^{\mathrm{f}} \tau^{\mathrm{f}} \right)} \log_2 \left(\frac{\lambda^{\mathrm{f}} + \mu^{\mathrm{f}}}{\sigma_1^2 - \mu^{\mathrm{f}} \tau^{\mathrm{f}}} \right), \end{aligned} \tag{6.31}$$

and

$$C_{\gamma_{\mathrm{rd}}} = \frac{Q_2 \tau^{\mathrm{s}}}{2\sigma_2^2 - Q_2 \tau^{\mathrm{s}}} \log_2 \left(\frac{\sigma_2^2}{Q_2} \right) - \frac{\lambda^{\mathrm{s}} \tau^{\mathrm{s}}}{\sigma_2^2 - \lambda^{\mathrm{s}} \tau^{\mathrm{s}}} \log_2 (\tau^{\mathrm{s}})$$
$$+ \frac{\sigma_2^2 \tau^{\mathrm{s}} (Q_2 - 2\lambda^{\mathrm{s}})}{(2\sigma_2^2 - Q_2 \tau^{\mathrm{s}}) (\sigma_2^2 - \lambda^{\mathrm{s}} \tau^{\mathrm{s}})} \log_2 \left(\frac{\lambda^{\mathrm{s}} + \mu^{\mathrm{s}}}{\sigma_2^2 - \mu^{\mathrm{s}} \tau^{\mathrm{s}}} \right), \qquad (6.32)$$

respectively. Having obtained closed-form expressions for $C_{\gamma_{\mathrm{sr}}}$ and $C_{\gamma_{\mathrm{rd}}}$, we can evaluate the ergodic capacity of the system under consideration according to (6.28).

6.1.5   End-to-End Performance with Partial Relay Selection

In this section, we extend our cooperative system model by considering a cluster of relays between SS and SD nodes, which consists of L relays; R_{s_l}, $l = 1, \cdots, L$ (Fig. 6.3). We assume that the relays are located close to each other (optimal clustering [112]), which implies the same average received SNR at relays within a cluster[8]. However, it is worth noting that the instantaneous SNR values vary from relay to relay in a cluster. We define the channel power gain between SS and the l-th relay by β_l, and the interference channel from the SS to the PR by g_1, as shown in Fig. 6.3. We assume that the channel power gains $\{\beta_l\}_{l=1}^{L}$ are exponentially distributed with the same mean τ^{f}. Furthermore, it is assumed that the channel gains are mutually independent and that perfect CSI is available at the SS and the relays through appropriate feedback. Using this information, the SS selects the best relay that provides the maximum instantaneous SNR during the first-hop transmission. Hence, denoting the instantaneous SNR of each link as $\gamma_{\mathrm{sr}}(Z_l) = S_{\mathrm{sr}}(Z_l) \beta_l / \sigma_1^2$ where $Z_l = \beta_l / g_1$, the maximum instantaneous SNR of the first-hop transmission is given by $\gamma_{\mathrm{sr}} = \max_{l=1,\cdots,L} \{\gamma_{\mathrm{sr}}(Z_l)\}$. The chosen relay detects and forwards the received signal to the destination node SD. For more details about the above-described selection strategy, called partial relay selection (PRS), the readers are referred to [30] and [29].

As PRS strategy is employed in the first-hop, from the order statistics theory [57], the CDF of the first-hop can be expressed as

$$F_{\gamma_{\mathrm{sr}}}^{\mathrm{prs}}(\gamma) = [F_{\gamma_{\mathrm{sr}}}(\gamma)]^{L}, \qquad (6.33)$$

---

[8]Note that an important factor for the performance of cooperative relaying systems is the selection of appropriate relay stations out of a set of potential candidates [112], which might be either fixed relays part of a certain network infrastructure or simply other neighboring users in case of cooperative communication.
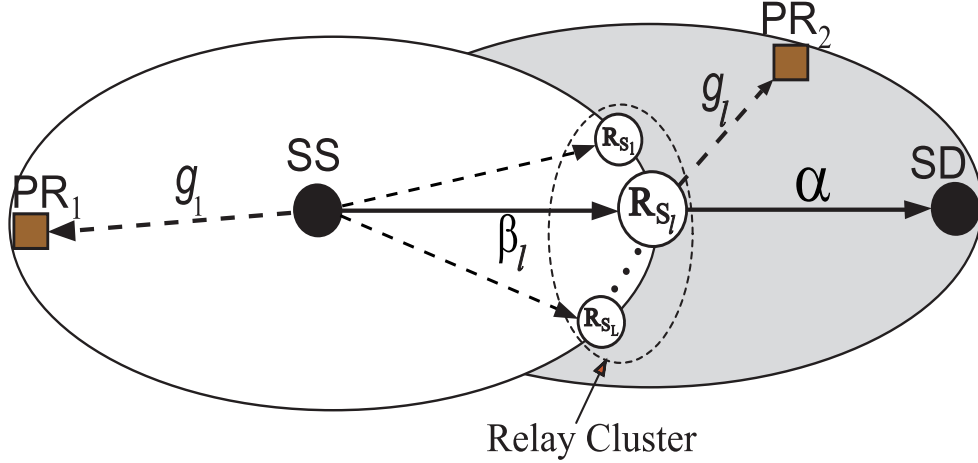
Figure 6.3: Dual-hop cooperative spectrum-sharing system with partial relay selection.

where $F_{\gamma_{sr}}(\gamma)$ is given by (6.12). Accordingly, we can obtain the PDF of the first-hop transmission by performing the derivative of the CDF expression in (6.33) with respect to γ_{sr}, i.e.,

$$f_{\gamma_{sr}}^{\mathrm{prs}}(\gamma) \triangleq \frac{dF_{\gamma_{sr}}^{\mathrm{prs}}(\gamma)}{d\gamma} = L\left(F_{\gamma_{sr}}(\gamma)\right)^{L-1} f_{\gamma_{sr}}(\gamma), \tag{6.34}$$

which, after appropriate substitutions and some mathematical manipulations, can be expressed as

$$f_{\gamma_{sr}}^{\mathrm{prs}}(\gamma) = \begin{cases} \dfrac{L\lambda^{\mathrm{f}}\tau^{\mathrm{f}}\left(\sigma_1^2\right)^L \gamma^{L-1}}{\left(\lambda^{\mathrm{f}}\tau^{\mathrm{f}} + \sigma_1^2\gamma\right)^{L+1}}, & 0 \le \gamma_{sr} \le \dfrac{\lambda^{\mathrm{f}}}{\mu^{\mathrm{f}}}, \\[4mm] \dfrac{LQ_1\tau^{\mathrm{f}}\left(\sigma_1^2\right)^L \left(\gamma-1\right)^{L-1}}{\left(Q_1\tau^{\mathrm{f}} + \sigma_1^2\left(\gamma-1\right)\right)^{L+1}}, & \gamma_{sr} > \dfrac{\lambda^{\mathrm{f}}}{\mu^{\mathrm{f}}}. \end{cases} \tag{6.35}$$

Note that the PDF and CDF of the second-hop, $f_{\gamma_{rd}}(\gamma)$ and $F_{\gamma_{rd}}(\gamma)$, remain the same as presented in (6.13) and (6.14), respectively. In what follows, considering PRS strategy, we obtain closed-form expressions for the average BER and the achievable ergodic capacity of the dual-hop cooperative spectrum-sharing system under the constraints on average and peak received interference at the primary receivers.

6.1.5.1 Average Bit Error Rate

Considering the above-mentioned relay selection strategy, the end-to-end average BER of the cooperative DF relaying spectrum-sharing communication system is calculated according to

$$P_{\text{e2e}}^{\text{prs}} = P_{\gamma_{\text{sr}}}^{\text{prs}} + P_{\gamma_{\text{rd}}} - 2P_{\gamma_{\text{sr}}}^{\text{prs}} P_{\gamma_{\text{rd}}}, \tag{6.36}$$

where $P_{\gamma_{\text{sr}}}^{\text{prs}}$ and $P_{\gamma_{\text{rd}}}$ are the average SERs corresponding to the first- and second-hop, respectively. Note that $P_{\gamma_{\text{rd}}}$ is calculated similar to (6.18) by making the necessary substitutions as explained in section 6.1.4. Furthermore, substituting the CDF (6.33) into (6.16) yields the expression for the average BER of the first-hop, $P_{\gamma_{\text{sr}}}^{\text{prs}}$, according to

$$P_{\gamma_{\text{sr}}}^{\text{prs}} = \frac{(\sigma_1^2)^L}{\sqrt{2\pi}} \left(I_1^{\text{prs}} + I_2^{\text{prs}} \right), \tag{6.37}$$

where

$$I_1^{\text{prs}} = \int_0^{\sqrt{\frac{\lambda^{\text{f}} C}{\mu^{\text{f}}}}} \left(\frac{\xi^2}{\lambda^{\text{f}} \tau^{\text{f}} C + \sigma_1^2 \xi^2} \right)^L \exp\left(-\frac{\xi^2}{2} \right) d\xi, \tag{6.38}$$

and

$$I_2^{\text{prs}} = \int_{\sqrt{\frac{\lambda^{\text{f}} C}{\mu^{\text{f}}}}}^{\infty} \left(\frac{(\xi^2 - C)}{C \left(Q_1 \tau^{\text{f}} - \sigma_1^2 \right) + \sigma_1^2 \xi^2} \right)^L \exp\left(-\frac{\xi^2}{2} \right) d\xi. \tag{6.39}$$

To calculate I_1^{prs} and I_2^{prs}, changing the variable to $t = \mu^{\text{f}} / \lambda^{\text{f}} C \xi^2$ and following the approach adopted in Section 6.1.4, we get

$$I_1^{\text{prs}} = \frac{\left(\mu^{\text{f}} \tau^{\text{f}} \right)^{-L} \sqrt{\lambda^{\text{f}} C}}{(2L+1) \sqrt{\mu^{\text{f}}}} \times \Phi_1 \left(L + \frac{1}{2}, L; L + \frac{3}{2}; \frac{-\sigma_1^2}{\mu^{\text{f}} \tau^{\text{f}}}, \frac{-\lambda^{\text{f}} C}{2\mu^{\text{f}}} \right), \tag{6.40}$$

and

$$I_2^{\text{prs}} = \frac{\sqrt{\lambda^{\text{f}} C}}{2\sqrt{\mu^{\text{f}}} \left(\sigma_1^2 - Q_1 \tau^{\text{f}} \right)^L} \left(\begin{array}{l} \sqrt{\pi} \Phi_2 \left(\frac{1}{2}, -L, L; \frac{3}{2}; \frac{-\lambda^{\text{f}}}{\mu^{\text{f}}}, \frac{-\sigma_1^2 \lambda^{\text{f}}}{\left(\sigma_1^2 - Q_1 \tau^{\text{f}} \right) \mu^{\text{f}}}, \frac{\lambda^{\text{f}} C}{2\mu^{\text{f}}} \right) \\ -2\Phi_1 \left(\frac{1}{2}, -L, L; \frac{3}{2}; \frac{\lambda^{\text{f}}}{\mu^{\text{f}}}, \frac{\sigma_1^2 \lambda^{\text{f}}}{\left(\sigma_1^2 - Q_1 \tau^{\text{f}} \right) \mu^{\text{f}}}, \frac{-\lambda^{\text{f}} C}{2\mu^{\text{f}}} \right) \end{array} \right). \tag{6.41}$$

Then, substituting the expressions in (6.40) and (6.41) into (6.37), the average BER of the

first-hop link, $P_{\gamma_{\text{sr}}}^{\text{prs}}$, can be obtained as

$$
\begin{aligned}
P_{\gamma_{\text{sr}}}^{\text{prs}} &= \frac{\left(\sigma_1^2\right)^L \left(\mu^{\text{f}}\tau^{\text{f}}\right)^{-L} \sqrt{\lambda^{\text{f}}C}}{(2L+1)\sqrt{2\pi\mu^{\text{f}}}} \; \Phi_1\left(L+\frac{1}{2}, L; L+\frac{3}{2}; \frac{-\sigma_1^2}{\mu^{\text{f}}\tau^{\text{f}}}, \frac{-\lambda^{\text{f}}C}{2\mu^{\text{f}}}\right) \\
&+ \frac{\left(\sigma_1^2\right)^L \sqrt{\lambda^{\text{f}}C}}{\sqrt{8\mu^{\text{f}}}\left(\sigma_1^2 - Q_1\tau^{\text{f}}\right)^L} \; \Phi_2\left(\frac{1}{2}, -L, L; \frac{3}{2}; \frac{-\lambda^{\text{f}}}{\mu^{\text{f}}}, \frac{-\sigma_1^2\lambda^{\text{f}}}{\left(\sigma_1^2 - Q_1\tau^{\text{f}}\right)\mu^{\text{f}}}, \frac{\lambda^{\text{f}}C}{2\mu^{\text{f}}}\right) \\
&- \frac{\left(\sigma_1^2\right)^L \sqrt{\lambda^{\text{f}}C}}{\sqrt{2\pi\mu^{\text{f}}}\left(\sigma_1^2 - Q_1\tau^{\text{f}}\right)^L} \; \Phi_1\left(\frac{1}{2}, -L, L; \frac{3}{2}; \frac{\lambda^{\text{f}}}{\mu^{\text{f}}}, \frac{\sigma_1^2\lambda^{\text{f}}}{\left(\sigma_1^2 - Q_1\tau^{\text{f}}\right)\mu^{\text{f}}}, \frac{-\lambda^{\text{f}}C}{2\mu^{\text{f}}}\right).
\end{aligned} \tag{6.42}
$$

Finally, incorporating $P_{\gamma_{\text{sr}}}^{\text{prs}}$ and $P_{\gamma_{\text{rd}}}$ (given in Section 6.1.4) into (6.36) yields the average BER expression of the spectrum-sharing cooperative system when using PRS strategy.

6.1.5.2 Ergodic Capacity

Herein, we investigate the ergodic capacity of the cooperative transmission system under consideration when PRS strategy is used in the first-hop transmission, which is mathematically given by

$$
C^{\text{prs}} = \frac{1}{2} \min\left\{C_{\gamma_{\text{sr}}^{\text{prs}}}, \; C_{\gamma_{\text{rd}}}\right\}, \tag{6.43}
$$

where $C_{\gamma_{\text{rd}}}$ is calculated according to (6.32), and $C_{\gamma_{\text{sr}}^{\text{prs}}}$ is obtained using the expectation of $\log_2\left(1 + \gamma_{\text{sr}}^{\text{prs}}\right)$ given by

$$
C_{\text{sr}}^{\text{prs}} = \mathrm{E}_{\gamma_{\text{sr}}^{\text{prs}}}\left[\log_2\left(1 + \gamma_{\text{sr}}^{\text{prs}}\right)\right]. \tag{6.44}
$$

Then, considering the PDF of the received SNR for the L relays participating in PRS over the first transmission link, given in (6.35), we can express (6.44) as

$$
C_{\text{sr}}^{\text{prs}} = \frac{L\left(\sigma_1^2\right)^L \tau^{\text{f}}}{\ln(2)}\left(\lambda^{\text{f}} J_1 + Q_1 J_2\right), \tag{6.45}
$$

where

$$
J_1 = \int_0^{\frac{\lambda^{\text{f}}}{\mu^{\text{f}}}} \frac{\gamma^{L-1}\ln(1+\gamma)}{\left(\lambda^{\text{f}}\tau^{\text{f}} + \sigma_1^2\gamma\right)^{L+1}}d\gamma \tag{6.46}
$$

and

$$J_2 = \int_{\frac{\lambda^{\mathrm{f}}}{\mu^{\mathrm{f}}}}^{\infty} \frac{(\gamma - 1)^{L-1} \ln (1 + \gamma)}{(Q_1 \tau^{\mathrm{f}} + \sigma_1^2 (\gamma - 1))^{L+1}} d\gamma. \tag{6.47}$$

In the following, we derive approximated closed-form expressions for the integrals J_1 and J_2. For the first integral, we use the following expansion series given by [84, Eq. 1.11]

$$\frac{1}{(a + z)^p} = \begin{cases} \frac{1}{(a)^p} \sum_{n=0}^{N} \left(\frac{-1}{a}\right)^n \binom{P+n-1}{n} z^n + \varepsilon\left(\frac{z}{a}\right) & \forall \left|\frac{z}{a}\right| \leq 1, \\ \sum_{n=0}^{N} (-a)^n \binom{P+n-1}{n} z^{-n-p} + \varepsilon\left(\frac{z}{a}\right) & \forall \left|\frac{z}{a}\right| > 1, \end{cases} \tag{6.48}$$

where $\binom{a}{b} := \frac{a!}{(a-b)!b!}$ represents the Binomial coefficients [84] and $\varepsilon(\frac{z}{a})$ is the truncation error[9]. Now, for the sake of accuracy in using these series in (6.46) and since the integral limit $\frac{\lambda^{\mathrm{f}}}{\mu^{\mathrm{f}}}$ is always larger than unity, owing to the fact that $\mu^{\mathrm{f}} = \lambda^{\mathrm{f}} - Q_1$, we split the integration interval $[0, \frac{\lambda^{\mathrm{f}}}{\mu^{\mathrm{f}}}]$ into two intervals. Thus, considering (6.48) and after expressing the logarithm function in terms of Meijer's G-function [109], namely, using $\ln (1 + \gamma) = G_{2,2}^{1,2}\left(\gamma \left|^{1,1}_{1,0}\right.\right)$, J_1 can be expressed as

$$J_1 = \frac{1}{(\lambda^{\mathrm{f}} \tau^{\mathrm{f}})^{L+1}} \sum_{n=0}^{N} \left(\frac{-\sigma_1^2}{\lambda^{\mathrm{f}} \tau^{\mathrm{f}}}\right)^n \binom{L+n}{n} \int_0^{\frac{\lambda^{\mathrm{f}} \tau^{\mathrm{f}}}{\sigma_1^2}} \gamma^{L+n-1} G_{2,2}^{1,2}\left(\gamma \left|^{1,1}_{1,0}\right.\right) d\gamma$$

$$+ \frac{1}{(\sigma_1^2)^{L+1}} \sum_{n=0}^{N} \left(\frac{-\lambda^{\mathrm{f}} \tau^{\mathrm{f}}}{\sigma_1^2}\right)^n \binom{L+n}{n} \int_{\frac{\lambda^{\mathrm{f}} \tau^{\mathrm{f}}}{\sigma_1^2}}^{\frac{\lambda^{\mathrm{f}}}{\mu^{\mathrm{f}}}} \gamma^{-n-2} G_{2,2}^{1,2}\left(\gamma \left|^{1,1}_{1,0}\right.\right) d\gamma. \tag{6.49}$$

Then, knowing that the integral of a Meijer's G-functions is also a Meijer's G-function [113], i.e.,

$$\int z^{\alpha-1} G_{2,2}^{1,2}\left(z \left|^{a_1,a_2}_{b_1,b_2}\right.\right) dz = G_{3,3}^{1,3}\left(z \left|^{1,\alpha+a_1,\alpha+a_2}_{\alpha+b_1,0,\alpha+b_2}\right.\right), \tag{6.50}$$

---

[9]In numerical results, the parameter N is considered such that the truncation error always satisfies $\left|\varepsilon(\frac{z}{a})\right| < 3 \times 10^{-3}$.

and after some mathematical manipulations, (6.49) can be expressed as [84, Eq. 9.31.2]

$$J_1 = \frac{1}{(\lambda^{\mathrm{f}}\tau^{\mathrm{f}})^{L+1}} \sum_{n=0}^{N} \left(\frac{-\sigma_1^2}{\lambda^{\mathrm{f}}\tau^{\mathrm{f}}}\right)^n \binom{L+n}{n} G_{3,3}^{1,3}\left(\frac{\lambda^{\mathrm{f}}\tau^{\mathrm{f}}}{\sigma_1^2} \left|_{L+n+1,0,L+n}^{1,L+n+1,L+n+1}\right.\right)$$

$$+ \frac{1}{(\sigma_1^2)^{L+1}} \sum_{n=0}^{N} \left(\frac{-\lambda^{\mathrm{f}}\tau^{\mathrm{f}}}{\sigma_1^2}\right)^n \binom{L+n}{n}$$

$$\times \left[G_{3,3}^{3,1}\left(\frac{\mu^{\mathrm{f}}}{\lambda^{\mathrm{f}}} \left|_{0,n+1,n+1}^{1+n,1,n+2}\right.\right) - G_{3,3}^{3,1}\left(\frac{\sigma_1^2}{\lambda^{\mathrm{f}}\tau^{\mathrm{f}}} \left|_{0,n+1,n+1}^{1+n,1,n+2}\right.\right) \right]. \tag{6.51}$$

It is worth noting that the Meijer's G-functions are implemented in most popular computing softwares such as Matlab and Mathematica.

As for the integral J_2, by considering the integral complementary characteristic, (6.47) can be rewritten as

$$J_2 = \underbrace{\int_0^\infty \frac{(\gamma-1)^{L-1}\ln(1+\gamma)}{(Q_1\tau^{\mathrm{f}} + \sigma_1^2(\gamma-1))^{L+1}}d\gamma}_{J_2^a} - \underbrace{\int_0^{\frac{\lambda^{\mathrm{f}}}{\mu^{\mathrm{f}}}} \frac{(\gamma-1)^{L-1}\ln(1+\gamma)}{(Q_1\tau^{\mathrm{f}} + \sigma_1^2(\gamma-1))^{L+1}}d\gamma}_{J_2^b}. \tag{6.52}$$

To solve the integral J_2^a in (6.52), using the change of variable $x = \gamma-1$ and substituting the logarithm function representation in terms of Meijer's G-function [109] followed by some mathematical manipulations, J_2^a can be simplified as follows [84, Eq. 9.31.5]:

$$J_2^a = \int_{-1}^\infty \frac{G_{2,2}^{1,2}\left(x+1 \left|_{L,L-1}^{L,L}\right.\right)}{(Q_1\tau^{\mathrm{f}} + \sigma_1^2 x)^{L+1}}dx. \tag{6.53}$$

Now, representing the denominator of the fraction in (6.53) in terms of Meijer's G-function as [84, Eq. 9.31.2]

$$\frac{1}{(Q_1\tau^{\mathrm{f}} + \sigma_1^2 x)^{L+1}} = \frac{\left(Q_1\tau^{\mathrm{f}}\right)^{-L-1}}{\Gamma(L+1)} G_{1,1}^{1,1}\left(\frac{\sigma_1^2 x}{Q_1\tau^{\mathrm{f}}} \left|_0^{-L}\right.\right) \tag{6.54}$$

and substituting (6.54) into (6.53), we obtain

$$J_2^a = \frac{\left(Q_1\tau^{\mathrm{f}}\right)^{-L-1}}{\Gamma(L+1)} \int_{-1}^\infty G_{1,1}^{1,1}\left(\frac{\sigma_1^2 x}{Q_1\tau^{\mathrm{f}}} \left|_0^{-L}\right.\right) G_{2,2}^{1,2}\left(x+1 \left|_{L,L-1}^{L,L}\right.\right) dx. \tag{6.55}$$

Then, after some further manipulations, J_2^a can be derived as follows:

$$J_2^a = \frac{\mathrm{H}_L}{L\left(Q_1\tau^{\mathrm{f}}\sigma_1^2\right)\left(\sigma_1^2\right)^L} - \frac{1}{L\left(\sigma_1^2\right)^{L+1}}\left(\begin{array}{c} {}_2F_1^{(1,0,0,0)}\left(1,L+1;L+1;2-\frac{Q_1\tau^{\mathrm{f}}}{\sigma_1^2}\right) \\ +{}_2F_1^{(0,0,1,0)}\left(1,L+1;L+1;2-\frac{Q_1\tau^{\mathrm{f}}}{\sigma_1^2}\right) \end{array}\right),$$

(6.56)

where $\mathrm{H}_L := \sum_{l=1}^{L} 1/l$ denotes the L-th harmonic number [51]. Furthermore, in (6.56), ${}_2F_1^{(1,0,0,0)}\left(a,b;c;z\right)$ and ${}_2F_1^{(0,0,1,0)}\left(a,b;c;z\right)$ represent the first-order symbolic differentiation of the Gauss hypergeometric function [75] with respect to parameters a and c, respectively, and defined as [75]

$${}_2F_1^{(1,0,0,0)}\left(a,b;c;z\right) = \sum_{k=0}^{\infty} \frac{(b)_k}{(c)_k k!} \frac{\partial (a)_k}{\partial a} z^k,$$

(6.57)

$${}_2F_1^{(0,0,1,0)}\left(a,b;c;z\right) = \sum_{k=0}^{\infty} \frac{(a)_k(b)_k}{(c)_k k!} \frac{\partial^{1}\!/\!(c)_k}{\partial c} z^k$$

(6.58)

with $(a)_i \triangleq \frac{\Gamma(a+i)}{\Gamma(a)}$ denoting the Pochammer symbol, $|z| < 1$. It is worth noting that the symbolic differentiation of Gauss hypergeometric function used in (6.56) can be easily implemented in most popular numerical softwares such as Mathematica.

For the integral J_2^b in (6.52), making the change of variable $x = \gamma - 1$, J_2^b can be simplified to

$$J_2^b = \int_{-1}^{\frac{Q_1}{\mu^{\mathrm{f}}}} \frac{x^{L-1}\ln\left(2+x\right)}{\left(Q_1\tau^{\mathrm{f}} + \sigma_1^2 x\right)^{L+1}} dx.$$

(6.59)

Then, making use of the expansion series given in (6.48) and using the same approach

applied for the derivation of J_1, (6.59) can be rewritten as

$$
\begin{aligned}
J_2^b &= \frac{1}{(\sigma_1^2)^{L+1}} \sum_{n=0}^{N} \left(\frac{-Q_1 \tau^{\mathrm{f}}}{\sigma_1^2} \right)^n \binom{L+n}{n} \int_{-1}^{\frac{-Q_1 \tau^{\mathrm{f}}}{\sigma_1^2}} x^{-n-2} G_{2,2}^{1,2} \left(x+1 \,\middle|\, {}_{1,0}^{1,1} \right) dx \\
&+ \frac{1}{(Q_1 \tau^{\mathrm{f}})^{L+1}} \sum_{n=0}^{N} \left(\frac{-\sigma_1^2}{Q_1 \tau^{\mathrm{f}}} \right)^n \binom{L+n}{n} \int_{\frac{-Q_1 \tau^{\mathrm{f}}}{\sigma_1^2}}^{\frac{Q_1 \tau^{\mathrm{f}}}{\sigma_1^2}} x^{L+n-1} G_{2,2}^{1,2} \left(x+1 \,\middle|\, {}_{1,0}^{1,1} \right) dx \\
&+ \frac{1}{(\sigma_1^2)^{L+1}} \sum_{n=0}^{N} \left(\frac{-Q_1 \tau^{\mathrm{f}}}{\sigma_1^2} \right)^n \binom{L+n}{n} \int_{\frac{Q_1 \tau^{\mathrm{f}}}{\sigma_1^2}}^{\frac{Q_1}{\mu^{\mathrm{f}}}} x^{-n-2} G_{2,2}^{1,2} \left(x+1 \,\middle|\, {}_{1,0}^{1,1} \right) dx, \qquad (6.60)
\end{aligned}
$$

which, after some mathematical manipulations [84, Eq. 9.31.2], yields

$$
\begin{aligned}
J_2^b &= \frac{1}{(Q_1 \tau^{\mathrm{f}})^{L+1}} \sum_{n=0}^{N} \binom{L+n}{n} \left(\frac{-\sigma_1^2}{Q_1 \tau^{\mathrm{f}}} \right)^n \left(\begin{array}{c} G_{3,3}^{1,3} \left(\frac{\sigma_1^2 + Q_1 \tau^{\mathrm{f}}}{\sigma_1^2} \,\middle|\, {}_{L+n+1,0,L+n}^{1,L+n+1,L+n+1} \right) \\ -G_{3,3}^{1,3} \left(\frac{\sigma_1^2 - Q_1 \tau^{\mathrm{f}}}{\sigma_1^2} \,\middle|\, {}_{L+n+1,0,L+n}^{1,L+n+1,L+n+1} \right) \end{array} \right) \\
&+ \frac{1}{(\sigma_1^2)^{L+1}} \sum_{n=0}^{N} \binom{L+n}{n} \left(\frac{-Q_1 \tau^{\mathrm{f}}}{\sigma_1^2} \right)^n
\end{aligned}
$$

$$
\times \left(\begin{array}{c} G_{3,3}^{3,1} \left(\frac{\mu^{\mathrm{f}}}{\lambda^{\mathrm{f}}} \,\middle|\, {}_{0,1+n,1+n}^{1+n,1,n+2} \right) + G_{3,3}^{3,1} \left(\frac{\sigma_1^2}{\sigma_1^2 - Q_1 \tau^{\mathrm{f}}} \,\middle|\, {}_{0,1+n,1+n}^{1+n,1,n+2} \right) \\ -G_{3,3}^{3,1} \left(\frac{\sigma_1^2}{Q_1 \tau^{\mathrm{f}} + \sigma_1^2} \,\middle|\, {}_{0,1+n,1+n}^{1+n,1,n+2} \right) \end{array} \right). \qquad (6.61)
$$

Finally, incorporating the expressions in (6.52) and (6.51) into (6.45), gives the ergodic capacity expression for the first-hop transmission when PRS strategy is used in the first-hop transmission. Then, the overall achievable capacity of the dual-hop DF cooperative spectrum-sharing system is calculated according to the expression in (6.43).

6.1.6   Numerical Results and Discussions

Using the analysis in the previous sections, we now investigate the performance and benefits of the proposed cooperative spectrum-sharing system when using PRS strategy. Simulation results are also provided, and as will be seen, a good agreement is achieved between the analytical and simulated curves[10]. In our simulations, the fading channels pertaining to the first- and second-hop links are modeled according to Rayleigh PDFs with

---

[10]Note that, for clarity of presentation, simulation data have been omitted in some of the curves.
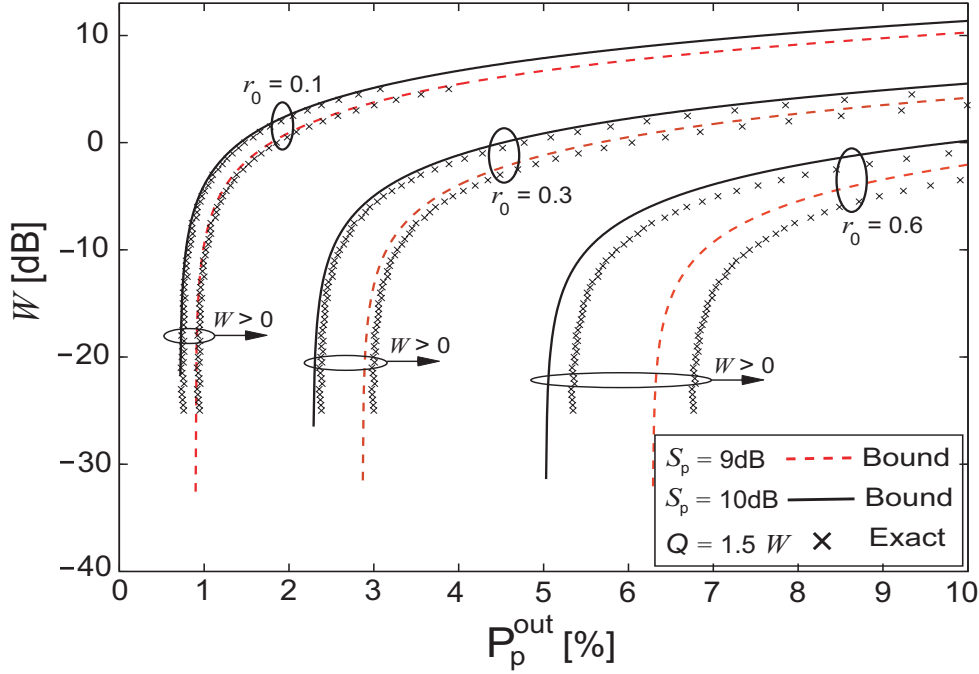
Figure 6.4: Interference limit, W, versus $P_{\text{p}}^{\text{out}}$ for $r_0 = 0.1$, 0.3, 0.6 bits/sec/Hz and different values for S_{p}.

$\mathrm{E}\left[\beta_l\right] = \tau^{\text{f}}$ and $\mathrm{E}\left[\alpha\right] = \tau^{\text{s}}$, respectively. We consider an exponential distribution for the associated interference channels, g_1 and g_2, with expected values of unity. It is also assumed that $\sigma_1^2 = \sigma_2^2 = 1$.

At first, we start by investigating the range of interference-limits tolerable at the PRs for different primary QoS requirements defined in terms of minimum required rate r_0 with a certain outage probability $P_{\text{p}}^{\text{out}}$. Fig. 6.4 depicts the upper bounds for the average interference-limit ($W = W_1 = W_2$) versus the outage probability in percentage for $r_0 = 0.1$, 0.3, 0.6 bits/sec/Hz and different values for S_{p} (9 dB and 10 dB). In this figure, we set $\delta_1^2 = \delta_2^2 = 1$. The figure shows that after certain values for $P_{\text{p}}^{\text{out}}$, the interference-limit, W, decreases rapidly as the outage probability, $P_{\text{p}}^{\text{out}}$, decreases or as the minimum required rate, r_0, increases. For comparison purposes, the exact calculated values of the interference-limit are shown for the case considering $Q = 1.5W$, where $Q = Q_1 = Q_2$. It is worth noting that when $W < 0$, no feasible power allocation satisfying the constraints in (6.2) exists. The arrows indicate the regions for which $W > 0$ holds true.
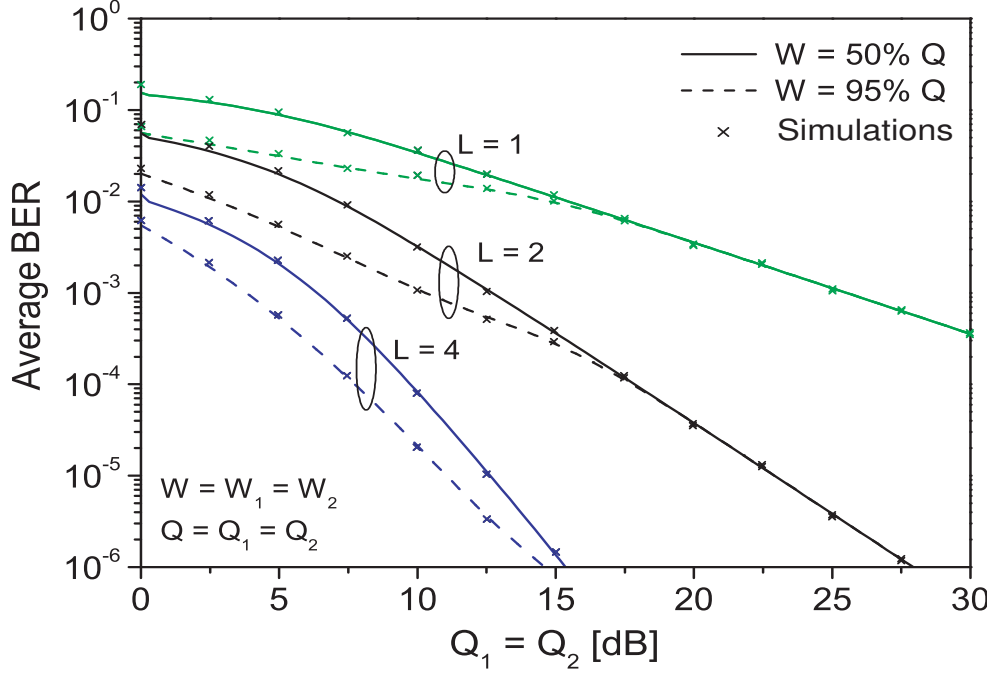
Figure 6.5: Average BER for BPSK spectrum-sharing cooperative relaying system, with $L = 1, 2$ or 4 relays and balanced resource limits, i.e., $Q_1 = Q_2$ and $W_1 = W_2$.

6.1.6.1   Error Rate Performance

Figs. 6.5-6.7 plot the end-to-end average BER as a function of the peak transmit power limits for each hop and considering different numbers for the relays participating in the selection. In Fig. 6.5, we set $Q_1 = Q_2 = Q$ and $W_1 = W_2 = W$, and vary the interference-limit as $W = 0.5Q$ or $W = 0.95Q$ for the number of relays $L = 1, 2, 4$, considering $\tau^{\mathrm{f}} = 0$ dB and $\tau^{\mathrm{s}} = 2$ dB. The figure shows that as W increases, the system performance improves, but for higher values of Q, it converges towards that of the system with no peak transmit-power constraints. Analysis of the number of relays shows substantial improvements in performance as L increases.

Fig. 6.6 investigates the effect of imbalanced resource limits, defined by the parameters Q_i and W_i for $i = 1, 2$, corresponding to the first- and second-hop transmission constraints. In this figure, we observe the significant effect of the imbalance between the resource limits on the dual-hop spectrum-sharing system. Fig. 6.6 also shows that for a fixed value of $Q_1 = Q_2$, as the average interference limit increases, e.g., as W_2 increases (or $\frac{W_2}{Q_2}$ increases), the system performance increases and converges towards that of the system with no average received-interference constraints. In fact, this means that a higher W_i can be considered
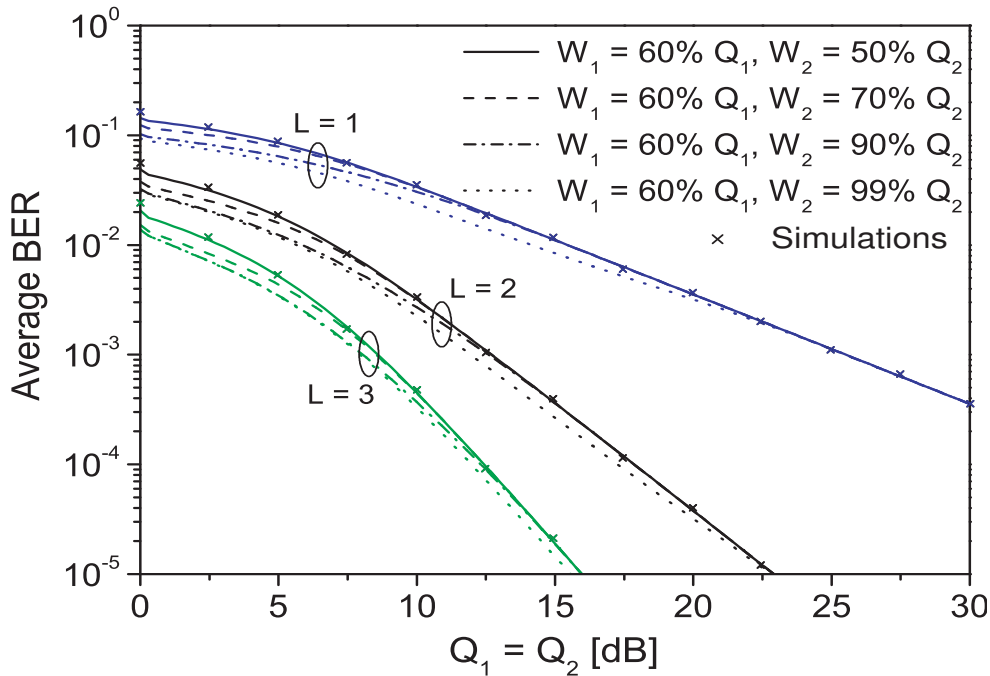
Figure 6.6: Average BER for BPSK spectrum-sharing cooperative relaying system, with $L = 1, 2$ or 3 relays and imbalanced resource limits.

as an advantage for the system performance and decreases the average BER, but after a certain value of W_i, for instance when $W_2 > Q_2$, the average BER is only limited by the peak received-interference constraints and does not increase as W_i increases.

In Fig. 6.7, we analyze the advantages of implementing PRS strategy in the dual-hop cooperative spectrum-sharing system. In this figure, setting $W_1 = 0.5Q_1$ and $W_2 = 0.7Q_2$, the variation of τ^{f} is investigated when $\tau^{\mathrm{s}} = 2$ dB. We observe the significant improvement in the overall performance of the cooperative system when the first transmission link is in weak propagation conditions, i.e., with lower values of τ^{f}, by increasing the number of relays participating in the selection over the first-hop transmission. It is worth noting that, although we consider a system with binary phase shift keying (BPSK) modulation, which implies $C = 2$ in the derived average BER expressions, the obtained expressions can easily be evaluated for other modulation schemes.

6.1.6.2   Ergodic Capacity Performance

The ergodic capacity of the dual-hop cooperative spectrum-sharing system is investigated in Figs. 6.8 and 6.9, for different values of the average interference-limit $W = W_1 =$
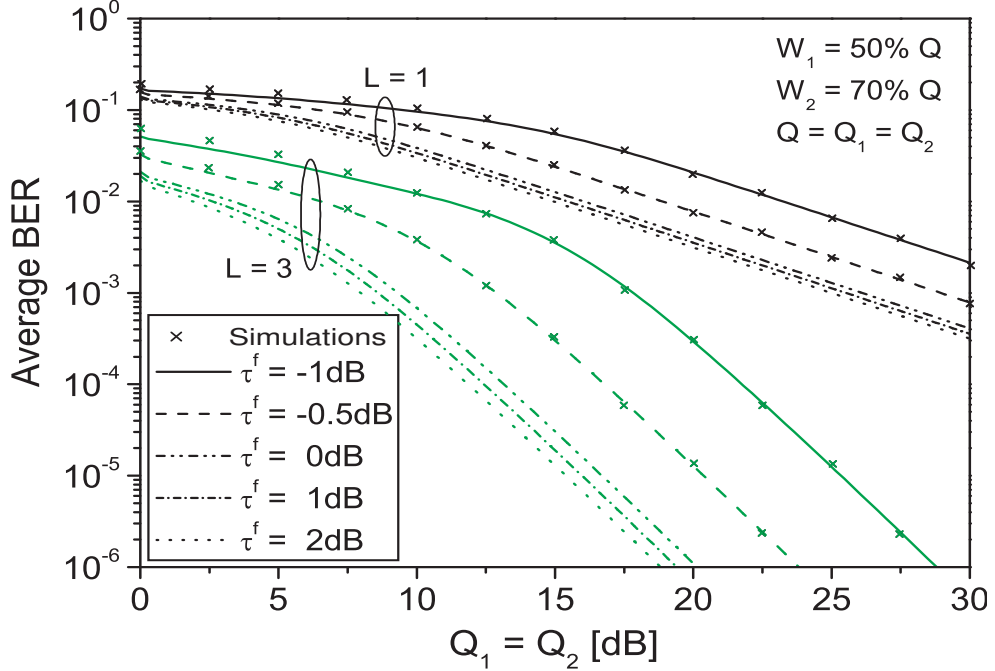
Figure 6.7: Average BER for BPSK spectrum-sharing cooperative relaying system, with $L = 1$ or 3 relays and imbalanced resource limits for different τ^{f} and $\tau^{\mathrm{s}} = 2$ dB.

W_2 and number of relays L. In Fig. 6.8, we set $\tau^{\mathrm{f}} = -1$ dB and $\tau^{\mathrm{s}} = 2$ dB. As observed, the overall achievable capacity of the dual-hop cooperative system increases as Q_1 or the number of relays increases. On the other hand, in Fig. 6.9, we set $Q_1 = 1.1W$ and $Q_2 = 1.5W$. From the plots, we observe a capacity gain achievement by increasing the number of relays available for the PRS strategy, especially when the transmission of the first link is more restricted than the second link, i.e., $Q_1 < Q_2$ or $\tau^{\mathrm{f}} < \tau^{\mathrm{s}}$.

6.1.6.3 Outage Probability Performance

Outage probability is one of the most commonly used performance measures in wireless systems and defined as the probability that the received SNR falls below a predetermined threshold γ_{th}. Particularly, in spectrum-sharing systems, given that the first and second-hop transmissions are limited by constraints on the average and peak interference at the primary receivers, it is obvious that some percentage of outage is unavoidable [8]. The outage probability may mathematically be defined as $P_{\mathrm{out}} = \mathrm{Pr}\left(\gamma_{\mathrm{sr}} \& \gamma_{\mathrm{rd}} < \gamma_{\mathrm{th}}\right)$, where γ_{th} is a predefined threshold. Indeed, the received signal power, or specifically the received SNR, has to be kept above a certain threshold at the secondary receivers to assure the sec-

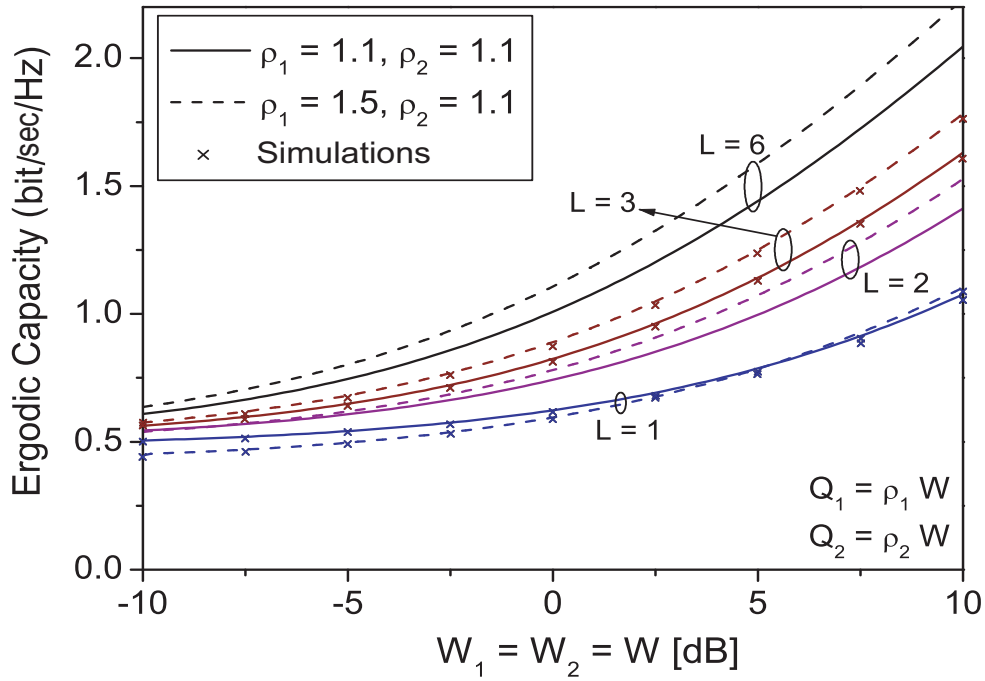Figure 6.8: Ergodic capacity of spectrum-sharing cooperative relaying system with DF relays versus $W = W_1 = W_2$, with $L = 1, 2, 3$ or 6 relays and imbalanced resource limits.
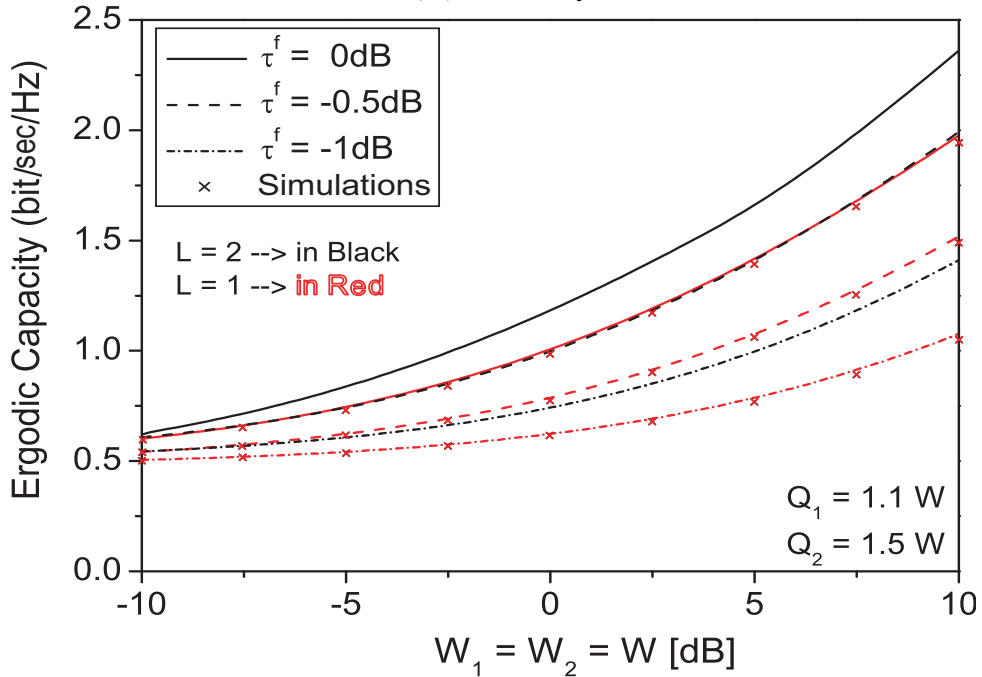

Figure 6.9: Ergodic capacity of spectrum-sharing cooperative relaying system with DF relays versus $W = W_1 = W_2$, with $L = 1$ or 2 relays and imbalanced resource limits for different τ^f and $\tau^s = 2$ dB.
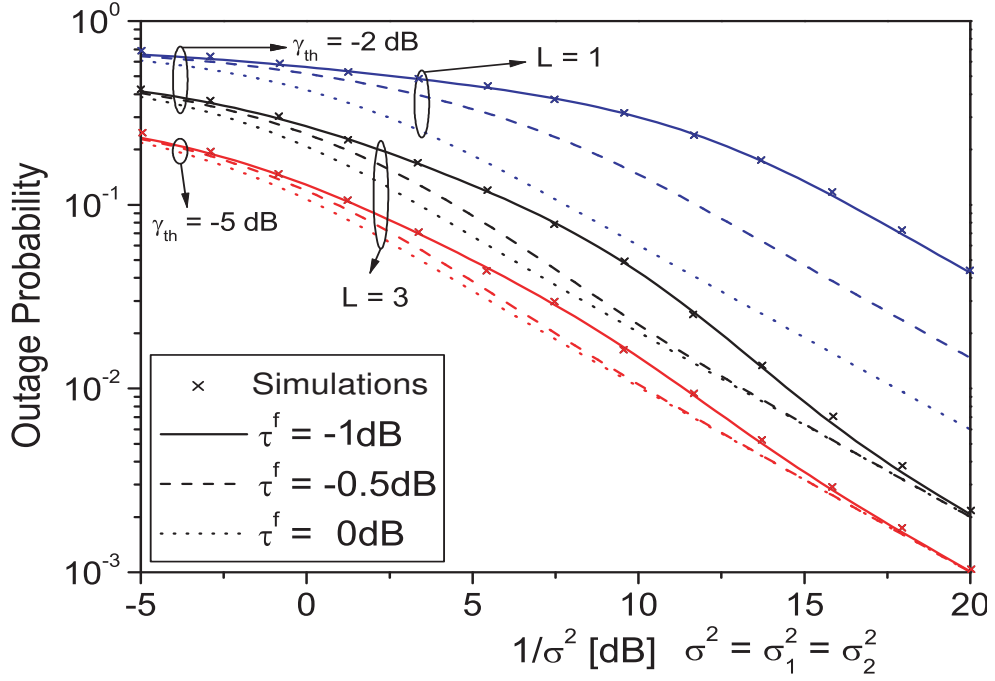
Figure 6.10: Outage probability of cooperative spectrum-sharing system with $L = 1$ or 3 relays and $\gamma_{\text{th}} = -2$ dB or -5 dB, for different τ^{f} and $\tau^{\text{s}} = 2$ dB.

ondary QoS is guaranteed. In this regard, the outage probability of the dual-hop cooperative spectrum-sharing system in terms of channel CDFs is given by

$$P_{\text{out}} = F_{\gamma_{\text{sr}}} \left(\gamma_{\text{th}} \right) + F_{\gamma_{\text{rd}}} \left(\gamma_{\text{th}} \right) - F_{\gamma_{\text{sr}}} \left(\gamma_{\text{th}} \right) F_{\gamma_{\text{rd}}} \left(\gamma_{\text{th}} \right). \tag{6.62}$$

Accordingly, the outage probability of the system under consideration when implementing the PRS strategy can be obtained by

$$P_{\text{out}}^{\text{prs}} = F_{\gamma_{\text{sr}}}^{\text{prs}} \left(\gamma_{\text{th}} \right) + F_{\gamma_{\text{rd}}} \left(\gamma_{\text{th}} \right) - F_{\gamma_{\text{sr}}}^{\text{prs}} \left(\gamma_{\text{th}} \right) F_{\gamma_{\text{rd}}} \left(\gamma_{\text{th}} \right), \tag{6.63}$$

which, after substituting the results obtained in (6.33), can be rewritten as

$$P_{\text{out}}^{\text{prs}} = \left[F_{\gamma_{\text{sr}}} \left(\gamma_{\text{th}} \right) \right]^{L} + F_{\gamma_{\text{rd}}} \left(\gamma_{\text{th}} \right) - \left[F_{\gamma_{\text{sr}}} \left(\gamma_{\text{th}} \right) \right]^{L} F_{\gamma_{\text{rd}}} \left(\gamma_{\text{th}} \right). \tag{6.64}$$

Note that the CDFs involved in (6.62) and (6.64) are obtained in section 6.1.3, and L in (6.64) denotes the number of relays participating in the PRS strategy.

Numerical results corresponding to the above expressions are shown in Fig. 6.10.

In this figure, we plot the outage probability performance of the dual-hop cooperative spectrum-sharing system in terms of the effective noise power (ENP) pertaining to the first- and second-hop defined by $1/\sigma_1^2$ and $1/\sigma_2^2$, respectively. For illustration purposes, it is assumed that $\sigma_1^2 = \sigma_2^2$. In these figures, we keep the peak and average interference limits at $Q_1 = Q_2 = 3$ dB and $W_1 = W_2 = -1$ dB, and vary the outage threshold γ_{th} or τ^{f}, while considering various values for the number of relays L. As observed, for $\gamma_{\text{th}} = -2$ dB, when the first link condition gets stronger, i.e., τ^{f} increases, the outage probability decreases, and for higher values of ENP, i.e., lower values of σ_1^2 or σ_2^2, it converges towards that of the system with better channel condition. On the other hand, as γ_{th} decreases, the outage probability decreases as well. As expected, analysis of the number of relays shows a significant improvement in the outage performance as L increases.

6.1.7 Summary

In this section, we studied a spectrum-sharing system that implements cooperative relaying in order to more efficiently use the available transmission resources such as power and rate in the shared spectrum, while adhering to predefined interference constraints to guarantee the PU's QoS is always satisfied. Specifically, we considered that the secondary source-destination communication relies on an intermediate relay node in the transmission process. In this context, we obtained the first-order statistics (PDF and CDF) pertaining to the first and second transmission channels. Then, making use of these statistics, we investigated the end-to-end performance of the proposed cooperative spectrum-sharing system under interference power constraints satisfying the QoS requirements at the PU side. More specifically, we obtained closed-form expressions for the average BER, ergodic capacity and outage probability of the secondary communication, while the PU's QoS requirements are specified in terms of appropriate resource constraints on the average and peak received interference power at the primary receiver. We further generalized our results for the case when multiple relays are available between the secondary source and destination nodes. In this case, considering partial relay selection technique for the first-hop transmission, the performance of the cooperative spectrum-sharing system has been studied under the underlying resource constraints. Our theoretical analysis was sustained by numerical and simulation results illustrating the performance and benefits of the proposed spectrum-sharing cooperative relaying system.

In the next section, we consider that the communication between the secondary source and destination nodes is assisted by an intermediate relay that uses AF strategy. In this context, making use of the standard convolutional approach, we obtain closed-form expressions for the PDF of the received SNR at the secondary destination node for different channel fading distributions, namely, Rayleigh and Nakagami. Then, the overall performance of the cooperative spectrum-sharing system is investigated for different propagation conditions.

6.2   Performance of Cooperative Amplify-and-Forward Relaying in Spectrum-Sharing Systems

Spectrum-sharing CR communication is a promising way to alleviate the spectrum scarcity in current wireless communication systems [114]. This technology offers tremendous potential to improve the radio spectrum usage by allowing SUs to access the spectrum bands licensed to PUs while adhering to the interference limitations of the licensed users. On the other hand, during the last decade, cooperative relaying has shown significant potential to increase the coverage area and enhance capacity in wireless communication systems [30, 96, 115] and has recently been shown to be of great interest in CR systems [105]. Applying the concept of cooperation in spectrum-sharing CR systems can even become a necessity when the available spectrum resources are not sufficient to guarantee reliable transmission and satisfy the SUs' service requirements.

A typical cooperative relaying spectrum-sharing CR system consists of a pair of secondary source and destination nodes with an intermediate relay located in the vicinity of the primary users. In this context, considering DF relaying [96], the effective capacity of the relay channel under Rayleigh fading in a spectrum-sharing CR system has been studied in [37] and [105], when the transmission of the SU is limited by interference constraint at the primary receiver. In Section 6.1, on the other hand, we considered that the SU communication is assisted by some intermediate relays that implement the DF technique onto the SU's relayed signal, and investigated the end-to-end performance of the dual-hop cooperative spectrum-sharing CR system under resource constraints defined so as to ensure the primary's quality-of-service is unaffected.

In this section, we investigate the end-to-end performance of dual-hop cooperative

AF relaying in spectrum-sharing CR systems while considering constraints on the average received-interference at the primary receivers. In particular, Section 6.2.1 presents the system and channel models of the proposed cooperative CR system and the assumed interference constraints. In Section 6.2.2, we obtain the PDF of the received SNR at the secondary destination node for different channel fading distributions, namely, Rayleigh and Nakagami. Then in Section 6.2.6, making use of these statistics, the overall achievable capacity and outage probability of the SU's communication process are investigated and numerical results and comparisons are provided. Finally, concluding remarks and summary are presented in Section 6.2.7.

6.2.1   The System Model

We consider a spectrum-sharing CR system where AF relays are employed to help in the SU's communication process. More specifically, our system consists of a pair of secondary source and destination nodes (SS and SD) located in the vicinity of the primary receiver (PR), and an AF relay node (R_s), as shown in Fig. 6.11. There is no direct link between the associated source and destination nodes, and the communication is established only via the relay in a dual-hop fashion. In this way, during the first hop, the SS communicates with the relay node, R_s. As the primary and secondary users share the same frequency band, the cognitive (secondary) user is allowed to operate in the licensee's spectrum as long as the primary communication is unaffected. For such, the SS listens to the interference channel, q_1, and adjusts its transmit power under predefined resource constraints in order to ensure the primary's operation is unaffected. Similar to the first-hop transmission, in the second-hop one, R_s node uses the same spectrum band originally assigned to the primary in order to communicate with SD.

During the second transmission hop, the relay node R_s listens to the interference channel, q_2, in order to adhere to the primary requirements and amplifies the received signal by a *gain factor* G. It is assumed that the first and second hops' transmissions are independent, e.g., through a time-division channel allocation scheme. It is also conjectured that SS and R_s have perfect knowledge of their respective interference channel gains. This can be obtained through a spectrum-band manager that mediates between the licensed and unlicensed users [105, 116]. We further assume that the channel power gain between SS and R_s is given by h with mean τ^f, and the one between R_s and SD by g with mean τ^s. The
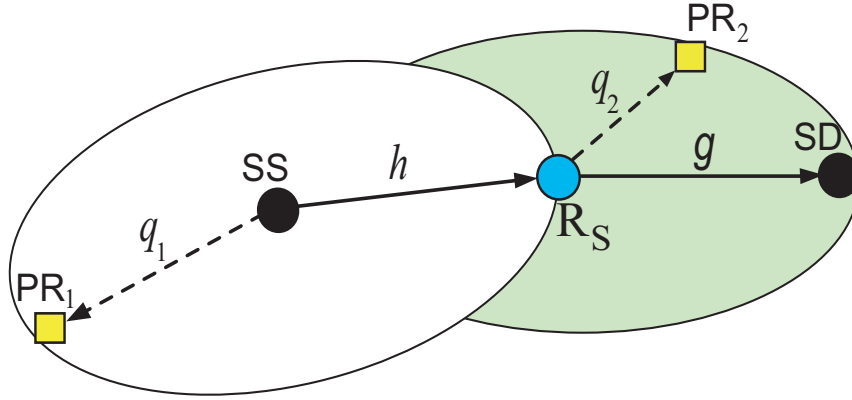
Figure 6.11: Spectrum-sharing system with dual-hop cooperative relaying.

interference channels' power gains, q_1 and q_2, are mutually independent with unit-mean distribution functions. Perfect CSI is available at terminals SS, $\mathrm{R_s}$ and SD. Accordingly, the received signal y at the destination node can be written as $y = G(hgx_\mathrm{s} + gn_\mathrm{sr}) + n_\mathrm{rd}$, where x_s stands for the signal transmitted by SS and, n_sr and n_rd denote the additive noise including the interference generated by the primary transmitter (PT) operating in the secondary transmission area, of the first hop and the second hop, respectively. We consider that the interference generated by the PT is modeled as additive zero-mean Gaussian noise at $\mathrm{R_s}$ and SD, with noise variance σ_1^2 and σ_2^2, respectively. Furthermore, for the sake of simplicity and mathematical tractability, herein we set the amplification gain according to $G^2 = 1/h^2$, which yields an extremely tight upper bound for the end-to-end SNR [117]. In this case, the relay just amplifies the incoming signal with the inverse of the channel of the first-hop, regardless of the noise level of that hop[11], leading to the following expression for the end-to-end instantaneous SNR:

$$\gamma_\mathrm{eq} = \left(\frac{1}{\gamma_\mathrm{sr}} + \frac{1}{\gamma_\mathrm{rd}} \right)^{-1}, \qquad (6.65)$$

where γ_sr and γ_rd are the instantaneous received-SNR at the secondary relay and destination, respectively.

In a spectrum-sharing CR system, a SU is allowed to operate in the licensee's spectrum as long as the average interference power it causes to the PR remains below a certain threshold. For such, in the primary/secondary cooperative spectrum-sharing system under

---

[11]This assumption serves as a benchmark for the design of practical relay systems.

study, the secondary nodes (SS, SD and R_{s}) are allowed to operate in the same spectrum band with the primary user as long as the following average interference constraints, for the first hop and second hop respectively, are satisfied

$$\mathcal{E}_{h,q_1}\left[S\left(h, q_1\right) q_1\right] \leq W_1, \tag{6.66a}$$

$$\mathcal{E}_{g,q_2}\left[S\left(g, q_2\right) q_2\right] \leq W_2, \tag{6.66b}$$

where $S\left(h, q_1\right)$ and $S\left(g, q_2\right)$ represent the instantaneous transmit power at SS and R_{s}, respectively, and $\mathcal{E}_X[\cdot]$ denotes statistical average with respect to X. Furthermore, W_1 and W_2 are the average received-interference power limits pertaining to the first- and second-hop, respectively.

6.2.2   Statistical Analysis under Average Power Constraints

Based on the average received-interference constraints detailed above, we derive the PDF of the instantaneous SNR pertaining to each hop on the secondary link. As well known, this statistic is an important metric that can be used to study the performance of cooperative communication systems in general. In our case, this statistic will be crucial in the analysis of the proposed cooperative relaying spectrum-sharing system, which is illustrated in Fig. 6.11. Note that, in this scenario, the relay, R_{s}, is used by the SU to enable communication between SS and SD and, consequently, improves the spectral efficiency of the system.

From the interference constraint given in (6.66a) and making use of the Lagrangian optimization technique, the optimal power transmission policy that maximizes the ergodic capacity of the secondary's first-hop link can be obtained as [101]

$$\mathrm{S}\left(h, q_1\right) = \left[\frac{\lambda^{\mathrm{f}}}{q_1} - \frac{\sigma_1^2}{h}\right]^+, \quad \frac{\sigma_1^2}{\lambda^{\mathrm{f}}} \leq \frac{h}{q_1}, \tag{6.67}$$

where λ^{f} is the first-hop optimization parameter which should be found such that the power constraint in (6.66a) is satisfied with equality. Accordingly, the instantaneous received SNR

at the secondary relay (R_s) can be expressed as

$$\gamma_\mathrm{sr} = \frac{S_\mathrm{sr}\left(h, q_1\right) h}{\sigma_1^2} = \left[\frac{\lambda^\mathrm{f}}{\sigma_1^2} \cdot \frac{h}{q_1} - 1\right]^+. \tag{6.68}$$

Now, considering the distribution function of the ratio h/q_1 to be $f_V\left(v\right)$, the required PDF statistic of γ_sr, can be obtained as follows:

$$f_{\gamma_\mathrm{sr}}\left(\gamma\right) = \left.\frac{\sigma_1^2}{\lambda^\mathrm{f}} f_V\left(v\right)\right|_{v=\frac{\sigma_1^2}{\lambda^\mathrm{f}}\left(\gamma+1\right)}. \tag{6.69}$$

Next, we will study the effect of the fading on the gain of opportunistic spectrum access by evaluating the instantaneous received SNR in (6.68) for different channel fading environments.

6.2.3 Rayleigh/Rayleigh Channels

With the fading following the Rayleigh distribution, which means that we consider all channel power gains to be independent exponential random variables, it is easy to show that the PDF of $V = h/q_1$ is given by $f_V\left(v\right) \triangleq \dfrac{\tau^\mathrm{f}}{\left(\tau^\mathrm{f} + v\right)^2}$ [107]. Thus, applying (6.69), the PDF of γ_sr can be obtained after some mathematical manipulations as

$$f_{\gamma_\mathrm{sr}}\left(\gamma\right) = \frac{\sigma_1^2 \lambda^\mathrm{f} \tau^\mathrm{f}}{\left(\lambda^\mathrm{f} \tau^\mathrm{f} + \sigma_1^2 \gamma\right)^2}, \ \gamma_\mathrm{sr} \geq 0. \tag{6.70}$$

Using the same approach described above, the PDF of the instantaneous SNR associated with the second-hop transmission can be obtained as

$$f_{\gamma_\mathrm{rd}}\left(\gamma\right) = \frac{\sigma_2^2 \lambda^\mathrm{s} \tau^\mathrm{s}}{\left(\lambda^\mathrm{s} \tau^\mathrm{s} + \sigma_2^2 \gamma\right)^2}, \ \gamma_\mathrm{rd} \geq 0, \tag{6.71}$$

where λ^s denotes the second-hop optimization parameter, which can be obtained from (6.66b) when set to equality.

Now, our aim is to find the PDF of γ_eq by making use of the direct convolutional approach. Thus, considering the end-to-end SNR function in (6.65), we define $Z = \gamma_\mathrm{eq}^{-1}$

by

$$Z \triangleq X + Y, \tag{6.72}$$

where $X \triangleq 1/\gamma_{\mathrm{sr}}$ and $Y \triangleq 1/\gamma_{\mathrm{rd}}$. Based on the PDFs in (6.70) and (6.71) and using the latter definitions for the random variables X and Y, it is easy to obtain the PDFs $f_X(x)$ and $f_Y(y)$ as follows:

$$f_X(x) = \frac{\sigma_1^2 \lambda^{\mathrm{f}} \tau^{\mathrm{f}}}{\left(\lambda^{\mathrm{f}} \tau^{\mathrm{f}} x + \sigma_1^2\right)^2}, \tag{6.73}$$

$$f_Y(y) = \frac{\sigma_2^2 \lambda^{\mathrm{s}} \tau^{\mathrm{s}}}{\left(\lambda^{\mathrm{s}} \tau^{\mathrm{s}} y + \sigma_2^2\right)^2}. \tag{6.74}$$

Since the random variables X and Y are independent, the density of their sum, i.e., $f_Z(z)$, simply equals the convolution of their densities [57], i.e.,

$$f_Z(z) = \int_0^z f_X(x) f_Y(z - x)\, dx. \tag{6.75}$$

Accordingly, substituting (6.73) and (6.74) into (6.75) and after some mathematical manipulations, $f_Z(z)$ can be simplified as follows [84, Eq. 2.173]:

$$
\begin{aligned}
f_Z(z) = & \frac{\lambda^{\mathrm{f}} \lambda^{\mathrm{s}} \tau^{\mathrm{f}} \tau^{\mathrm{s}} \left(\left(\sigma_1^2 \lambda^{\mathrm{f}} \tau^{\mathrm{f}} \left(\lambda^{\mathrm{s}} \tau^{\mathrm{s}}\right)^2 + \sigma_2^2 \lambda^{\mathrm{s}} \tau^{\mathrm{s}} \left(\lambda^{\mathrm{f}} \tau^{\mathrm{f}}\right)^2 \right) z + \left(\sigma_1^2 \lambda^{\mathrm{s}} \tau^{\mathrm{s}}\right)^2 + \left(\sigma_2^2 \lambda^{\mathrm{f}} \tau^{\mathrm{f}}\right)^2 \right) z}{\left(\sigma_1^2 + \lambda^{\mathrm{f}} \tau^{\mathrm{f}} z\right) \left(\sigma_2^2 + \lambda^{\mathrm{s}} \tau^{\mathrm{s}} z\right) \left(\sigma_1^2 \lambda^{\mathrm{s}} \tau^{\mathrm{s}} + \sigma_2^2 \lambda^{\mathrm{f}} \tau^{\mathrm{f}} + \lambda^{\mathrm{f}} \lambda^{\mathrm{s}} \tau^{\mathrm{f}} \tau^{\mathrm{s}} z\right)^2} \\
& + \frac{2\sigma_1^2 \sigma_2^2 \left(\lambda^{\mathrm{f}} \lambda^{\mathrm{s}} \tau^{\mathrm{f}} \tau^{\mathrm{s}}\right)^2}{\left(\sigma_1^2 \lambda^{\mathrm{s}} \tau^{\mathrm{s}} + \sigma_2^2 \lambda^{\mathrm{f}} \tau^{\mathrm{f}} + \lambda^{\mathrm{f}} \lambda^{\mathrm{s}} \tau^{\mathrm{f}} \tau^{\mathrm{s}} z\right)^3} \ln \left(\frac{\left(\sigma_1^2 + \lambda^{\mathrm{f}} \tau^{\mathrm{f}} z\right) \left(\sigma_2^2 + \lambda^{\mathrm{s}} \tau^{\mathrm{s}} z\right)}{\sigma_1^2 \sigma_2^2} \right).
\end{aligned} \tag{6.76}
$$

Therefore, in the case that the channel gains are Rayleigh distributed, the PDF of γ_{eq}, i.e., $f_{\gamma_{\mathrm{eq}}}(\gamma)$, is given by

$$
\begin{aligned}
f_{\gamma_{\mathrm{eq}}}(\gamma) = & \frac{\Sigma \Pi^2 + \left(\Sigma^2 \Pi - 2\sigma_1^2 \sigma_2^2 \Pi^2\right) \gamma}{\left(\sigma_1^2 \gamma + \lambda^{\mathrm{f}} \tau^{\mathrm{f}}\right) \left(\sigma_2^2 \gamma + \lambda^{\mathrm{s}} \tau^{\mathrm{s}}\right) \left(\Sigma \gamma + \Pi\right)^2} \\
& + \frac{2\Pi^2 \sigma_1^2 \sigma_2^2 \gamma}{\left(\Sigma \gamma + \Pi\right)^3} \ln \left(\frac{\left(\sigma_1^2 \gamma + \lambda^{\mathrm{f}} \tau^{\mathrm{f}}\right) \left(\sigma_2^2 \gamma + \lambda^{\mathrm{s}} \tau^{\mathrm{s}}\right)}{\gamma^2 \sigma_1^2 \sigma_2^2} \right),
\end{aligned} \tag{6.77}
$$

where parameters Σ and Π are defined as $\Sigma \triangleq \sigma_1^2 \lambda^{\mathrm{s}} \tau^{\mathrm{s}} + \sigma_2^2 \lambda^{\mathrm{f}} \tau^{\mathrm{f}}$ and $\Pi \triangleq \lambda^{\mathrm{f}} \lambda^{\mathrm{s}} \tau^{\mathrm{f}} \tau^{\mathrm{s}}$.

6.2.4 Nakagami/Nakagami Channels

With the fading following Nakagami distribution [118], both h and q_1 of the first-hop transmission (also g and q_2 of the second-hop) are independent random variables following Gamma distribution. In this case, it can be shown that the ratio $V \triangleq h/q_1$ is Beta-prime distributed [101]

$$f_V(v) = \left(\frac{m_0}{m_1}\right)^{m_0} \frac{v^{m_1-1}}{B(m_0, m_1)\left(v + \frac{m_0}{m_1}\right)^{m_0+m_1}}, \ v \geq 0, \tag{6.78}$$

where m_0 and m_1 are fading shape parameters pertaining to the channels h and q_1, respectively, with $m_0, m_1 \geq 0.5$, and $B(a, b) \triangleq \frac{\Gamma(a)\Gamma(b)}{\Gamma(a+b)}$ denotes the Beta function. Then, substituting (6.78) in (6.69), the PDF of the instantaneous SNR for the first-hop link, can be obtained as follows:

$$f_{\gamma_{sr}}(\gamma) = \left(\frac{\lambda^f m_0}{\sigma_1^2 m_1}\right)^{m_0} \frac{\gamma^{m_1-1}}{B(m_0, m_1)\left(\gamma + \frac{\lambda^f m_0}{\sigma_1^2 m_1}\right)^{m_0+m_1}}, \ \gamma_{sr} \geq 0. \tag{6.79}$$

For the second-hop transmission, we also consider that the channel power gains (g and q_2) follow Nakagami fading distribution. Thus, applying the same approach as explained for the first-hop, the PDF of γ_{rd} is obtained as

$$f_{\gamma_{rd}}(\gamma) = \left(\frac{\lambda^s \mu_0}{\sigma_2^2 \mu_1}\right)^{\mu_0} \frac{\gamma^{\mu_1-1}}{B(\mu_0, \mu_1)\left(\gamma + \frac{\lambda^s \mu_0}{\sigma_2^2 \mu_1}\right)^{\mu_0+\mu_1}}, \ \gamma_{rd} \geq 0, \tag{6.80}$$

where μ_0 and μ_1 are fading shape parameters pertaining to the channels g and q_2, respectively, with $\mu_0, \mu_1 \geq 0.5$. Subsequently, we use the convolutional approach presented in Section 6.2.3, to obtain the PDF of the instantaneous SNR at node SD, i.e., the PDF of γ_{eq}. In this regard, considering the definition of variables X and Y in (6.72), the PDFs $f_X(x)$

and $f_Y(y)$ can be written as

$$f_X(x) = \left(\frac{\lambda^{\mathrm{f}} m_0}{\sigma_1^2 m_1}\right)^{m_0} \frac{x^{m_0-1}}{\mathrm{B}(m_0, m_1)\left(1 + \frac{\lambda^{\mathrm{f}} m_0}{\sigma_1^2 m_1} x\right)^{m_0+m_1}}, \tag{6.81}$$

$$f_Y(y) = \left(\frac{\lambda^{\mathrm{s}} \mu_0}{\sigma_2^2 \mu_1}\right)^{\mu_0} \frac{y^{\mu_0-1}}{\mathrm{B}(\mu_0, \mu_1)\left(1 + \frac{\lambda^{\mathrm{s}} \mu_0}{\sigma_2^2 \mu_1} y\right)^{\mu_0+\mu_1}}. \tag{6.82}$$

Then, substituting the above functions into the convolution expression in (6.75), we get

$$f_Z(z) = \frac{\left(\frac{\lambda^{\mathrm{f}} m_0}{\sigma_1^2 m_1}\right)^{m_0} \left(\frac{\lambda^{\mathrm{s}} \mu_0}{\sigma_2^2 \mu_1}\right)^{\mu_0}}{\mathrm{B}(m_0, m_1)\,\mathrm{B}(\mu_0, \mu_1)} \underbrace{\int_0^z \frac{x^{m_0-1}}{\left(1 + \frac{\lambda^{\mathrm{f}} m_0}{\sigma_1^2 m_1} x\right)^{m_0+m_1}} \frac{(z-x)^{\mu_0-1}}{\left(1 + \frac{\lambda^{\mathrm{s}} \mu_0}{\sigma_2^2 \mu_1} z - \frac{\lambda^{\mathrm{s}} \mu_0}{\sigma_2^2 \mu_1} x\right)^{\mu_0+\mu_1}} dx}_{I},$$

$$\tag{6.83}$$

in which the integral I can be simplified after applying the change of variable $t = \dfrac{x}{z}$ as

$$I = z^{m_0+\mu_0-1} \left(1 + \frac{\lambda^{\mathrm{s}} \mu_0 z}{\sigma_2^2 \mu_1}\right)^{-\mu_0-\mu_1} \int_0^1 \frac{t^{m_0-1}(1-t)^{\mu_0-1}}{\left(1 + \frac{\lambda^{\mathrm{f}} m_0 z}{\sigma_1^2 m_1} t\right)^{m_0+m_1} \left(1 - \frac{\lambda^{\mathrm{s}} \mu_0 z}{\sigma_2^2 \mu_1 + \lambda^{\mathrm{s}} \mu_0 z} t\right)^{\mu_0+\mu_1}} dt. \tag{6.84}$$

Then, after some algebraic manipulations, (6.84) can be expressed as

$$I = \frac{\mathrm{B}(m_0, \mu_0)\, z^{m_0+\mu_0-1}}{\left(1 + \frac{\lambda^{\mathrm{s}} \mu_0 z}{\sigma_2^2 \mu_1}\right)^{\mu_0+\mu_1}} F_1\left(m_0, m_0+m_1, \mu_0+\mu_1, m_0+\mu_0; \frac{-\lambda^{\mathrm{f}} m_0 z}{\sigma_1^2 m_1}, \frac{\lambda^{\mathrm{s}} \mu_0 z}{\sigma_2^2 \mu_1 + \lambda^{\mathrm{s}} \mu_0 z}\right), \tag{6.85}$$

where $F_1(a, b_1, b_2, c; u, v)$ denotes the integral representation of the Appell hypergeometric function of the first kind, which is given by [84, Eq. 3.211]

$$F_1(a, b_1, b_2, c; u, v) = \frac{1}{\mathrm{B}(a, c-a)} \int_0^1 \frac{t^{a-1}(1-t)^{c-a-1}}{(1-ut)^{b_1}(1-vt)^{b_2}} dt, \tag{6.86}$$

for $\mathfrak{Re}[a] > 0$ and $\mathfrak{Re}[c-a] > 0$. It is worth noting that the Appell hypergeometric functions are implemented in most popular computing softwares such as Mathematica.

Now, incorporating (6.85) into (6.83) yields the final closed-form expression for $f_Z(z)$ as

$$f_Z(z) = \frac{\left(\frac{\lambda^{\mathrm{f}} m_0}{\sigma_1^2 m_1}\right)^{m_0} \left(\frac{\lambda^{\mathrm{s}} \mu_0}{\sigma_2^2 \mu_1}\right)^{\mu_0}}{\left(1 + \frac{\lambda^{\mathrm{s}} \mu_0 z}{\sigma_2^2 \mu_1}\right)^{\mu_0 + \mu_1}} \frac{\mathrm{B}(m_0, \mu_0) \, z^{m_0 + \mu_0 - 1}}{\mathrm{B}(m_0, m_1) \, \mathrm{B}(\mu_0, \mu_1)}$$

$$\times F_1\left(m_0, m_0 + m_1, \mu_0 + \mu_1, m_0 + \mu_0; \frac{-\lambda^{\mathrm{f}} m_0 z}{\sigma_1^2 m_1}, \frac{\lambda^{\mathrm{s}} \mu_0 z}{\sigma_2^2 \mu_1 + \lambda^{\mathrm{s}} \mu_0 z}\right), \qquad (6.87)$$

which, after applying the convolution theorem [57], yields the following expression for the PDF of γ_{eq} in the Nakagami fading case.

$$f_{\gamma_{\mathrm{eq}}}(\gamma) = \frac{\mathrm{B}(m_0, \mu_0)}{\mathrm{B}(m_0, m_1) \, \mathrm{B}(\mu_0, \mu_1)} \frac{\left(\frac{\lambda^{\mathrm{f}} m_0}{\sigma_1^2 m_1}\right)^{m_0} \left(\frac{\lambda^{\mathrm{s}} \mu_0}{\sigma_2^2 \mu_1}\right)^{\mu_0}}{\left(1 + \frac{\lambda^{\mathrm{s}} \mu_0}{\sigma_2^2 \mu_1 \gamma}\right)^{\mu_0 + \mu_1} \gamma^{m_0 + \mu_0 + 1}}$$

$$\times F_1\left(m_0, m_0 + m_1, \mu_0 + \mu_1, m_0 + \mu_0; \frac{-\lambda^{\mathrm{f}} m_0}{\sigma_1^2 m_1 \gamma}, \frac{\lambda^{\mathrm{s}} \mu_0}{\lambda^{\mathrm{s}} \mu_0 + \sigma_2^2 \mu_1 \gamma}\right). \qquad (6.88)$$

6.2.5 Special Cases

The PDF expression provided in (6.88) can be reduced to some particular cases for the fading in relation with the first and second hops. For each case, we determine the simplified form of the received-SNR density function.

6.2.5.1 Rayleigh/Rayleigh Channels

In this case, it is assumed that the communication channels (h, q_1) and (g, q_2) undergo Rayleigh fading with unit variances. Considering Rayleigh as a special case of the Nakagami distributions considered above, the fading shape parameters are unity, i.e., $m_0 = \mu_0 = m_1 = \mu_1 = 1$. Substituting these values into the PDF expression in (6.88), we get

$$f_{\gamma_{\mathrm{eq}}}(\gamma) = \frac{\lambda^{\mathrm{f}} \lambda^{\mathrm{s}} \left(\sigma_2^2 \gamma\right)^2}{\sigma_1^2 \sigma_2^2 \left(\lambda^{\mathrm{s}} + \sigma_2^2 \gamma\right)^2 \gamma^3} F_1\left(1, 2, 2, 2; \frac{-\lambda^{\mathrm{f}}}{\sigma_1^2 \gamma}, \frac{\lambda^{\mathrm{s}}}{\lambda^{\mathrm{s}} + \sigma_2^2 \gamma}\right). \qquad (6.89)$$

Then considering that $F_1\left(1, 2, 2, 2; u, v\right)$ can be reduced as [84, Eq. 2.173.1]

$$F_1\left(1, 2, 2, 2; u, v\right) = \frac{u^2\left(v-1\right) + v^2\left(u-1\right)}{\left(v-u\right)^3\left(u-1\right)\left(v-1\right)} + \frac{2uv}{\left(u-v\right)^3}\ln\left(\frac{v-1}{u-1}\right),\qquad(6.90)$$

and after some mathematical manipulations, $f_{\gamma_{\text{eq}}}\left(\gamma\right)$ can be expressed as

$$f_{\gamma_{\text{eq}}}\left(\gamma\right) = \frac{\lambda^{\text{f}}\lambda^{\text{s}}\left(\sigma_1^2\lambda^{\text{f}}\left(\lambda^{\text{s}}\right)^2 + \sigma_2^2\lambda^{\text{s}}\left(\lambda^{\text{f}}\right)^2 + \left(\left(\sigma_1^2\lambda^{\text{s}}\right)^2 + \left(\sigma_2^2\lambda^{\text{f}}\right)^2\right)\gamma\right)}{\left(\lambda^{\text{f}} + \sigma_1^2\gamma\right)\left(\lambda^{\text{s}} + \sigma_2^2\gamma\right)\left(\lambda^{\text{f}}\lambda^{\text{s}} + \left(\sigma_1^2\lambda^{\text{s}} + \sigma_2^2\lambda^{\text{f}}\right)\gamma\right)^2}$$
$$+ \frac{2\sigma_1^2\sigma_2^2\left(\lambda^{\text{f}}\lambda^{\text{s}}\right)^2\gamma}{\left(\lambda^{\text{f}}\lambda^{\text{s}} + \left(\sigma_1^2\lambda^{\text{s}} + \sigma_2^2\lambda^{\text{f}}\right)\gamma\right)^3}\ln\left(\frac{\left(\sigma_1^2\gamma + \lambda^{\text{f}}\right)\left(\sigma_2^2\gamma + \lambda^{\text{s}}\right)}{\sigma_1^2\sigma_2^2\gamma^2}\right).\qquad(6.91)$$

It is worth noting that (6.91) can also be assumed as a special case of the expression presented in (6.77) with $\tau^{\text{f}} = \tau^{\text{s}} = 1$.

6.2.5.2 Nakagami/Rayleigh Channels

In this case, it is considered that the secondary channel power gains (h, g) are distributed according to Nakagami PDF with fading shape parameters m_1 and μ_1, and the interference channels (q_1, q_2) experience Rayleigh fading with unit variance, i.e., $m_0 = \mu_0 = 1$. Thus, applying the above values into the PDF expression in (6.88), we obtain

$$f_{\gamma_{\text{eq}}}\left(\gamma\right) = \frac{\lambda^{\text{f}}\lambda^{\text{s}}\left(\sigma_2^2\mu_1\right)^{1+\mu_1}\gamma^{\mu_1-2}}{\sigma_1^2\sigma_2^2\left(\lambda^{\text{s}} + \sigma_2^2\mu_1\gamma\right)^{1+\mu_1}}F_1\left(1, 1+m_1, 1+\mu_1, 2; \frac{-\lambda^{\text{f}}}{\sigma_1^2 m_1\gamma}, \frac{\lambda^{\text{s}}}{\lambda^{\text{s}} + \sigma_2^2\mu_1\gamma}\right).$$
$$(6.92)$$

Then, considering the reduced expression of the Appell hypergeometric function in (6.92), i.e., [84]

$$F_1\left(1, b_1, b_2, 2; u, v\right) = \frac{1}{v\left(b_2 - 1\right)}$$
$$\times\left(\frac{\left(1-v\right)^{1-b_1}v}{\left(1-u\right)^{b_1}}\,_2F_1\left(1, b_1; 2-b_2; \frac{u-uv}{v-uv}\right) - \,_2F_1\left(1, b_1; 2-b_2; \frac{u}{v}\right)\right),\quad(6.93)$$

the PDF expression for the end-to-end SNR in the Nakagami/Rayleigh fading case can be obtained as

$$
\begin{aligned}
f_{\gamma_{eq}}\left(\gamma\right) =\ & \frac{\lambda^{\mathrm{f}}\left(\lambda^{\mathrm{s}}\right)^{m_1+1}\left(\sigma_2^2\mu_1\right)^{\mu_1}\gamma^{\mu_1-2}}{\sigma_1^2\left(\lambda^{\mathrm{s}}+\sigma_2^2\mu_1\gamma\right)^{\mu_1}} \\
& \times\left(\begin{array}{l}
\frac{\left(\lambda^{\mathrm{s}}+\sigma_2^2\mu_1\gamma\right)^{m_1}\left(\sigma_1^2 m_1\right)^{m_1+1}\gamma}{\left(\sigma_2^2\mu_1\right)^{m_1}\left(\lambda^{\mathrm{f}}+\sigma_1^2 m_1\gamma\right)^{1+m_1}}\ {}_2F_1\left(1,1+m_1;1-\mu_1;\frac{-\sigma_2^2\lambda^{\mathrm{f}}\mu_1\gamma}{\lambda^{\mathrm{f}}\lambda^{\mathrm{s}}+\lambda^{\mathrm{s}}\sigma_1^2 m_1\gamma}\right) \\
-\ {}_2F_1\left(1,1+m_1;1-\mu_1;\frac{\lambda^{\mathrm{f}}\lambda^{\mathrm{s}}+\sigma_2^2\lambda^{\mathrm{f}}\mu_1\gamma}{-\sigma_1^2\lambda^{\mathrm{s}}m_1\gamma}\right)
\end{array}\right),\quad (6.94)
\end{aligned}
$$

where ${}_2F_1\left(a,b;c;z\right)$ represents the Gauss hypergeometric function [84].

In the following section, making use of the derived statistics and focusing on the secondary communication, we investigate the end-to-end performance of the cooperative spectrum-sharing CR system with AF relaying.

6.2.6 Performance Analysis and Discussion

The overall achievable capacity of the proposed dual-hop cooperative spectrum-sharing system with AF relaying is given by

$$
C = \frac{1}{2}\int_0^{+\infty}\log_2\left(1+\gamma\right)f_{\gamma_{eq}}\left(\gamma\right)d\gamma. \tag{6.95}
$$

Numerical results regarding the achievable capacity are investigated in Figs. 6.12 and 6.13, for the different channel fading distributions studied in Section 6.2.2 and different average interference limits W_1 and W_2. In our simulations, it is assumed that $\sigma_1^2 = \sigma_2^2 = 1$. In Fig. 6.12, we consider the Rayleigh/Rayleigh scenario as described in Section 6.2.3, where the channel gains $\sqrt{h}$ and $\sqrt{g}$ are modeled according to Rayleigh PDFs with $\mathrm{E}\left[h\right] = \tau^{\mathrm{f}}$ and $\mathrm{E}\left[g\right] = \tau^{\mathrm{s}}$, respectively. It is also assumed that the interference channels q_1 and q_2, follow Rayleigh distributions with unit variances. In this figure, the variation of τ^{f} and the average interference limits, W_1 and W_2, are investigated while τ^{s} is set to 2 dB. We observe the significant improvement on the overall achievable capacity of the proposed cooperative spectrum-sharing system as the transmission of the first link is restricted, i.e., $\tau^{\mathrm{f}} < \tau^{\mathrm{s}}$ or $W_1 < W_2$.

Fig. 6.13 investigates the end-to-end capacity of the proposed cooperative system in the Nakagami/Nakagami scenario described in Section 6.2.4. In particular, it is consid-
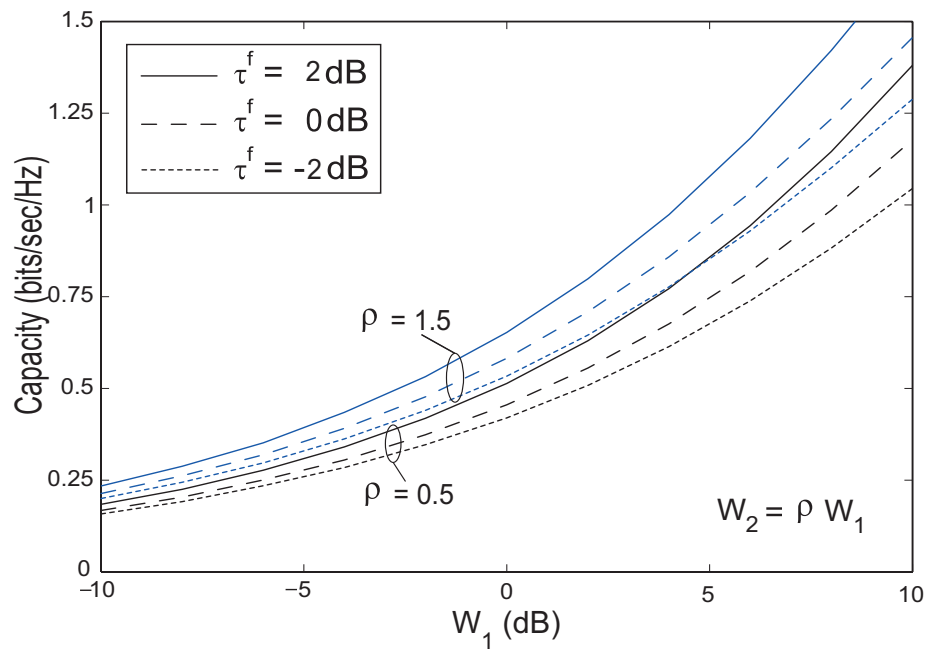
Figure 6.12: Achievable capacity of cooperative relaying spectrum-sharing system with AF relay versus W_1, with $\tau^s = 2$ dB.
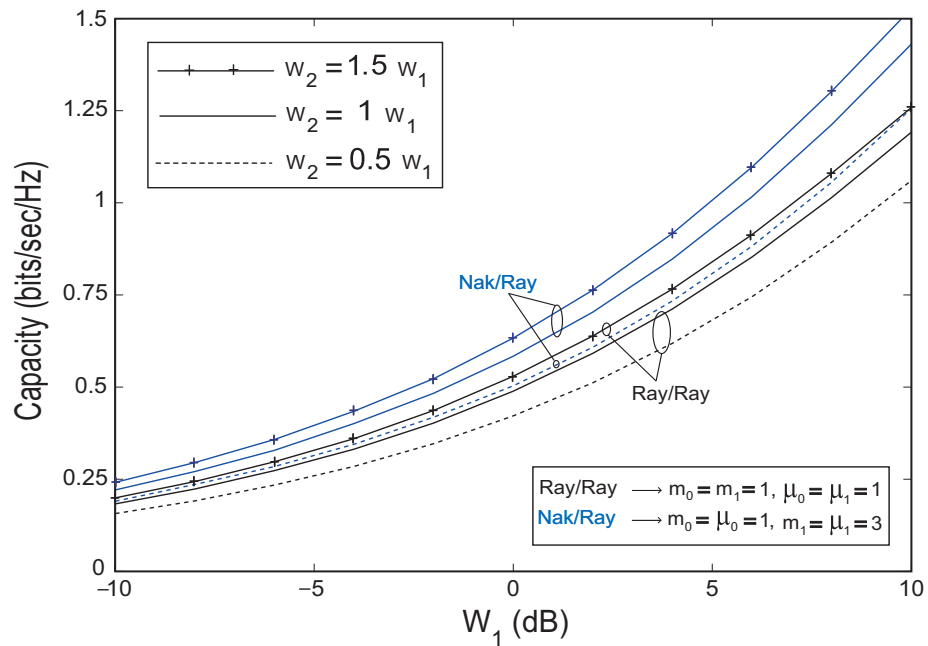

Figure 6.13: Achievable capacity of cooperative relaying spectrum-sharing system with AF relay versus W_1.

ered that the fading channel power gains pertaining to the first and second transmission hops, i.e., $(\sqrt{h}, \sqrt{q_1})$ for the first-hop and $(\sqrt{g}, \sqrt{q_2})$ for the second-hop, are distributed according to Nakagami fading PDFs with fading shape parameters (m_0, m_1) and (μ_0, μ_1), respectively. In this figure, we compare the performance of the special cases in this scenario, i.e., Nakagami/Rayleigh $(m_0 = \mu_0 = 1, m_1 = \mu_1 = 3)$ and Rayleigh/Rayleigh $(m_0 = \mu_0 = 1, m_1 = \mu_1 = 1)$, for different values of the interference limits W_1 and W_2. As observed, the overall achievable capacity of the dual-hop cooperative system increases as the secondary transmission channels, h and g, have stronger fading conditions than the interference channels, q_1 and q_2, i.e., higher $m_0 > m_1$ and $\mu_0 > \mu_1$, respectively. Furthermore, for a fixed value of W_1, we observe a capacity gain achievement as the average interference limit W_2 increases in both aforementioned cases.

On the other hand, one important performance measure in noise-limited systems is the outage probability, P_{out}, which is defined as the probability that the received SNR at the destination node falls below a predetermined threshold, γ_{th}. This threshold can be considered as a protection level for the received-SNR at the SU destination node to ensure the secondary quality-of-service is satisfied. In the system under study, the outage probability performance can be calculated according to the following integral expression:

$$P_{\text{out}} = \Pr\left(\gamma_{\text{eq}} < \gamma_{\text{th}}\right) = \int_0^{\gamma_{\text{th}}} f_{\gamma_{\text{eq}}}\left(\gamma\right) d\gamma, \tag{6.96}$$

where $f_{\gamma_{\text{eq}}}(\cdot)$ is as obtained in Section 6.2.2.

In Fig. 6.14, we analyze the outage probability performance of the dual-hop AF cooperative spectrum-sharing systems for different average interference limits $(W_1 = W_2 = W)$ and threshold values $(\gamma_{\text{th}} = 2 \text{ dB and} -3 \text{ dB})$. As shown in this figure, we compare the outage probability of the proposed cooperative system for various fading scenarios, namely, Nakagami/Nakagami $(m_0 = \mu_0 = 2, m_1 = \mu_1 = 3)$, Nakagami/Rayleigh $(m_0 = \mu_0 = 1, m_1 = \mu_1 = 3)$ and Rayleigh/Rayleigh $(m_0 = \mu_0 = 1, m_1 = \mu_1 = 1)$. As observed, for a given threshold value, the performance improves with increasing interference limit W. By comparing the fading scenarios in Fig. 6.14, it is observed that at high threshold values such as $\gamma_{\text{th}} = 2$ dB, the Nakagami/Nakagami scenario shows a poor performance for low-to-moderate interference limits and that its performance gradually improves as the interference limit (W) increases. On the other hand, at low threshold values such as $\gamma_{\text{th}} = -3$ dB, the Nakagami/Nakagami scenario shows a better performance than the other scenarios.
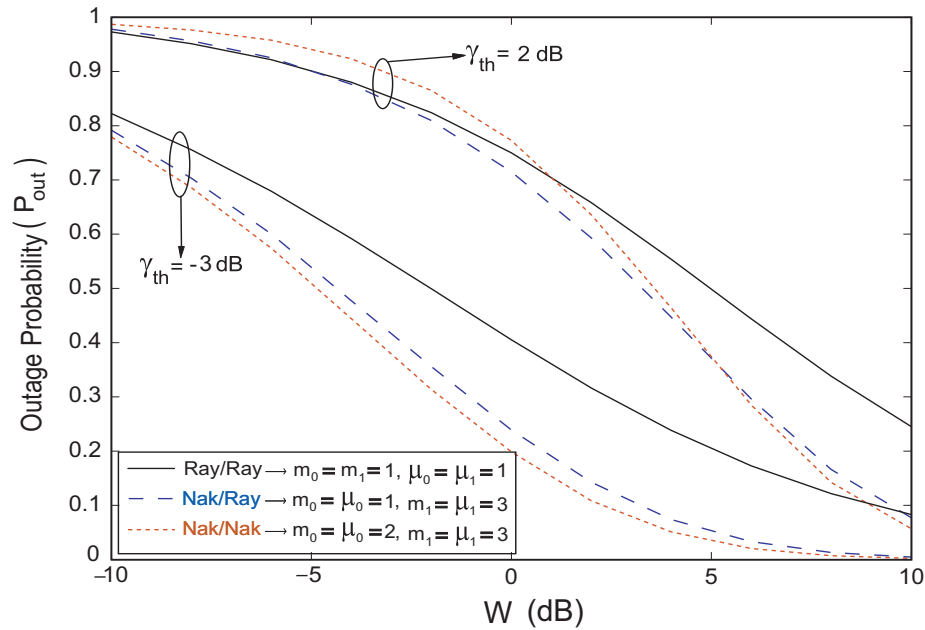
Figure 6.14: Outage probability of cooperative relaying spectrum-sharing system for equal interference limits ($W_1 = W_2 = W$) and different threshold values ($\gamma_{\text{th}} = 2, -3$ dB).

6.2.7   Summary

In this section, we considered a cooperative relaying scheme in order to improve the spectrum efficiency in spectrum-sharing CR systems while considering constraints on the average received-interference at the primary receivers. The relaying was implemented using the AF technique and we considered no direct link between the secondary source and destination nodes. In this context, closed-form expressions for the PDF of the received SNR at the secondary destination node have been derived considering different channel fading distributions, namely, Rayleigh and Nakagami. Then making use of these PDF expressions, we investigated the end-to-end performance of the proposed dual-hop cooperative spectrum-sharing system in different fading scenarios. Particularly, the overall achievable capacity and outage probability of the SU communication were investigated under average received-interference constraints at the primary receivers. Our theoretical analysis was sustained by numerical results illustrating the performance and benefits of the proposed cooperative relaying spectrum-sharing system.

Chapter 7

Conclusions of the Dissertation

In this dissertation, we investigated different approaches for adaptive resource allocation in spectrum-sharing CR networks. At first, we considered spectrum-sharing CR networks operating under interference constraints and where the SUs' transmission parameters can be adjusted based on the secondary channel variations and soft-sensing information about the activity of the PUs. Different resource allocation schemes were developed to increase the transmission opportunities and perform of the SUs while the QoS requirements of the PUs are satisfied. The existence and specification of such schemes were investigated for different system models and scenarios such as BC channels. Then, we proposed adopting cooperative relaying in spectrum-sharing CR networks to more effectively and efficiently utilize the available transmission resources, such as power, rate and bandwidth, while adhering to the QoS requirements of the PUs of the shared spectrum band. In this regard, while MGF-based approach is commonly utilized for performance analysis of the relaying communications, we proposed a unified framework based on first-order statistics and convolutional methods to obtain the end-to-end performance of the cooperative relaying spectrum-sharing system. Specifically, the contributions of the dissertation are summarized as follows:

• We considered a CR spectrum-sharing system where the SU's transmit power and rate can be adjusted based on the secondary channel variations and soft-sensing information about the activity of the PU. The spectrum-sharing system was assumed to operate under constraints on average interference and peak transmit power. Analysis and numerical results were provided and illustrated the throughput benefits of using soft-sensing infor-

mation and CSI at the SU in CR systems. It has been shown that by using a soft-sensing technique, the SU may opportunistically control its transmission parameters such as rate and power, according to different PU's activity levels observed by the sensing detector. Moreover, we analyzed the gap between the capacities achieved based on the *variable rate* and *variable power* transmission policies. Furthermore, we characterized the uncertainty of the sensing information calculated at the sensing detector, in terms of the false-alarm and detection probabilities, and investigated the effect of imperfect spectrum sensing on the performance of spectrum-sharing CR systems. (Chapter 2)

• Considering availability of soft-sensing information at the ST and adopting adaptive power transmission technique, we studied three capacity notions, namely, ergodic, delay-limited and service-rate (with and without outage), for CR spectrum-sharing systems operating under constraints on the average received-interference and peak transmit-power. Numerical results and comparisons for different fading environments, have shown that each capacity notion has some features that can be used according to different system requirements. Specifically, the service-rate capacity has been proposed as an appropriate capacity metric in CR networks which combines the advantages of the short- and long-term transmission strategies. (Chapter 3)

• We investigated adaptive resource sharing in CR fading BC channels when spectrum sensing information is utilized at the secondary BS so as to more effectively and efficiently use the shared spectrum resources. We proposed using soft-sensing information to fairly allocate the transmission time and power, among SUs, under appropriate constraints on the average interference at the PR and peak transmit-power at the secondary BS. Numerical results and comparisons have shown that spectrum sensing information allows for an efficient allocation of the time and power resources among the SUs and, consequently, the resulting interference onto the primary system. For instance, in the scenario with two SUs, it has been shown that as the primary system activity decreases in an area, more transmission time and power can be allocated to a SU located in that area and vice-versa. We further considered quantized spectrum sensing mechanism in order to reduce the overall system complexity, and as observed, performance with discrete levels are laid within the soft and two levels (hard) sensing mechanism results. (Chapter 4)

• We developed a performance analysis of conventional cooperative communications in order to have some ideas about the performance of cooperative CR spectrum-sharing sys-

tems which were then investigated in Chapter 6. First, considering a generalized fading scenario in a classical communication system and using the MGF approach, we obtained a general closed-form expression for the average SEP of arbitrary M-ary QAM constellations in MRC schemes over non-identical η-μ correlated fading channels. Thereafter, we analyzed the performance of multi-hop cooperative relaying networks in terms of the overall average SEP, ergodic capacity and outage probability subject to independent but non-identically distributed Nakagami-m fading. Furthermore, numerical and simulation results corroborating our analysis were provided and the impact of several parameters such as the number of relaying nodes and Nakagami fading indexes was investigated. (Chapter 5)

• Finally, we considered a cooperative relaying spectrum-sharing system where the secondary source-destination communication process relies on an intermediate relay node. In this regard, we investigated the end-to-end performance of the cooperative spectrum-sharing system under both DF and AF transmission relaying schemes by proposing a unified framework which relies on the first-order statistics and convolutional approaches, respectively. Specifically, we obtained closed-form expressions for the average BER, ergodic capacity and outage probability of the secondary communication, while the PU's QoS requirements are specified in terms of appropriate resource constraints on the average and peak received interference power at the PU receiver. Numerical results and comparisons showed the benefits of the proposed spectrum-sharing cooperative relaying system in different fading scenarios. (Chapter 6)

Appendix A

A.1 Conventional energy detection technique

It is worth noting that there is no restriction on the type of sensing technique that can be considered at the detector. The sensing information can be obtained based on the instantaneous power level pertaining to the PU transmission, or on statistics of such power level. In this paper, a conventional energy detection technique is adopted by the sensing module to calculate the sensing metric, ξ, [8, 119].
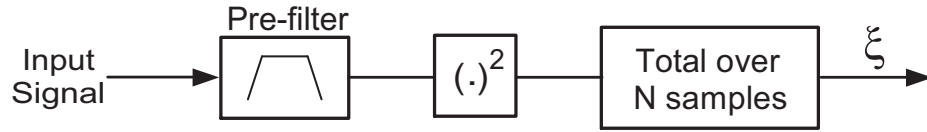

Figure A.1: A simple spectrum sensing model.

As shown in Fig. A.1, a conventional energy detector consists of a low-pass noise pre-filter that limits the noise bandwidth and adjacent signals and a square-law device followed by an integrator that evaluates the total received power over N independent signal samples. Hence, ξ is given by

$$\xi = \begin{cases} \sum_{n=1}^{N} \left(\sqrt{\gamma_{\mathrm{m}}[n]} x[n] + z[n] \right)^2, & \text{PU is ON}, \\ \sum_{n=1}^{N} \left(z[n] \right)^2, & \text{PU is OFF}, \end{cases} \tag{A.1}$$

where N is the observation time, $\sqrt{\gamma_{\mathrm{m}}[n]}$ is the channel gain between PT and ST, $x[n]$ denotes the PT's signal, $z[n]$ indicates the white Gaussian noise with unit variance at the detector, and n is the time sample index. As formulated in the above expression, we con-

sider fast channel fading, i.e., the channel coefficients change at every sample (n).

A.2 Proof of *Theorem* 1, regarding the average interference limits

From (6.1a), due to the independence of h_1, β and g_1, and the convexity of the function $f(x) = \log_2(1 + \frac{a}{x+b})$, for a, b and $x \geq 0$, the minimum rate inequality in (6.1a) can be simplified by using Jensen's inequality[1] as follows:

$$\mathrm{E}_{\beta,g_1}\left[\log_2\left(1 + \frac{S_\mathrm{p}h_1}{\mathrm{S}_\mathrm{sr}\left(\beta, g_1\right) g_1 + \delta_1^2}\right)\right] \geq \log_2\left(1 + \frac{S_\mathrm{p}h_1}{\mathrm{E}_{\beta,g_1}\left[\mathrm{S}_\mathrm{sr}\left(\beta, g_1\right) g_1\right] + \delta_1^2}\right)$$
$$\geq \log_2\left(1 + \frac{S_\mathrm{p}h_1}{W_1 + \delta_1^2}\right), \qquad (A.2)$$

where the second inequality results from the fact that the average received interference power is assumed to be constrained: $\mathrm{E}_{\beta,g_1}\left[\mathrm{S}_\mathrm{sr}\left(\beta, g_1\right) g_1\right] \leq W_1$. Now, substituting the upper bound presented in (A.2) into (6.1a), we obtain

$$\mathrm{Pr}\left\{\log_2\left(1 + \frac{S_\mathrm{p}h_1}{W_1 + \delta_1^2}\right) < r_0\right\} \leq P_\mathrm{p}^\mathrm{out}. \qquad (A.3)$$

Reorganizing (A.3) according to the primary channel h_1, and after some manipulations, the constraint simplifies to:

$$P_\mathrm{p}^\mathrm{out} \geq \mathrm{Pr}\left\{h_1 < \hat{\eta}\left(W_1 + \delta_1^2\right)\right\}$$
$$= \int_0^{\hat{\eta}\left(W_1 + \delta_1^2\right)} f_{h_1}\left(h_1\right) dh_1$$
$$= F_{h_1}\left(\hat{\eta}\left(W_1 + \delta_1^2\right)\right), \qquad (A.4)$$

where $\hat{\eta} = \dfrac{2^{r_0} - 1}{S_\mathrm{p}}$. Now, since we consider that the primary channel is exponentially distributed, then $F_{h_1}(x) = 1 - \exp\left(-x\right)$, and the above expression can be simplified to

$$P_\mathrm{p}^\mathrm{out} \geq 1 - \exp\left(-\hat{\eta}\left(W_1 + \delta_1^2\right)\right). \qquad (A.5)$$

---

[1]i.e., $\mathrm{E}\left[f\left(\mathrm{X}\right)\right] \geq f\left(\mathrm{E}\left[\mathrm{X}\right]\right)$.

For achieving a target $P_{\mathrm{p}}^{\mathrm{out}}$ value, the above inequality can be used to adjust the transmission power, $S_{\mathrm{sr}}(\beta, g_1)$. Thus, after simple manipulations of (A.5), for a given outage target $P_{\mathrm{p}}^{\mathrm{out}}$, the constraint limit W_1 is as expressed in (6.3). Furthermore, applying the same approach in (6.1b) for the second-hop, yields the constraint limit W_2 provided in (6.3).

A.3 Details pertaining to the derivations of optimization parameters

Substituting the optimal power allocation policy shown in (6.5), into the average received power constraint given by (6.2a) with equality, we obtain

$$\int_{\frac{\sigma_1^2}{\lambda^{\mathrm{f}}}}^{\frac{\sigma_1^2}{\mu^{\mathrm{f}}}} \left(\lambda^{\mathrm{f}} - \frac{\sigma_1^2}{z} \right) f_Z(z)\, dz + \int_{\frac{\sigma_1^2}{\mu^{\mathrm{f}}}}^{\infty} Q_1 f_Z(z)\, dz = W_1, \tag{A.6}$$

where $Z \triangleq \dfrac{\beta}{g_1}$ with PDF given by $f_Z(z) = \dfrac{\tau^{\mathrm{f}}}{\left(\tau^{\mathrm{f}} + z\right)^2}$ [107]. After evaluating the integrations in (A.6), the latter equation can be simplified according to

$$W_1 = Q_1 + \frac{\sigma_1^2}{\tau^{\mathrm{f}}} \ln\left(\frac{\sigma_1^2 + \left(\lambda^{\mathrm{f}} - Q_1\right)\tau^{\mathrm{f}}}{\sigma_1^2 + \lambda^{\mathrm{f}}\tau^{\mathrm{f}}} \right), \tag{A.7}$$

which, after further manipulation, yields (6.6). Then, substituting (6.6) into $\mu^{\mathrm{f}} = \lambda^{\mathrm{f}} - Q_1$, results in the expression shown in (6.7).

Bibliography

[1] Canadian Radio-Television Telecommunications Commission (CRTC), "Moving to Digital Television," *http://www.crtc.gc.ca*.

[2] Federal Communication Commission (FCC), "Notice of Proposed Rule Making and Order – In the Matter of Facilitating Opportunities for Flexible, Efficient, and Reliable Spectrum Use Employing Cognitive Radio Technologies Authorization and Use of Software Defined Radios," *FCC ET Docket No. 03-322*, Dec. 2003.

[3] IEEE 802.22 Working Group, "on Wireless Regional Area Netwok," *http://www.ieee802.org/22/*.

[4] IEEE 802.22 Working Group Document, "Functional Requirements for the 802.22 WRAN Standard," July 2009.

[5] X. Kang, Y.-C. Liang, H.K. Garg, and L. Zhang, "Sensing-based spectrum sharing in cognitive radio networks," *IEEE Trans. Veh. Tech.*, vol. 58, no. 8, pp. 4649–4654, Oct. 2009.

[6] N.S. Shankar, C. Cordeiro, and K. Challapali, "Spectrum agile radios: utilization and sensing architectures," in *Proc. IEEE DySPAN'05*, Baltimore, MD, USA, Nov. 2005, pp. 160–169.

[7] H. Kim, and K.G. Shin, "In-band spectrum sensing in cognitive radio networks: energy detection or feature detection?," in *Proc. Inte. Conf. Mobile Computing and Net.*, California, USA, Sep. 2008, pp. 14–25.

[8] Vahid Asghari and Sonia Aïssa, "Resource sharing in cognitive radio systems: Outage capacity and power allocation under soft sensing," in *Proc. IEEE Global Telecomm. Conf. (GLOBECOM'08)*, New Orleans, LA, USA, Nov.-Dec. 2008, pp. 1–5.

[9] I. F. Akyildiz, W. Y. Lee, M. C. Vuran, and S. Mohanty, "NeXt generation/dynamic spectrum access/cognitive radio wireless networks: A survey," *Computer Networks: The Int. J. of Computer and Telecommu. Networking*, vol. 50, no. 13, pp. 2127–2159, Sept. 2006.

[10] Anh Tuan Hoang and Ying-Chang Liang, "Downlink channel assignment and power control for cognitive radio networks," *IEEE Trans. Wire. Commun.*, vol. 7, no. 8, pp. 3106–3117, Aug. 2008.

[11] Jan Mietzner, Lutz Lampe, and Robert Schober, "Distributed transmit power allocation for multihop cognitive-radio systems," *IEEE Trans. Wire. Commun.*, vol. 8, no. 10, pp. 5187–5201, Oct. 2009.

[12] D. I. Kim, L. Le, and E. Hossain,, "Joint rate and power allocation for cognitive radios in dynamic spectrum access environment," *IEEE Trans. Wire. Commun.*, vol. 7, no. 12, pp. 5517–5527, Dec. 2008.

[13] Haipeng Yao, Zheng Zhou, He Liu, and Luyong Zhang, "Optimal power allocation in joint spectrum underlay and overlay cognitive radio networks," in *Proc. of 4th Inter. Conf. on CROWNCOM*, Germany, June 2009, pp. 1–5.

[14] S. Haykin, "Cognitive radio: brain-empowered wireless communications," *IEEE Jour. Selec. Areas in Commu.*, vol. 23, no. 2, pp. 201–220, Feb. 2005.

[15] A. Ghasemi and E. S. Sousa, "Capacity of fading channels under spectrum-sharing constraints," in *Proc. IEEE Int. Conf. Commun. (ICC'06)*, Istanbul, Turkey, June 2006, pp. 4373–4378.

[16] Leila Musavian and Sonia Aïssa, "Ergodic and outage capacities of spectrum-sharing systems in fading channels," in *Proc. IEEE Global Telecomm. Conf. (GLOBECOM'07)*, Washington, DC, USA, Nov. 2007, pp. 3327–3331.

[17] X. Kang, Ying-Chang Liang, and A. Nallanathan, "Optimal power allocation for fading channels in cognitive radio networks: Delay-limited capacity and outage capacity," in *Proc. IEEE Vehi. Tech. Conf. (VTC'08)*, Singapore, May 2008, pp. 1544–1548.

[18] Leila Musavian and Sonia Aïssa, "Quality-of-service based power allocation in spectrum-sharing channels," in *Proc. IEEE Global Telecomm. Conf. (GLOBE-COM'08)*, New Orleans, LA, USA, Nov. 2008, pp. 1–5.

[19] Rui Zhang, "Optimal power control over fading cognitive radio channel by exploiting primary user CSI," in *Proc. IEEE Global Telecomm. Conf. (GLOBECOM'08)*, New Orleans, LA, USA, Nov.-Dec. 2008, pp. 1–5.

[20] Himal A. Suraweera, Jason Gao, Peter J. Smith, Mansoor Shafi, and Michael Faulkner, "Channel capacity limits of cognitive radio in asymmetric fading environments," in *Proc. IEEE Int. Conf. Commun. (ICC'08)*, Beijing, China, May 2008, pp. 4048–4053.

[21] S. V. Hanly and D. N. Tse, "Multi-access fading channels: Shannon and delay-limited capacities," in *Proc. 33rd Allerton Conf.*, Monticello, IL, USA, Oct. 1995, pp. 1–10.

[22] Leila Musavian and Sonia Aïssa, "Capacity and power allocation for spectrum-sharing communications in fading channels," *IEEE Trans. Wireless Commun.*, vol. 8, no. 1, pp. 148–156, Jan. 2009.

[23] X. Kang, Y.-C. Liang, A. Nallanathan, H. K. Garg, and R. Zhang, "Optimal power allocation for fading channels in cognitive radio networks: Ergodic capacity and outage capacity," *IEEE Trans. Wireless Commun.*, vol. 8, no. 2, pp. 940–950, Feb. 2009.

[24] J. Luo, R. Yates, and P. Spasojević, "Service outage based power and rate allocation for parallel fading channels," *IEEE Trans. Inform. Theory*, vol. 51, no. 7, pp. 2594–2611, July 2005.

[25] N. Jindal and A. J. Goldsmith, "Capacity and optimal power allocation for fading broadcast channels with minimum rates," *IEEE Trans. Inform. Theory*, vol. 49, no. 11, pp. 2895–2909, Nov. 2003.

[26] Lifang Li and A. J. Goldsmith, "Capacity and optimal resource allocation for fading broadcast channels–part I: Ergodic capacity," *IEEE Trans. Inform. Theory*, vol. 47, no. 3, pp. 1083–1102, Mar. 2001.

[27] Y. Zhao, R. Adve, and T. J. Lim, "Improving amplify-and-forward relay networks: optimal power allocation versus selection," *IEEE Trans. Wirel. Commun.*, vol. 6, no. 8, pp. 3114–3123, Aug. 2007.

[28] M.D. Renzo, F. Graziosi, and F. Santucci, "On the performance of CSI-assisted cooperative communications over generalized fading channels," in *Proc. IEEE International Commun. Conf., "ICC'08"*, China, May 2008, p. 1001 Ű 1007.

[29] I. Krikidis, J. Thompson, S. McLaughlin, and N. Goertz, "Amplify-and-forward with partial relay selection," *IEEE Commun. Lett.*, vol. 12, no. 4, pp. 235–237, Apr. 2008.

[30] D. B. da Costa and Sonia Aïssa, "End-to-end performance of dual-hop semi-blind relaying systems with partial relay selection," *IEEE Trans. Wireless Commun.*, vol. 8, no. 8, pp. 4306–4315, Aug. 2009.

[31] D. B. da Costa and Sonia Aïssa, "Cooperative dual-hop relaying systems with beamforming over Nakagami-m fading channels," *IEEE Trans. Wireless Commun.*, vol. 8, no. 8, pp. 3950–3954, Aug. 2009.

[32] M.D. Renzo, F. Graziosi and F. Santucci, "A unified framework for performance analysis of CSI-assisted cooperative communications over fading channels," *IEEE Trans. on Commun.*, vol. 57, no. 9, pp. 2551–2557, Sep. 2009.

[33] M. O. Hasna and M.-S. Alouini, "Outage probability of multihop transmissions over Nakagami fading channels," *IEEE Commun. Lett.*, vol. 7, no. 5, pp. 216–218, May 2003.

[34] G. Farhadi and N. C. Beaulieu, "On the performance of amplify-and-forward cooperative systems with fixed gain relays," *IEEE Trans. Wirel. Commun.*, vol. 7, no. 5, pp. 1851–1856, May 2008.

[35] M. O. Hasna and M.-S. Alouini, "End-to-end performance of transmission systems with relays over Rayleigh-fading channels," *IEEE Trans. Wireless Commmun.*, vol. 2, no. 6, pp. 1126–1131, Nov. 2003.

[36] N. Devroye, P. Mitran, O.-S. Shin, H. Ochiai, V. Tarokh, "Cooperation and cognition in wireless networks," *SK Telecom Review, special issue on 4G Spectrum and System Engineering issues*, Feb. 2007.

[37] L. Musavian and S. Aïssa, "Cross-layer analysis of cognitive radio relay networks under quality of service constraints," in *Proc. IEEE Vehi. Tech. Conf. (VTC-S'09)*, Barcelona, Spain, Apr. 2009, pp. 1–5.

[38] K. Ben Fredj, L. Musavian, and S. Aïssa, "Closed-form expressions for the capacity of spectrum-sharing constrained relaying systems," in *Proc. IEEE 17th Inter. Conf. on Telecommun. (ICT)*, Doha, Qatar, Apr. 2010, pp. 476–480.

[39] Q. Zhang, J. Jia and J. Zhang, "Cooperative relay to improve diversity in cognitive radio networks," *IEEE Communications Magazine*, vol. 47, no. 2, pp. 111–171, Feb. 2009.

[40] A. J. Goldsmith and P. Varaiya, "Capacity of fading channels with channel side information," *IEEE Trans. Inform. Theory*, vol. 43, no. 6, pp. 1986–1992, Nov. 1997.

[41] E. Biglieri, J. Proakis, and S. Shamai, "Fadding channels: Information-theoretic and communications aspects," *IEEE Trans. Inform. Theory*, vol. 44, no. 6, pp. 2619–2692, Oct. 1998.

[42] M. A. Khojastepour and B. Aazhang, "The capacity of average and peak power constrained fading channels with channel side information," in *Proc. IEEE Wireless Commun. and Networking Conference (WCNC'04)*, Atlanta, CA, USA, Mar. 2004, pp. 77–82.

[43] C. Cordeiro, K. Challapali, D. Birru, and N. Sai Shankar, "IEEE 802.22: the first worldwide wireless standard based on cognitive radios," in *First IEEE Inte. Sym. New Fron. in Dyn. Spec. Access Net., DySPAN '05'*, Washington, DC, USA, Nov. 2005, pp. 328–337.

[44] N. Sai Shankar, "Overview of blind sensing techniques considered in IEEE 802.22 WRANs," in *Proc. 5th IEEE Annual Communications Society Conference on Sensor, Mesh and Ad Hoc Communications and Networks Workshops (SECON'08)*, San Diego, CA, USA, June 2008, pp. 1–4.

[45] H. Urkowitz, "Energy detection of unknown deterministic signals," *Proceedings of the IEEE*, vol. 55, no. 4, pp. 523–531, Apr. 1967.

[46] D. Cabric, A. Tkachenko, and R.W. Brodersen, "Spectrum sensing measurements of pilot, energy, and collaborative detection," in *Proc. IEEE Military Commun. Conf. (MILCOM'06)*, Washington, DC, Oct. 2006, pp. 1–7.

[47] S. Srinivasa and S. A. Jafar, "Soft sensing and optimal power control for cognitive radio," in *Proc. IEEE Global Telecomm. Conf. (GLOBECOM'07)*, Washington, DC, USA, Nov. 2007, pp. 1380–1384.

[48] M. Gastpar, "On capacity under received-signal constraints," in *Proc. 42nd Annu. Allerton Conf. on Communi. Control and Comp.*, Monticello, IL, USA, Oct. 2004, pp. 1322–1331.

[49] A. J. Goldsmith and Soon-Ghee Chua, "Variable-rate Variable-power MQAM for fading channels," *IEEE Trans. Communications*, vol. 45, no. 10, pp. 1218–1230, Oct. 1997.

[50] M.-S. Alouini and A. J. Goldsmith, "Capacity of Rayleigh fading channels under different adaptive transmission and diversity-combining techniques," *IEEE Trans. Veh. Technol.*, vol. 48, no. 4, pp. 1165 – 1181, July 1999.

[51] Milton Abramowitz and Irene A. Stegun, *Handbook of Mathematical Functions: with Formulas, Graphs, and Mathematical Tables*, Dover, New York, 9th edition, 1972.

[52] Stephen Boyd and Lieven Vandenberghe, *Convex Optimization*, Cambridge university Press, New York, USA, 2004.

[53] Leila Musavian and Sonia Aissa, "Fundamental capacity limits of cognitive radio in fading environments with imperfect channel information," *IEEE Trans. on Commun.*, vol. 57, no. 11, pp. 3472Ű3480, Nov. 2009.

[54] D. Cabric, S. Mishra, and R. Brodersen, "Implementation issues in spectrum sensing for cognitive radios," in *Proc. Thirty-Eighth Asilomar Conference on Signals, Systems and Computers*, Pacific Grove, California, Nov. 2004, vol. 1, pp. 772–776.

[55] S. Akin and M. C. Gursoy, "Effective capacity analysis of cognitive radio channels for quality of service provisioning," in *Proc. IEEE Global Telecommunications Conference (GLOBECOM'09)*, Honolulu, HI, USA, Nov.-Dec. 2009, pp. 1–6.

[56] Y.-C. Liang, Y. Zeng, E. C.Y. Peh, and A. T. Hoang, "Sensing-throughput tradeoff for cognitive radio networks," *IEEE Trans. Wireless Communications*, vol. 7, no. 4, pp. 1326–1337, Apr. 2008.

[57] A. Papoulis, *Probability, Random Variables, and Stochastic Processes*, 4 edition, 2002.

[58] I.F. Akyildiz, W. Su, Y. Sankarasubramaniam and E. Cayirci, "A survey on sensor networks," *IEEE Communication Mazazine*, vol. 40, no. 8, pp. 102–114, Aug. 2002.

[59] Y. Q. Shi and H. Sun, *Image and Video Compression for Multimedia Engineering: Fundamentals, Algorithms, and Standards*, CRC Press, Inc., FL, USA, 1st edition, 1999.

[60] Mark A. McHenry, "NSF spectrum occupancy measurments project summary," *Available at http://www.Sharedspectrum.com*, Aug. 2005.

[61] J. G. Proakis, *Digital Communications*, McGraw-Hill, 4th edition, 2001.

[62] A. J. Goldsmith, *Wireless Communications*, Cambridge University Press, 2005.

[63] G. Caire, G. Taricco, and E. Biglieri, "Optimum power control over fading channels," *IEEE Trans. Inform. Theory*, vol. 45, no. 5, pp. 1468–1489, July 1999.

[64] R. Zhang, S. Cui, and Y.-C. Liang, "On ergodic sum capacity of fading cognitive multiple-access and broadcast channels," *IEEE Trans. Inform. Theory*, vol. 55, no. 11, pp. 5161–5178, Nov. 2009.

[65] L. Zhang, Y. Xin, and Y.-C. Liang, "Weighted sum rate optimization for cognitive radio mimo broadcast channels," *IEEE Trans. Wire. Commun.*, vol. 8, no. 6, pp. 2950–2959, June 2009.

[66] Wei Yu, "Sum-capacity computation for the Gaussian vector broadcast channel via dual decomposition," *IEEE Trans. Inform. Theory*, vol. 52, no. 2, pp. 754–759, Feb. 2006.

[67] G. D. Durgin, T. S. Rappaport, and D. A. de Wolf, "New analytical models and probability density functions for fading in wireless communications," *IEEE Trans. Commun.*, vol. 50, no. 6, pp. 1005–1015, Jun. 2002.

[68] M. D. Yacoub, "The κ-μ distribution and the η-μ distribution," *IEEE Ant. and Prop. Magazine*, vol. 49, no. 1, pp. 68–81, Feb. 2007.

[69] M. K. Simon and M. S. Alouini, *Digital Communication over Fading Channels*, John Wiley Sons, second edition, 2005.

[70] N.C. Beaulieu, "A useful integral for wireless communication theory and its application to rectangular signaling constellation error rates," *IEEE Trans. Commun.*, vol. 54, no. 5, pp. 802–805, May 2006.

[71] Amine Maaref and Sonia Aïssa, "Exact error probability analysis of rectangular QAM for single- and multichannel reception in Nakagami-m fading channels," *IEEE Trans. Commun.*, vol. 57, no. 1, pp. 214–221, Jan 2008.

[72] N.Y. Ermolova, "Useful integrals for performance evaluation of communication systems in generalised η-μ and κ-μ fading channels," *IET Communications*, vol. 3, no. 2, pp. 303–308, Feb. 2009.

[73] D. B. da Costa and M. D. Yacoub, "Accurate approximations to the sum of generalized random variables and applications in the performance analysis of diversity systems," *IEEE Trans. Commun.*, vol. 57, no. 5, pp. 1271–1274, May 2009.

[74] P. R. Krishnaiah and M. M. Rao, "Remarks on a multivariate Gamma distribution," *The American Mathematical Monthly*, vol. 68, no. 4, pp. 342–346, Apr. 1961.

[75] H. Exton, *Multiple Hypergeometric Functions and Applications*, Wiley, New York, NY, 1976.

[76] M. S. Alouini, A. Abdi, and M. Kaveh, "Sum of Gamma variates and performance of wireless communication systems over Nakagami-fading channels," *IEEE Trans. Veh. Tech.*, vol. 50, no. 6, pp. 1471–1480, Nov. 2001.

[77] M. Z. Win, and G. Chrisikos, and J.H. Winters, "MRC performance for M-ary modulation in arbitrarily correlated Nakagami fading channels," *IEEE Commun. Lett.*, vol. 4, no. 10, pp. 301–303, Oct. 2000.

[78] M.V. Clark, L.J. Greenstein, W.K. Kennedy, and M. Shafi, "Matched filter performance bounds for diversity combining receivers in digital mobile radio," *IEEE Trans. Vehi. Tech.*, vol. 41, no. 4, pp. 356–362, Nov. 1992.

[79] H. Vincent Poor, *An Introduction to Signal Detection and Estimation*, Springer-Verlag, New York, NY, 2nd edition, 1994.

[80] T. Q. Duong and V. N. Q. Bao, "Performance analysis of selection decode-and-forward relay networks," *IEE Electron. Lett.*, vol. 44, no. 20, Sep. 2008.

[81] Z. Yi and I. Kim, "Diversity order analysis of the decode-and-forward cooperative networks with relay selection," *IEEE Trans. Wireless Commmun.*, vol. 7, no. 5, pp. 1792–1799, May 2008.

[82] M. Chiani, and D. Dardari, and M.K. Simon, "New exponential bounds and approximations for the computation of error probability in fading channels," *IEEE Trans. Wirel. Commun.*, vol. 2, no. 4, pp. 840–845, July 2003.

[83] J. N. Laneman and G. W. Wornell, "Energy efficient antenna sharing and relaying for wireless networks," in *Proc. IEEE Wireless Commun. & Networking Conf., WCNC'00"*, Chicago, IL, Oct. 2000, pp. 7 – 12.

[84] I. S. Gradshteyn and I. M. Ryzhik, *Table of Integrals, Series, and Products*, New York: Academic, 7th edition, 2007.

[85] Wolfran Functions Site, "Bessel-Type Functions," *Available at http://functions.wolfram.com/03.01.26.0003.01*.

[86] J. Boyer, D. D. Falconer, and H. Yanikomeroglu, "Multihop diversity in wireless relaying channels," *IEEE Trans. Commun.*, vol. 52, no. 10, pp. 1820–1830, Oct. 2004.

[87] G. K. Karagiannidis, T. A. Tsiftsis, and R. K. Mallik, "Bounds for multihop relayed communications in Nakagami-*m* fading," *IEEE Trans. Commun.*, vol. 54, no. 1, pp. 18–22, Jan. 2006.

[88] B. Maham and A. Hjorungnes, "Asymptotic performance analysis of amplify-and-forward cooperative networks in a Nakagami fading environment," *IEEE Commun. Lett.*, vol. 13, no. 5, pp. 300–302, May 2009.

[89] P. L. Yeoh, M. Elkashlan, and I. B. Collings, "Selection diversity with multiple amplify-and-forward relays in Nakagami-m fading channels," in *Proc. Int. Vehicular Technology Conf. (VTC'08) - Fall*, Ottawa, Canada, Sep. 2010, pp. 1–5.

[90] Y. Li and S. Kishore, "Asymptotic analysis of amplify-and-forward relaying in nakagami-fading environments," *IEEE IEEE Trans. on Wireless Commun.*, vol. 6, no. 12, pp. 4256–4262, Dec. 2007.

[91] L-L Yang and H.-H. Chen, "Error probability of digital communications using relay diversity over Nakagami-m fading channel," *IEEE IEEE Trans. on Wireless Commun.*, vol. 7, no. 5, pp. 1806–1811, May 2008.

[92] G. K. Karagiannidis, "Performance bounds of multihop wireless communications with blind relays over generalized fading channels," *IEEE Trans. Wireless Commun.*, vol. 5, no. 3, pp. 498–503, Mar. 2006.

[93] J. Vazifehdan and R. Hekmat, "Performance evaluation of multi-hop detect-and-forward and amplify-and-forward wireless transmission systems," in *Proc. IEEE 19th International Symposium on Personal, Indoor and Mobile Radio Communications (PIMRC'08)*, Cannes, France, Sep. 2008, pp. 1–5.

[94] S. Chen, W. Wang, and X. Zhang, "Ergodic and outage capacity analysis of coopera-tive diversity systems under Rayleigh fading channels," in *Proc. IEEE International Commun. Conf., "ICC'09"*, Germany, June 2009, pp. 1–5.

[95] G. Farhadi and N. C. Beaulieu, "On the ergodic capacity of multi-hop wireless relaying systems," *IEEE Trans. Wireless Commun.*, vol. 8, no. 5, pp. 2286–2291, May 2009.

[96] J. N. Laneman, D. N. C. Tse and G.W. Wornell, "Cooperative diversity in wireless networks: Efficient protocols and outage behavior," *IEEE Trans. Info. Theory*, vol. 50, no. 12, pp. 3062–3080, Dec. 2004.

[97] Wolfran Functions Site, "Bessel-Type Functions," *Available at http://functions.wolfram.com/Bessel-TypeFunctions/BesselK/26/01/02/*.

[98] Y.-C. Ko, and M. S. Alouini and M. K. Simon, "Outage probability of diversity systems over generalized fading channels," *IEEE Trans. Commun.*, vol. 48, no. 11, pp. 1783–1787, Nov. 2000.

[99] J. M. Romero-Jerez and A. J. Goldsmith, "Performance of multichannel reception with transmit antenna selection in arbitrarily distributed Nagakami fading channels," *IEEE Trans. on Wireless Commun.*, vol. 8, no. 4, pp. 2006–2013, Apr. 2009.

[100] Anvar Hasanov and H.M. Srivastava, "Decomposition formulas associated with the Lauricella multivariable hypergeometric functions," *Computers and Mathematics with Applications*, vol. 53, no. 7, pp. 1119–1128, Apr. 2007.

[101] A. Ghasemi and E. S. Sousa, "Fundamental limits of spectrum-sharing in fading environments," *IEEE Trans. Wireless Commun.*, vol. 6, no. 2, pp. 649–658, Feb. 2007.

[102] D. Chen and J. N. Laneman, "Modulation and demodulation for cooperative di-versity in wireless systems," *IEEE Trans. Wireless Commun.*, vol. 5, no. 7, pp. 1785–1794, July 2006.

[103] Y. Zhu and H. Zheng, "Understanding the impact of interference on collaborative relay," *IEEE Trans. Mobile Computing*, vol. 7, no. 6, pp. 724–736, June 2008.

[104] A. Høst-Madsen and J. Zhang, "Capacity bounds and power allocation for wireless relay channels," *IEEE Trans. Info. Theory*, vol. 51, no. 6, pp. 2020–2040, June 2005.

[105] Leila Musavian, Sonia Aïssa, and S. Lambotharan, "Effective capacity for interference and delay constrained cognitive-radio relay channels," *IEEE Trans. Wireless Commun.*, vol. 9, no. 5, pp. 1698–1707, May 2010.

[106] A. Jovicic and P. Viswanath, "Cognitive radio: An information-theoretic perspective," *IEEE Trans. Infor. Theory*, vol. 55, no. 9, pp. 3945–3958, Sep. 2009.

[107] Leon Garcia, *Probability, Statistics, And Random Processes For Electrical Engineering*, Prentice Hall, 2 edition, 1999.

[108] Y. Zhao, R. Adve, and T. J. Lim, "Symbol error rate of selection amplify-and-forward relay systems," *IEEE Commun. Lett.*, vol. 10, no. 11, pp. 757–759, Nov. 2006.

[109] A.P. Prudnikov, Y.A. Brychkov, and O.I. Marichev, *Integrals and series*, vol. 3, Gordon and Breach Science Publishers, 1990.

[110] T. Cover and A.E. Gamal, "Capacity theorems for the relay channel," *IEEE Trans. Inf. Theory*, vol. 25, no. 5, pp. 572–584, Sep. 1979.

[111] Boris Rankov and Armin Wittneben, "Spectral efficient protocols for half-duplex fading relay channels," *IEEE J. Select. Areas Commun.*, vol. 25, no. 2, pp. 379–389, Feb. 2007.

[112] J. N. A. Karaki and A. E. Kamal, "Routing techniques in wireless sensor networks: a survey," *IEEE Wireless Commun.*, vol. 11, no. 5, pp. 6–28, Dec. 2004.

[113] Wolfran Functions Site, "Meijer G-Functions," *Available at http://functions.wolfram.com/07.34.21.0002.01*.

[114] J. Mitola *et al.*, "Cognitive radio: making software radio more personal," *IEEE Pers. Commun.*, pp. 13–18, Aug. 1999.

[115] A. Sendonaris, E. Erkip, and B. Aazhang, "User cooperation diversity - part I: system description," *IEEE Trans. Commun.*, vol. 51, no. 11, pp. 1927–1938, Nov. 2003.

[116] J. M. Peha, "Approaches to spectrum sharing," *IEEE Communications Magazine*, vol. 8, no. 1, pp. 10–11, Feb. 2005.

[117] T. Tsiftsis, G. Karagiannidis and S. Kotsopoulos, *Wireless Transmissions with Combined Gain Relays over Fading Channels*, vol. 197 of *IFIP International Federation for Information Processing*, Springer Boston, 2006.

[118] L. Rubio, N. Cardona, S. Flores, J. Reig and L. Juan-Llacer, "The used of semi-deterministic propagation models for the prediction of the short-term fading statistics in urban environments," in *IEEE 49th Veh. Technol. Conf. (VTC)*, Amsterdam, Netherland, 1999, pp. 1460–1464.

[119] Fadel F. Digham, M.-S. Alouini, and Marvin K. Simon, "On the energy detection of unknown signals over fading channels," *IEEE Trans. Commun.*, vol. 55, no. 1, pp. 21–24, Jan. 2007.

Appendix B

Résumé

B.1 Introduction

B.1.1 Contexte et Motivation

À la fin de juin 2009, les États-Unis d'Amérique (USA) ont terminé le processus de fermeture de la radiodiffusion terrestre analogique. Le Conseil de la radiodiffusion et des télécommunications canadiennes (CRTC) a également fixé la date limite pour la transition vers la télévision numérique (DTV), à savoir au 31 août 2011 [1]. À cette date, des stations de télévision canadiennes en liaison radio cesseront la diffusion dans le domaine analogique et utiliseront des signaux numériques à la place. Partout dans le monde, les pays les plus développés ont commencé l'arrêt de l'analogique; un processus qui va s'accélérer au cours des cinq prochaines années. Le passage au numérique va libérer des ressources précieux du spectre pour d'autres services importants comme les services sans fil évolués, et la sécurité publique, comme pour les applications de la police et d'urgence. En effet, la DTV utilise moins les ressources du spectre que la TV analogique. En outre, la transmission DTV est moins affectée par les interférences et aussi opère dans des niveaux de puissance plus faibles que les signaux de TV analogiques.

D'autre part, conduit par l'intérêt croissant des consommateurs pour les services sans fil, la demande pour le spectre radio a augmenté de façon spectaculaire. Par ailleurs, l'approche classique de la gestion du spectre est très rigide dans le sens où une licence exclusive est accordée à chaque opérateur pour fonctionner dans une bande de fréquence donnée. Cependant, avec la plupart du spectre radioélectrique utile étant déjà attribuée, il

devient excessivement difficile de trouver des bandes vacantes soit pour déployer de nouveaux services ou pour améliorer ceuy existants. Dans ce contexte, le but d'améliorer l'efficacité spectrale dans les bandes TV, la Federal Communications Commission (FCC) aux États-Unis a permis les systèmes sans licence (secondaire) à fonctionner dans la bande de fréquences attribuée aux services de DTV, tout en assurant qu'aucune interférence préjudiciable ne soit causée sur la diffusion DTV [2]. Compte tenu de cela, le groupe de travail de la norme IEEE 802.22 élabore la norme communément appelé réseau sans fil régionaux zone (WRAN) qui fonctionnera comme un système secondaire dans les bandes de DTV basées sur la technologie de radio cognitive.

La technologie de radio cognitive (CR) a la capacité de détection de l'environnement dans lequel elle opère, et d'exploiter ces informations pour opportuément fournir des liens sans fil qui peuvent mieux répondre à la demande de l'utilisateur et de son environnement radio. La technologie CR offre un potentiel énorme pour améliorer l'utilisation du spectre radioélectrique par la réutilisation et le partage efficace des bandes licenciées du spectre tout en respectant les limitations d'interférence de leurs utilisateurs principaux. En conséquence, deux fonctions principales dans les systèmes CR sont la *détection du spectre* et l'*accès au spectre*.

La détection du spectre consiste à observer la bande de fréquences radio et de traiter les observations en vue d'acquérir d'information sur la transmission licenciée dans la bande de fréquences partagée. La détection du spectre est une tâche importante dans les systèmes CR, et considérée comme obligatoire dans la norme IEEE 802.22. Divers problèmes de détection du spectre ont été observés dans la littérature. La condition nécessaire dans la détection du spectre est d'adopter des techniques sophistiquées de détection et des algorithmes pratiques pour échanger les informations de détection entre les nœuds secondaires.

D'autre part, l'accès au spectre consiste à fournir l'allocation et la gestion efficaces des ressources disponibles parmi les utilisateurs secondaires. Parmi les principaux défis dans les réseaux CR opportunistes est l'accès au spectre. En effet, comment efficacement et équitablement répartir les ressources radio entre les utilisateurs secondaires dans un réseau CR est un problème fondamental.

Dans cette thèse, nous nous concentrons sur plusieurs questions liées aux systèmes de partage du spectre CR à savoir, l'allocation des ressources adaptatives, les limites de capacité, la communication multi-utilisateurs, l'analyse de performance des communications

coopératives relayées et les communications CR coopératives relayées.

L'allocation Adaptative des Ressources

L'allocation adaptative des ressources est une technique prometteuse pour améliorer la performance des systèmes de communication CR [14]. En utilisant cette technique, un nœud CR a la capacité de changer ses paramètres de transmission basé sur la surveillance active de plusieurs facteurs dans l'environnement radio, comme le spectre radioélectrique, le trafic et l'activité des utilisateurs licenciés, et les variations du canal à évanouissement [9]. Dans ce contexte, généralement dans les systèmes de partage du spectre, l'information de l'état du canal secondaire (CSI) est utilisé à l'émetteur secondaire pour ajuster adaptativement les ressources de transmission [15, 16]. À cet égard, la connaissance de la liaison secondaire CSI et des informations sur le canal entre l'émetteur secondaire (ST) et le récepteur principal (PR), les deux à la ST, ont été utilisés dans [16] pour obtenir la politique de puissance optimale de transmission de l'utilisateur secondaire (SU) sous des contraintes sur la crête et la puissance moyenne reçue à la PR. La même approche a également été utilisée dans [17] et [18] pour optimiser la politique de transmission du SU dans le cadre de différents types de ressources et contraintes de qualité de service (QoS). Dans [19], en plus de l'information du canal susmentionné, la CSI relatif au lien de l'utilisateur principal (PU) a également supposé étre disponible à la ST pour ajuster la puissance d'émission de façon optimale afin de maximiser la capacité passible d'une contrainte sur la perte moyenne de capacité du lien primaire.

Limites de Capacité

Pour l'évaluation des performances et la conception de systèmes CR, utiliser la métrique de capacité adéquate est d'une importance primordiale. Habituellement, la capacité ergodique est utilisée comme une mesure de débit à long terme dans ces systèmes [20]. La capacité ergodique est le taux moyen maximale atteignable sur tous les états évanouis sans aucune contrainte de délai. Toutefois, dans les systèmes CR, en imposant des contraintes sur les interférences générées par les utilisateurs cognitives tout en adhérant àux niveaux d'activité des PUs, il est évident qu'un certain pourcentage de panne est inévitable [16]. Ainsi, pour applications sensibles au délai, la capacité limitée par le délai est une métrique plus appropriée [21]. À cet égard, la capacité limitée par le délai des systèmes à spectre partagé sous différents types de contraintes de puissance, a été étudiée dans [22] et [23], en considérant la disponibilité de la CSI relative au lien SU et celui correspondant au canal

d'interférence entre l'émetteur secondaire (ST) et le récepteur principal (PR), les deux à la ST. D'autre part, dans de nombreuses applications en temps réel, le taux requis n'est pas nécessairement constant. Par exemple, dans les systèmes sans fil, où un taux spécifique est nécessaire pour la communication vocale, un taux en excès peut être utilisé pour d'autres applications. Motivé par ce fait, la notion de capacité basée sur taux de service a été proposée dans [24, 25]. En particulier, dans les systèmes CR où la transmission est limitée par l'activité des PUs, il est souhaitable que les PUs utilisent pleinement les ressources de radio alors qu'ils ont accès à la bande de fréquences partagées. À cet égard, compte tenu de la disponibilité de la CSI secondaire et de l'information sur le canal d'interférence à la ST, la capacité de taux de service des systèmes de partage du spectre est étudiée dans [22].

Réseau de Communications Multi-Utilisateurs

Comme mentionné précédemment, l'accès au spectre signifie comment repartir efficacement et équitablement les ressources radio entre SUs dans un réseau CR [12]. Cette question est similaire au problème du canal de diffusion (*en anglais Broadcast Channels*, BC) dans les systèmes actuels de communication sans fil. Dans les systèmes BC, habituellement et traditionnellement, la CSI a été utilisée pour allouer les ressources de transmission de façon adaptative tels que le temps, la puissance, la bande passante et la vitesse, parmi les utilisateurs [26]. En particulier, en considérant une CSI parfaite à la station de base et les récepteurs, le temps optimal et les politiques d'allocation de puissance qui maximisent la capacité ergodique des BCs évanouis a été étudié dans [26]. Dans les réseaux de partage du spectre CR, le problème de la répartition équitable des ressources parmi les SU a été étudiée dans [12] soumis à des contraintes de QoS dans les SUs et des contraintes d'interférence aux PRs. Dans ces dernier travaux, la CSI est la seule information sur laquelle la station de base décide comment répartir les ressources entre les utilisateurs.

Analyse du Rendement des Communications Coopératives

L'analyse de performance des signaux à modulation numérique dans les environnements évanŏis est une question de longue date qui a été le centre des recherches au cours des dernières années [69]. Un aspect crucial de ces efforts est la dérivation d'expressions de forme fermée prêtes à l'emploi, et faciles à utiliser pour les mesures clé de rendement tels que la probabilité moyenne d'erreur de symboles (SEP) induite par les schémas de modulation M-aires sur les canaux à évanouissements, des expressions qui fournissent souvent des

informations précieuses sur la conception de systèmes sans fil. Une fois mis en IJuvre, tels résultats de forme fermée diminuent le besoin de simulations Monte Carlo, donc permettant un étalonnage facile des paramètres du système sans fil afin d'optimiser sa performance globale. Cette métrique a été étudiée pour certains scénarios d'évanouissement sous différentes hypothèses. D'autre part, avec la nécessité permanente d'un débit plus élevé et une augmentation du débits de données dans les systèmes de communication sans fil, le concept de diversité coopérative a été récemment suscité un intérêt grandissant [27–31]. L'idée clé est que les terminaux situés dans différentes positions géographiques peuvent partager leurs antennes afin de mimer un réseau d'antennes virtuelles et d'exploiter les avantages de la diversité spatiale, même lorsque les nœuds de source et destination sont des dispositifs à une seule antenne. En fait, les transmissions coopératives permettant à deux nœuds, une source et une destination, atteindre mutuellement à travers un ensemble de relais coopératifs, dont le but est de propager le signal de la source à la destination en vue d'améliorer la couverture et d'augmenter le débit réalisables entre les nœuds d'extrémité. Dans ce contexte, l'évaluation des performances des systèmes sans fil multi-branche et multi-sauts coopératives a été étudiée dans [32] en proposant un cadre unifié qui repose sur l'approche basée sur MGF. Par ailleurs, la probabilité de coupure ainsi que la performance de bout en bout des systèmes de relais coopératifs ont été analysés dans [33, 34].

Relayage Coopératifs dans les Communications CR

La gestion des ressources est en effet d'une importance fondamentale dans le spectre des systèmes de partage comme expliqué précédemment dans cette section. Toutefois, lorsque les ressources de fréquences disponibles ne sont pas suffisantes pour garantir une transmission fiable à la partie secondaire, la politique d'allocation des ressources ne peut pas être en mesure de remplir les exigences des SUs. Dans de tels cas, le système secondaire doit mettre en IJuvre des techniques sophistiquées pour répondre à ses exigences de performance. Une technique notable est la communication coopérative qui exploite la diversité spatiale naturelle des systèmes multiutilisateurs. En effet, la transmission coopérative (communication en utilisant des noeuds relais) est une voie prometteuse pour lutter contre l'évanouissement du signal causé par la propagation radio multi-trajets, et améliorer les performances du système et la zone de couverture [35]. Grosso modo, il y a deux principaux types de traitement du signal au niveau des nœuds relais: Amplifier et retransmettre (*en anglais Amplify-and-Forward*, AF) par lequel le relais amplifie simplement le signal

reçu sans aucune sorte de décodage et transmet la version amplifiée au nœud de destination, qui est l'option la plus simple et pratique, décoder et de retransmettre (*en anglais Decode-and-Forward*, DF) par lequel le relais décode le signal reçu, puis réencode avant de le transmettre au nœud de destination. Dans ce contexte, le concept de relais a été appliqué dans le contexte de CR pour aider la transmission de SUs et améliorer l'efficacité du spectre, par exemple, voir [36–39].

B.1.2   Objectifs de la Recherche

Dans cette thèse, comme souligné plus haut, nous considérons les réseaux CR en faisant usage de l'information de détection sur l'activité des PUs dans la région voisine du CR et fonctionnant sous des contraintes d'interférence. Dans ce cas, une bonne gestion des ressources est nécessaire afin de garantir les exigences de QoS des PUs. L'existence et spécification de telle allocation de ressources en vertu des differents exigences de service dans le système secondaire sont des questions nécessaires et seront étudiés dans cette thèse. Nous allons également développer des techniques d'allocation dynamique des ressources et proposer des politiques d'adaptation appropriées pour les réseaux CR. En particulier, nous considérerons un scénario de partage du spectre BC et développerons des techniques de pointe pour la détection du spectre et la gestion des ressources en conjonction avec les politiques d'adaptation et les protocoles de manière à utiliser le spectre radio de manière efficace. Par la suite, nous allons adopter la technique de relais coopérative pour la transmission secondaire dans un système de partage du spectre CR, pour utiliser plus efficacement les ressources spectrales disponibles et réduire les interférences au niveau des récepteurs primaires. Dans ce contexte, nous allons commencer par faire une analyse de performance des communications coopératives dans des environnements évanouis. Ensuite, nous allons considérer un système par relais coopératif typique de partage du spectre d'enquêter sa performance de bout en bout lorsque les transmissions sont limitées par des contraintes sur l'interférence admissible au niveau du récepteur primaire.

B.1.3   Contribution de la Dissertation

La contribution de cette thèse peut être résumée à plusieurs égards comme suit:

- On considère un système de partage du spectre où la puissance de la ST est contrôlé

basé sur la détection douce (soft-sensing) des informations sur l'activité du PU et CSI appartenant à la liaison secondaire. L'information de sondage spectral est obtenue par un détecteur de sondage spectral monté sur le côté secondaire pour évaluer l'état d'activité du PU dans la bande de fréquences partagées et le système est caractérisé par des contraintes de ressources sur l'interférence moyenne à la PR et la crête de puissance de transmission à la ST. Compte tenu de ces limites, la capacité ergodique du canal du SU dans l'environnement evanoui est étudié, et le régime d'allocation de puissance optimale pour obtention de capacité, à savoir politique de puissance variable, est dérivé. Cependant, alors que la plupart des schémas de modulation n'adaptent pas leurs performances dans les conditions d'évanouissements, un CR reconfigurable est en mesure de choisir une stratégie de modulation qui adapte la vitesse de transmission et de puissance pour fournir des communications fiables à travers le canal tout le temps. Dans ce contexte, nous examinons aussi la stratégie de transmission de puissance *Multilevel Quadrature Amplitude Modulation* (M-QAM) de taux et puissance variable dans un système de communication CR où le taux et la puissance de la ST sont adaptativement contrôlées basée sur la disponibilité de la liaison secondaire CSI et la détection douce (soft-sensing) des informations sur l'activité du PU. En outre, considérant que une information "soft-sensing" imparfaite est utilisée au niveau du système secondaire, nous étudions la politique de transmission de puissance optimale en termes de fausses alarmes et probabilités de détection et explorons l'impact des incertitudes sur la performance de détection des systèmes cognitifs de radio par partage du spectre.

• Les notions de capacité différentes, à savoir, les capacités ergodiques, limitées par délai et taux de service dans les systèmes CR sont étudiés tandis que les paramètres de transmission des utilisateurs cognitives sont adaptativement changés basé sur la disponibilité de la CSI appartenant au lien SU, et information "soft-sensing" sur l'activité de la PU. Nous étudions d'abord la capacité ergodique du lien SU dans les environnements évanouis et dérivons la politique d'allocation de puissance optimale associé. Ensuite, la politique d'allocation de puissance sous la contrainte de probabilité de coupure est obtenue, et la capacité réalisable avec telle politique de transmission est étudiée dans différents environnements évanouis. Enfin, nous proposons la capacité de taux de service comme une notion de capacité basée en service pour les réseaux CR qui fournit non seulement un taux minimal constant pour les utilisateurs cognitifs, mais aussi augmente le taux réalisable moyen à long terme du lien de communication secondaire à travers l'utilisation de la puissance en excès disponible.

• Nous considérons un système de partage du spectre primaire/secondaire et étudions la gestion des ressources adaptative en canaux de diffusion à évanouissements CR-BC. Dans ce contexte, tout en se concentrant sur la capacité des systèmes CR pour apercevoir l'environnement dans lequel ils opèrent, nous obtenons une politique d'allocation de puissance de transmission et partage du temps optimale pour les systèmes CR-BC, basée sur des observations locales sur l'activité du système primaire autour de chaque SR. Notre approche est nouvelle par rapport à l'utilisation des informations locales "soft-sensing" afin de déterminer quel SU devrait avoir accès à la bande de fréquences partagées à chaque état de détection. Nous avons également implémenté un mécanisme de détection discrète afin de limiter la complexité globale du système, sans compromettre les performances du système de manière significative.

• Nous présentons une analyse de performances des systèmes de communication par relais coopératif. Dans ce contexte, d'abord, en considérant un scénario d'évanouissement généralisé dans un système de communication classique, nous étudions la performance d'un système de communication typique en termes de la probabilité moyenne d'erreur de symbole (SEP) des constellations M-aires QAM arbitraires de régimes de combinaison par rapport maximal (MRC) sur des canaux corrélés non-identiques. Ensuite, nous considérons un système de sauts multiples par relais de coopératifs avec transmission amplifier et transférer (AF) par de ligne de visage directe entre les nœuds de source et destination, en fonctionnent sur des canaux à évanouissement Nakagami avec des paramètres d'évanouissement arbitraires. Dans ce contexte, nous étudions la performance des réseaux par relais coopératifs en matière de SEP moyenne, la capacité ergodique et probabilité de coupure soumise à évanouissement Nakagami-m indépendants et non identiquement distribuées.

• Nous adoptons la technique de relais coopératifs pour la transmission secondaire dans un système de partage du spectre, pour utiliser plus efficacement les ressources spectrales disponibles, et de diminuer les interférences au niveau des PRs. Dans ce contexte, nous considérons un système de partage du spectre par relais coopératif relais à double saut et étudions les performances de bout en bout de ce système coopératif tout en respectant les exigences de QoS des PUs de la bande de fréquences partagée. Plus précisément, en supposant qué un régime de relayage décoder et transférer (DF) est employé dans la communication entre les nœuds source secondaire (émetteur) et la destination (récepteur), les
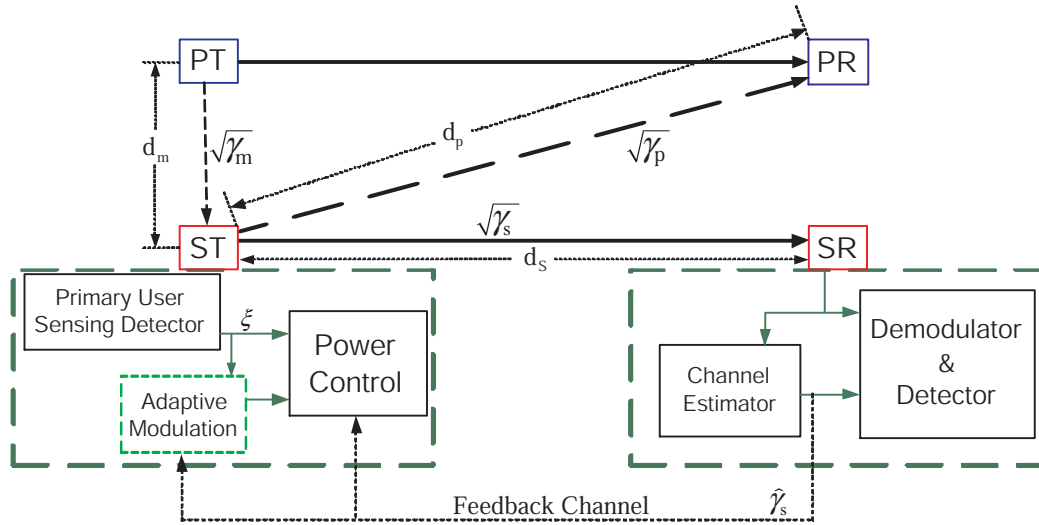
Figure B.1: Modèle de système de partage du spectre de schéma.

performances de bout en bout du système coopératif double saut est étudiée tout en tenant
compte un relais intermédiaire entre la source et la destination secondaire pour aider le pro-
cessus de communication secondaire. En outre, nous considérons le scénario où un groupe
de relais est disponible entre les nœuds source secondaire et destination. Dans ce cas,
l'utilisation schéma de sélection de relais partiel, les résultats présentés pour le scénario
de relais simple sont généralisés. Enfin, nous considérons que la communication entre les
nœuds source secondaire et destination est assistée par un relais intermédiaire qui utilise un
régime de relayage AF. Dans ce contexte, la performance globale du système coopératif de
partage du spectre est étudiée pour différentes conditions de propagation.

B.2   L'allocation Adaptative des Ressources

Dans cette section, nous considérons un système de partage du spectre où la puissance
de la ST est contrôlé en se basant sur la détection douce (soft sensing) des informations
sur l'activité de la PU et CSI relatives à la liaison secondaire. Le modèle du système est
illustré dans la Fig. B.1, qui montre deux paires d'émetteurs primaires et secondaires et les
récepteurs. Le système est caractérisé par des contraintes de ressources sur l'interférence
de la puissance d'émission moyenne au niveau du PR et de la puissance pic transmise
par le ST. Compte tenu de ces limitations, nous étudions la capacité ergodique du canal
à évanouissement de la SU, et extrayons le schéma d'alimentation optimale pour la réal-

isation d'allocation de capacité, soit la puissance variable. Cependant, alors que la plupart des schémas de modulation n'adaptent pas leurs performances dans les conditions d'évanouissements, un CR reconfigurable est en mesure de choisir une stratégie de modulation qui adapte la vitesse de transmission et de puissance pour fournir des communications fiables à travers le canal à tout temps [14]. Cette stratégie, appelée à puissance et taux variable, a été proposée dans [49]. Dans ce dernier travail, en supposant que la disponibilité de CSI à côté de l'émetteur, le taux et la stratégie de puissance qui maximise la capacité des canaux ont été étudiés sous les contraintes jointes de puissance d'émission moyenne et de taux d'erreur binaire (BER) cible. Dans ce contexte, nous examinons aussi une stratégie de transmission de puissance M-QAM à taux et puissance variable dans un système de communication CR où le taux et la puissance de la ST sont dynamiquement contrôlée se basant sur la disponibilité de la liaison secondaire CSI et détection douce des informations sur l'activité du PU. Enfin, les avantages de l'utilisation de soft-détection des informations sur l'activité du PU sur la puissance et des stratégies d'adaptation de taux sont évalués, et des résultats numériques et des comparaisons illustrant les performances de notre système de partage de spectre dans les scénarios d'exploitation différents sont fournis. En particulier, nous montrons que l'utilisation de la technique soft-détection, le SU peut contrôler ses paramètres de transmission tels que le débit et la puissance, en fonction de différents niveaux d'activités observés PU par le détecteur de détection.

Par ailleurs, nous caractérisons l'incertitude de l'information de détection calculée au niveau du détecteur de détection en prenant en compte les fausses alarmes prédéterminées et les probabilités de détection dans le modèle du système. Le système CR est limité par la contrainte appropriée sur la puissance moyenne reçue à la PR. Dans ce contexte, la transmission de puissance optimale a été dérivée en termes de probabilités de fausses alarmes et la détection, de telle sorte que la capacité du canal réalisables SU est maximisée. Enfin, les résultats numériques et les comparaisons illustrent la performance du système de CR dans les informations de détection imparfaite. Les résultats étudiés ont montré une amélioration de la performance du SU comme l'incertitude sur l'information augmente la détection.

B.3   Limites de Capacité

Dans cette section, nous considérons un système de communication sans fil CR où la puissance de la ST est contrôlé en se basant sur l'information de détection douce (en anglais soft-sensing information, SSI) sur les états d'activité du PU, et CSI relatives à la liaison secondaire. Il est à noter que l'interférence sur le principal lien vers le récepteur SU est également considéré dans ce modèle de système. Comme le montre la Fig. B.2, nous considérons un système de partage du spectre avec une paire d'émetteurs-récepteurs primaires / secondaires, à savoir, (PT, PR) et (ST, SR). Le système considéré est soumis à des contraintes sur l'interférence moyenne à la PR et sur la puissance d'émission maximale de la ST. Compte tenu de ces deux contraintes, nous avons d'abord étudier la capacité ergodique du lien entre le SU dans les environnements évanouissements et dériver les politiques optimales d'allocation de puissance associée. Ensuite, nous obtenons la politique d'allocation de puissance sous contrainte de probabilité de coupure, et enquêtons sur la capacité réalisable avec la politique de telle transmission dans des environnements à évanouissements. Enfin, nous proposons la capacité de service à taux comme un service basé sur la notion des capacités pour les réseaux CR qui fournit non seulement un taux minimal constant pour les utilisateurs cognitifs, mais aussi augmente la moyenne à long terme à taux réalisable de la liaison de communication secondaire à travers l'utilisation des disponibles excès de puissance.

L'analyse théorique en plus des résultats numériques et des comparaisons pour différents environnements à évanouissements, sont présentés à ce que chaque notion de capacité a quelques fonctionnalités qui peuvent être utilisées selon les différentes exigences de système. En particulier, la capacité de service à taux a été proposée comme une capacité appropriée métriques dans les réseaux de CR qui combine les avantages des stratégies de transmission à court et à long terme.

B.4   Gestion des ressources dans les CR à canaux de diffusion (CR-BC)

Dans le scénario de CR-BC présenté dans la norme WRAN [3], plutôt que l'information de canal, la station de base secondaire (CR) peut employer ses observations sur le milieu
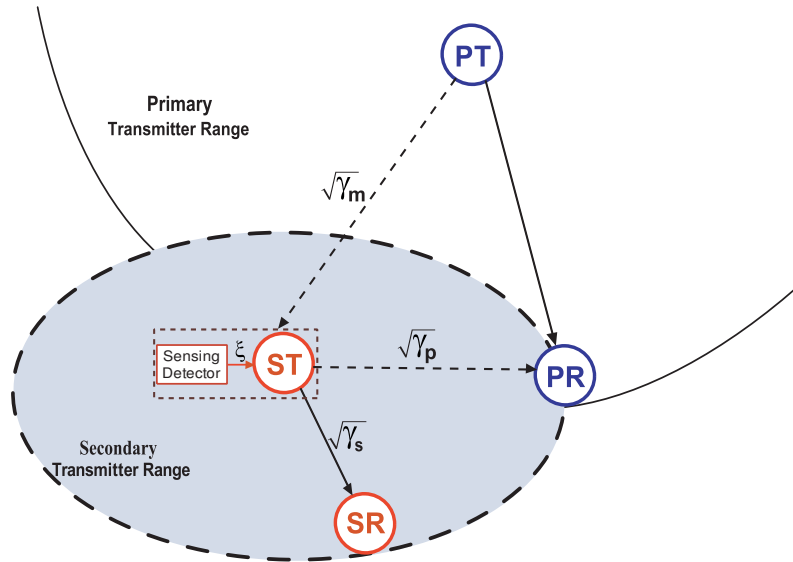
Figure B.2: Modèle de système de partage du spectre.

environnant pour allouer de manière optimale ses ressources, telles que le temps de transmission et de puissance, entre les utilisateurs secondaires. Dans cette section, tout en se concentrant sur la capacité des systèmes de CR au sens de l'environnement dans lequel ils opèrent, notre objectif est d'obtenir une optimalité de partage des ressources pour les systèmes CR-BC, basée sur des observations locales sur l'activité du système primaire autour de chaque récepteur secondaire. Notre approche est nouvelle par rapport à l'utilisation des informations locales par détection douce afin de déterminer quel SU devrait avoir accès à la bande de fréquences partagées à chaque état de détection. Dans ce contexte, un scénario classique de BC est considéré comme un réseau de partage du spectre avec un CR ST comme station de base (BS) et un nombre K de SR, comme le montre la Fig. B.3. Le réseau CR-BC est limité par des contraintes appropriées sur la moyenne reçus-ingérence à la PR et sur la puissance crête émise par la ST. Nous avons également en œuvre un mécanisme de détection discrète afin de limiter la complexité globale du système, sans compromettre les performances du système de manière significative. Dans ce schéma, on ne considère que les niveaux d'activité restreint primaire pour les observations de télédétection.

Enfin, les résultats numériques illustrent les performances de la proposition de CR-BC du système en termes de capacité ergodique sous contraintes prédéfinies sur l'interférence moyen ne générée par le réseau secondaire à la PR et le pic de transmission de puissance au secondaire BS. Par ailleurs, nous étudions la peine de capacité de l'approche proposée
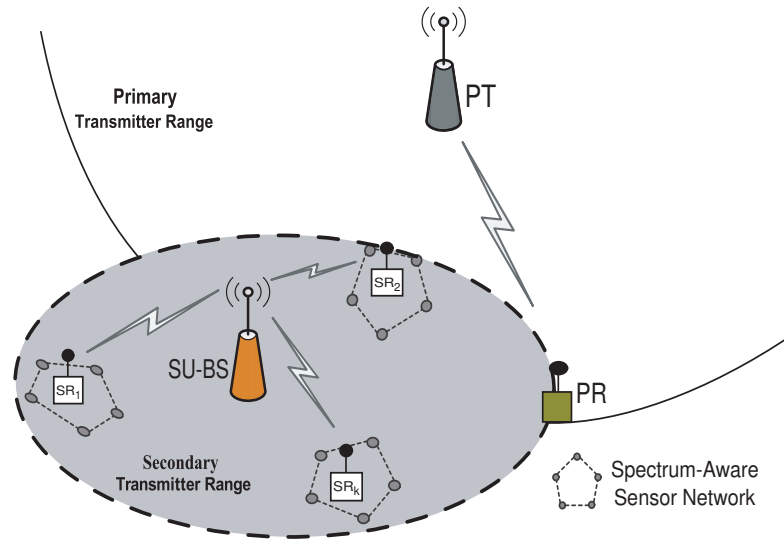
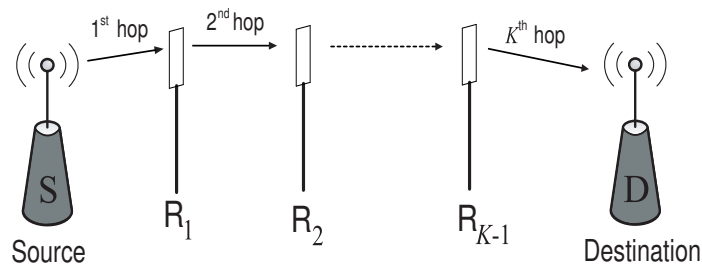Figure B.3: Spectre de partage configuration du système BC.

Figure B.4: Multi-Hop système de relais de la coopération.

par détection quantifiée pour le système en cours d'examen.

B.5 Analyse du Rendement des Communications Coopératives

Dans cette section, notre objectif est d'enquêter sur l'analyse des performances de la CR à relayage coopérative dans un contexte de partage du spectre. Dans ce contexte, nous commençons par enquêter sur l'analyse des performances des communications coopérative. En particulier, au premier abord, en considérant un scénario généralisé fondu dans un système de communication classique, nous enquêtons sur l'analyse des performances du
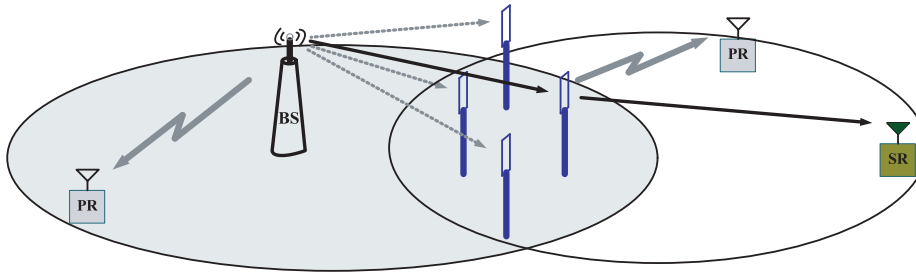
Figure B.5: Double-Hop coopératives de partage du spectre du système de relais avec sélection partielle.

système de communication typiques en termes de la SEP moyenne de différentes constellations M-aires QAM avec MRC sur les canaux non-identiquement corrélés.

Par la suite, nous étudions l'analyse des performances des réseaux de relais coopératifs en matière de SEP moyenne, la capacité ergodique et sous réserve des performances de probabilité de panne indépendante et non identiquement distribuées à évanouissements Nakagami-m. Dans ce contexte, nous considérons le modèle du système illustré à la figure B.4, où un ensemble de K-1 relais intermédiaires permet d'amplifier et de transmettre le signal à partir d'une source à une destination, coopérant ainsi à créer un système de transmission multi-sauts AF. Enfin, les résultats numériques de simulation qui corroborent notre analyse ont été fournis et l'impact de plusieurs paramètres tels que le nombre de nœuds de reparcage et les indices d'évanouissements Nakagami sont étudiés pour différentes modulations QAM rectangulaires.

B.6   Relayage Coopératifs dans les Communications CR

L'utilisation de la transmission coopérative dans les systèmes CR de partage du spectre peut donner une plus grande efficacité dans l'utilisation des ressources du spectre. Dans ce contexte, nous adoptons la technique de coopération pour relayer la transmission secondaire dans un système de partage du spectre, et ce afin d'utiliser plus efficacement les ressources spectrales disponibles et de réduire les interférences générées à la RR. Dans cette section, nous considérons un système de partage du spectre CR, où les relais DF sont employés pour aider à la communication de la procédure SU, comme le montre la figure B.5. Plus précisément, nous considérons un système coopératif relais à deux sauts de partage du spectre, et d'enquêter sur sa bout à bout des performances lorsque les transmissions sont

limitées par des contraintes sur l'interférence tolérable par le PU tels que sa transmission est soutenue avec un taux constant pour une certaine période de temps.

Les Relais DF sont employées dans la communication entre la source secondaire (émetteur) et destination (récepteur) des nœuds, et nous obtenons le BER moyen et la capacité ergodique du système de relais de partage du spectre avec coopération avec un relais intermédiaire entre la source et de destination pour aider les processus de communication secondaire. Nous considérons par ailleurs le scénario où un groupe de relais est disponible entre la source secondaire et des nœuds de destination. Dans ce cas, la sélection à l'aide de relais partielle [30], nous généralisons les résultats présentés ici pour le scénario de simple relais, et d'obtenir le BER moyen et la capacité ergodique du système coopératif avec un cluster de relais L disponibles. Enfin, nous étudions les performances de probabilité de coupure de la coopérative de partage du spectre du système en cours d'examen pour les deux, les régimes mono-relais et de multiples relais.

Nous avons en outre étudier la performance de bout en bout de double-Hop AF relayer coopératives dans les systèmes CR de partage du spectre tout en tenant compte des contraintes sur la moyenne reçue-ingérence dans la RR. En particulier, nous obtenons les statistiques de l'reçues SNR au niveau du noeud de destination secondaire pour différentes distributions de la décoloration de canal, à savoir, de Rayleigh et Nakagami. Puis, faisant usage de ces statistiques, la capacité globale réalisable et la probabilité de coupure du processus de la communication de la SU sont étudiés et des résultats numériques et les comparaisons sont fournis.

B.7   Conclusions de la Dissertation

Dans cette thèse, nous avons considéré de partage du spectre des réseaux CR soumis à des contraintes d'interférence et de paramètres de transmission du SUs peut être ajusté sur la base des variations de canaux secondaires et de l'information soft de détection de l'activité du PUs. Dans ce contexte, une bonne gestion des ressources a été développé de sorte à garantir les exigences de QoS du PUs. L'existence et la spécification d'allocation des ressources et la gestion de telle transmission pour différents scénarios tels que les canaux BC ont été étudiés dans ce projet. Nous avons également proposé d'adopter la technique de coopération dans les systèmes de relais CR de partage du spectre de manière plus efficace

et utiliser efficacement les ressources de transmission disponibles, telles que l'énergie, le taux et la bande passante, tout en respectant les exigences de QoS du PUs de la bande de fréquences partagées. À cet égard, nous avons étudié les performances de bout en bout de la proposition de partage du spectre système de relais de coopération dans le cadre des contraintes de ressources définis de manière à garantir la QoS primaires n'est pas affectée. Plus précisément, les contributions de la thèse sont conclues comme suit:

• Nous avons considéré un CR de partage du spectre du système où le pouvoir à transmettre le SU et le taux peut être ajusté sur la base des variations de canaux secondaires et de l'information soft de détection de l'activité de la PU. Le système de partage du spectre a été supposé pour fonctionner sous des contraintes sur les interférences moyennes et la puissance d'émission maximale. Les résultats numériques et les comparaisons ont été fournis et illustré les avantages de l'utilisation de débit soft de détection de l'information et à la secondaire de la CSI dans les systèmes CR. Il a été démontré qu'en utilisant soft de détection technique, le SU peut opportuniste contrôler ses paramètres de transmission tels que le débit et la puissance, en fonction de différents niveaux d'activité observés PU par le détecteur de détection. Par ailleurs, nous avons observé un écart entre les capacités réalisées sur la base des taux variables et variables politiques de transmission de puissance. Par ailleurs, nous avons caractérisé l'incertitude de l'information de détection calculée au niveau du détecteur de détection, en termes de fausses alarmes et les probabilités de détection et étudié l'effet du spectre imparfaite de détection sur la performance des systèmes CR de partage du spectre.

• Considérant la disponibilité du soft de détection de l'information à la ST et en adoptant la technique de transmission de puissance adaptative, nous avons étudié trois notions de capacité, à savoir, ergodique, délai limité et un service de débit (avec et sans coupure), pour le CR de partage du spectre des systèmes d'exploitation sous contraintes sur la moyenne reçus-ingérence et d'émission de crête-puissance. Les résultats numériques et des comparaisons pour différents environnements de décoloration, ont montré que chaque notion de capacité a quelques fonctionnalités qui peuvent être utilisés selon les exigences de système différent. Plus précisément, la capacité de service à taux a été proposée comme une capacité appropriée métriques dans les réseaux de CR qui combine les avantages des stratégies de transmission à court et à long terme.

• Nous avons enquêté sur le partage des ressources adaptatives dans le CR-BC canaux où

l'information est utilisée spectre de détection au niveau du secondaire BS afin de répondre plus efficacement et d'utiliser efficacement les ressources partagées spectre. Nous avons proposé l'aide de soft-détection d'informations pour répartir équitablement le temps de transmission et de puissance, entre SU, sous des contraintes appropriées sur l'interférence moyenne à la PR et le pic de transmission de puissance-au secondaire BS. Les résultats numériques et les comparaisons ont montré que les informations relatives au spectre de détection permet une gestion efficace du temps et des ressources de pouvoir entre les SU et, par conséquent, l'ingérence résultant sur le système principal. Par exemple, dans le scénario avec deux SUs, il a été démontré que l'activité du système primaire diminue dans un secteur, plus de temps de transmission et de puissance peuvent être attribués à un SU situé dans cette zone et vice-versa. Nous avons également considéré comme un mécanisme de détection de spectre quantifié afin de réduire la complexité globale du système, et comme on l'observe, la performance avec des niveaux discrets sont définies dans le doux et deux niveaux (dur) de détection des résultats mécanisme.

• Nous avons développé une analyse des performances des communications traditionnelles de coopération afin d'avoir quelques idées sur la performance des coopératives relayer CR de partage du spectre des systèmes. Dans ce contexte, d'abord, en considérant un scénario généralisé la décoloration dans un système de communication classique, nous avons obtenu un général forme fermée expression pour le SEP moyen de constellations QAM arbitraires M-aires dans les régimes de la MRC sur les non-identiques η-μ corrélée canaux à évanouissement. Par la suite, nous avons étudié l'analyse des performances des réseaux multi-sauts relais en termes de coopération de l'ensemble septembre moyenne, la capacité ergodique et sous réserve des performances probabilité de panne indépendante à but non identiquement distribuées Nakagami-m à la décoloration. Par ailleurs, les résultats numériques de simulation et de corroborer notre analyse ont été fournis et l'impact de plusieurs paramètres tels que le nombre de nœuds relais et index Nakagami la décoloration a été étudiée.

• Enfin, nous avons considéré un relais coopératifs de partage du spectre du système dont la source secondaire de destination de la communication repose sur un nœud relais inter- médiaire dans le processus de transmission. À cet égard, nous avons étudié les perfor- mances de bout en bout du projet de coopérative de partage du spectre du système sous les deux systèmes DF et AF relayer la transmission. Plus précisément, nous avons obtenune

forme fermée des expressions pour le BER moyenne, la capacité ergodique et probabilité de coupure de la communication secondaire, tandis que les exigences du PU de QoS sont spécifiées en termes de contraintes de ressources appropriés sur le pouvoir d'interférence reçue moyenne et de pointe à la PR. Les résultats numériques et les comparaisons ont montré les avantages de la proposition de partage du spectre système de relais de coopération dans différents scénarios de décoloration.